



HAL
open science

Inter-organ cooperation during late *D. melanogaster* embryogenesis

Baptiste Tesson

► **To cite this version:**

Baptiste Tesson. Inter-organ cooperation during late *D. melanogaster* embryogenesis. *Development Biology*. Ecole normale supérieure de lyon - ENS LYON, 2022. English. NNT : 2022ENSL0042 . tel-04001230

HAL Id: tel-04001230

<https://theses.hal.science/tel-04001230>

Submitted on 22 Feb 2023

HAL is a multi-disciplinary open access archive for the deposit and dissemination of scientific research documents, whether they are published or not. The documents may come from teaching and research institutions in France or abroad, or from public or private research centers.

L'archive ouverte pluridisciplinaire **HAL**, est destinée au dépôt et à la diffusion de documents scientifiques de niveau recherche, publiés ou non, émanant des établissements d'enseignement et de recherche français ou étrangers, des laboratoires publics ou privés.



Numéro National de Thèse : 2022ENSL0042

THESE

en vue de l'obtention du grade de Docteur, délivré par
l'ECOLE NORMALE SUPERIEURE DE LYON

Ecole Doctorale N° 340

Biologie Moléculaire Intégrative et Cellulaire

Discipline : Sciences de la vie et de la santé

Soutenue publiquement le 28/11/2022, par :

Baptiste TESSON

Inter-organ cooperation during late *D.melanogaster* embryogenesis

Coopération entre organes lors de l'embryogénèse tardive de *D. melanogaster*

Devant le jury composé de :

MAO, Yanlan
LEVAYER, Romain
CROZATIER-BORDE, Michelle
REYMANN, Anne-Cécile
DERR, Julien
HEITZLER, Pascal
VINCENT, Stéphane

Professeure des universités
Directeur de recherche
Directrice de recherche
Chargée de recherche
Professeur des universités
Directeur de recherche
Maître de conférences

LMCB, UCL
Pasteur
CBP
IGBMC
ENS de Lyon
IBMP
ENS de Lyon

Rapporteuse
Rapporteur
Examinatrice
Examinatrice
Examinateur
Examinateur
Directeur de thèse



À mon père.

Remerciements

First, I would like to thank my two rapporteurs, Yanlan Mao and Romain Levayer, who took the time to read and correct this work. More generally, I would like to extend these thanks to all the members of the jury, whose wise remarks and advice meant a lot to me both scientifically and personally.

Then, I would like to thank my colleagues and friends that accompanied me during this nearly four years adventure. First, my mentor Stéphane Vincent who pushed me to always think outside of the box, thus leading to the production of this work rethinking entirely the late morphogenesis of drosophila, despite having being studied for decades prior to my arrival in the lab. Then, Muriel Grammont, Stève De Bosoreille and Megha Jacob, my team members, whose counseling, ideas and advice helped me shape my experiments and my comprehension of the morphogenesis field. Moreover, I cannot forgot to thank thoroughly the PLATIM team, and especially Claire Lionnet and Elodie Chatre, who helped me to master the rather capricious spinning disk microscope at the origin of the entirety of the microscopy images and movies used for this work. Finally, even if they were not directly implicated in my project, I want to thank my friends from the other teams of the M4 ground floor whose support has been crucial for the accomplishment of this project.

Comme une bonne partie des personnes que je vais désormais remercier ne sont pas anglophones, je choisis d'écrire la suite de ce texte en français. S'il y a une certitude que j'ai, c'est qu'en aucun cas je n'aurais pu réussir l'épreuve qu'a représenté

cette thèse sans mes proches. Je n'aurai pas la place de les remercier tous ici, et je ne suis de toute façon pas extrêmement doué dans cet exercice. Je tiens tout d'abord à remercier mes amis. Être chercheur c'est risquer en permanence d'être submergé par sa propre recherche et les nombreuses suites d'échecs qui l'accompagnent. Votre présence m'aura permis au cours de ces années de garder un ancrage dans la réalité, une réalité bien plus positive et pleine d'aventure que ma lutte pour la compréhension des déformations cellulaires des embryons de mouches. Vous êtes pour moi une source d'inspiration, ce qui m'a permis de garder le pied à l'étrier face aux doutes les plus renversants. De plus, la plupart des idées à l'origine de mes découvertes émergent de discussions que j'ai eues avec vous, de manière volontaire ou non, dans tous types de lieux et situations allant de bureaux de laboratoires aux débits de boisson les plus insolites ou en passant par des paysages des plus grandioses.

Enfin, ma famille. Maman, Florian, ces années auront été éprouvantes pour chacun d'entre nous mais c'est grâce à vous que j'ai pu les surmonter. Je suis et resterai extrêmement heureux de pouvoir compter sur vous, tout comme du fait que vous pouvez compter sur moi.

Enfin, Papa. Devenir biologiste était ton rêve, et tu m'as élevé dans l'amour et la curiosité envers ce monde fascinant. Sans toi, jamais je n'aurais réalisé le parcours qui m'a mené jusqu'ici, et j'aurais aimé que tu sois là pour le voir. Cette thèse, et tout mon travail de recherche, est pour toi.

Summary

Dorsal closure and head involution are among the last major events in the morphogenesis of the *Drosophila melanogaster* embryo, taking place during stages 13 to 15. During dorsal closure, the cells of the dorsal epidermis elongate until they fuse with their counterparts on the dorsal midline, pulled by an extra-embryonic tissue: the amnioserosa. At the same time, the dorsal epidermis of the thoracic segments, having just fused, covers the head of the embryo: that is the head involution. I dedicated this thesis to the understanding of the morphogenetic processes at the origin of these two phenomena and to their regulation by two signaling pathways: JNK and DPP (the TGF β homolog in *D. melanogaster*).

First, I unravel and clarify the distinct roles of each of these two signaling pathways for dorsal closure. Indeed, embryos mutated for components of the JNK or DPP pathway fail to achieve dorsal closure and undergo a fatal evisceration marking the failure of their development. I identify that DPP defines the domain and the contractile activity of the amnioserosa early in embryogenesis, during stages 5-7. DPP then determines the dorsal epidermis, to which it confers visco-plastic properties during stage 9, long before dorsal closure. This property proves crucial for the epidermis to reach the required size without the traction provided by the amnioserosa varying over time. Finally, I describe how JNK and DPP act in concert to ensure cohesion between the amnioserosa and the dorsal epidermis from stage 11 until the end of dorsal closure. I then identify that it is the loss of this adhesion that is responsible for the common evisceration of mutants of each of these signaling pathways.

Second, I clarify the role of apoptosis in the evisceration of DPP mutants. Indeed,

until now, it was supposed that in the absence of the DPP pathway, the activation of the JNK pathway in the dorsal epidermis cells would provoke their death. Thus, it would be this episode of cell death that would be at the origin of the evisceration of these mutants. However, I demonstrate here that in these mutants the cells of the dorsal epidermis do not die by apoptosis and that apoptosis has no role in their evisceration.

In a third step, I identify the role of internal organ morphogenesis in the evisceration of DPP mutants. I demonstrate that it is the involution of the head coupled with the closure of the midgut and the migration of the hindgut that is responsible for the evisceration rather than the traction performed by the amnioserosa. I also observe that defects in the morphogenesis of internal organs in these mutants contribute to the precocity of evisceration without being solely responsible.

Finally, I identify how a subpopulation of cells from the head epidermis participate in the migration of the thoracic epidermis over it. These cells are organized in two bands located laterally on either side of the head epidermis. During head involution, these two bands contract thanks to the intercalation of their cells as well as the reduction of their apical area. Thus, these bands act as suspenders pulling on the thoracic epidermis via the dorsal ridge. Concomitantly, the dorsal ridge also contracts and acts as a belt to synchronize the migration of the thoracic epidermis over the head. Altogether, this work demonstrates that the role of the DPP pathway in the regulation of late epidermal morphogenesis in the *Drosophila* embryo originates much earlier than previously thought. It also sheds light on the crucial role of inter-organ cooperation during this process.

Résumé

La fermeture dorsale et l'involution de la tête sont parmi les derniers événements majeurs de la morphogénèse de l'embryon de *Drosophila melanogaster*, se déroulant lors des stades 13 à 15 de celle-ci. Lors de la fermeture dorsale, les cellules de l'épiderme dorsal s'allongent jusqu'à fusionner avec leurs semblables sur la ligne médiane dorsale, tractées par un tissu extra-embryonnaire: l'amnioséreuse. Au même moment, l'épiderme dorsal des segments thoraciques, venant tout juste de fusionner, recouvre la tête de l'embryon: c'est l'involution de la tête. J'ai consacré ce travail de thèse à la compréhension des procédés morphogénétiques à l'origine de ces deux phénomènes ainsi qu'à leur régulation par deux voies de signalisation: JNK et DPP (l'homologue des $TGF\beta$ chez *D. melanogaster*).

Dans un premier temps, je décortique et précise les rôles distincts de chacune de ces deux voies de signalisation pour la fermeture dorsale. En effet, les embryons mutés pour des composants de la voie JNK ou DPP ne parviennent pas à réaliser la fermeture dorsale et subissent une éviscération fatale marquant l'échec de leur développement. J'identifie ainsi que DPP définit le domaine ainsi que l'activité contractile de l'amnioséreuse précocement chez l'embryon, lors des stades 5 à 7. DPP détermine ensuite l'épiderme dorsal et lui confère des propriétés visco-plastiques lors du stade 9, bien avant la fermeture dorsale. Cette propriété s'avère cruciale pour que l'épiderme puisse atteindre la taille requise sans que la traction fournie par l'amnioséreuse ne varie au cours du temps. Enfin, je décris comment JNK et DPP agissent de concert pour assurer la cohésion entre l'amnioséreuse et l'épiderme dorsal, du stade 11 jusqu'à la fin de la fermeture dorsale. J'identifie alors que c'est

la perte de cette adhésion qui est à l'origine de l'éviscération commune des mutants de chacune de ces voies de signalisation.

Dans un second temps j'éclaircis le rôle de l'apoptose quant à l'éviscération des mutants de la voie DPP. En effet jusqu'alors, il était supposé qu'en l'absence de la voie DPP l'activation de la voie JNK dans les cellules de l'épiderme dorsal leur serait fatale. Ainsi, ce serait cet épisode de mort cellulaire qui serait à l'origine de l'éviscération de ces mutants. Néanmoins, je démontre ici que chez ces mutants les cellules de l'épiderme dorsal ne meurent pas par apoptose et que celle-ci n'a par ailleurs aucun rôle dans leur éviscération.

Dans un troisième temps, j'identifie le rôle de la morphogénèse des organes internes dans l'éviscération des mutants de la voie DPP. Je démontre que c'est l'involution de la tête couplée à la fermeture de l'intestin moyen et à la migration du gros intestin qui en est responsable, et non la traction réalisée par l'amnioséreuse. J'observe également que les défauts de morphogénèse des organes internes dans ces mutants contribuent à la précocité de l'éviscération sans pour autant en être les seuls responsables.

Finalement, j'identifie comment une sous population de cellules de l'épiderme de la tête participe à la migration de l'épiderme thoracique par dessus celui-ci. Ces cellules sont organisées en deux bandes situées latéralement de part et d'autre de l'épiderme de la tête. Lors de l'involution de la tête, ces deux bandes se contractent grâce à l'intercalation de leurs cellules ainsi qu'à la réduction de leur aire apicale. Ainsi, ces bandes agissent telles des bretelles tirant sur l'épiderme thoracique via la crête dorsale. Celle-ci, se contractant également, agit comme une ceinture permettant la synchronisation de la migration de l'épiderme thoracique par dessus la tête. Ainsi, ce travail permet de démontrer que le rôle de la voie DPP dans la régulation de la morphogénèse tardive de l'épiderme de l'embryon de drosophile puise son origine bien plus précocement que ce qui était pensé jusqu'alors. Il permet également d'éclairer le rôle crucial de la coopération entre organes lors de celle-ci.

Contents

Remerciements	5
Summary	7
Contents	11
List of Figures	17
I Introduction	21
I) Morphogenesis	21
A) Definition and history of the morphogenesis field	21
B) The morphogenesis toolbox	24
a) Morphogenesis through variation of cell shape	24
b) Morphogenesis through changes in cell position	26
i) Morphogenesis through cell migration	26
ii) Morphogenesis through cell contact reorga- nization	28
c) Morphogenesis through variation of cell number	29
i) Morphogenesis through oriented cell division	29
ii) Morphogenesis through localized cell death	29
C) The control of morphogenesis	31
a) Spatio-temporal patterning of morphogenesis through molecular signaling	31

i)	From self-organization to tissue communication during patterning and morphogenesis	31
ii)	From signaling to morphogenesis	32
b)	Physical forces are both required and produced by the tissues that change shape	33
i)	Cellular forces required for morphogenesis	34
ii)	Biological tissues behavior in response to forces	36
iii)	Forces and signals generated by tissues undergoing morphogenesis	37
II)	The early morphogenesis of <i>D. melanogaster</i>	39
A)	From zygote to cellularized embryo	40
B)	The gastrulation and concomitant morphogenetic events	42
a)	Formation of the mesoderm	42
i)	Patterning of the mesoderm	42
ii)	The invagination, detachment and spreading of the mesoderm	43
b)	The endoderm	45
c)	Morphogenesis of the ectoderm during gastrulation	47
C)	Germband extension and nervous system emergence	49
a)	The germband extension	49
b)	Central nervous system morphogenesis	51
D)	Germband retraction	54
III)	The Dorsal closure of <i>D. melanogaster</i>	56
A)	Internal organs morphogenesis during dorsal closure	57
a)	The midgut and hindgut	57
b)	The mesoderm derived tissues	59
c)	Tracheal dorsal branch morphogenesis	61

<i>CONTENTS</i>	13
B) The Dorsal closure process	63
a) Dorsal Closure morphogenesis	63
i) Dorsal Closure initiation	63
ii) Dorsal Closure onset	64
iii) The Dorsal Closure zipping phase	66
b) Physical cues during dorsal closure	68
i) Traction from the amnioserosa	68
ii) Forces generated by the zipping process	69
iii) The actin cable	69
iv) Dorsal epidermis resistance	70
v) Forces transmission during dorsal closure	71
c) Signaling during dorsal closure	71
i) The JNK and DPP cascades	71
ii) Spatio-temporal activity of the JNK and DPP pathway during dorsal closure	73
iii) The dorsal-open phenotype and JNK/DPP target genes during dorsal closure	76
C) Head involution	78
a) Morphogenesis during head involution	78
b) Physical cues during head involution	80
c) Signaling during head-involution	80
II Results	83
I) DPP signaling and morphogenesis potential	83
II) DPP signaling and apoptosis during dorsal closure	104
A) <i>rpr</i> induction in the dorsal epidermis induces apoptosis events invisible in <i>tkv</i> mutants	106
B) JNK+ leading-edge cells do not undergo apoptosis during dor- sal closure in <i>tkv</i> mutants	108

C)	Apoptosis is not involved in the <i>tkv</i> mutant evisceration phenotype	110
III)	Evisceration and internal organ morphogenesis	113
A)	Internal organ rather than amnioserosa contraction induces evisceration of <i>tkv</i> mutants	114
B)	Both heart and midgut morphogenesis are affected in <i>tkv</i> mutants	116
C)	Impairment of DPP signaling in both the dorsal epidermis and the internal organs increases the risks of evisceration	119
D)	Rescue of internal organ morphogenesis delays evisceration in <i>tkv</i> mutants	122
IV)	Suspender cells and head-involution	124
A)	Head-involution initiation does not require dorsal ridge or dorsal closure in <i>tkv</i> mutants	125
B)	The contraction of a stripe of head epidermis cells tracts the dorsal ridge towards the anterior of the embryo	127
C)	Contraction of a supra cellular actin web is associated with cellular contraction and convergent extension in the head epidermis	131
III Discussion		135
I)	A fresh look on the dorsal closure process	136
A)	The dorsal closure fails after its initiation in dorsal-open embryos	136
B)	DPP and JNK cooperate during dorsal closure while assuming non-overlapping functions	138
a)	Early DPP signaling determines the properties of dorsal closure actors	138
b)	DPP signaling turns the dorsal epidermis from a visco-elastic into a visco-plastic tissue	140
c)	JNK signaling: the wound-healer	143

d)	DPP and JNK signaling cooperate to promote dorsal epidermis/amnioserosa adhesion	144
C)	Is dorsal closure a great model for wound-healing?	147
II)	Inter-organ cooperation & epidermis morphogenesis	150
A)	Amnioserosa and Suspender cells: the motors of dorsal epidermis morphogenesis	150
B)	The dorsal epidermis is directionally predetermined for massive morphological changes	151
C)	The synchronization of independent motors	153

IV Material and Methods 155

I)	Fly stocks	155
A)	Gal4 lines	155
B)	UAS lines	156
C)	Mutant lines	156
D)	Lines used as live-markers	157
E)	Additional stable lines from combination of the previous lines	158
II)	Live microscopy and image analysis	159
A)	Embryo collection and preparation for live microscopy	159
B)	Spinning disk microscopy	160
a)	Spinning disk specifications	160
b)	Imaging and laser ablation	162
C)	Image analysis	162
III)	Statistical analysis and model fitting	164
A)	Statistical analysis	164
B)	Model fitting for speed extraction	164
IV)	Modelling the physical behavior of the dorsal epidermis	167
A)	Building of the visco-plastic model	167
B)	Stress estimation using laser ablation	169
C)	Stretching time estimation using laser ablation	171

Bibliography

173

List of Figures

I.1	Ernst Haeckel, Wilhelm His and Wilhelm Roux	21
I.2	Morphogenesis through variation of cell shape	25
I.3	Morphogenesis through cell migration	27
I.4	Convergent extension drives tissue elongation	28
I.5	Oriented cell division as a driver of morphogenesis	29
I.6	Localized cell death finalizes digit morphogenesis	30
I.7	SHH and VEGF signaling during dorsal aorta morphogenesis of <i>D. rerio</i>	33
I.8	Morphogenetic processes interact through forces or signal transmission	37
I.9	Morphogenesis of the early syncytial embryo	40
I.10	Surface microvilli as a membrane reservoir for cellularization	42
I.11	Mesoderm morphogenesis during gastrulation	44
I.12	Anterior and Posterior Midgut invagination during gastrulation	45
I.13	Ectoderm folding during gastrulation	47
I.14	Germband extension at the embryo and cellular scale	49
I.15	Germband retraction at the embryo and cellular scale	54
I.16	Midgut and hindgut morphogenesis during dorsal closure	58
I.17	Somatic musculature morphogenesis during dorsal closure	60
I.18	Tracheal dorsal branch morphogenesis	61
I.19	Dorsal Closure initiation	63
I.20	Amnioserosa morphogenesis during dorsal closure	64

I.21	Leading edge cells produce a supra-cellular acto-myosin cable and filopodia	65
I.22	The Dorsal Closure zipping phase	66
I.23	Contralateral fusion at the canthus is initiated by filopodia	67
I.24	DPP and JNK signaling during <i>D. melanogaster</i> embryogenesis . . .	74
I.25	Dorsal view of the head involution process	79
II.1	The leading-edge is supposed to undergo JNK induced apoptosis . . .	104
II.2	<i>rpr</i> induction in the <i>pnr</i> domain does not phenocopy <i>tkv</i> mutants . .	107
II.3	JNK+ cells of <i>tkv</i> mutants do not undergo apoptosis during dorsal closure	108
II.4	Preventing apoptosis does not rescue <i>tkv</i> mutants	111
II.5	Internal organ rather than amnioserosa contraction induces evisceration of <i>tkv</i> mutants	114
II.6	Both heart and midgut morphogenesis are affected in <i>tkv</i> mutants . .	117
II.7	Impairment of DPP signaling in both the dorsal epidermis and the internal organs increases the risks of evisceration	120
II.8	Rescue of internal organ morphogenesis delays evisceration of <i>tkv</i> mutants	123
II.9	Head-involution initiation does not require dorsal ridge or dorsal closure in <i>tkv</i> mutants	125
II.10	The contraction of a stripe of head epidermis cells tracts the dorsal ridge towards the anterior of the embryo	128
II.11	Contraction of a supra-cellular actin web is associated with cellular contraction and convergent extension in the head epidermis	132
III.1	3 waves of DPP signaling define tissue properties required for Dorsal Closure	146
III.2	Inter-organ cooperation in epidermis morphogenesis during late <i>D. melanogaster</i> embryogenesis	154

IV.1 Embryo collection and preparation 159

IV.2 The PLATIM home-built spinning-disk microscope 161

IV.3 The simplified visco-plastic model 167

IV.4 The output of the model 169

IV.5 Simulation of the stretching and relaxation of a visco-elastic tissue
undergoing laser ablation 171

Chapter I

Introduction

I) Morphogenesis

A) Definition and history of the morphogenesis field

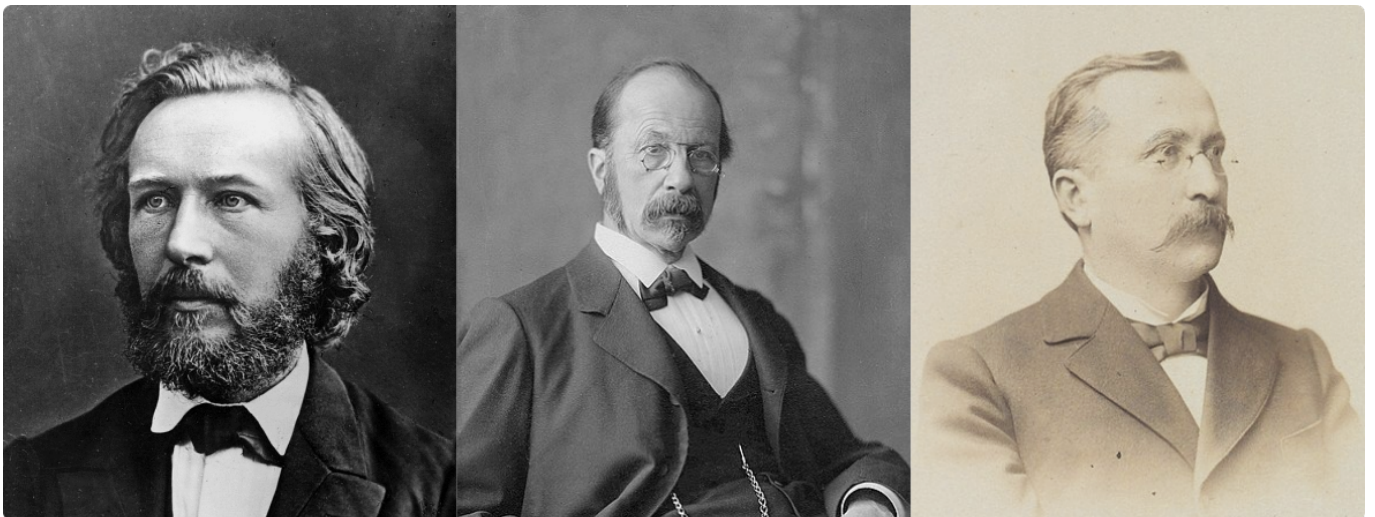


Figure I.1: Ernst Haeckel, Wilhelm His and Wilhelm Roux: pictures from wikipedia.org

The term "morphogenesis" stems from the compaction of two Greek words: *morphê*, the form, and *genesis*, the creation. Meaning literally the generation of form, it is today the part of the developmental biology field that focuses on how multi-cellular organisms, animals and plants, or large unicellular organisms acquire their shape. Morphogenesis can occur in a variety of situations: during organism

development such as the continuous formation of new leaves on a tropical tree for example. It can also be mobilized in a specific time-window during regeneration, for example when a crab regrows a leg that got severed. However, in the animal kingdom, the vast majority of morphogenetic events occurs during either embryogenesis -the development from a zygote to a juvenile organism- or metamorphosis that is the transition from the larval to the adult stage. Hence, the study of morphogenesis is intrinsically bound to the study of embryology.

The field of embryology arose in the 19th century, in Germany, when Wilhelm Roux -seen in Figure I.1- proposed the concept of *Entwicklungsmechanik*. *Entwicklungsmechanik* can be translated literally as "developmental mechanics" [Maienschein, 1991]. German embryologists at the time, led by Ernst Haeckel (Figure I.1), thought of the embryo only as a tool to study phylogeny. Their claim was motivated by the fact that ontogeny closely relates to phylogeny. Hence, they believed that early developmental events had little to no influence on the final form of an organism [Acot et al., 1998]. Wilhelm His -seen in Figure I.1- was the first scientist to challenge this theory which he deemed unfounded. He declared that embryos should be studied as physical objects and that the mechanical aspect was crucial during development. Although he could not prove his point, his assumptions justified the use of an experimental approach to study embryogenesis that inspired German scientists for the next decades. Wilhelm Roux, ironically a student of Ernst Haeckel, was one of them. He hypothesized that each cell of a developing embryo is able to develop independently. Instead of making its point by observation only, he used an experimental approach. He burnt one blastomere of 2-cell stage frog embryos and observed that the remaining blastomere continued to develop for some time but failed to form a fully grown tadpole. Therefore he concluded that all cells develop in a predetermined manner [Roux, 1888]. We know today that his interpretation was wrong and that the failure of development he observed was caused by the interference of the burnt blastomere still attached to the embryo. However his result showed to the scientific community the necessity and importance of conducting experiments

to understand development.

This way of conducting developmental biology studies, by combining careful observation of organism development to elaborate hypothesis and to propose experiments to assess them, is still applied today and led to all the major discoveries on morphogenesis regulation.

B) The morphogenesis toolbox

Living tissues are composed of a multitude of smaller units: their cells. The main realization of the last decades is that tissue shape modifications rely on specific cellular behaviours. Cells can change their own shape, position -through migration or rearrangement- or their number -through division, delamination or cell death. In the following section I will describe examples on how those cellular mechanisms contribute to morphogenesis at the tissue scale

a) Morphogenesis through variation of cell shape

Cells are biological units that can modify their own shape and influence the global geometry of a tissue. These alterations can generate variations of tissue properties such as thickness, size or folding.

If all the cells of a tissue change their thickness, so will the thickness of the tissue itself. An example of this phenomenon can be observed during *D. melanogaster* oogenesis (Figure I.2 A). The *D. melanogaster* egg chamber is composed of an epithelium, the follicular cells, surrounding the germline that is the nurse cells and the oocyte. Its development includes 14 distinct stages [Deng and Bownes, 1998]. From stages 8 to 10, follicular cells undergo major changes in shape. At stage 8, follicular cells form a cuboidal epithelium. However, from this stage, follicular cells in contact with the nurse cells flatten and become squamous whereas follicular cells in contact with the oocyte become columnar [Kolahi et al., 2009]. Therefore, two homogeneous changes of cell shape produce two distinct shape of epithelia: one thin anterior squamous follicular epithelium and one thick posterior follicular epithelium. Cell elongation in a particular direction can also drive the elongation of the tissue in the same direction. It is the case of plant roots: at the tip of the root, a population of dividing cells form the root apical meristem, thus producing cells entering the extension zone. Cells in the extension zone then elongate in a polarized manner, hence driving the elongation of the whole root [Gregory, 2006] (Figure I.2 B).

A striking example of how cell shape changes can impact the global geometry of

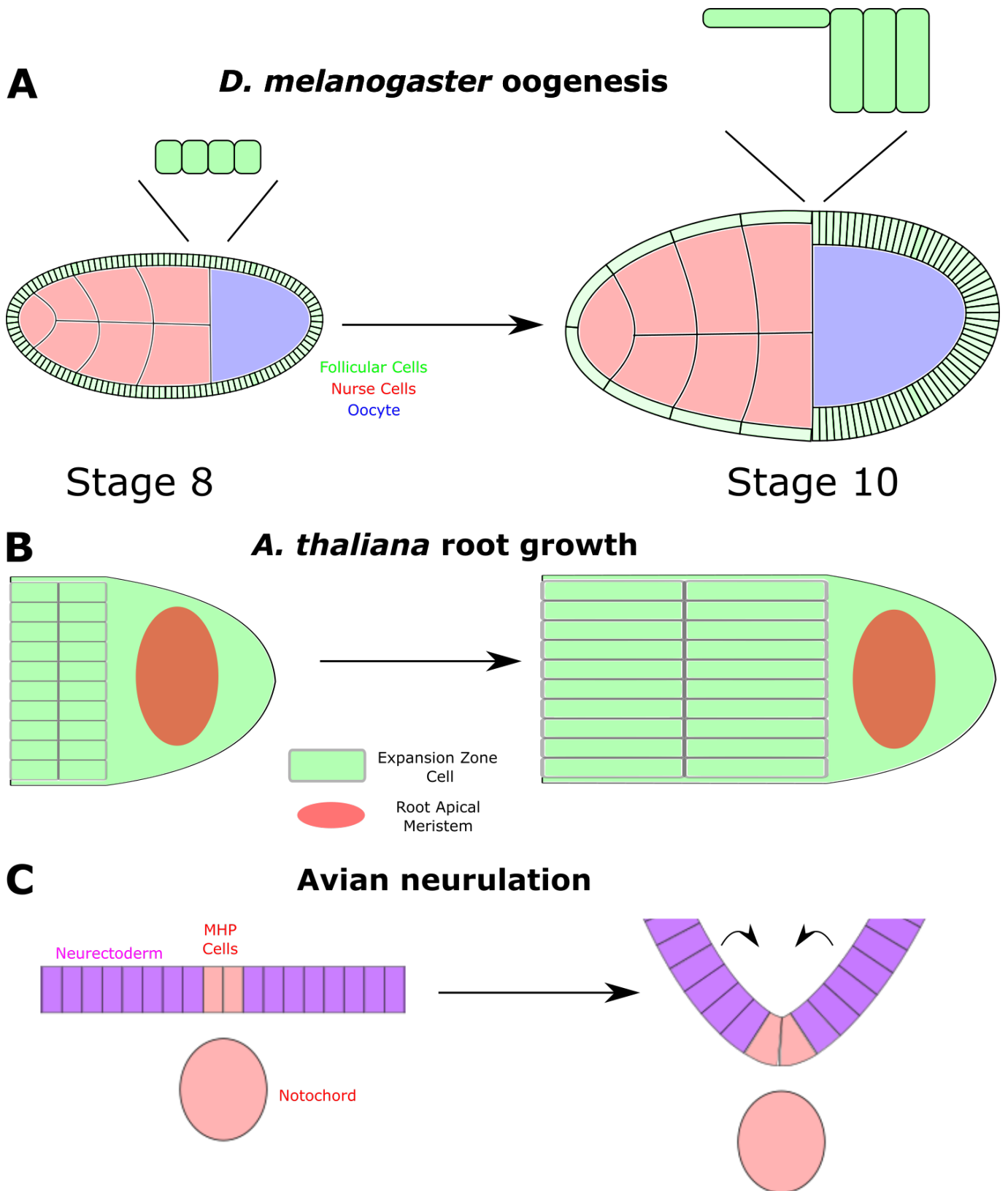


Figure I.2: Morphogenesis through variation of cell shape: **A:** *D. melanogaster* oogenesis from stage 8 to 10, follicular cells that undergo cell shape changes are shown in green, nurse cells in red and the oocyte in blue. **B:** *A. thaliana* root growth. The outline of the cells of the elongation zone is displayed. **C:** Avian neurulation, Medial Hinge Point (MHP) cells that undergo deformation are displayed in red as the notochord with which they share a common origin, neuroectoderm cells are displayed in magenta.

a tissue occurs during avian neurulation (Figure I.2 C). Prior to neurulation, the neural plate, the tissue that will later form the central nervous system, is a flat structure. Its bending relies on a subset of cells from mesodermal origin, fixed to the notochord [Catala et al., 1996]. These cells constrict their apical side, slightly invaginate, and hence act as a hinge during the bending of the whole neural plate [Schoenwolf and Franks, 1984, Schoenwolf and Smith, 1990]. These Medial Hinge Point cells do not generate the forces responsible for the bending of the neural plate alone, but rather determine the location where the tissue folds. Moreover, their change of cell shape prevents the neural plate from tearing, just as a brittle material would do as it is bent [Smith and Schoenwolf, 1991].

b) Morphogenesis through changes in cell position

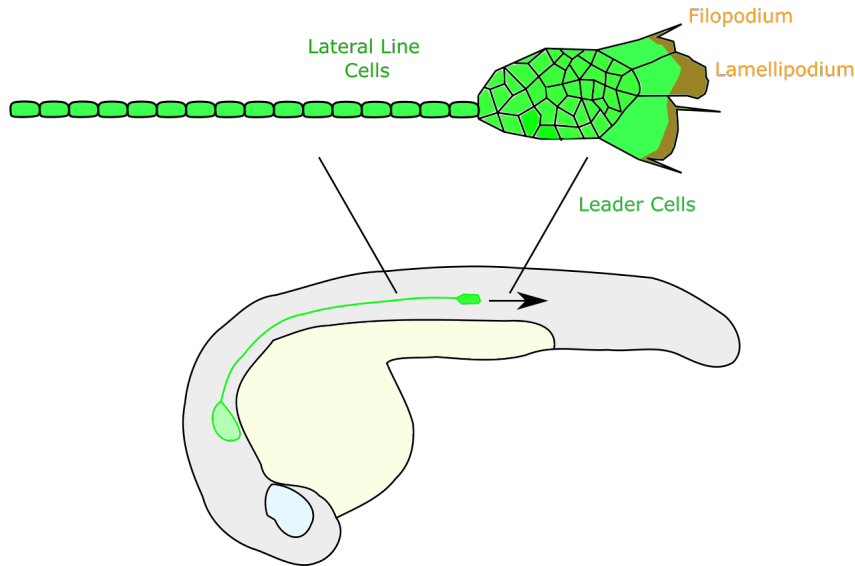
Cells use two main strategies to change their position: through migration or neighbor re-arrangements. Both contribute to tissue morphogenesis as shown by the next examples.

i) Morphogenesis through cell migration

Cell-migration is either collective or individual. For example in the zebrafish *D. rerio*, the shape of the lateral line relies on collective cell migration of its primordium (Figure I.3 A). The lateral line is a sensory organ that allows fish and amphibians to sense the movements of water in an aquatic environment and corresponds to the inner ear of terrestrial tetrapods [Ghyssen and Dambly-Chaudière, 2004]. As suggested by its name, the lateral line is a linear sensory organ that connects the zebrafish inner-ear to the caudal most area. The primordium collectively migrates from the otic vesicle of the developing zebrafish embryo to its caudal extremity. The migration front is composed of leader cells that display large lamellipodia and filopodia and that drag epithelial-like follower cells that deposit the connected neuromasts [Haas and Gilmour, 2006].

On the other hand, the development of the zebrafish dorsal aorta involves individual cell migration (Figure I.3 B). Cells that will form the dorsal aorta originate from

A: *D. rerio* lateral line morphogenesis



B: *D. rerio* dorsal aorta morphogenesis

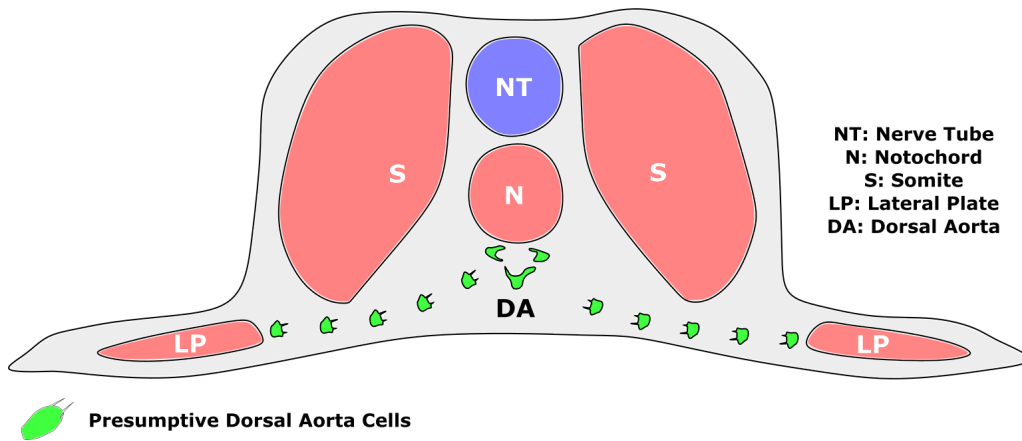


Figure I.3: Morphogenesis through cell migration: **A:** Collective cell migration at the origin of the *D. rerio* lateral line. Lateral Line cells are shown in green, filopodia and lamellipodia are highlighted in orange within the leader cells. **B:** Individual cell migration at the origin of *D. rerio* dorsal aorta, Mesoderm derived tissues are displayed in red, the neural tube is shown in blue. Migrating presumptive dorsal aorta cells are shown in green.

the lateral plate mesoderm [Torres-Vázquez et al., 2003]. These cells detach from the lateral plate mesoderm through an epithelial to mesenchymal transition process (EMT) [Poole et al., 2001]. These cells then migrate individually to the midline, right under the embryo notochord, where they aggregate and form the dorsal aorta [Jin et al., 2005], thus determining the localization and elongated shape of the dorsal aorta.

ii) Morphogenesis through cell contact reorganization

Modification in the geometry of junctions can have dramatic effects on morpho-

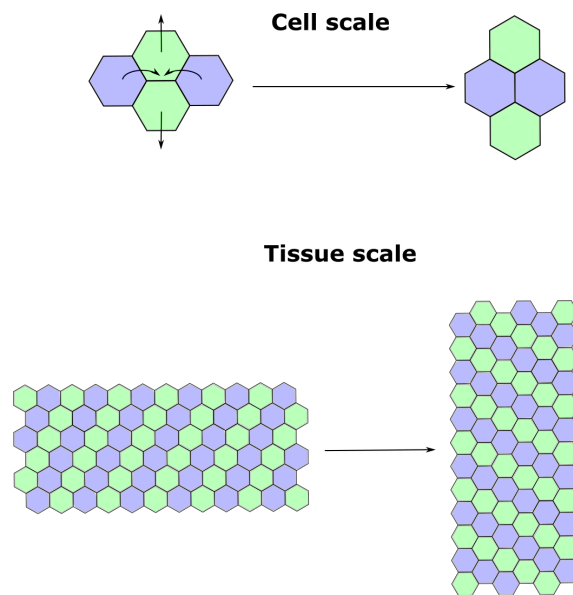


Figure I.4: Convergent extension drives tissue elongation: Example of four cells undergoing rearrangements that drives elongation of the vertical axis. Consequences of such convergent extension events at the tissue scale.

genesis, as in the development of the neural plate of the xenopus (*X. laevis*) embryo [Keller et al., 1992]. The elongated shape of the neural plate emerges through cell contact rearrangements known as convergent extension (Figure I.4). Neural-plate cells progressively intercalate in the midline direction. Hence, the length of the tissue in the midline increases as its width decreases. Therefore, changes in cell position directly contribute to the elongated shape of the neural plate.

c) Morphogenesis through variation of cell number

Variations of cell number at specific locations within a tissue, either by addition or removal, can impact both its size and its shape.

i) Morphogenesis through oriented cell division

The orientation of cell division can remodel the shape of a tissue. For example, it

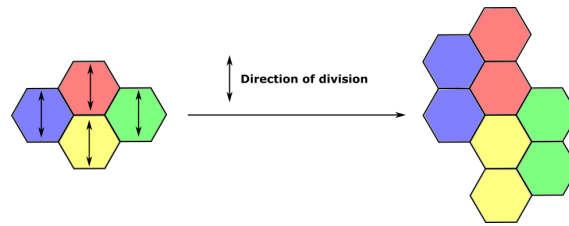


Figure I.5: Oriented cell division as a driver of morphogenesis: Restriction of cell division to the vertical axis drives the elongation of the tissue in this direction.

can drive the elongation of a tissue when coordinated in a single direction (Figure I.5). Indeed, oriented cell division has also been shown to be important for neural plate morphogenesis, in addition of convergent-extension. In the development of the avian neural plate, the neuroectoderm cells of the neural plate divide along the midline axis, therefore contributing to the elongation of the tissue. Further, the surrounding epidermal cells also divide in a stereotyped manner, either in parallel or perpendicular to the midline axis. This drives the growth of the epidermis both along and towards the midline [Sausedo et al., 1997].

ii) Morphogenesis through localized cell death

Selectively removing cells from a tissue can produce the emergence of new shapes. This is the case in vertebrate digits morphogenesis (Figure I.6). At the onset of its development, the limb bud grows as a rod-like structure perpendicular to the midline of the embryo's trunk. However, the branch-like structure of the digits, at the end of the bud, do not form by ectopic growth from the presumptive digits base. In fact, the digit emerge from the limb bud as cells localized in the interdigit necrotic zone undergo synchronized cell death [Montero and Hurlé, 2010]. The remaining cells

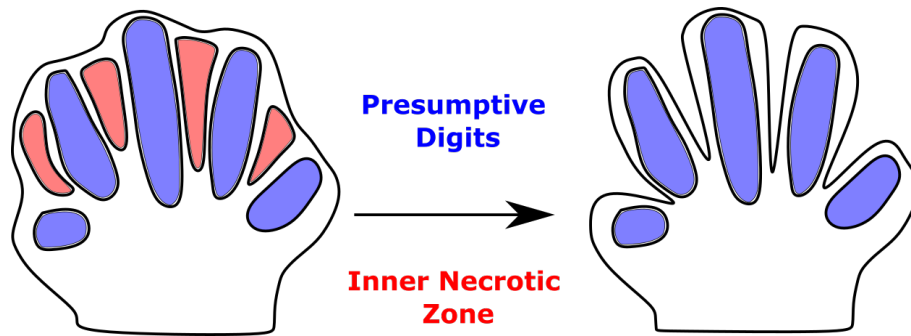


Figure I.6: Localized cell death finalizes digit morphogenesis Cell death in the Inner Necrotic Zone (in red) drives the individualization of the digits (in blue).

outside the Inner Necrotic Zone then continue their development, hence forming the final digits of the animal.

C) The control of morphogenesis

In the previous part, I discussed the different cellular mechanisms that contribute to morphogenesis. As His foresaw in the 19th century, mechanical forces are necessary to produce shape changes observed during morphogenesis. However, one might wonder how they originate. In this part I will discuss the critical role of molecular signals in the control of the sub-cellular forces at the origin of morphogenesis and their complex interaction at the tissue scale.

a) Spatio-temporal patterning of morphogenesis through molecular signaling

i) From self-organization to tissue communication during patterning and morphogenesis

I already described how morphogenesis results from the active behavior of cells within a tissue. The origin of such changes has long been a mystery. According to W. Roux, the answer relies in a hard-rooted program contained within each cell [Roux, 1888]. However, his conclusion would soon be contradicted. In 1891 Hans Driesch discovered that separating the two blastomeres from a 2-cell stage sea urchin embryo would give rise to two normal larvae [Driesch, 1892]. In 1895, Thomas Morgan definitely invalidated Roux's results by pipetting out one of the 2 blastomere of xenopus embryos instead of burning it, thus showing that the remaining cell could develop into a full tadpole. These experiments were crucial to prove the importance of the cellular environment during morphogenesis [Morgan, 1895]. In the early 20th century, Hans Spemann showed that it is possible to generate two newt tadpoles from one blastula cut in half only if the two parts received a portion of the blastopore lip [Spemann, 1988]. He further demonstrated the critical influence of the cellular environment by performing microsurgery. He observed that the presumptive epidermis from one species of newt would still produce forebrain tissues even if implanted into the developing forebrain of another newt species [Spemann, 1921]. Altogether, those observation led him and his student Hilde Mangold to perform transplant of

the upper lip of the blastopore, even from different newt species, in different parts of the blastula. Together, they showed that it produces an ectopic neural chord that fully develops [Spemann and Mangold, 1924]. Therefore, the environment at the origin of different morphogenetic events can be generated by the cells from the developing embryos themselves.

ii) From signaling to morphogenesis

The entity that mediates the influence of the local cell environment on morphogenesis remained a mystery for Spemann and Mangold: they even wrote in the discussion of their paper "*The causal relationships in the origin of the secondary embryonic anlage are still completely in the dark*" [Spemann and Mangold, 1924]. The gap would be filled a few years later by Conrad Hal Waddington. He hypothesized and demonstrated that cells within an organism, although sharing the same genome, would only express a subset of genes defining their identity. This gene subset would be influenced by both the intrinsic and extrinsic environment of the cell, hence linking the environment to cell identity [Waddington and Kacser, 1957].

Cell identity patterned by genetic cues directly controls morphogenesis. It is the case in the examples described so far in this introduction. During *D. melanogaster* oogenesis, the cuboidal to squamous follicular cells transition is spatially and temporally controlled by BMP signaling. The anterior follicular cells must receive the *D. melanogaster* BMP ligand DPP in order to initiate their flattening. Conversely, early exposure to BMP signaling induces a premature flattening of these cells [Brigaud et al., 2015].

During the development of the dorsal aorta of *D. rerio*, the subset of cells that differentiate into the angioblast acquire its identity from a complex interplay between *SHH* and *VEGF* signaling (Figure I.7). *SHH* expressed by the notochord stimulates *VEGF* secretion by the somites. Cells from the lateral plate mesoderm that receive *VEGF* differentiate into angioblasts and initiate their EMT-dependent migration [Lawson et al., 2002]. Moreover, it has been shown that *X. laevis* angioblasts migrate towards the midline through *VEGF* mediated chemotaxis [Clever and Krieg,

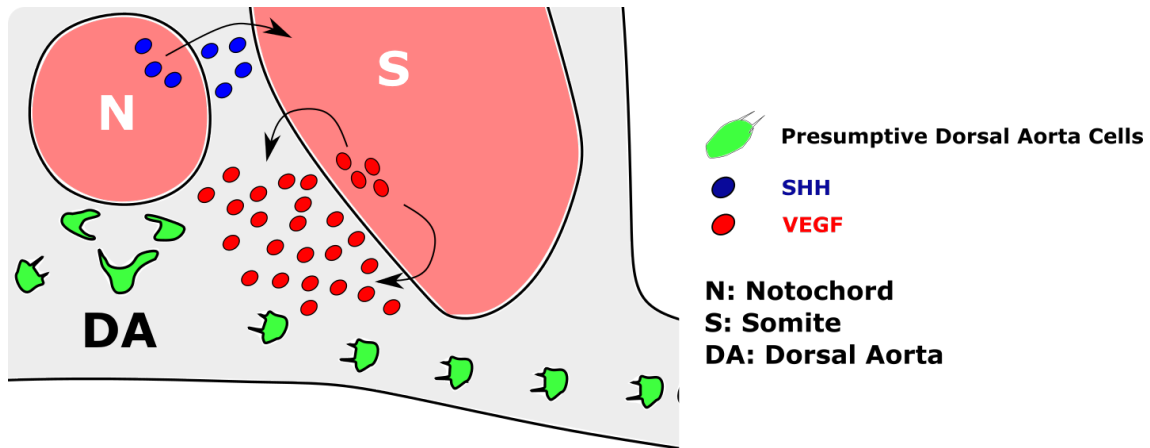


Figure I.7: SHH and VEGF signaling during dorsal aorta morphogenesis of *D. rerio*

1998]. A similar mechanism has been proposed for *D. rerio* [Lawson and Weinstein, 2002].

During limb bud morphogenesis, the cell identity between Inner Necrotic zone Cells and presumptive digit cells is determined by a Turing pattern involving *BMP*, *Sox9* and *Wnt* signaling. Both *BMP* and *Wnt* are diffusible molecules that respectively induce and repress *Sox9* expression, whereas the non diffusible *Sox9* inhibits both in return. The spatial regulation of these activities generates the pattern alternating between *Sox9* and *BMP* expressing cells that shape the digits. Cells that express *BMP* and that are able to receive *Wnt* signaling turn into the Inner Necrotic Zone cells, hence initiating the selective apoptosis required for digit morphogenesis [Raspopovic et al., 2014].

b) Physical forces are both required and produced by the tissues that change shape

Forces required for morphogenesis are first generated by the cells themselves. However, such forces can also be transmitted to neighbouring cells and tissue. Consequently, morphogenetic events and even cell identity changes can be driven by morphogenetic events occurring in other tissues.

i) Cellular forces required for morphogenesis

Cells own two major tools to exert forces on their environment: their internal cytoskeleton and the adhesion with their surroundings.

Cytoskeleton mediated forces

The two main actors of the cytoskeleton are the actin filaments and the microtubules. Both can generate forces, by polymerization or through their molecular motors.

Part of the elongation of the *D. melanogaster* wing disc relies on the elongation of its cells along the proximo-distal axis. It has been recently shown that this cell elongation relies on the polymerization of microtubules [Singh et al., 2018]. In these cells, microtubules polarized in the proximo-distal axis polymerize until they buckle onto the membrane, thus exerting a pressure on it. Thus, microtubules provide the force driving cell elongation.

Cytoskeleton polymerization can also provide forces during cell migration. In migrating cells, actin polymerizes at the front of the cells within the lamellipodia, in the direction of the movement [Gardel et al., 2010]. This polymerization has been proposed to generate the forces necessary to propel the cell, providing energy through a Brownian ratchet mechanism [Mogilner and Oster, 1996].

The coupling of the cytoskeleton to molecular motors provides a widely used force generator during morphogenesis. For example, the coupling of the actin cytoskeleton to its molecular motor, Myosin2, is used in a recurrent manner throughout morphogenesis [Murrell et al., 2015]. For example, it is involved in several morphogenesis events occurring during the neural plate folding. I described how cells at the Middle Hinge Point undergo apical constriction in order to specify the location of the neural plate folding. This process requires the recruitment of the actin-binding protein Shroom3 to their apical junctions. Shroom3 in turn recruits Rho kinases to the apical junction, which activate Myosins by phosphorylation. Activation of the myosins coupled to the actin cytoskeleton at the apical junction then generates the

traction force necessary for the apical constriction of the Middle Hinge Point cells [Nishimura and Takeichi, 2008]. The cell intercalation necessary for the neural plate elongation also requires acto-myosin generated forces. In the medio-lateral cells of the neural plate, Rho kinases are recruited to the apical junctions perpendicular to the midline through a planar cell polarity mechanism. As in the previous example, Rho kinases activate myosin at those junctions. The traction generated on the actin cytoskeleton results in the junction shortening perpendicular to the midline hence driving the convergence and intercalation of the medio-lateral cells towards it [Nishimura et al., 2012].

The role of cell adhesion on force transduction and shape maintenance

During morphogenesis, forces generated intrinsically by individual cells need to propagate to their environment in order to produce larger scale effects. The propagation of forces across epithelia has been shown to be mediated mostly by cadherin cell/cell adhesion. Particularly enriched at epithelial cells apical junctions, they link the cytoskeleton of each cell within a tissue thus forming a large continuum [Lecuit and Lenne, 2007]. In their absence, morphogenesis often fails. For example, adhesion through cadherins is required for the morphogenetic movements I described during the folding of the neural plate [Nandadasa et al., 2009]. Moreover, during the formation of the *D. rerio* lateral line, loss of cadherin expression results in the detachment of the follower cells from the leader cells hence preventing the transduction of their traction towards the posterior end of the embryo [Matsuda and Chitnis, 2010].

Cell adhesion to the extracellular matrix (ECM) also plays a role during morphogenesis. The actin cytoskeleton is coupled to the ECM via transmembrane proteins, the integrins. During cell migration the force generated by the actin cytoskeleton is transduced to the extracellular matrix via integrin-rich focal adhesions [Li et al., 2016]. Focal adhesions are assembled at the front of the migrating cell and pushed to the rear where they disassemble as the cell moves forward [De Pascalis and Etienne-Manneville, 2017]. This link between the polymerized actin and ECM induces a

treadmill motion that propels the cell forward [Jurado et al., 2005].

Cell adhesion stabilizes the shape of a tissue and must be remodeled during morphogenesis. For example, cells that undergo EMT in order to migrate out of their original tissue need to disassemble from their neighbour. This elimination of cell-cell adhesion is performed by both down-regulation and cleavage of cadherin junctions [Chu et al., 2006, Shoval et al., 2007]. Cells changing their shape also need to remodel their junctions with neighbours. For example, during *D. melanogaster* oogenesis, the flattening of the anterior follicular cells necessitates Notch-mediated apical junction remodeling as its absence leads to impaired squamous cells morphogenesis [Grammont, 2007].

ii) Biological tissues behavior in response to forces

The immediate response of living tissues to external forces is of visco-elastic nature [Desprat et al., 2005, Plotnikov et al., 2014, Bufi et al., 2015, Forgacs et al., 1998]. A visco-elastic material can be described as follows: *"A material with both viscous and elastic properties. Such a material regains its initial shape after deformation, but more slowly than a purely elastic body because of the viscous dampening."* [Molnar and Labouesse, 2021]. Hence, due to its intrinsic viscosity, a tissue takes a few minutes to adapt to external forces.

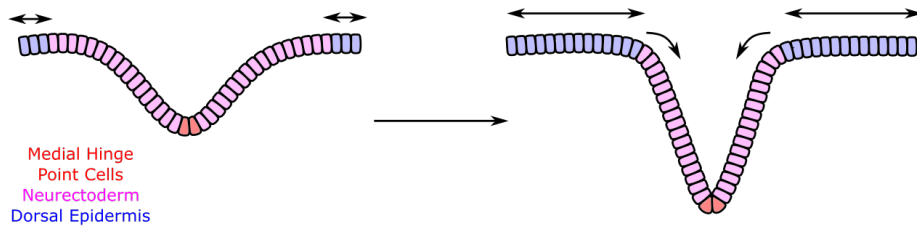
However, when external forces are applied on a longer time-scale, living tissues exhibit a different form of behavior, which is plastic. Indeed, the tissue will decrease tensions or compression by undergoing remodeling through cell division, death, extrusion or intercalation [Guillot and Lecuit, 2013]. Moreover, recent studies have underlined that plastic behavior are also exhibited at the sub-cellular scale, a phenomenon attributed to both actin and apical junctions dynamics but yet poorly understood [Clément et al., 2017, Iyer et al., 2019].

Therefore, biological tissues react differently if they are subjected to brief or long-lasting external forces. From reversible stretching to permanent deformation, they exhibit properties of both visco-elastic and visco-plastic materials.

iii) Forces and signals generated by tissues undergoing morphogenesis

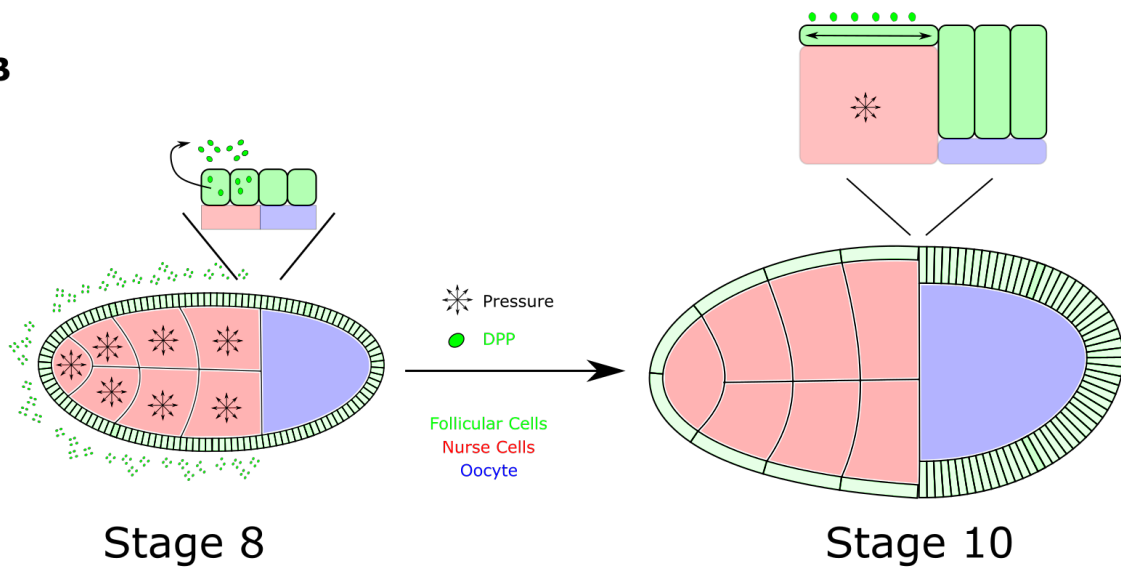
I detailed the forces provided intrinsically by the cells to fuel morphogenesis and

A



Avian Neurulation

B



***D. melanogaster* oogenesis**

Figure I.8: Morphogenetic processes interact through forces or signal transmission: A: Dorsal epidermis oriented cell division provide the compression necessary for neural plate folding. **B:** Increase in Nurse Cells pressure drives DPP expression in surrounding follicular cells, which in turn drives their flattening.

described how they can be transduced even at long distances thanks to cell contacts and adhesion. However, in some situations, the forces required for the morphogenesis of a tissue can also be provided by the morphogenesis of the adjacent tissues. A compelling illustration comes again from the morphogenesis of the avian neural plate (Figure I.8). I described in previous sections how the apical constrictions of Middle

Hinge Plate cells directs the neural plate folding but mentioned that the force they generate cannot bend the plate by itself. However, I also mentioned how oriented cell divisions drive the expansion of the neighboring dorsal epidermis in the direction of the midline. As the epidermis expands towards the midline, it exerts pressure from both sides of the neural plate. This source of energy coming from both sides of the neural plate induces the bending at the Middle Hinge Point, which in return leads to the dorsal expansion of the epidermis [Sausedo et al., 1997]. Thus, two distinct morphogenetic events from two distinct tissues are dependent from each-other and share forces.

Productive interactions between morphogenetic processes can also be mediated by juxtacrine signaling. I described in previous sections the importance of the $TGF\beta$ pathway for the ovary anterior follicular cells flattening in *D. melanogaster*. It has recently been shown that $TGF\beta$ activation in the follicular cells directly depends on the growth of the nurse cells underneath. As nurse cells grow, they exert pressure on the overlying follicular epidermis. In response, the follicular cells turn in their $TGF\beta$ pathway on, thus inducing their differentiation followed by their cuboidal to squamous transition [Lamiré et al., 2020] (Figure I.8). Hence, morphogenetic events can both depend and influence diffusible signals, thus allowing their coordination.

II) The early morphogenesis of *D. melanogaster*

Since initial studies by Thomas Hunt Morgan, *D. melanogaster* has become a powerful model organism, especially for embryogenesis. *D. melanogaster* is easy and cheap to breed. Its generation time is short, only 10 days. Moreover, a female can lay over 1500 eggs during its life. The embryos produced are small and fully develop in about 24 hours, thus making them ideal subjects for microscopical observations. Furthermore, the extensive study and manipulation of their genetics led to the building of a plethora of genetic tools that allows deeper and deeper understanding of their development. In this section, I will depict the main morphogenetic events of the early embryogenesis of *D. melanogaster*. From the zygote to the stage 13 embryo, *D. melanogaster* embryogenesis is a sequence of sometimes simultaneous morphogenetic processes as defined in the first section.

A) From zygote to cellularized embryo

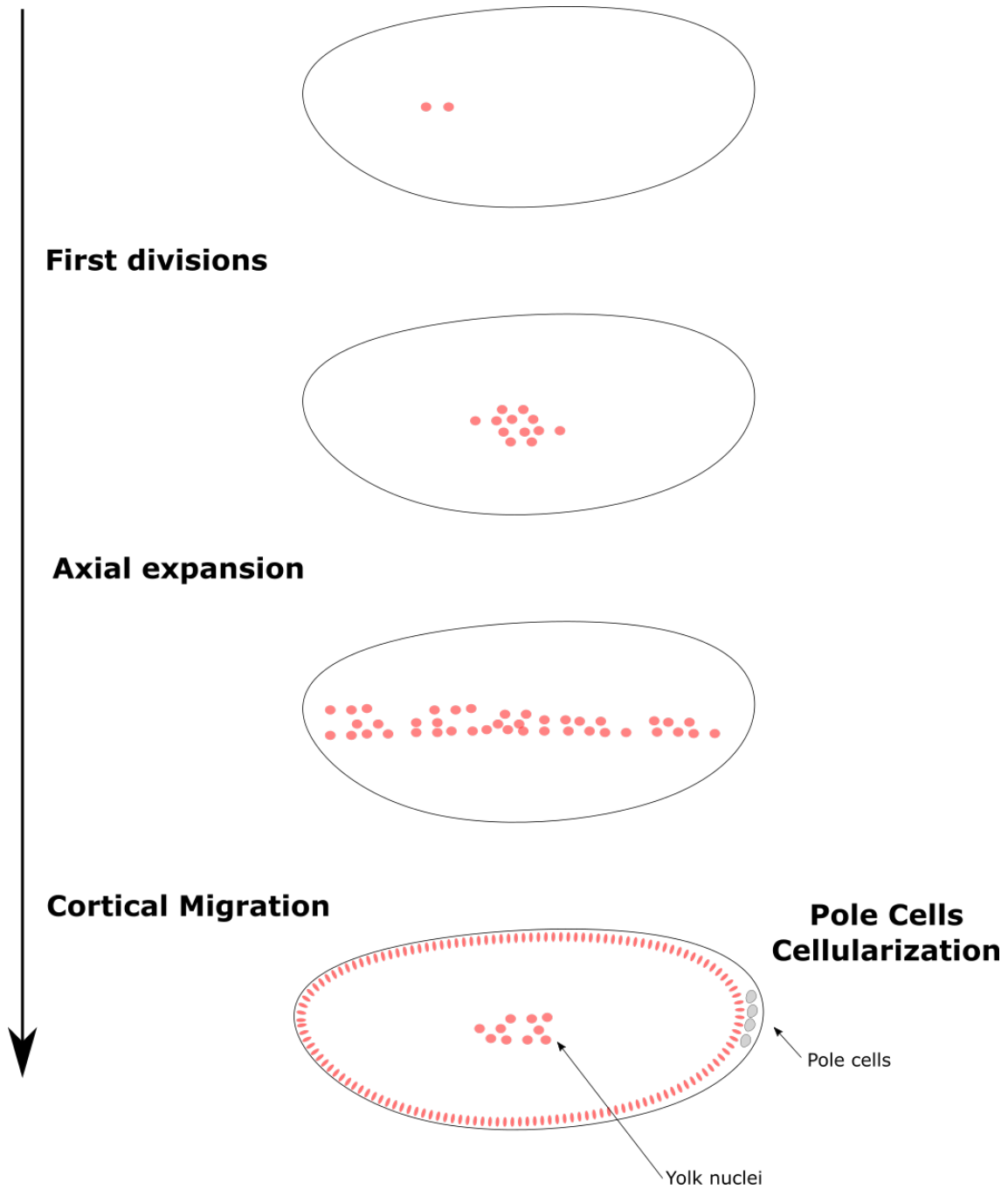


Figure I.9: Morphogenesis of the early syncytial embryo: Sagittal cuts, anterior is left, dorsal up. Nuclei are shown in red

The first steps of *D. melanogaster* morphogenesis differ from vertebrate morphogenesis as it occurs without cellularization. After fertilization, the first nuclear divisions occur without cell individualization. The embryo is formed by a syncytium of dividing nuclei until the 13th round of division as cellularization occurs [Zalokar,

1976] (Figure I.9). The first seven divisions occur synchronously in the center of the embryo, within the yolk [Rabinowitz, 1941a]. During this set of divisions, the nuclei are spread in the antero-posterior axis (Figure I.9). This process known as axial expansion is driven by the acto-myosin cytoskeleton of the embryo [Royou et al., 2002].

During the next three mitotic cycles, most of the nuclei then migrate towards the surface of the embryo in a step-wise manner, a phenomenon known as cortical migration [Foe and Alberts, 1983] (Figure I.9). The exact process underlying cortical migration remains unclear but it seems powered by the microtubule cytoskeleton as its reorganization both correlates and is required for nuclei movement [Baker et al., 1993]. At this stage, two or three of the remaining cells are incorporated in the germinal plasma, at the posterior pole of the embryos. These nuclei then divide two times and cellularize, thus forming the pole cells, precursors of the germline [Zalokar and Erk, 1977] (Figure I.9). This incorporation and cellularization is directly mediated by microtubules [Lerit and Gavis, 2011]. Another twenty cells remain within the yolk sac, divide three times and become polyploid, thus forming the yolk cells that will no longer divide from this stage on [Rabinowitz, 1941b]. The next three cycles of divisions occur in the somatic and germline cells are no longer synchronized [Foe, 1993].

The approximately 6000 somatic nuclei then undergo cellularization. This de-novo formation of membrane that expands the membrane surface of the embryo by 25-folds was previously thought to be the consequence of the exocytosis of membranes from inside the embryo [Lecuit and Wieschaus, 2000]. However, a new theory recently emerged. At first, the membrane at the surface of the embryo forms microvilli [Fullilove and Jacobson, 1971] (Figure I.10). Those finger-like structures progressively disappear and have been hypothesized to serve as a membrane reservoir as they ingress from the surface between the nuclei [Figard et al., 2013]. The embryo is thus formed of a continuous single-layered epithelium -plus a group of budding cells at the posterior end- surrounding the yolk sac.

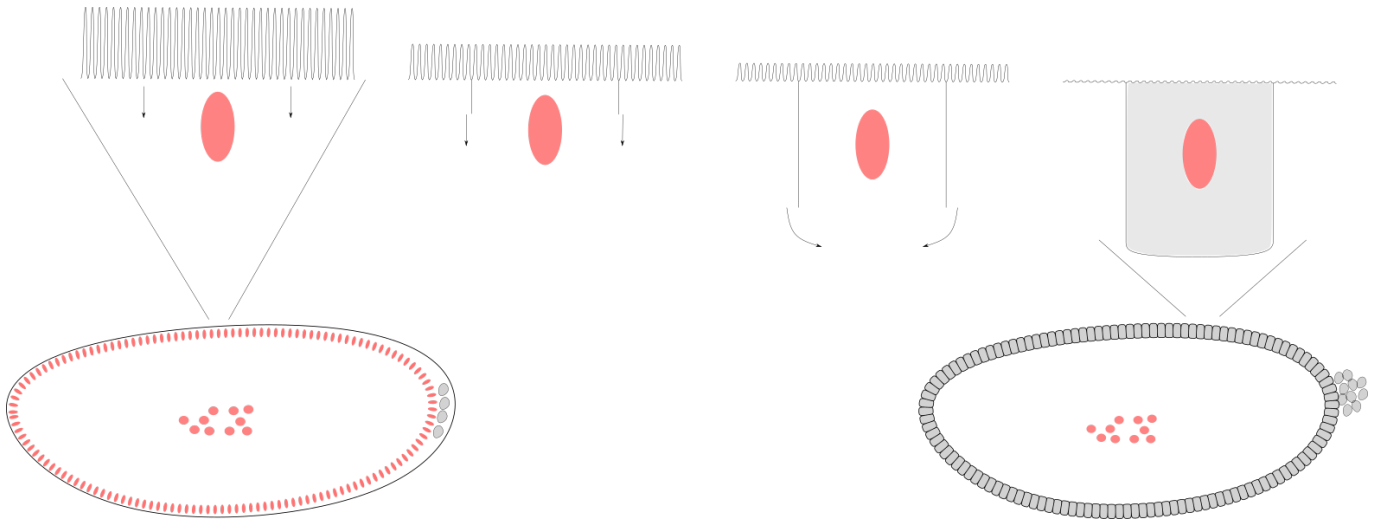


Figure I.10: Surface microvilli as a membrane reservoir for cellularization: Sagittal cuts, anterior is left, dorsal up. Nuclei are shown in red, individualized cytoplasm in grey

B) The gastrulation and concomitant morphogenetic events

The next step of embryogenesis is the gastrulation where the layer of somatic cells gives rise to three distinct germ layers, the ectoderm the mesoderm and the endoderm. In this section, I describe the origin and cellular processes required for this morphogenetic event.

a) Formation of the mesoderm

i) Patterning of the mesoderm

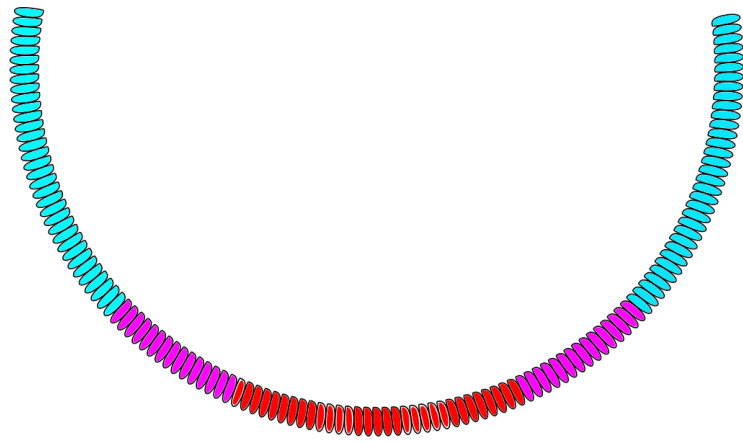
The presumptive mesoderm arises from the ventral most cells of the blastoderm. This patterning results from the interaction of different signaling cascades that originate from oogenesis. It starts with the segregation of *gurken* mRNA at the posterior part of the oocyte. *gurken* encodes a diffusible TGF- α like ligand [Neuman-Silberberg and Schüpbach, 1993]. From there, it is translated and secreted towards the overlying follicle cells [Peri et al., 1999]. This results in the repression of the transcription of the gene *pipe* in the dorsal follicular cells, thus confining *pipe* expression in the "ventral" follicular cells. Pipe, an heparan sulfate 2-O-sulfotransferase,

hence modifies the vitelline membrane of the egg ventrally [Sen et al., 1998]. Those modifications activate the protease Easter, that cleaves the diffusible protein Spätzle [Cho et al., 2012, Rahimi et al., 2019]. The cleaved and activated form of Spätzle forms a dorso-ventral gradient over time and acts as a morphogen through its activation of the Toll pathway [Rahimi et al., 2019, Weber et al., 2003]. The spatially graduated activation of the Toll pathway results in proportional translocation of the Dorsal transcription factor to the nuclei from the syncitial stage [Rushlow et al., 1989]. High levels of nuclear Dorsal drive the expression of *twist* and *snail*, thus defining the pattern of the mesoderm [Chopra and Levine, 2009].

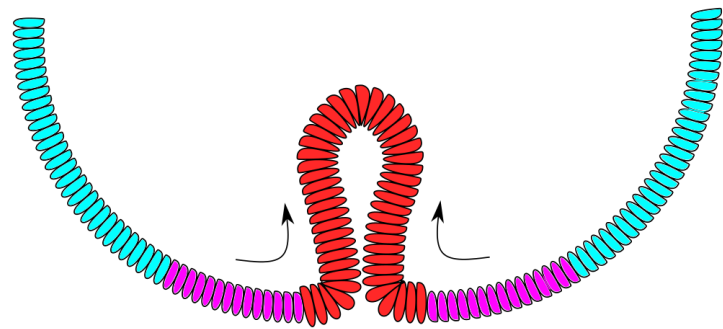
ii) The invagination, detachment and spreading of the mesoderm

The joint activity of Twist and Snail transcription factors activates the GPCR pathway through its ligand Fog and downstream effectors [Seher et al., 2007, Manning et al., 2019]. This sustains persistent apical constriction through RhoA activation within the mesoderm cells that allows subsequent formation of a supracellular mesh of myosin2 coupled to apical junctions that strengthen and support apical tensions, leading to mesoderm invagination [Häcker and Perrimon, 1998, Weng and Wieschaus, 2016, Martin et al., 2010]. The sustained apical constriction at constant volume drives cell apico-basal elongation [Gelbart et al., 2012]. Moreover, myosin depletion basally drives basal extension and cells become wedge-shaped [Polyakov et al., 2014]. This collective cell shape change drives the invagination of the whole mesoderm which forms a tube-like structure inside the embryo and forms the ventral furrow [Leptin, 1999] (Figure I.11).

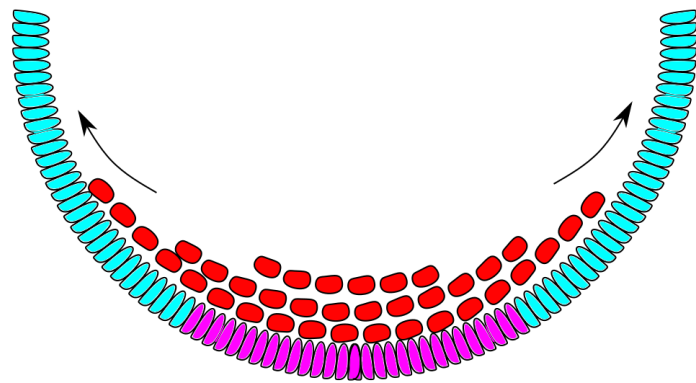
Once internalized, the mesoderm cells undergo EMT, a most-likely consequence of Snail activity which is a key regulator of EMT [Hemavathy et al., 1997] (Figure I.11). By inhibiting Bazooka and stimulating the switch from E to N-cadherin, Snail destabilizes adherent junctions between the mesoderm and ectoderm and facilitates the detachment of the two tissues [Weng and Wieschaus, 2017, Oda et al., 1998]. Interestingly, this apical junction destabilization must be performed after internalization, as early destabilization results in internalization failure and tissue



Invagination



EMT and spreading



Mesoderm
Neurogenic
ectoderm
Presumptive
Epidermis

Figure I.11: Mesoderm morphogenesis during gastrulation: Transversal cuts, dorsal is up.

disruption [Martin et al., 2010]. Once detached, the mesoderm cells undergo two rounds of division [Foe, 1989]. They spread dorsally on the neuroectoderm floor. This spreading results from a combination of cell intercalation, spreading and collective migration stimulated by the FGF ligand secreted by the underlying ectoderm [Murray and Saint, 2007, Clark et al., 2011]. This process hence turns the embryo from a single-layered to a stratified multilayered structure.

b) The endoderm

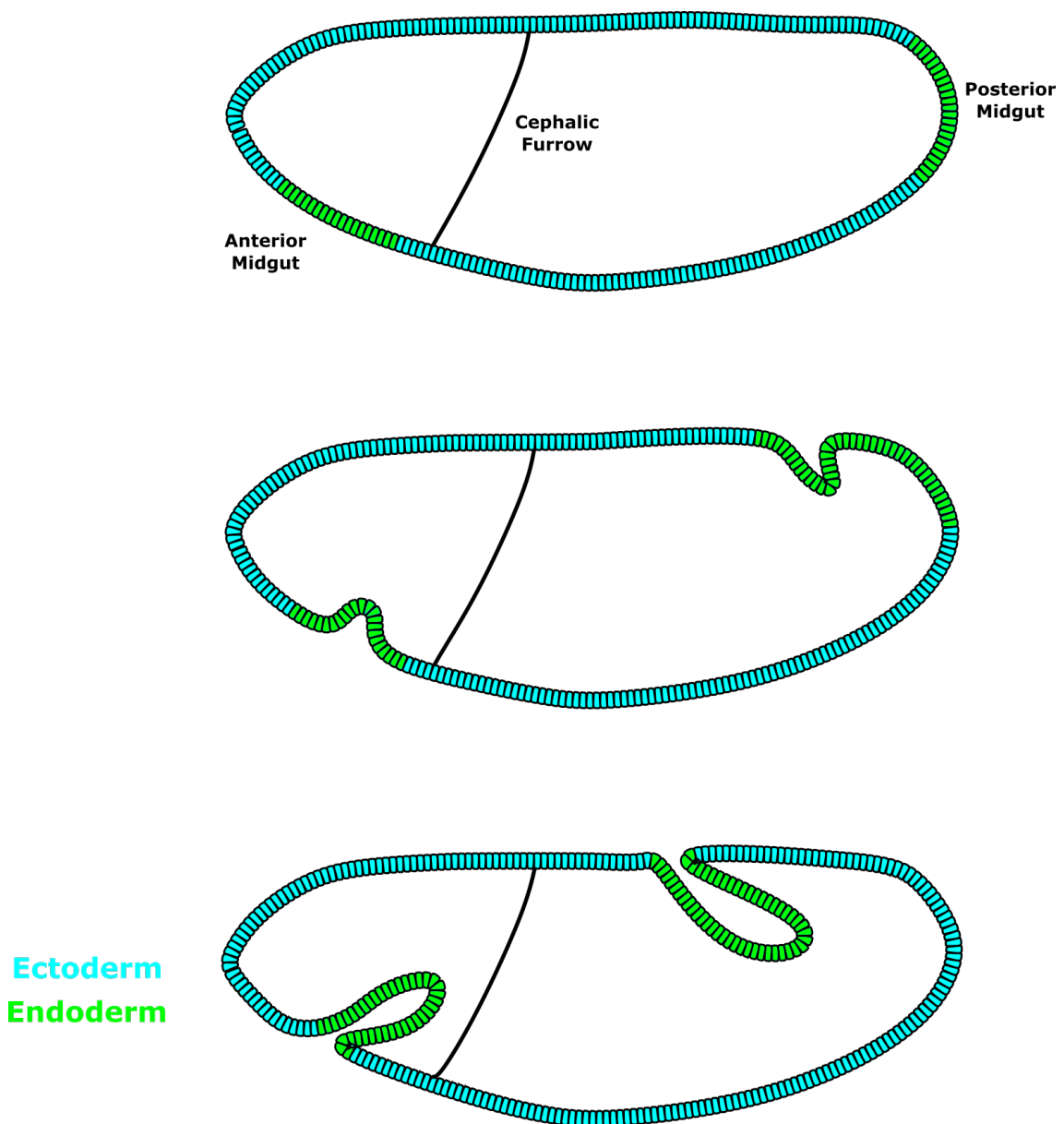


Figure I.12: Anterior and Posterior Midgut invagination during gastrulation: Sagittal cuts are displayed, anterior is left, dorsal up.

The individualization of the endoderm also requires tissue invagination (Figure I.12). It arises from two different locations, one anterior that forms the Anterior Midgut (AMG) primordium and one posterior that forms the Posterior Midgut (PMG) primordium. PMG is patterned by Torso signaling [Nüsslein-Volhard et al., 1987]. PMG cells can be distinguished from surrounding ectodermal cells prior to invagination by their columnar shape [Poulson, 1950]. In these cells the Torso pathway induces its target Tailless [Chen et al., 2009]. Tailless afterwards activates the GPCR pathway through Fog, which drives apical constriction of the PMG cells and their invagination as during mesoderm internalization [Costa et al., 1994]. Interestingly, the invagination of the PMG can be distinguished from mesoderm morphogenesis as it does not proceed simultaneously but gradually from posterior to anterior as a wave of myosin activity is observed. Posterior most PMG cells undergo apical constriction which initiates the invagination. The tension resulting from the apical constriction of the cells is transduced to the anterior neighbouring cells, hence driving their apical extension through stretching. This provokes the rolling of the apically contracted cells under their neighbours. Therefore, as the wave of apical constriction progresses, the PMG ingresses. Surprisingly, this anterior to posterior wave of myosin activity does not depend on Fog levels [Bailles et al., 2019]. Little is known about the precise mechanisms at the origin of AMG morphogenesis. It starts from a patch of cells resulting from post-blastoderm division, just anterior to the cephalic furrow but in contact with the ventral furrow [Foe, 1989]. Therefore, it is not surprising that its patterning depends on Bicoid, the morphogen responsible for the anterior identity within the embryo [Schüpbach and Wieschaus, 1986]. Thus, despite their resemblance, spatial and temporal simultaneity, mesoderm internalization and AMG invagination depend of two independent induction sources, Dorsal and Bicoid respectively.

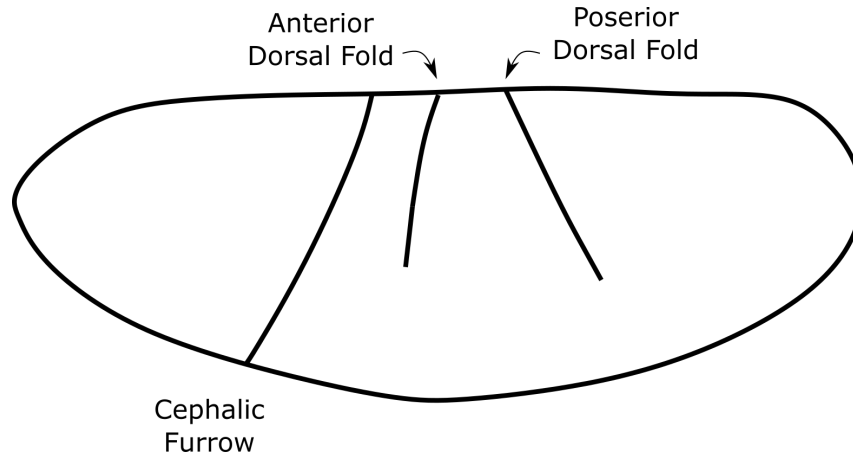


Figure I.13: Ectoderm folding during gastrulation: Lateral view, anterior is left, dorsal is up.

c) Morphogenesis of the ectoderm during gastrulation

While the ectoderm remains at the surface of the embryo, it undergoes several folding events (Figure I.13).

The most anterior fold consists in the formation of the cephalic furrow. At about one third of the embryo along the antero-posterior axis, the cephalic furrow forms a transversal ring-like cleft which is 30 μ m deep [Spencer et al., 2015]. The cephalic furrow individualizes the presumptive head from the rest of the ectoderm and delimits its boundary with the thoracic segments. Its localization depends on the antero-posterior morphogen Bicoïd, which activates the pair rule gene *evenskipped* in the anterior domain. The cephalic furrow forms from ectoderm cells from the second row of *evenskipped* expression [Vincent et al., 1997a]. The initiation of the folding appears as a line of initiator cells that undergo apical shortening, therefore cleaving the ectoderm. As the initiator cells undergo apical constriction coupled to basal expansion, the anterior and posterior neighbouring cells are dragged and roll into the fold. The mechanics behind this change of cell shape remain unclear as of today, but it has been proposed that actin cytoskeleton remodelling is a sufficient driver, independently of Myosin 2 activity [Spencer et al., 2015].

Two other transversal folds, restricted to the dorsal domain, also appear during gastrulation. Their antero-posterior positions are determined by the stripes 3 and 5

of the pair ruled gene *runt* [Wang et al., 2012b]. Their presence on the dorsal side is determined by the gradient of Dorsal that I extensively described regarding the mesoderm patterning [Nüsslein-Volhard et al., 1987]. The folding appears as the initiator cells proceed in an apical to basal adherent junction switch. This switch results in a shortening of the initiator cells that plunge within the embryo, hence dragging their neighbours [Wang et al., 2012b]. The force necessary for the folding events is thought to be provided by the initiator cells cytoskeleton and molecular motors, through both microtubule coupled Dynein and actin coupled Myosin [Takeda et al., 2018, Wang et al., 2013].

C) Germband extension and nervous system emergence

Gastrulation defines and sets apart the three germ-layers. It is followed by a large convergent extension event that shapes the definitive proportions of the embryo: the germ band extension (GBE). Subsequently the formation of the central nervous system occurs.

a) The germband extension

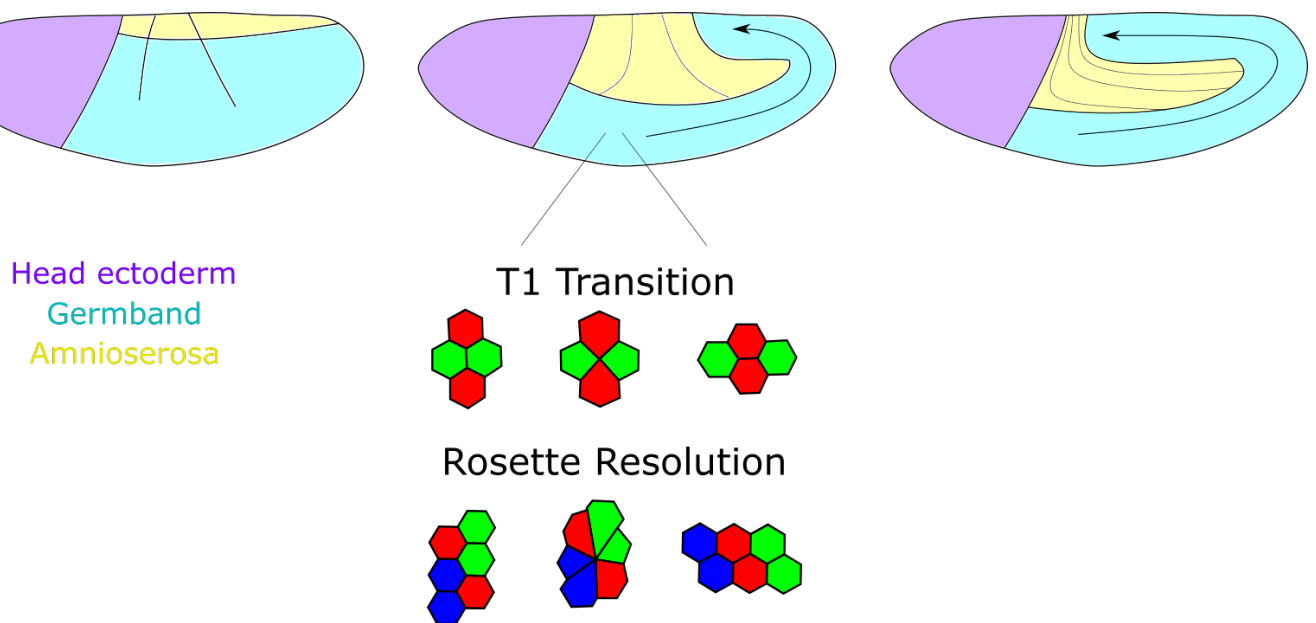


Figure I.14: Germband extension at the embryo and cellular scale: Lateral view, anterior is left, dorsal is up.

All the ectoderm cells posterior to the cephalic furrow and ventral to the dorsal most cells of the presumptive amnioserosa -whose morphogenesis begins during the GBE- participate to a major convergent extension event: the GBE [Irvine and Wieschaus, 1994] (Figure I.14). The process of GBE is critical to define the final proportions of the embryo. During that process, the antero-posterior length of the embryo is increased 2.5 folds whereas its dorso-ventral length shrinks by half [Hartenstein et al., 1985]. It is divided in two-phases: one fast 45 minute phase during which 60 percent of the elongation occurs and one slow that lasts 100 minutes [Hartenstein et al., 1985].

This change of cells position within the tissue requires both polarized acto-myosin

contraction and adherent junction remodelling [Zallen and Wieschaus, 2004, Tepass, 2014]. Specifically, Myosin-2 gets polarized at the antero-posterior junctions between segments upon the heterophilic binding of Toll-2, Toll6 and Toll-8 receptors. These 3 genes are under the control of the *evenskipped* and *runt* pair-rule genes and are expressed in overlapping bands in the embryonic trunk. Therefore, the heterophilic binding of those receptors is enriched at the interface between those bands along the dorso-ventral axis. This binding in turn recruits Myosin 2, which allows the coordinated contraction of the cells at their common antero-posterior contact [Pare, 2014]. In regions where Toll receptors overlap, another couple of proteins, Tartan and Ten-m, drive recruitment of the myosin in a similar fashion [Paré et al., 2019]. As adherent junctions are compressed by the contraction of the cell cortical acto-myosin network, they are remodelled. This remodelling is allowed by E-cadherin endocytosis, powered by a medio-apical Myosin flow underneath the adherent junctions [Levayer et al., 2011, Levayer and Lecuit, 2013]. Interestingly, this flow also drives apical junction oscillations that is reminiscent of the ones observed during ventral furrow formation. Similarly, this process requires the activation of the GPCR pathway [Kerridge et al., 2016]. Therefore, enrichment of myosin at the antero-posterior adherent junctions within the whole tissue coupled to their remodelling drive their shrinkage and the overall convergence of the cells towards the ventral midline.

At the cellular level, the contraction of the adherent junctions induces the exchange of neighbours and therefore the extension of the germ band. Two kinds of exchanges are observed during GBE, the T1 transition and the resolution of rosettes [Bertet et al., 2004, Blankenship et al., 2006] (Figure I.14). T1 transitions consist in the rearrangement of 4 cells. Cells are organized in a 1-2-1 configuration on the dorso-ventral axis. The adherent junction between the antero-posterior faces of the two middle cells shrinks until a 4-cells vertex is formed. The 2 middle cells are then separated by a new adherent junction that grows between the dorsal-most and ventral most cells, thus creating a new cell organisation with a 1-2-1 configuration in the antero-posterior axis [Bertet et al., 2004]. The rosette resolution involves 6 to

8 cells, linked together by a supra-cellular myosin cable [Fernandez-Gonzalez et al., 2009]. This cable, oriented in the dorso-ventral axis results from the reaction of the tissue to its endogenous tension [Fernandez-Gonzalez and Zallen, 2009]. As the cable contracts, the adherent junctions along the dorso-ventral axis shrink until all the cells are transiently linked by a single vertex. Then, as in T1 transition, new adherent junctions grow between the neighbours along the antero-posterior axis, hence leading to both neighbor exchange and elongation along the antero-posterior axis [Blankenship et al., 2006].

The elongation of the germband is further accentuated by oriented cell division in the antero-posterior axis [da Silva and Vincent, 2007]. Altogether, both convergent extension and oriented cell divisions result in the elongation of the germband without elongation of the egg. This has a dramatic effect on the embryo shape, which is now composed of a head at the anterior pole, followed by a U-shaped trunk.

b) Central nervous system morphogenesis

The central nervous system (CNS) arises from cells of the ventral and lateral part of the neuroectoderm. It is composed of the brain, that emerges from the head neuroectoderm, and the ventral nerve cord that arises from the ventral part of the germband. From the end of GBE, structures of 5-7 cells form proneural clusters [Skeath and Carroll, 1992]. They are characterized by the expression of *achaete*, *scute* and *lethal of scute* transcription factors that are crucial for the subsequent differentiation of neuroblasts [Skeath et al., 1992, Jiménez and Campos-Ortega, 1990]. Those clusters can easily be spotted thanks to cells enlargement at the expense of the surrounding neighbours [Stollewerk, 2000]. However, in the ventral nerve cord, only one cell from each cluster acquires the neuroblast identity. The role of Notch signaling in neuroblast selection has been discovered as mutations in components of its pathway results in CNS hypertrophy [Lehmann et al., 1983]. In the absence of Notch signaling, all cells within the cluster keep expressing proneural genes and select the neuroblast fate [Skeath and Carroll, 1992]. However, a recent study deciphered more precisely

the regulation of the neuroblast fate and linked it with genes implicated in the next step of its development. The cells express a set of pro-EMT genes prior to ectoderm detachment [Arefin et al., 2019]. The authors found that in the neural clusters, two pro-EMT genes, *SoxNeuro* of the *SoxB* family and *worniu* from the *Snail* family, are expressed and required for NB formation. These genes are inhibited by Notch signaling and in turn induce the transcription of *Delta*, the Notch ligand. Hence, a lateral inhibition process occurs, resulting in only one *Delta SoxNeuro worniu* positive cell in the proneural cluster. At the same time, SoxN and worniu downregulate *E-Cadherin* and *Crumbs*. This results in the weakening of its adherent junctions and therefore to an inhibition of Notch signaling that relies on Crumbs. Therefore, both Notch driven lateral inhibition process and EMT are intertwined and result in the emergence of a unique neuroblast per pro-neural cluster. Interestingly, during brain formation, all the cells within the pro-neural cluster become neuroblasts, Notch signaling being only involved in the selection of the neuroblast type [Hwang and Rulifson, 2011].

After delamination, neuroblasts undergo several rounds of asymmetric divisions in a stem-cell like mode, producing one neuroblast and one progenitor cell [Gallaud et al., 2017]. Progenitor cells can also divide or directly differentiate into different types of neurons and glia. The determination of the final type of neuron obtained by the end of central nervous system formation is regulated both spatially and temporally at the neuroblast cell stage. The final identity of the neurons on the antero-posterior axis is regulated by segment polarity genes [Bhat, 1999]. Dorso-ventral identity of neuroblasts is determined through DPP signaling, hence allowing a 3 dimensional distribution of neuroblast identity [Esteves et al., 2014, Garcia and Stathopoulos, 2011]. Moreover, final neuron and glial identity is regulated by a temporal transcription factors cascade within the neuroblasts. In the neuroblasts undergoing asymmetric divisions, the following transcription factors are sequentially produced and induce the next as follows: Hunchback (Hb) \rightarrow Krüppel (Kr) \rightarrow Pdm2/Nubbin (Pdm) \rightarrow Castor (Cas) \rightarrow Grainy head (Grh) [Doe, 2017]. The transcription factor expressed

by the neuroblast as it undergoes its asymmetric division determines the fate of the daughter cells, hence finally defining a supplementary layer of neuron and glia specification within the CNS.

CNS cell generation and specification is directly followed by a dramatic wave of programmed cell death. About half of the generated neurons and 75 percent of the glial cells are eliminated through apoptosis [Rogulja-Ortmann et al., 2007, Jacobs, 2000]. Therefore, CNS morphogenesis is defined spatially and temporally by several signaling cascades that control EMT, proliferation and cell-death.

D) Germband retraction

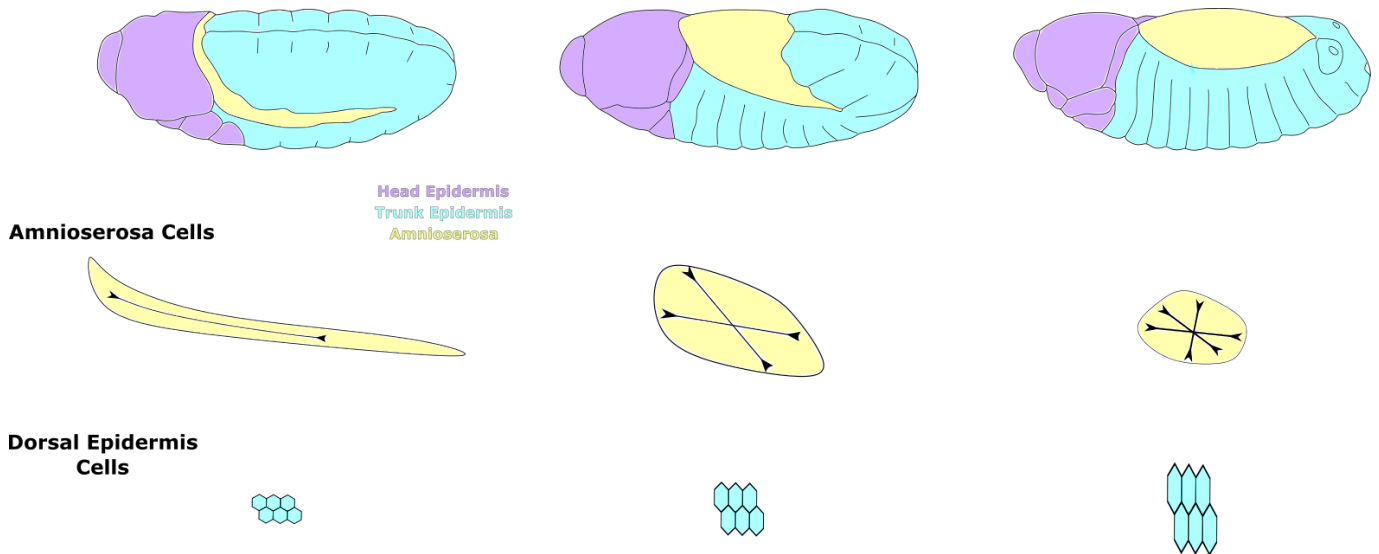


Figure I.15: Germband retraction at the embryo and cellular scale: Lateral view, anterior is left, dorsal is up.

By stage 11, the embryo is composed of 4 main layers: the ectoderm surrounding the central nervous system, the mesoderm and the endoderm. However, the trunk of the embryo is still folded in a U shape.

The retraction of the Germ-band (GBR) requires an extra-embryonic tissue, the amnioserosa (AS). The term extra-embryonic tissue is used as the AS does not participate in the formation of larval tissues. The AS presumptive cells are differentiated from the early blastoderm stage, from a stripe of 6 cells at the dorsal midline. Their fate is determined by DPP signaling that induces *zen* expression in the presumptive AS cells [Rushlow et al., 2001]. These cells continue to replicate as the rest of the ectoderm, but do not perform cytokinesis and therefore become polyploid [Hartenstein et al., 1985]. As the GBE occurs, the extending germband exerts a significant traction on the AS cells that are still attached to the underlying yolk sac, inducing their elongation [Pope and Harris, 2008]. This tension causes the AS cells to elongate dramatically, up to 10 times their original length while dividing their width by 5, and switch from cuboidal to squamous shape (Figure I.15). This cell deformation requires the remodelling of the AS cells microtubule cytoskeleton, a process driven by Myosin 2 that redirects their direction of polymerization [Pope and Harris, 2008].

The process also requires an intensive adherent junction remodelling, mediated by synthesis of new adherent junction proteins or their recycling/relocalization by endocytosis/exocytosis [Goldenberg and Harris, 2013].

Germband retraction (GBR) requires the interaction between the AS with the dorsal cells of the germband. During the process, the AS cells switch from an elongated to isometric squamous shape while the germband cells elongate dorsally [Schöck and Perrimon, 2002] (Figure I.15. Interestingly, the GBR process that produces a macroscopic effect inverse to the one of GBE does not involve cell intercalation nor oriented cell division [Schöck and Perrimon, 2002]. Laser ablation experiments have shown that the contraction of the AS cells drives the germband cell directed elongation [Lynch et al., 2013]. Thus, GBR results from the coordination and transmission of forces between two tissues undergoing morphogenesis. It results in an embryo with a straight antero-posterior axis but whose trunk is cut in half by a hole in the dorsal side, covered by the AS. This thesis focuses on the morphogenesis events that result in the closure of this hole, a process known as dorsal closure.

III) The Dorsal closure of *D. melanogaster*

I focused my thesis on the understanding of the mechanics driving dorsal closure. The mechanics of dorsal closure have been thoroughly investigated in the last decades, but few studies considered the embryo as a whole while trying to understand the matter. My bet was to take into account all the different organs and associated morphogenetic movements in order to understand fully the dorsal closure mechanism. Therefore, in this section, I will first describe the morphogenesis of the internal organs during dorsal closure. I will then give an overview of what is currently known about dorsal closure, from the cell biology to the mechanics and signaling standpoint. I will finally recapitulate what is known about the head-involution process, that is concomitant and results as well in large-scale embryo morphogenesis.

A) Internal organs morphogenesis during dorsal closure

a) The midgut and hindgut

Two presumptive digestive organs undergo major morphogenetic events during dorsal closure, the midgut and the hindgut.

Midgut formation requires subsequent EMT and Mesenchymal to Epithelial Transition (MET). Following their internalization during gastrulation, both the anterior and posterior midgut primordia undergo EMT. The process is driven by the expression of the GATA factor *serpent*, that represses *crumbs* in order to disorganize adherent junctions thus allowing EMT [Campbell et al., 2011]. By the end of GBE, the midgut is formed by two pools of mesenchymal cells at the anterior and posterior poles of the embryo. During GBR, the two pools migrate concomitantly towards each other, using the visceral mesoderm as a substrate [Reuter et al., 1993, Martin-Bermudo et al., 1999]. Subsequently, the two primordia fuse and undergo MET, through downregulation of *serpent* and of proteins mediating the adhesion with the underlying visceral mesoderm. Subsequently, this results in the formation of adherent junction and construction of an apico-basal polarity by the onset of dorsal closure [Tepass and Hartenstein, 1994, Campbell et al., 2011, Pitsidianaki et al., 2021]. The two newly formed epithelial lobes therefore extend and fuse both ventrally and dorsally and surround the yolk sac, through a mechanical process that has yet to be understood [Tepass and Hartenstein, 1994](Figure I.16). A first hypothesis is that the elongation of the midgut is the result of two cycles of endo-replication followed by a columnar to squamous cell shape transition [Smith and Schoenwolf, 1991, Fuss et al., 2001]. Interestingly, a recent study demonstrated that the yolk cell undergoes massive Myosin-2 dependent contraction during midgut closure. The authors hypothesized that the midgut extension could result from the traction generated by the yolk sac, thus allowing midgut lumen formation [Selvaggi et al., 2022]. Altogether, midgut lumen formation might result from the combination of the two phenomena, the polyploidisation allowing surface increase and the yolk contraction

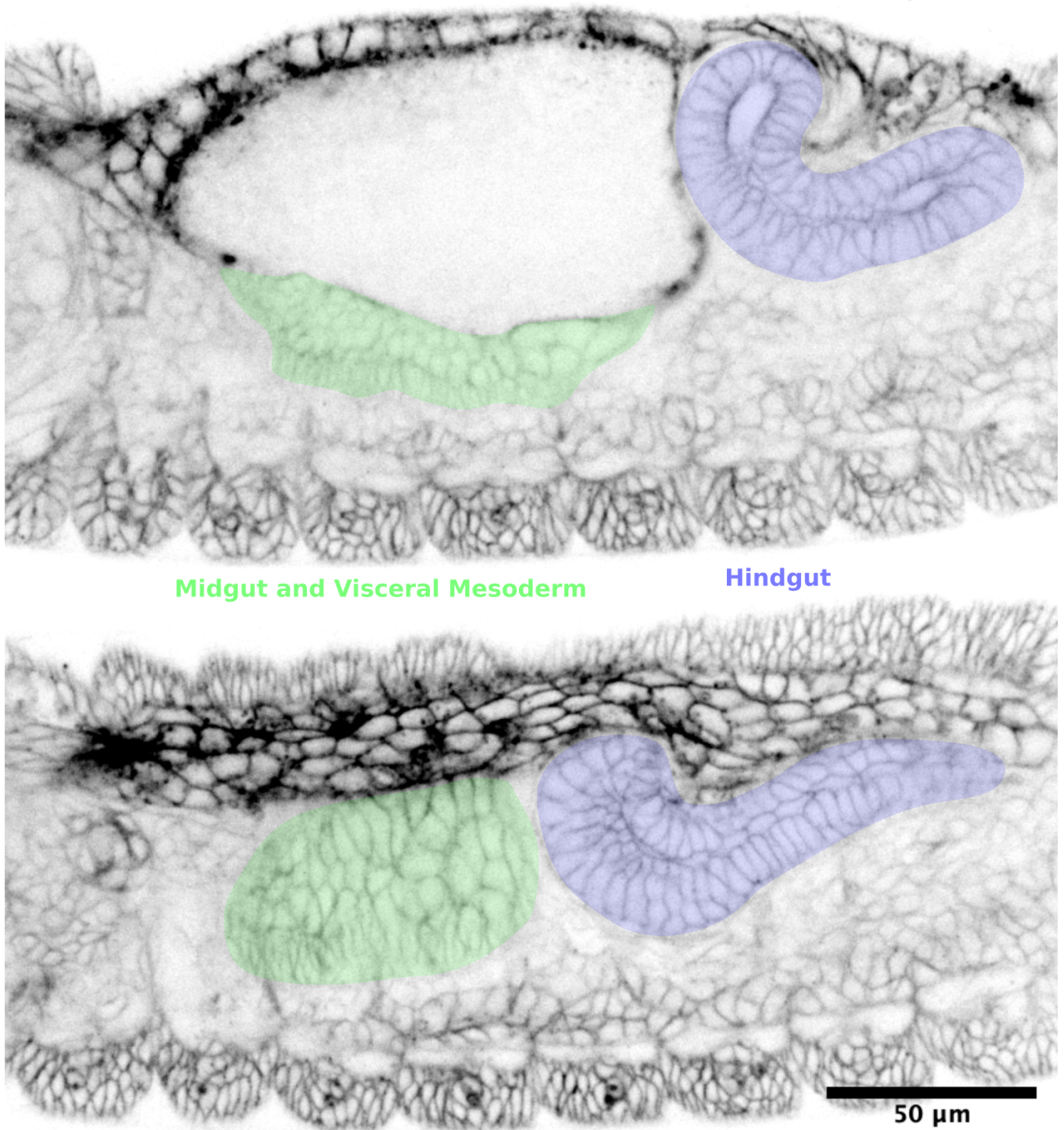


Figure I.16: Midgut and hindgut morphogenesis during dorsal closure: Optical slices of a *CAAX::GFP* embryo at the onset and at mid dorsal closure.

providing the directional information for expansion.

Both the hindgut and midgut anlagen undergo internalization during gastrulation. By the end of gastrulation, the hindgut forms a thick tubular structure at the posterior end of the embryo [Campos-Ortega and Hartenstein, 1997]. During dorsal closure, the hindgut expands from posterior to anterior and forms the elongated tube that will become the larval small intestine (Figure I.16). This elongation is driven by both cell shape changes and contact rearrangements. During dorsal closure, the hindgut cells undergo columnar to cuboidal transition, thus increasing the tissue surface. Concomitantly, the tissue reorganizes through a convergent extension mechanism along the antero-posterior axis [Iwaki et al., 2001]. Therefore, the combination of the two phenomena drives an expansion of the tissue directed towards the anterior pole of the embryo during dorsal closure.

b) The mesoderm derived tissues

By the end of GBE, the mesoderm gets subdivided in two main domains, the visceral and somatic musculature primordia, corresponding to the mesoderm from the *evenskipped* and *sloppy-paired* domains respectively [Lee and Frasch, 2005, Frasch, 1999]. More specifically, the visceral mesoderm arises from the dorsal most cells of the mesoderm, in response to DPP signaling [Frasch, 1995]. These cells receive DPP signaling from the overlying ectoderm which induces the genetic cascade *tinman* → *bapppipe* → *biniou*, thus maintaining the visceral mesoderm identity [Zaffran et al., 2001]. Following their differentiation, the visceral mesoderm cells from the different *evenskipped* positive bands fuse together on the embryo floor and act as rails for the migration of the overlying midgut primordia during GBR [Sun et al., 2020, Reuter et al., 1993, Martin-Bermudo et al., 1999]. During dorsal closure, the visceral mesoderm cells migrate in concert with the midgut [Campos-Ortega and Hartenstein, 1997]. Concomitantly with the end of dorsal closure, a cooperation between *biniou* potentiates Ubx activation within the PS7 of the visceral mesoderm, thus driving DPP expression [Zaffran et al., 2001]. This activation results in the constriction

of the midgut and overlying visceral mesoderm [Staebling-Hampton and Hoffmann, 1994].

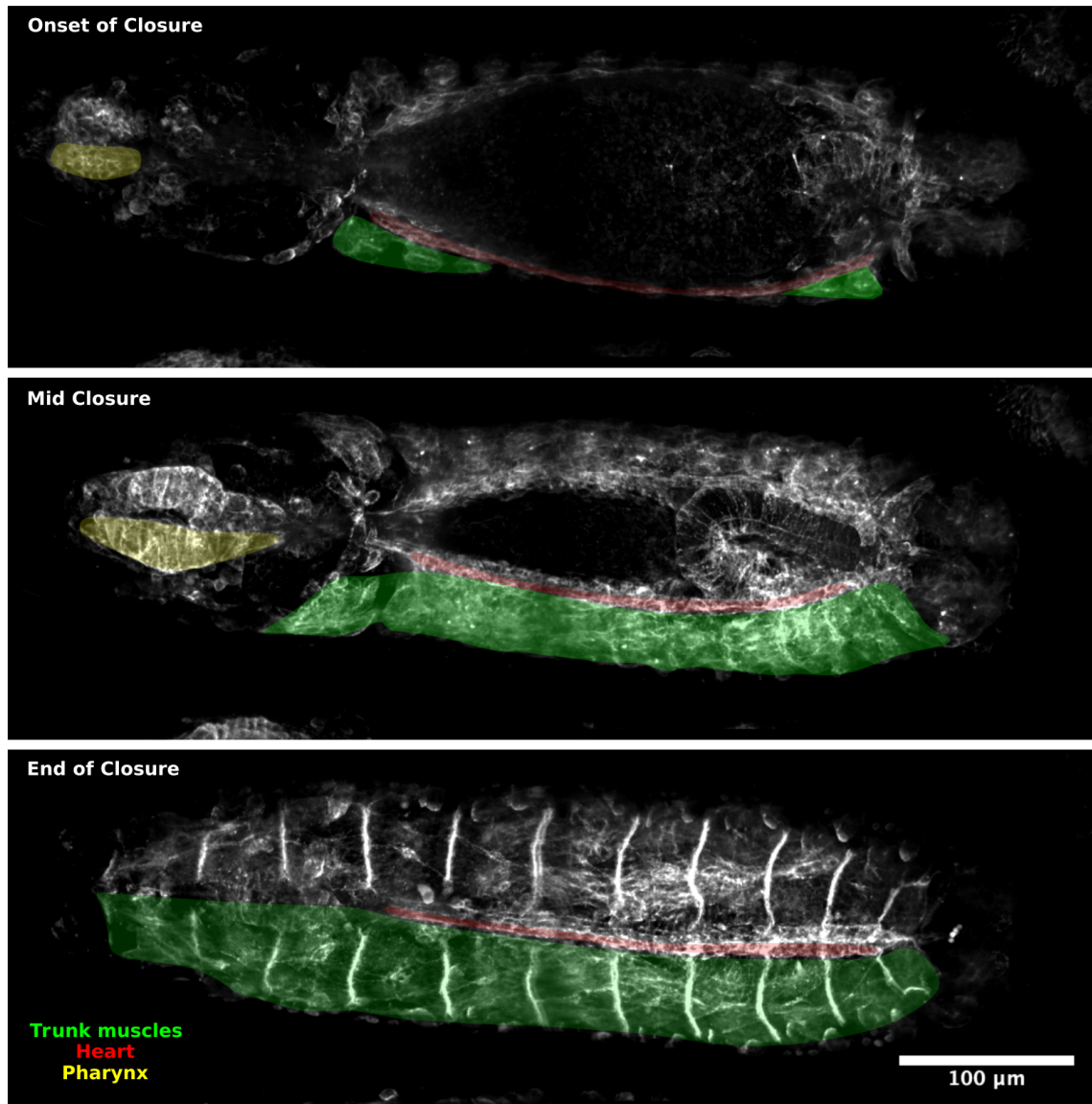


Figure I.17: Somatic musculature morphogenesis during dorsal closure: Time-lapse imaging of a *twist-Gal4*, *UAS-APC2::GFP* embryo. Only the left side is annotated so that the right side stays perfectly visible.

DPP signaling also plays a crucial role during somatic mesoderm morphogenesis. Somatic muscles that receive high levels of DPP express *tinman*, as in the visceral mesoderm, which drives their differentiation into cardiac mesoderm [Frasch, 1995]. The cardiac cells subsequently undergo MET and align as two rows of cells on the antero-posterior axis, one on each side of the embryo at the end of GBE [Poulson,

1950, Fremion et al., 1999]. During dorsal closure, the cardioblasts migrate towards the midline, just under the epidermis [Haack et al., 2014] (Figure I.17). By the end of dorsal closure, the bilateral rows of cardioblasts meet their counterpart at the midline and fuse, thus forming the cardiac tube of the embryo [Medioni et al., 2008]. Myoblast ventral to the *tinman* activation pattern do not undergo MET, but rather fuse in order to form myotubes [Schulman et al., 2015]. During dorsal closure, the musculature is displaced dorsally, towards the midline, but little is known about the mechanics of the process (Figure I.17).

Therefore, two internal layers of mesoderm derived tissues migrate dorsally during dorsal closure, concomitantly with the dorsal epidermis.

c) Tracheal dorsal branch morphogenesis

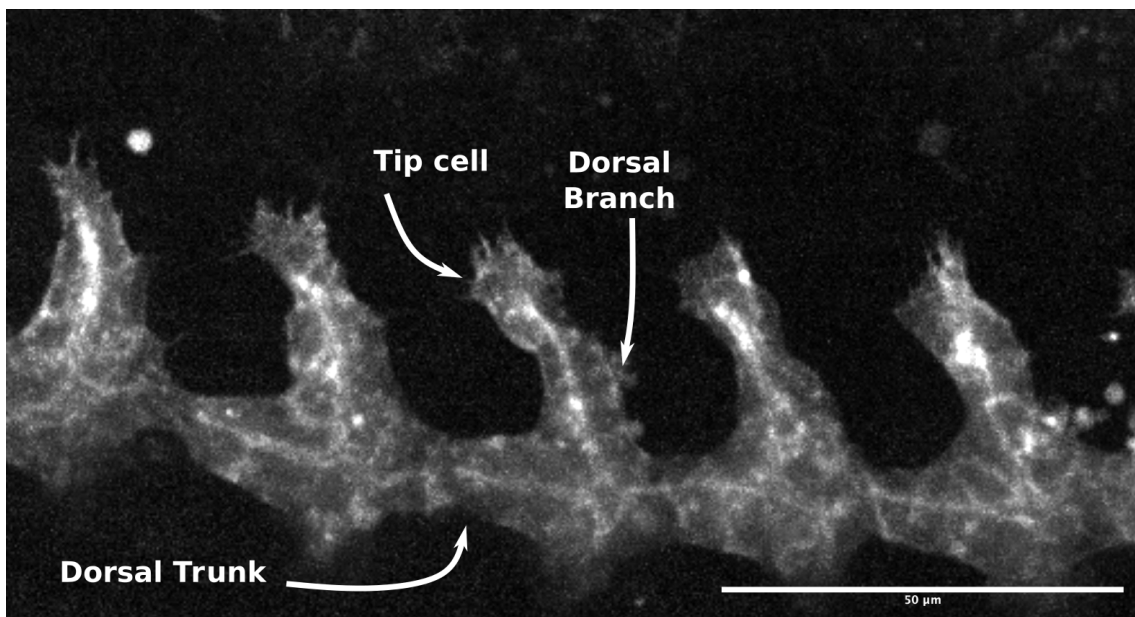


Figure I.18: Tracheal dorsal branch morphogenesis Maximum projection of a *Bnl:Moesin::RFP* embryo during dorsal closure, courtesy of Hugo Raveton.

The dorsal tracheal network develops concomitantly with dorsal closure. The dorsal branch cells are determined by DPP signaling, which induces *knirps* while inhibiting *spalt* expression [Vincent et al., 1997b]. One dorsal branch forms as a single tip cell migrates towards the dorsal midline while dragging the follower cells towards the midline. Selection of the tip cell among the dorsal branch cells requires a

complex interplay between the FGF ligand *Brancheless* and Notch signaling. DPP is important for the localized expression of *brancheless* in the dorsal epidermis [Vincent et al., 1997b]. Dorsal branch cells receiving Bnl express the Notch ligand *delta*. In turn, Notch expression in the other cells turns off MAPK signaling, the target of Bnl [Ikeya and Hayashi, 1999]. Delta-Notch lateral inhibition results in the selection of a single cell expressing *delta*, and hence the ability to receive Bnl signaling [Ghabrial and Krasnow, 2006]. This tip cell therefore drags the other dorsal branch cells, defined as stalk cells, towards the embryo dorsal midline while being guided by the Bnl gradient [Caussinus et al., 2008, Sutherland et al., 1996] (Figure I.18). The dorsal branch elongation relies on the progressive intercalation of the stalk cells in response to the tip cell traction, promoted by expression of *knirps* and turnover of surface E-cadherin [Caussinus et al., 2008, Chen et al., 1998, Shindo et al., 2008]. Once it reaches the midline, the tip cell dorsal migration is inhibited by DPP emanating from the leading edge cells of the dorsal epidermis. Therefore, the tip cell makes a U-turn towards the anterior of the embryo, thus ending the dorsal migration of the dorsal branch [Hayashi and Kondo, 2018]. The second cell then fuses with the second cell of the contralateral side and form the dorsal anastomosis.

B) The Dorsal closure process

Dorsal Closure is the morphogenetic event that turns the embryo of *D. melanogaster* from an open kayak-like shape into a seamless closed maggot. My PhD work is dedicated to the understanding of the physical interplay between the embryo's organs that drive such morphogenesis, and how it is regulated by the interplay between JNK and DPP signaling. In this section, I will first describe the morphogenesis of the two main actors of dorsal closure: the dorsal epidermis and the amnioserosa. Then, I will recapitulate the current knowledge about the nature of the forces responsible for the morphogenesis process. At last for this section, I will summarize what is known about the JNK and DPP signaling interplay, and how they are involved in processes described above.

a) Dorsal Closure morphogenesis

i) Dorsal Closure initiation

Dorsal closure starts at the 13th stage of the embryo development, about 10 hours

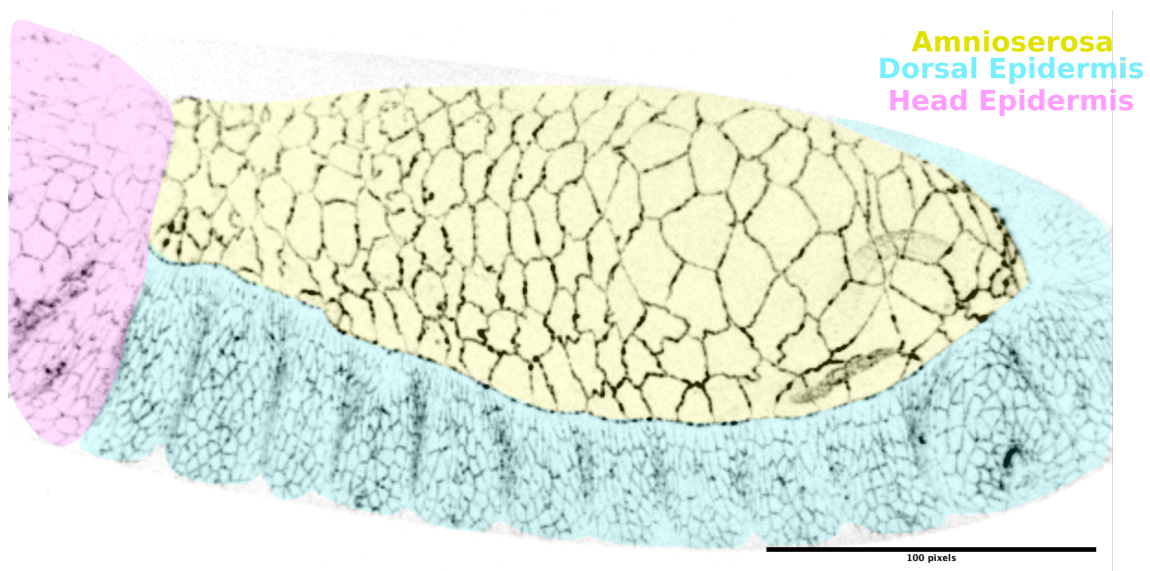


Figure I.19: Dorsal Closure initiation: Maximum projection of a *shg::mKate2* embryo

after fertilization at 25°C [Kiehart et al., 2017]. Prior to dorsal closure, during GBR, the leading-edge cells of the dorsal epidermis adhere to the amnioserosa and

already start to elongate dorsally [Narasimha and Brown, 2004, Gorfinkiel and Arias, 2007, Schöck and Perrimon, 2002]. In parallel, the amnioserosa tightly adheres to the underlying yolk cell [Narasimha and Brown, 2004, Reed et al., 2004]. Therefore, at the onset of closure, the embryo's dorsal trunk is composed of two dorsal epidermal sheets, separated but tightly linked by the squamous extra-embryonic amnioserosa that represents about 40 percent of the whole embryo circumference at the middle of the trunk [Campos-Ortega and Hartenstein, 1997]. Interestingly, at this stage, the amnioserosa possesses a right left symmetry but not an antero-posterior one. A large blunt interface separates the head and the amnioserosa at the anterior pole, leaving the thoracic segments on each side of the embryo far apart, whereas the posterior abdominal 8 segments of the dorsal epidermis start dorsal closure almost in contact [Kiehart et al., 2017] (Figure I.19).

ii) Dorsal Closure onset

As dorsal closure starts, the amnioserosa cells apical face start to oscillate with a 4

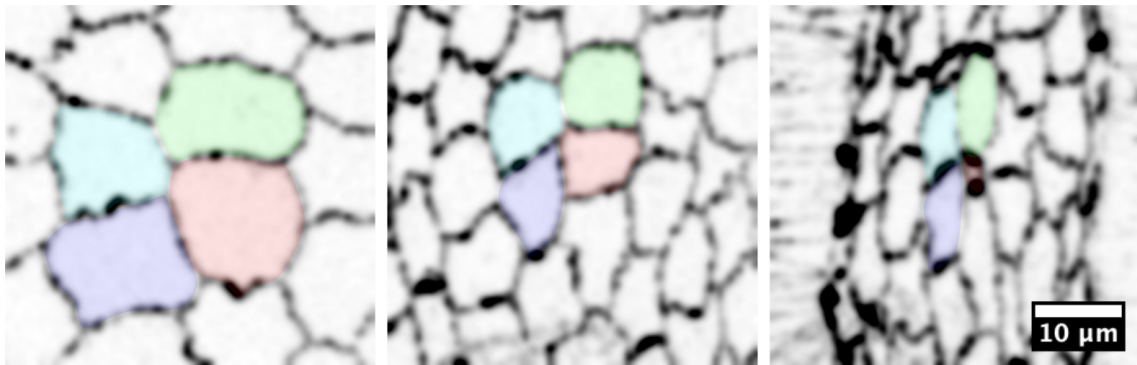


Figure I.20: Amnioserosa morphogenesis during dorsal closure: Close up on the amnioserosa of a *shg::mKate2* embryo, single cells are tracked and color coded.

minute period. This oscillatory behavior is associated with a graduated decrease of the amnioserosa cells area, hence promoting the apical area shrinking of the whole tissue [Solon et al., 2009] (Figure I.20). However, as dorsal closure progresses, amnioserosa cells cease to oscillate and start to contract even faster [Gorfinkiel et al., 2009]. This apical behavior is coupled with a progressive loss of the amnioserosa

cells internal volume [Saia et al., 2015]. Furthermore, a subset of cells, approximately 10 to 30 percent of the total number of cells at the onset of closure, undergoes apoptosis-dependent delamination during dorsal closure preferentially in the anterior half of the amnioserosa [Toyama et al., 2008, Mulyil et al., 2011] (see the red cell of Figure I.20). Altogether, these processes lead to the progressive shrinkage of the dorsal hole of the embryo during dorsal closure.

In parallel with the amnioserosa shrinking, the dorsal epidermal cells get polar-

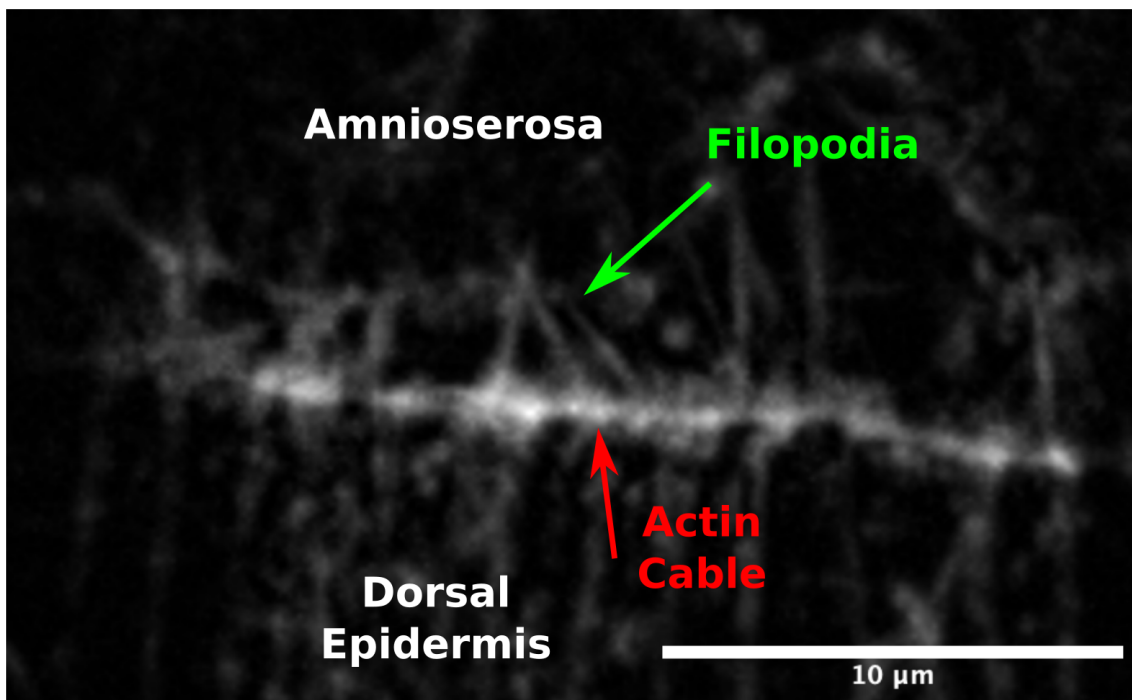


Figure I.21: Leading edge cells produce a supra-cellular acto-myosin cable and filopodia: Close up of the leading edge of a *UAS-lifect, pnr-Gal4* embryo

ized and elongate apically towards the midline. Two key mechanisms support this elongation. First, the adherent junctions at the antero-posterior boundary between dorsal epidermal cells elongate towards the midline [Kaltschmidt et al., 2002]. Second, the apical microtubule cytoskeleton of dorsal epidermal cells get transiently polarized along the dorso-ventral axis during dorsal closure [Jankovics and Brunner, 2006]. Concomitantly, the leading edge cells of the dorsal epidermis, at the interface with the amnioserosa, start to expand dynamic lamellipodia and filopodia over the amnioserosa [Jacinto et al., 2000] (Figure I.21). Interestingly, this migratory behavior is not associated with migration of the epidermis over the amnioserosa.

Instead, the leading edge cells keep their attachment with the same amnioserosa cell which they progressively cover until they reach their contra-lateral counterparts [Wada et al., 2007]. Moreover, the leading edge cells do not lose their epithelial nature, as they keep strong adherent junctions with their neighboring dorsal epidermis cells [Kaltschmidt et al., 2002]. Simultaneously, leading edge cells produce a supra-cellular actomyosin cable at the interface of with amnioserosa, thus resulting in the interface linearization [Kiehart et al., 2000, Jacinto et al., 2002](Figure I.21).

iii) The Dorsal Closure zipping phase

As the amnioserosa contracts and both dorsal epidermis sheets elongate, the leading

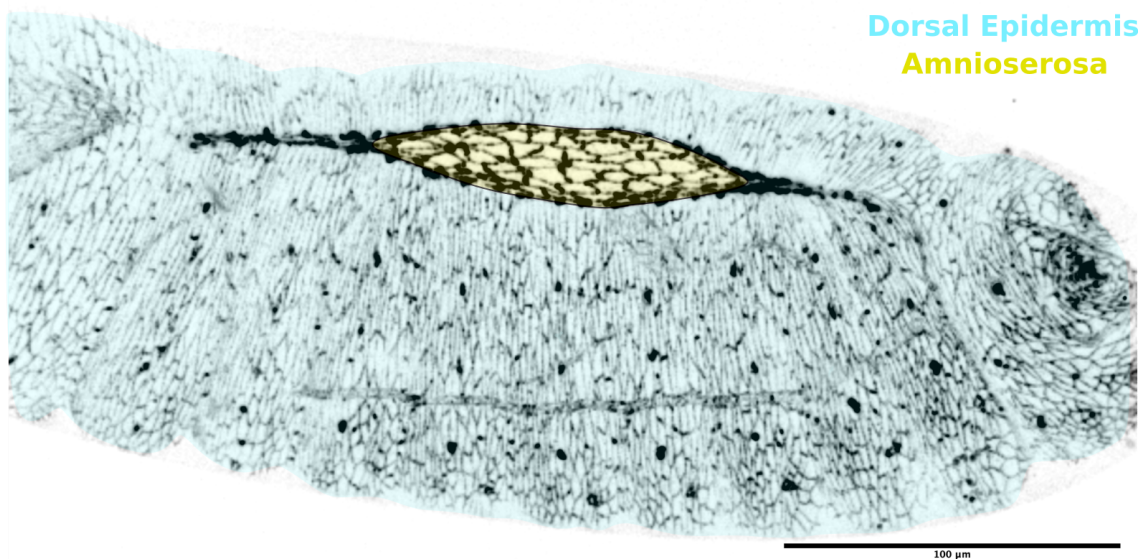


Figure I.22: The Dorsal Closure zipping phase: Maximum projection of a *shg::mKate2* embryo

edge cells meet at the midline. The two epidermal sheets meet first at the posterior and then at the anterior pole thus forming structures known as canthi. Thus, the amnioserosa adopts an eye-shaped morphology (Figure I.22). Progressively, the two sides of the dorsal epidermis zip together as the canthi progress towards the center of the antero-posterior axis of the embryo. As the cells zip together, they form new adherent junction thus definitively closing the gap [Bahri et al., 2010]. This zipping process allows the perfect matching of the leading edge cells with

their counterparts on the opposite side, thus leading to a seamless single dorsal epidermis layer. Interestingly, the filopodia from the dorsal epidermis contribute to zipping, but seem to be required only for the perfect matching of the two epidermis sides [Jacinto et al., 2000, Millard and Martin, 2008] (Figure I.23). As closure progresses, amnioserosa cells that did not delaminate individually during the bulk of closure acquire a wedge shape visible in Z sections and delaminate together as they are covered by the fusing dorsal epidermis [Kiehart et al., 2000, Toyama et al., 2008, Sokolow et al., 2012, Saias et al., 2015].

By the end of closure, the two canthi meet. The dorsal epidermis is now composed of one single cell layer and the embryo is closed.

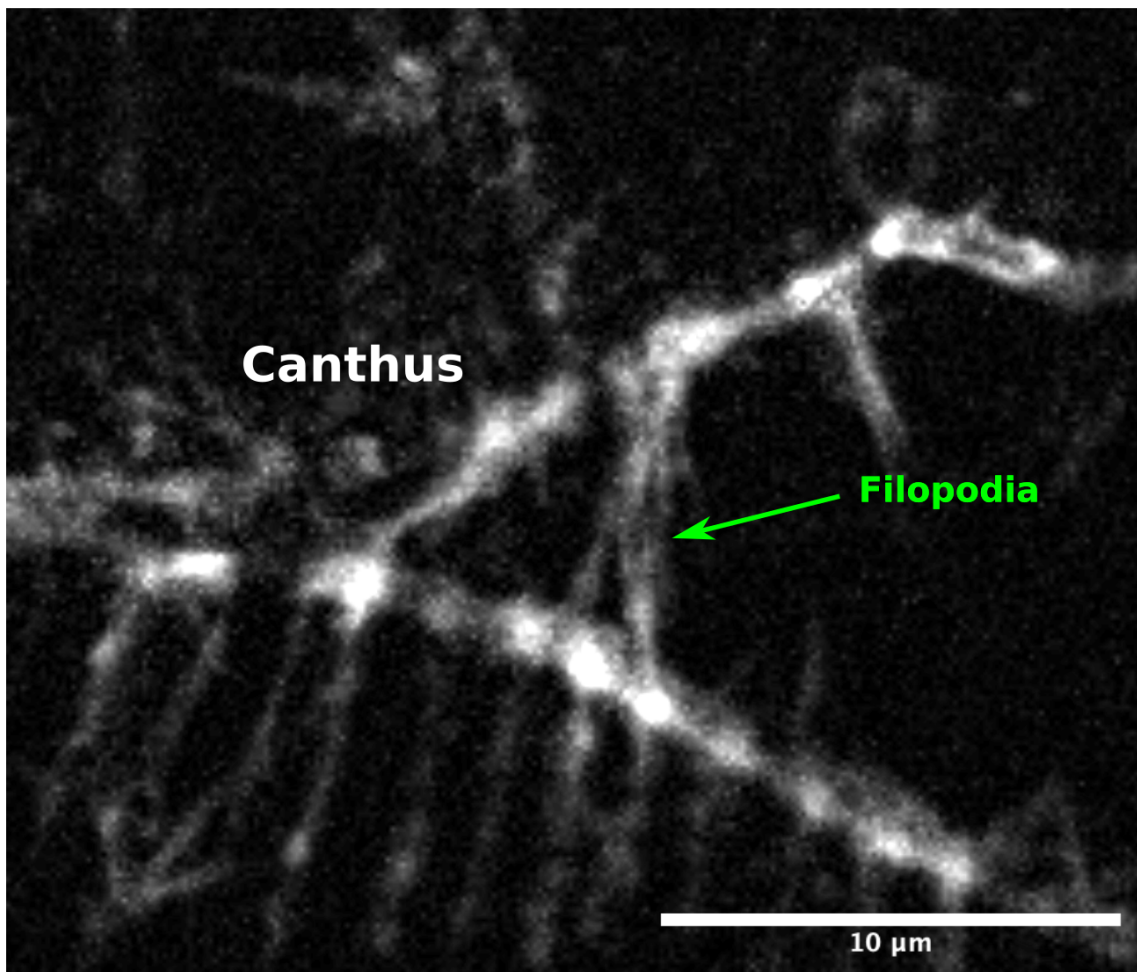


Figure I.23: Contralateral fusion at the canthus is initiated by filopodia: Close up of the canthus of a *UAS-lifect, pnr-Gal4* embryo

b) Physical cues during dorsal closure

Four distinct forces are thought to interact during closure: traction from the amnioserosa, zipping from the canthi, contraction of the supra-cellular actin cable and resistance from the dorsal epidermis. Moreover, distinct types of cell adhesion are crucial to resist such forces during dorsal closure.

i) Traction from the amnioserosa

The amnioserosa is under isotropic tension during dorsal closure [Lu et al., 2016]. Moreover, laser ablation experiments have demonstrated that the amnioserosa exerts traction on the dorsal epidermis, and that this traction force alone is sufficient to drive dorsal closure [Kiehart et al., 2000, Wells et al., 2014]. Each AS cell participates to the collective traction. Indeed, isolation from their neighbors of any single amnioserosa cell during dorsal closure using circular laser ablation resulted in their individual contraction and delamination [Jayasinghe et al., 2013].

Traction forces are thought to come from two phenomena, the acto-myosin oscillation and contraction of the amnioserosa cells combined with their delamination during dorsal closure. The amnioserosa cells oscillate and contract due spatio-temporal waves of activity of the non-muscle myosin 2 Spaghetti-squash (Sqh) within each AS cell, coupled with a ratchet-like mechanism of the leading edge actin cable [Solon et al., 2009]. The arrest of AS cell oscillation is associated with stabilization of the Sqh complexes within the cells that is thought to drive a more rapid contraction [Blanchard et al., 2010]. Furthermore, the complete removal of Sqh activity within the amnioserosa totally prevents amnioserosa contraction and leads to dorsal closure failure [Pasakarnis et al., 2016].

In parallel, the individual delamination of 10 to 30 percent of the AS cells contributes to the traction process [Toyama et al., 2008, Muliyl et al., 2011]. Indeed, the delamination of one AS cell drives the contraction of its neighbors that in turn increase tension. It is also thought to remove supernumerary AS cells that are in the way of the dorsal epidermis. However, it is important to note that preventing

cell delamination only slows dorsal closure down but does not stop it. Therefore, AS cell delamination during the bulk of closure contributes to AS traction, but is not absolutely required for the process.

A recent study proposed an alternative hypothesis [Saias et al., 2015]. The authors showed that preventing AS cell volume decrease through inhibition of water efflux prevents dorsal closure, whereas Sqh inhibition does not. Therefore, the traction from the amnioserosa would be the consequence of AS volume loss. However, the authors from [Pasakarnis et al., 2016] contested these results. They show that the Sqh inhibition method in the AS was incomplete. Therefore, as both the inhibition of apical contraction and cell volume decrease lead to dorsal closure failure, the two processes must be necessary to drive AS traction forces during dorsal closure, maybe in a related way. An alternative hypothesis would be that water efflux is driven by increased hydrostatic pressure due to the apical contraction of the AS cells.

ii) Forces generated by the zipping process

As of today, the physical contributions of the zipping to dorsal closure remain unclear. However, zipping contributions are computed within several physical mathematical models describing dorsal closure [Hutson et al., 2003, Peralta et al., 2007, Solon et al., 2009, Wang et al., 2012a, Almeida et al., 2011, Jayasinghe et al., 2013, Hayes and Solon, 2017]. This hypothesis is supported by experimental data showing that inhibition of the zipping process through microtubule function impairment prevents dorsal closure [Jankovics and Brunner, 2006]. However, it was previously showed that impairing filopodia production and maintenance would only affect tissue pairing accuracy without stopping dorsal closure [Jacinto et al., 2000]. However, one can still take into account that the zipping process stitches both sides of the dorsal epidermis together. Therefore, it could promote dorsal closure as a ratchet-like mechanism.

iii) The actin cable

The actin cable at the leading edge has long been thought to generate a force during

dorsal closure, that may stem from two distinct mechanisms. First, the cable may act as a ratchet for AS cells contraction [Solon et al., 2009]. However, it is mostly considered as a contractile purse string that drives tissue curvature and therefore brings the dorsal epidermis flanks together during dorsal closure [Young et al., 1993, Kiehart et al., 2000, Jacinto et al., 2002, Rodriguez-Diaz et al., 2008].

Nonetheless, two recent studies demonstrated that the actin-cable brings little to no forces during dorsal closure. In their study, *Pasakarnis et al* performed a total removal of Sqh activity within the dorsal epidermis, therefore preventing the actin cable contraction. As a result, they observed that it barely affects dorsal closure dynamics but rather impaired the zipping process [Pasakarnis et al., 2016]. The same observation were made by *Ducuing et al* who observed dorsal closure in embryos mutant for the *zasp52* gene, which is required for the actin cable assembly [Ducuing and Vincent, 2016]. Furthermore, they showed that the tension brought by the actin cable in wild-type embryos is two orders of magnitude weaker than what would be necessary to act as a purse-string according to mathematical modelling. Finally, they observed that the loss of the actin cable resulted in the loss of the linearity of the dorsal epidermis leading edge cells. Such loss of linearity results in a scar phenotype by the end of dorsal closure, thus suggesting that the actin cable function is to prevent scars in the future larva.

iv) Dorsal epidermis resistance

Laser ablation studies have demonstrated that the AS exerts tension on the dorsal epidermis which reciprocally resists to elongation [Kiehart et al., 2000]. However, the mechanical properties of the dorsal epidermis and how it reacts to traction remains unclear [Kiehart et al., 2017]. A recent study argued that the epidermis pulling increases more and more on the AS as the tissue elongates, thus behaving like a spring [Lv et al., 2022]. However, it was previously shown that the traction exerted on the dorsal epidermis is constant during dorsal closure, thus contradicting the former statement [Saias et al., 2015]. Therefore, these authors later hypothesized that the dorsal epidermis behaves as a spring whose stiffness decreases with time,

thus allowing continuous elongation under constant tension [Trubuil et al., 2021]. During my PhD I performed a series of experiments in order to decipher the precise mechanical properties of the dorsal epidermis (see the Result section).

v) Forces transmission during dorsal closure

As any other morphogenetic events, transmission of forces between cells requires adherent junctions between cells and fixation to their substrate. Indeed, in order to contract efficiently, AS cells need to adhere to the underlying yolk sac through integrin mediated adhesion [Goodwin et al., 2016, Goodwin et al., 2017]. Furthermore, transmission of the contraction between amnioserosa cells requires adherent junction [Goodwin et al., 2017]. Furthermore, cell-cell adhesion is also required to drive transmission of forces between the amnioserosa and the dorsal epidermis. The close juxtaposition of the leading edge cells with the AS is integrin mediated [Narasimha and Brown, 2004, Wada et al., 2007]. Moreover, embryos mutant for the *shotgun (shg)* E-cadherin show large ripping events at the interface between the AS and the leading edge, thus demonstrating the key role of adherent junction in the transmission of forces between the two tissues [Gorfinkiel and Arias, 2007].

c) Signaling during dorsal closure

Two signaling pathways are crucial for dorsal closure; the JNK and DPP pathways. In this section, I will first present the two pathways and their components, their spatio-temporal activation and target expression and finally I will expose the morphogenetic processes in which they are involved.

i) The JNK and DPP cascades

The JNK pathway

The JNK pathway belongs to the class of the MAPKs pathways. This pathway acts as a conserved stress mediator pathway in eukaryotic organisms. However

through the course of evolution it acquired other developmental functions [Ríos-Barrera and Riesgo-Escovar, 2013]. Components of the pathway have been identified from the famous Nüsslein-Vohldard/Wieschaus screens as their mutation results in the dramatic dorsal-open phenotype [Nüsslein-Vohldard et al., 1984, Jürgens et al., 1984, Wieschaus et al., 1984]. The most upstream component whose mutation results in dorsal closure failure is the JN3K Slipper (Slpr) [Stronach and Perrimon, 2002]. Once activated, it phosphorylates the JN2K Hemipterous (Hep) [Glise et al., 1995]. When phosphorylated, Hep phosphorylates the Basket (Bsk) JNK [Riesgo-Escovar et al., 1996, Sluss et al., 1996]. Last in the cascade is the homolog of c-Jun: Jun-related antigen (Jra). Once phosphorylated by Basket, it associates with Kayak (Kay/Fos) in order to form the AP-1 leucine-zipper transcription factor, which leads to the transcription JNK signaling targets [Bogoyevitch and Kobe, 2006].

JNK signaling is regulated spatio-temporally by a series of inhibitors, at different levels of the pathway. Puckered (Puc), a transcriptional target of JNK signaling, acts as a Basket phosphatase, thus creating a negative feedback loop of regulation of the pathway [Martín-Blanco et al., 1998]. Another negative feedback loop involves the gene *scarface* (*scaf*), which is a target of Jun signaling that encodes a secreted protein [Rousset et al., 2010]. However, the precise mechanism of JNK signaling inhibition by Scaf remains unknown. The *Yan/anterior-open* gene (*aop*) encodes a transcriptional inhibitor of JNK signaling targets. When phosphorylated, Basket in turn phosphorylates Aop thus resulting in its translocation to the cytoplasm and allowing AP-1 dependent transcription [Rebay and Rubin, 1995, Riesgo-Escovar and Hafen, 1997]. The gene *raw* also encodes an inhibitor of the pathway, impairing Jra phosphorylation by Basket [Bates et al., 2008]. Finally, the protein encoded by the gene *peb* prevents the translocation of AP-1 to the nucleus [Reed et al., 2001]. Those inhibitors are crucial for the dorsal closure process as they shape the pattern of JNK signaling activation during dorsal closure.

The DPP pathway

DPP is the *D. melanogaster* homologue of BMP 4 from the TGF- β BMP family.

The *dpp* gene encodes a secreted peptide that can act as a morphogen, for example during wing-disc development [Nellen et al., 1996, Affolter and Basler, 2007]. During early *drosophila* embryogenesis, it acts as a crucial organizer of dorsal tissues that I mentioned earlier in this introduction. Furthermore, mutation of *dpp* leads to ventralized embryos [Irish and Gelbart, 1987]. DPP signaling is initiated by its binding to its receptor complex, formed by the heterodimer of Thickveins (Tkv) and Punt [Brummel et al., 1994, Penton et al., 1994, Letsou et al., 1995, Ruberte et al., 1995, Nellen et al., 1996]. DPP binding results in the phosphorylation of Tkv by Punt, which in turn phosphorylates its target Mother against DPP (Mad) [Raftery et al., 1995, Sekelsky et al., 1995]. Mad therefore binds to its partner Medea (Med) and translocates to the nucleus. In the nucleus, they form a complex with Schnurri (Shn)[Arora et al., 1995, Grieder et al., 1995]. The complex acts as a transcriptional inhibitor of *brk*, a transcription factor that negatively regulates the targets of DPP signaling [Jaźwińska et al., 1999, Marty et al., 2000]. Interestingly, there are two classes of DPP targets: targets that just need loss of Brk repression to be transcribed and targets that need both Brk repression and Mad/Med binding to their promoter. During dorsal closure, targets of the DPP pathway require only Brk repression in order to be expressed [Marty et al., 2000].

As for JNK signaling, DPP signaling is also regulated by a negative feedback loop. Activation of the DPP pathway results in the transcription of *daughter-against-dpp* (*dad*) [Tsuneizumi et al., 1997]. The Dad protein in turn binds Tkv and prevents Mad phosphorylation, therefore impeding DPP signaling [Inoue et al., 1998].

ii) Spatio-temporal activity of the JNK and DPP pathway during dorsal closure

There are three waves of DPP signaling during *D. melanogaster* development. The first one, from stage 5 to the onset of GBE, specifies the amnioserosa while the second wave occurring at stage 9 specifies the dorsal epidermis [Dorfman and Shilo, 2001] (Figure I.24). From gastrulation to the onset of dorsal closure, DPP signaling

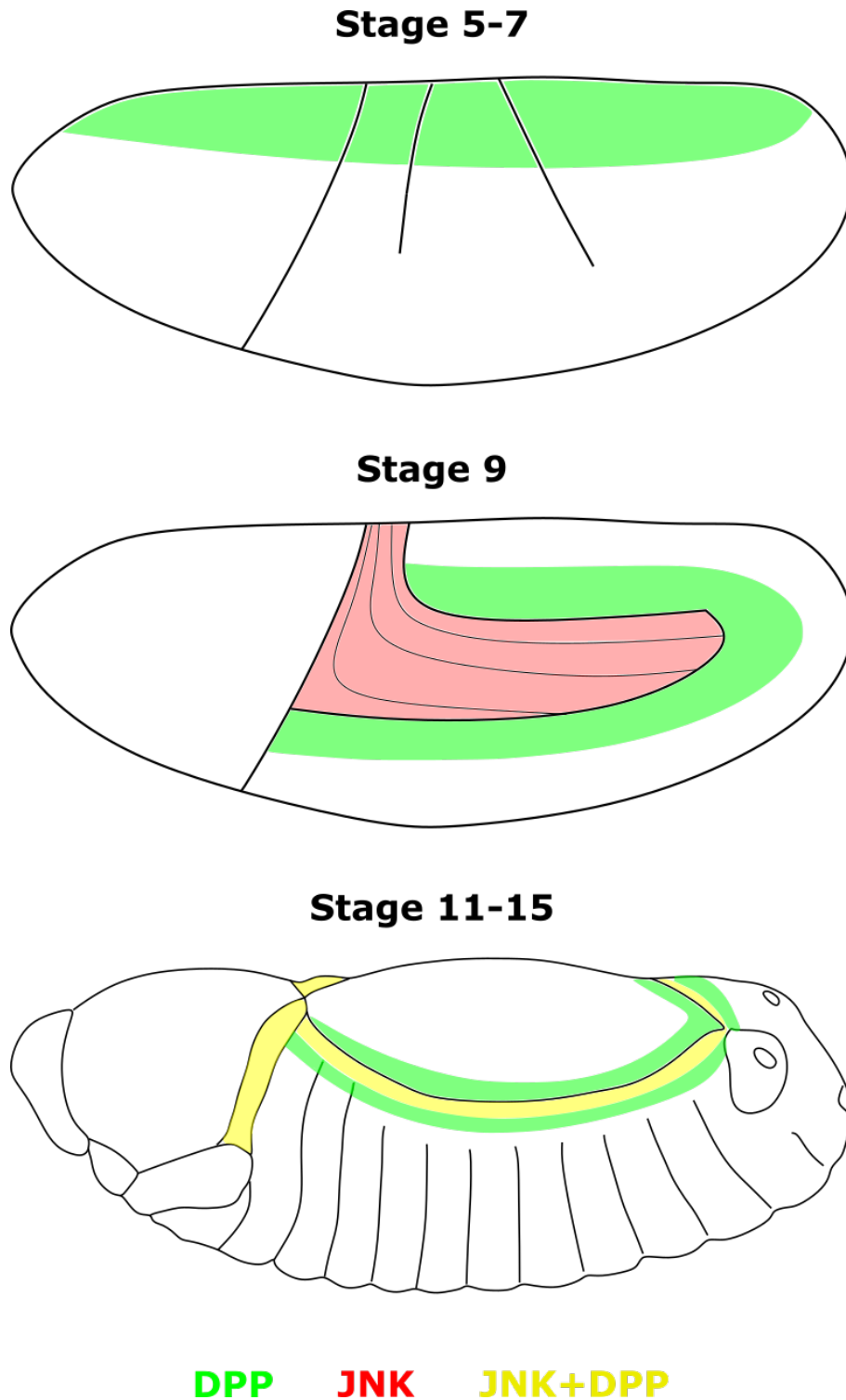


Figure I.24: DPP and JNK signaling during *D. melanogaster* embryogenesis: Two early waves of DPP pattern the amnioserosa and the dorsal epidermis. JNK signaling is transiently active in the amnioserosa by stage 9-10. Together, JNK and DPP signaling pattern the interface between the amnioserosa and the dorsal epidermis by stage 11.

drives the expression of the GATA factor gene *pannier* (*pnr*) in the dorsal ectoderm. As development proceeds, *pnr* expression is confined to the AS and dorsal epidermis before disappearing from the AS by the GBR stage [Herranz and Morata, 2001]. Another DPP target is expressed in both the AS and dorsal epidermis: the gene *u-shapped* (*ush*) [Ashe et al., 2000, Fernández et al., 2007]. Interestingly, contrary to *pnr*, its expression is kept in the AS throughout dorsal closure.

Prior to GBR, the JNK pathway is also active in the AS and the dorsal epidermis leading edge cells. Its activity is then shut down by *Peb* in the amnioserosa [Reed et al., 2001] (Figure I.24). Interestingly, *peb* has been shown to be a target of *Ush* in the amnioserosa only [Fernández et al., 2007]. Little is known so far about the genetic cascade that restricts the activation of the JNK signaling pathway to the first two rows of leading-edge cells. An interesting hypothesis is that at the onset of GBR, the entire epidermis would induce JNK signaling due to mechanical stress. However, *Peb* activation in the AS coupled with *Aop* and *Raw* inhibition in the lateral epidermis restricts JNK activity in the leading edge cells, thus allowing the precise patterning of JNK pathway activation [Ríos-Barrera and Riesgo-Escovar, 2013].

By the onset of GBR, JNK signaling activates DPP transcription [Glise and Noselli, 1997, Hou et al., 1997, Kockel et al., 1997, Riesgo-Escovar and Hafen, 1997] (Figure I.24). By this stage, it becomes the sole source of DPP within the dorsal epidermis as shown by phospho-Mad staining [Fernández et al., 2007]. JNK signaling also drives the expression of *puc* in the same subset of cells [Martín-Blanco et al., 1998]. Interestingly, it has been shown that induction of *dpp* by *Jra* necessitates both *ush* and *pnr*, the two DPP targets [Stronach and Perrimon, 2001, Herranz and Morata, 2001]. Additionally, *puc* expression at the leading-edge also requires *Ush* expression in the amnioserosa [Lada et al., 2012]. Nonetheless, *Pnr* is not involved in this process [Herranz and Morata, 2001]. Together, JNK and DPP signaling interact as a feed forward loop activating the transcription of a range of effector proteins during dorsal closure such as the E-Cadherin *Shg*, the microtubule binding protein *Jupiter*

and the actin binding protein Zasp52 [Ducuing et al., 2015].

iii) The dorsal-open phenotype and JNK/DPP target genes during dorsal closure

Loss of components from both these pathways result in a dramatic failure of dorsal closure, as identified in the Nüsslein-Vohlard/Wieschaus screens [Nüsslein-Volhard et al., 1984, Jürgens et al., 1984, Wieschaus et al., 1984]. The dorsal open phenotype consists in a complete evisceration of the embryos as the embryo fails to join the two sides of the dorsal epidermis sheet.

Several targets of both signaling pathways provide interesting clues about the reason of such failure. For example, both pathways are crucial to mediate adhesion between the AS and leading edge cells. JNK signaling is required for laminin synthesis within the basal membrane that links the two tissues [Narasimha and Brown, 2004, Sorrosal et al., 2010]. Moreover, JNK also regulates the transcription of the *scab* (*scb*) and *myospheroid* (*mys*) integrin genes in the leading-edge [Homsy et al., 2006]. Additionally, the transcription of the *scb* gene in the amnioserosa cells, which is required for its juxtaposition to the leading-edge, has been shown to require DPP signaling [Wada et al., 2007]. Furthermore, the *shg* gene essential for adherent junction between the two tissues is a target of the JNK/DPP feed forward [Ducuing et al., 2015]. Therefore, JNK/DPP signaling pathways are crucial to mediate adhesion between the AS and dorsal epidermis.

The protrusion of filopodia at the leading-edge and the formation of the actin cable also depends on the same feed-forward loop. Interestingly, the Jupiter protein, a target of the feed-forward, promotes microtubule polymerization in the early embryo, a process involved in filopodia formation [Karpova et al., 2006, Jankovics and Brunner, 2006].

Moreover, the mutation of the Zasp52 protein, also a feed-forward target, results in the absence of the actin-cable, like in mutants for the JNK/DPP pathways [Ducuing and Vincent, 2016, Homsy et al., 2006, Fernández et al., 2007]. Hence, cytoskeletal

rearrangements observed during dorsal closure depend on both JNK and DPP signaling targets.

A series of experiments also showed that both Jun activation in the leading-edge, AS cell contraction and dorsal epidermis cell elongation depend on DPP signaling in the AS, through the transcription of *ush* [Fernández et al., 2007, Lada et al., 2012]. Those results suggest that JNK and DPP signaling are required as early as the initiation of dorsal closure. Finally, it has been shown that DPP signaling prevents JNK-mediated apoptosis induction in the leading-edge cells [Beira et al., 2014]. Therefore, DPP signaling would promote cell survival in a mechanically stressful event such as dorsal closure.

Interestingly, numerous observations that I performed are in contradiction with the dogma that I just described. By carefully monitoring AS contraction, epidermis elongation and cell death using high temporal resolution confocal microscopy, I bring within this thesis a set of new hypotheses to explain the precise role of the JNK and DPP pathways during dorsal closure.

C) Head involution

Concomitantly to dorsal closure, another large morphogenetic event occurs at the embryo scale. The embryonic head invaginates within the thoracic segments, thus creating a major tissue movement orthogonal and underneath the epidermis involved in dorsal closure. During my PhD thesis I hypothesized that the dorsal open phenotypes of *tkv* and *jra* mutants could be the consequence of a loss of synchrony between dorsal closure and head-involution. Therefore, part of my thesis work is focused on the head-involution process.

a) Morphogenesis during head involution

Head-involution has been significantly less studied than dorsal closure, due to the complexity of the phenomenon and difficulty of accessibility through classical microscopy. The whole process has however been extensively described by Turner and Mahowald using scanning electron microscopy [Turner and Mahowald, 1979]. Head-involution starts concomitantly with GBR and ends by the end of dorsal closure. It starts by the complete invagination of the hypopharyngeal region within the stomodeum. Concomitantly, the labial appendages form salivary ducts and migrate ventrally. They fuse at the midline, thus forming only one salivary duct. The invagination of the hypopharyngeal region is followed by the partial invagination into the stomodeum of the dorsal clypeolabrum, ventral labium and lateral maxillary and mandibular appendages, thus forming the mouth parts of the future larva. By the end of head-involution, the clypeolabrum and labium are almost entirely invaginated within the stomodeum.

Dorsally, two ridges form and elongate towards the dorsal midline in synchrony with the first thoracic segment during dorsal closure (Figure I.25). They precede the thoracic segments and fuse at the midline. These events initiate the migration of the thoracic segments over the dorsal head epidermis as thoracic segments fuse at the dorsal midline in a synchronized manner [VanHook and Letsou, 2008]. The

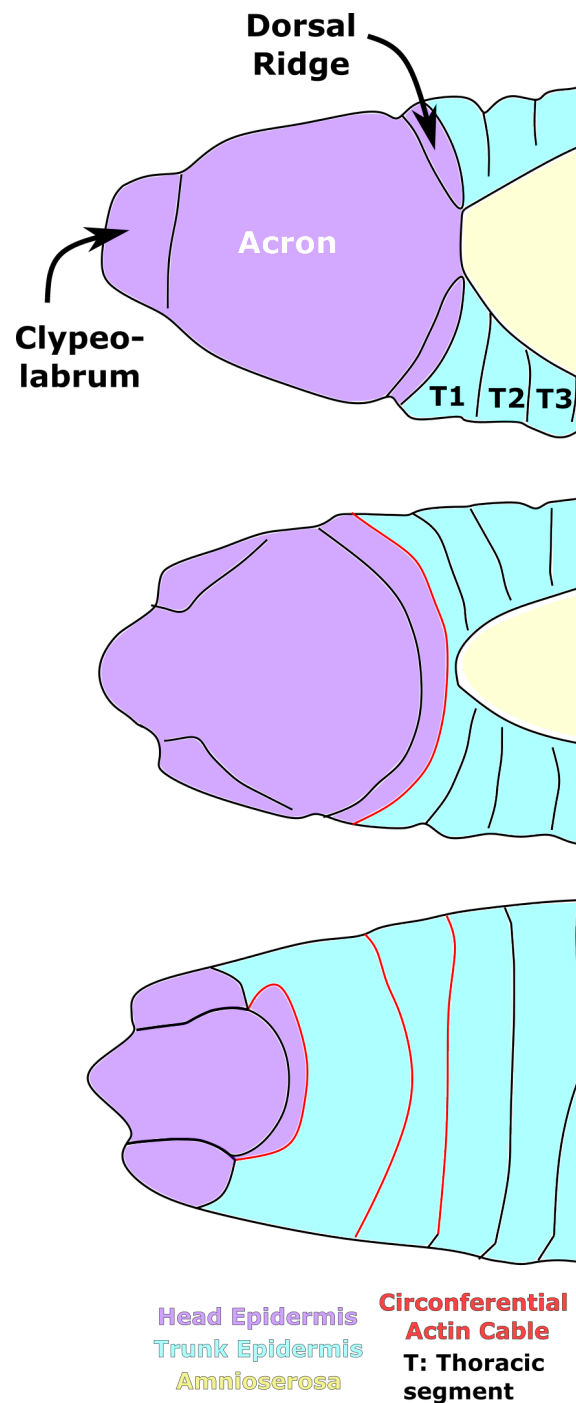


Figure I.25: Dorsal view of the head involution process: At stage 13, both sides of the dorsal-ridge are separated. By stage 14, the fuse and migrate over the head epidermis followed by the thoracic segments. By stage 15, the head epidermis is covered by the thoracic segments.

dorsal ridge acts as the leading edge of the thoracic segment anterior migration and will later on form the dorsal lip of the larva mouth. Simultaneously, the optic lobes are propelled towards the interior of the embryo.

b) Physical cues during head involution

As of today, only one model addresses the physical cues at play during head-involution [Czerniak et al., 2016]. This study states that the forces propelling and spreading the segments over the head during dorsal closure come from the contraction of circumferential supra-cellular actomyosin cables within the dorsal ridge and posterior parts of the thoracic segments (Figure I.25). This phenomenon is the consequence of *hedgehog* signaling, which is predictable as those regions differentiation depends on *hedgehog*.

However, observations I performed during my thesis show that thoracic anterior migration occurs independently of circumferential cables in the absence of dorsal closure. Furthermore, I identified a subset of cells in the head-epidermis involved in thoracic anterior traction (see the Results section).

c) Signaling during head-involution

Signaling during head-involution also remains elusive. It has mainly been studied through the observation of mutants. First, as dorsal closure and head-involution are simultaneous and involve common tissues, failure of dorsal closure involves subsequent failure of head-involution. Therefore, the JNK and DPP pathways are reported as regulator of head-involution [VanHook and Letsou, 2008].

However, other signals can result in head-involution failure associated with completion of dorsal closure. Morphological defects in head-involution have been mainly observed in mutants of pro-apoptotic genes: *head-involution-defective (hid)*, *reaper (rpr)*, *dronc*, *scylla (scyl)* and *charbyde (chrb)* [Abbott and Lengyel, 1991, Nassif et al., 1998, Scuderi et al., 2006]. Indeed, lack of apoptosis in the CNS results in the lack of neuron and glia elimination, therefore leading to a head volume that is too

important to involute within the thoracic segments as head-involution proceeds. Small GTPases signaling is also involved during dorsal closure. Indeed, *rho1* mutants manage to fulfil dorsal closure but the head-involution does not proceed at all [Magie et al., , Jacinto et al., 2002]. As of today, this remains the only known mutation that blocks head-involution entirely, apart from mutations in the ecdysone pathway that arrest both dorsal closure and head-involution.

Chapter II

Results

I) DPP signaling and morphogenesis potential

My main piece of work during this thesis consists in understanding the precise role that DPP plays during dorsal closure. When I started to address this matter, the consensus was that DPP signaling just preceding dorsal closure drives amnioserosa contraction and that JNK signaling, by inducing DPP from stage 11, drives epidermis elongation and its adherence to the amnioserosa [Fernández et al., 2007, Lada et al., 2012].

The story could have ended here. However, by observing contraction in the amnioserosa of *tkv* mutants, we started to question this model. My approach was to combine high resolution 4D imaging, laser ablations and precise quantification of morphological changes observed in embryos deficient for JNK and DPP signaling during dorsal closure to further understand their precise requirements and actions. In the following manuscript, I show how DPP signaling provides a morphogenetic potential to the organs that it patterns hours before rather than during dorsal closure. Indeed, I demonstrate that amnioserosa contraction relies on DPP emitted within the stage 5 to 7 of embryogenesis, when the tissue is patterned. Similarly, I identify that the visco-elastic to visco-plastic transition specific to the dorsal epidermis stems from DPP signaling during stage 9 while DPP patterns the dorsal epidermis. Finally, I show that the conjoint wave of JNK and DPP signaling, from stage 11 to the end

of dorsal closure, regulates adhesion at the interface between the amnioserosa and the dorsal epidermis. Altogether, I propose a model that drastically upgrades the former understatement of signaling regulation of the dorsal closure process.

The dorsal epidermis morphogenesis potential stems from DPP signaling during dorsal closure

Baptiste Tesson, Stéphane Vincent
LBMC, ENS de Lyon

The precise series of events underlying morphogenesis is one of the great questions in developmental biology. Morphogens play a key role in patterning but the cellular properties that they endow cells with remain mysterious. Here we show that during *Drosophila* embryogenesis, DPP, the best example of a secreted morphogen, provides a morphogenetic potential to dorsal epidermal cells. At the cellular level this potential consists in generating plastic deformation in response to mechanical forces. Hence, without induction by DPP cells deform in an elastic manner, leading to catastrophic events such as embryonic collapse. On the other hand, plastic deformations allow the tissues to adapt to extensive morphogenetic events and provide flexibility and robustness to development, allowing the embryo to obtain its perfect shape and size.

1 Introduction

Morphogenesis is paradoxically the most obvious manifestation of development and one of the least understood biological processes. Indeed, a number of studies unraveled the identity of inter-cellular signals, characterized cell shape changes and deciphered forces, yet their how they get integrated remains unclear. Furthermore a global perspective of the impact of inter-cellular signals on forces is still lacking. One of the issues is the lag between the ligand-receptor interaction and the production of a specific output, especially when this one involves transcription and translation. On the other hand, forces exert their effect orders of magnitude faster. Thus, the temporal integration of signaling and mechanics to produce a stereotyped choreography that is exactly conserved between embryos of a given species remains a mystery.

Dorsal closure (DC) is a key morphogenetic event of the late *D. melanogaster* embryogenesis that was proposed to exemplify the control of morphogenesis by the BMP homologue DPP [1, 2, 3, 4, 5, 6]. Typi-

cally at mid-embryogenesis the embryo is left with a dorsal opening that is covered by a squamous tissue called the amnioserosa [7]. By a complex interplay between Myosin dependant contraction, programmed cell death and volume loss [8, 9, 10], this tissue generates the main forces involved in dorsal closure by pulling on the epidermis that elongates until it fuses at the midline [11, 12, 13]. Interestingly DPP was proposed to act in a reiterative manner on several tissues: A first wave of DPP early in development patterns the amnioserosa [14, 15, 16, 17] whereas the a later wave of DPP signaling induces its constriction [5, 18]. In a similar fashion a second wave of DPP induces the identity of dorsal epidermal cells [19, 17], while the third and last wave of DPP, once more induces a morphogenetic change by controlling their elongation. In addition this third wave fosters a robust adhesion between the amnioserosa and the dorsal epidermis both baso-laterally and through adherent junctions [20, 21, 22]. This model is elegant as the sequential patterning that stems from the two first waves of DPP allows a precise definition of the geometry while the third wave coordinates the dy-

namics of closure. Thus, this last wave of DPP is considered as one of the finest example of signaling-controlled morphogenesis by a diffusible signal [5]. Importantly the last wave of DPP is induced by JNK signaling [1, 2, 3, 4], and impairment of either JNK or DPP signaling induces a dramatic developmental failure. Among them, embryos deficient for DPP signaling, like the mutants for the receptor *tkv* as well as embryos lacking JNK input, like the mutants for the transcription factor gene *jra* both display a dorsal-open phenotype where organs get extruded [23, 24, 25]. This points out the crucial importance of the third wave of DPP signaling and on the control of cell behavior. Further, it raises the question as to how a lack of coordination can lead to such striking developmental failure. Specifically, how are signaling and mechanics integrated in the wild type situation to produce a perfectly shaped embryo?

Here we used a dynamic approach including both high frequency 3D imaging and laser ablation to clarify DPP function during dorsal closure. Surprisingly, we identify key differences between DPP and JNK mutant phenotypes, despite the fact that both lead to dorsal open embryos. Specifically DPP deficient embryos display a phenotype of higher complexity than JRA deficient embryos that results from a deficit in both the second and third waves of DPP signaling. In contrast to former models, we find no evidence for a DPP mediated induction of amnioserosa contraction nor an induction of the elongation of the dorsal epidermis. These behaviors appear DPP independent once the tissues have been correctly patterned by the two first waves of DPP signaling. Rather, it is the second wave of DPP, in the first half of embryogenesis that controls a visco-elastic to visco-plastic transition that materializes later on during dorsal closure. This visco-plastic character is crucial to the elongation of the tissue. In turn, elongation appears to constitute a purely mechanical reaction to the contraction of the amnioserosa. Interestingly DPP patterning is setting up the initial conditions of a system that appears to run purely on mechanical control. Our data show that the physical properties such as cell plasticity are essential for the embryo to scale with the shape of the eggshell and obtain its 3D geometry, a part of the DPP phenotype that has been overlooked previ-

ously. We propose a model where DPP acts on patterning sequentially with two first waves controlling the identity of the amnioserosa and the dorsal epidermis, and the third wave that fosters adhesion between these two tissues. Altogether we propose that DPP does not control forces in real time but rather provides a morphogenetic potential that is crucial in determining the final volume of the embryo.

2 Results

2.1 JNK and DPP signaling assume different functions during dorsal closure

To understand tissue mechanics during late embryogenesis we quantified the dynamics of the striking mutant phenotypes of loss of JNK or DPP function. Indeed impairment of either signal not only prevents dorsal closure, but also leads to a dramatic evisceration phenotype (Figure 1A-A’). The rationale is that this event, massive at the scale of the embryo, can provide useful information at the cellular level on the forces underlying morphogenesis. Thus, membranes were marked with CAAX::GFP expressed in all tissues, thus allowing a global view of the embryo at a cellular resolution. In control embryos, the stereotyped process of amnioserosa contraction coupled with dorsal epidermis zipping occurs in approximately 180 minutes (Figure 1A, Movie1A). In *jra* embryos, closure initiation appears normal. However, before closure completion the dorsal epidermis breaks away from the amnioserosa in several locations along the leading edge (Figure 1A’, green arrowheads, Movie 1A’). As noted by others before [4], this phenotype is highly penetrant and all the *jra* embryos we observed undergo evisceration. In *tkv* embryos the epidermis breaks away from the amnioserosa preferentially at the anterior and posterior poles of the amnioserosa (Figure 1A’’, green arrowheads, Movie1A’’). These breaches correlate with the contraction of the thoracic segments along the antero-posterior axis. Interestingly, this compression was not observed in *jra* mutants. Further analysis revealed that the complete separation between the epidermis and the am-

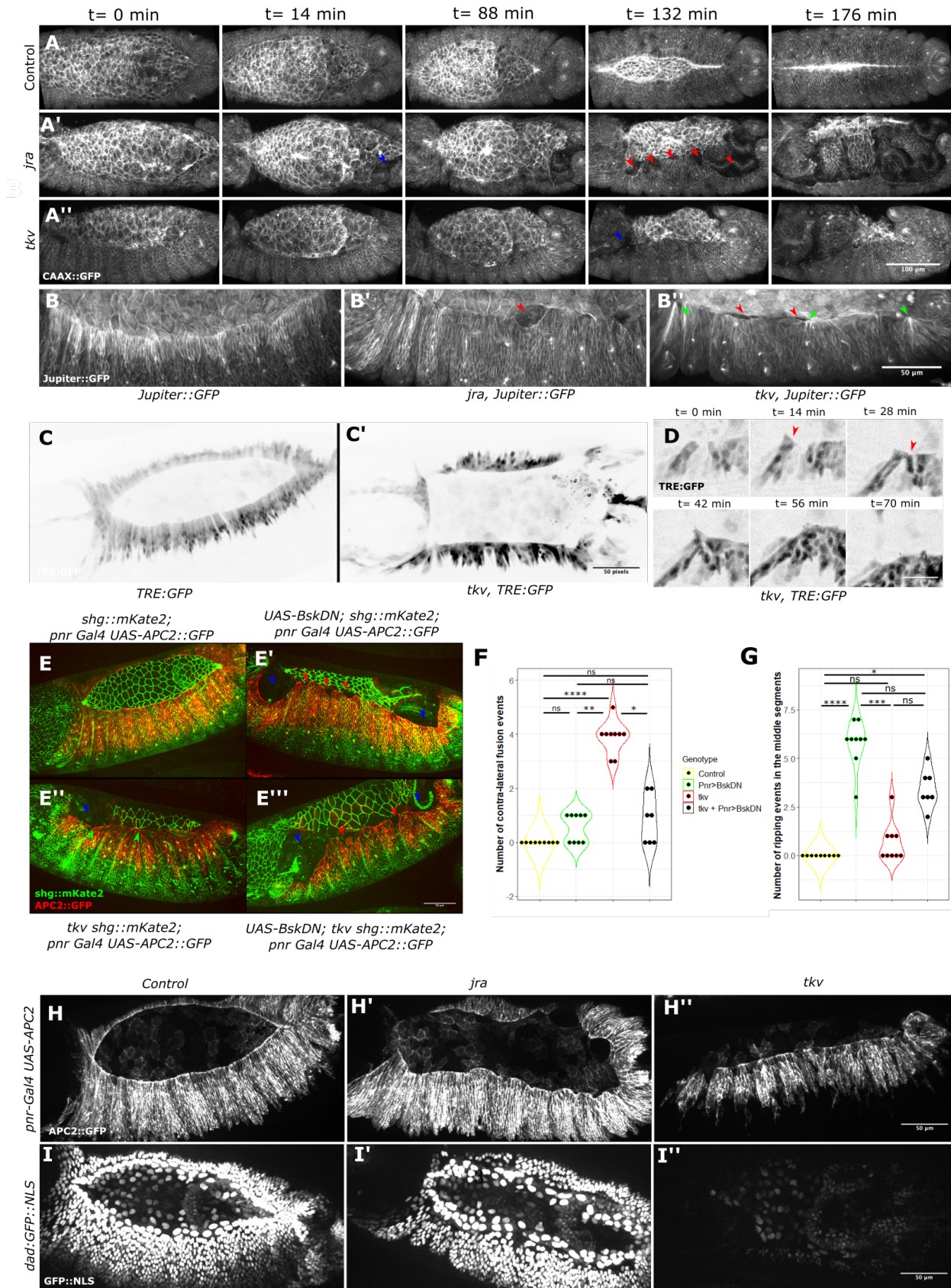


Figure 1: JNK and DPP signaling assume different functions during dorsal closure

A: Maximum of standard deviation projection of time-lapse imaging of *CAAX::GFP* (**A**), *jra/jra*; *CAAX::GFP* (**A'**) and *tkv4/tkv4*; *CAAX::GFP* embryos from the onset of DC. Blue arrowheads indicate ripping of the epidermis from the anterior or posterior pole of the amnioserosa, red arrowheads indicate ripping of the epidermis from the amnioserosa from the middle segments. **B:** Maximum projection of *Jupiter::GFP* (**B**), *jra/jra*; *Jupiter::GFP* (**B'**) or *tkv4/tkv4*; *Jupiter::GFP* (**B''**) at mid-DC. Red arrowheads indicate ripping of the epidermis from the amnioserosa from the middle segments, not associated with epidermis retraction for *tkv* mutant embryos. Green arrowheads indicate ipsilateral leading edge fusion events. **C:** Maximum projection of *TRE::GFP* (**C**), or *tkv8/tkv8*, *TRE::GFP::GFP* (**C'**) at mid-DC. **D:** Maximum projection of time-lapse imaging of *tkv8/tkv8*, *TRE::GFP::GFP* leading-edge during DC. Red arrowheads indicate protrusions from a LE cell fusing with its neighbor. **E:** Maximum projection of *shg::mKate2*; *pnr Gal4 UAS-APC2::GFP* (**E**), *UAS-BskDN*; *shg::mKate2*; *pnr Gal4 UAS-APC2::GFP* (**E'**), *tkv4/tkv4 shg::mKate2*; *pnr Gal4 UAS-APC2::GFP* (**E''**) and *UAS-BskDN*; *tkv4/tkv4 shg::mKate2*; *pnr Gal4 UAS-APC2::GFP* (**E'''**) at mid-DC. Blue arrowheads indicate ripping of the epidermis from the anterior or posterior pole of the amnioserosa, red arrowheads indicate ripping of the epidermis from the amnioserosa from the middle segments, green arrowheads indicate ipsilateral leading edge fusion events. **F:** Quantification of the number of ipsilateral fusion events observed in *pnr Gal4 UAS-APC2::GFP* (n=9), *UAS-BskDN*; *shg::mKate2*; *pnr Gal4 UAS-APC2::GFP* (n=9), *tkv4/tkv4 shg::mKate2*; *pnr Gal4 UAS-APC2::GFP* (n=9) and *UAS-BskDN*; *tkv4/tkv4 shg::mKate2*; *pnr Gal4 UAS-APC2::GFP* (n=7), compared by Kruskal-Wallis multiple comparison test, p-values adjusted with the Bonferroni method. **G:** Quantification of the number of leading-edge detachment observed in *pnr Gal4 UAS-APC2::GFP* (n=9), *UAS-BskDN*; *shg::mKate2*; *pnr Gal4 UAS-APC2::GFP* (n=9), *tkv4/tkv4 shg::mKate2*; *pnr Gal4 UAS-APC2::GFP* (n=9) and *UAS-BskDN*; *tkv4/tkv4 shg::mKate2*; *pnr Gal4 UAS-APC2::GFP* (n=7), compared by Kruskal-Wallis multiple comparison test, p-values adjusted with the Bonferroni method. **H:** Maximum projection of *pnr-Gal4 UAS-APC2::GFP* (**H**), *jra/jra*; *pnr-Gal4 UAS-APC2::GFP* (**H'**) or *tkv4/tkv4*; *pnr-Gal4 UAS-APC2::GFP* (**H''**) at mid-DC. **I:** Maximum projection of *dad::GFP::NLS* (**I**), *jra/jra*; *dad::GFP::NLS* (**I'**) or *tkv4/tkv4*; *dad::GFP::NLS* (**I''**) at mid-DC.
* : p - values < 0.05, ** : p - values < 0.01, *** : p - values < 0.001, **** : p - values < 0.0001

nioserosa in *tkv* embryos occurs progressively towards the center of the embryo. These preliminary observations indicate that while collective cell movements seem to occur in the mutants, tissue rupture is an important factor in the dorsal open phenotype, indicating that cell adhesion is a central component of dorsal closure [20, 21, 22]. Importantly, neither *jra* nor *tkv* mutants form any canthus and the contralateral epidermal sheets never fuse.

To better characterize the dynamics of the loss of adhesion between the dorsal epidermis and the amnioserosa, we performed time-lapse imaging of control, *jra* and *tkv* mutants (*jra* and *tkv* mutants were imaged on different occasions, maximum time-step = 15 minutes). We used a *Jupiter::GFP* background as *Jupiter* is a strong marker that is expressed in two overlapping patterns: The ubiquitous pattern marks all epidermal cells whereas the *JNK/DPP* controlled pattern displays a stronger signal at the leading edge (Figure 1B) [6]. Thus the lack of *Jupiter::GFP* accumulation allows the unambiguous identification of

jra or *tkv* mutants. In *jra* mutant embryos (Figure 1B', Movie1B'), the cells of the dorsal epidermis are polarized towards the dorso-ventral axis as in the wild type tissue. Detachment across the leading edge (green arrowhead) is associated with a rapid retraction of the dorsal epidermis. In *tkv* mutant embryos, dorso-ventral polarization is also observed at the onset of the process (Figure 1B'', Movie 1B''). However, the leading edge displays internal fusion events that correlate with cell autonomous accumulation of *Jupiter::GFP* (cyan arrowheads). Interestingly, the epidermal cells that detach from the amnioserosa (green-arrowheads) appear to bind to other cells from the same tissue, that is on the ipsilateral side. These "suture-like" autologous events appear to maintain the position of the tissue as we did not observe any ventral retraction at the detachment sites before the full rupture between the AS and the epidermis. This dynamic approach thus reveals clear differences between *JNK* and *DPP* loss of function and implies that *JNK* and *DPP* may control distinct

mechanical behavior at the cellular level.

As ipsilateral sutures observed in *tkv* embryos are absent in *jra* mutant, we investigated their potential link with JNK activity marked with TRE:GFP. Control embryos display a strong and rather homogenous pattern of TRE:GFP in the two rows of leading-edge cells (Figure 1C, Movie1C). As expected, TRE:GFP is also confined to the first two rows of cells in *tkv* mutant embryos (Figure 1C', Movie1C'). However, the TRE:GFP signal lacks homogeneity and ipsilateral sutures correlate with higher TRE:GFP expression (cyan arrowheads). Closer analysis of the ipsilateral sutures in a time dependent manner showed that ipsilateral sutures preferentially occur between cells expressing higher levels of early TRE:GFP (Figure 1D, Movie1D). These cells are able to extend protrusions over their neighbors and establish contact (red arrowheads). These contacts lead to ectopic adhesion between cells expressing high levels of TRE:GFP, that compress cells presenting low TRE:GFP. Thus, the suture mechanism observed in *tkv* mutants correlates with JNK pathway activity.

To test whether JNK signaling is required for the suture mechanism observed in *tkv* mutants, we inhibited JNK in the *tkv* context with UAS-BskDN driven by pnr-Gal4. We monitored the expression of shg::mKate2 and pnr Gal4 UAS-APC2::GFP constructs (Figure 1E-E', Movie1E-E') and quantified the number of ipsilateral sutures observed in each genotype (Figure 1F). Comparison using Kruskal-Wallis testing coupled with multiple-Dunn tests adjusted with the Bonferroni method showed that the number of ipsilateral sutures is significantly higher in *tkv* mutants compared to both control and embryos that lack JNK signaling. Furthermore, the number of ipsilateral sutures significantly dropped when JNK signaling was inhibited in *tkv* mutant embryos, suggesting that JNK signaling is required for ipsilateral sutures observed in *tkv* mutant embryos.

Next, we used live-imaging to quantify the number of detachment events between the epidermis and the amnioserosa (Figure 1G). We observed that the number of detachments was significantly higher in embryos lacking JNK activity at the leading edge compared to control and *tkv* mutant embryos as suggested by our previous observations. However, inhibition of

the JNK pathway in *tkv* mutants induced a 2.3-fold increase in epidermis retraction events, yet not significant after p-value adjustments. This suggests that JNK signaling is required for the adhesion between the dorsal-epidermis and the amnioserosa, even in the absence of DPP signaling.

To understand *jra* and *tkv* phenotypes at the tissue scale, we quantified dorsal epidermis elongation by monitoring cells in the Pannier domain using UAS-APC2::GFP driven by pnr Gal4 (Figure 1H-H', Movie1H-H'). Control embryos display a continuous elongation of the dorsal epidermis during DC. Surprisingly, *jra* mutants display elongation prior to detachment, while the dorsal epidermis fails to elongate in *tkv* mutants.

The presence of two distinct phenotypes is puzzling as JNK and DPP work together: not only JNK acts upstream of the late DPP expression that is restricted to the leading edge [1, 2, 3, 4], but JNK and DPP also form a feed-forward motif that controls the expression of several genes specifically expressed at the leading edge [6]. If *tkv* mutants prevent the interpretation of late DPP signals, we would predict identical phenotypes in JNK and *tkv* loss of function. A possible hypothesis would be that *tkv* mutants do not receive the input from earlier waves of DPP signaling. Indeed, *tkv* embryos present a maternal effect, but it remains unclear how long this effect precisely lasts. In order to test this hypothesis, we analyzed the pattern of DPP activity in JNK and *tkv* loss of function by monitoring the expression of Dad, an inhibitory SMAD that acts as a negative feed-back loop on DPP signaling [26, 27] (Figure 1I-I', Movie1I-I'). First we noticed that the pattern of Dad:GFP::NLS during DC is broader than the pMad pattern identified by *Fernandez et al* [5]. Indeed, cells from the whole pnr expression domain express Dad:GFP::NLS. This indicates that Dad:GFP::NLS reveals DPP activity present at the stage when DPP induces Pnr. As expected for a readout of DPP activity preceding DC, Dad:GFP::NLS pattern is wild-type in *jra* embryos. However, *tkv* embryos display a strong reduction of Dad:GFP::NLS expression in both their dorsal epidermis and amnioserosa. This indicates that *tkv* maternal effect stops before the onset of DC. Altogether *tkv* phenotype encompasses two distinct phases of

DPP activity, whereas *Jra* affects only the last wave. Specifically we conclude that the cell elongation phenotype of *tkv* embryos is not due to the DPP signal sent downstream of JNK, but rather to an earlier wave of DPP signaling.

2.2 Amnioserosa contraction and traction functions are not impaired in *tkv* mutants

The implication of an earlier wave of DPP in the phenotype of *tkv* embryos provides a useful avenue to understand the importance of cell elongation at the level of global morphogenesis. Recent studies showed that the traction generated by the amnioserosa is crucial to drive dorsal epidermis elongation [13]. Therefore, we studied the interaction between the amnioserosa and the dorsal epidermis in control, *jra* and *tkv* embryos expressing the CAAX::GFP membrane marker using time-lapse imaging. In order to visualize the association of the epidermis with the amnioserosa and its movement towards the midline, we performed transversal optical section of control embryos at the onset and mid closure (Figure 2A, associated to Movie2A). At the onset of closure (cyan channel), the amnioserosa forms a squamous tissue, overlying the circular yolk sac and linking the two sides of the dorsal epidermis [7] (Figure 2A). At mid-closure, the amnioserosa contracts, thus dragging the dorsal epidermis towards the midline, in close proximity to the vitelline membrane (see the yellow channel). At this stage, the peripheral amnioserosa cells and leading-edge cells are closely juxtaposed. The analysis of *jra* mutants revealed a similar tissue organization at the onset of closure (see the cyan channel of Figure 2A', and associated Movie2A'). At-mid closure (see the yellow channel), the amnioserosa contraction leads to the elongation of the dorsal epidermis towards the midline, close to the vitelline membrane. However, the close association between peripheral amnioserosa cells and leading-edge cells is lost. At the onset of closure, *tkv* embryos also show a similar tissue organization (see the cyan channel of Figure 2A'', and associated Movie2A''). However, at mid-closure the epidermis

fails to elongate towards the midline of the vitelline membrane (see the yellow channel). In contrast with WT and JRA embryos, the amnioserosa sinks towards the center of the embryo, thus resulting in a decrease of internal volume. We also noted the absence of juxtaposition between the peripheral amnioserosa cells and the leading-edge cells. Thus, the absence of epidermis elongation in *tkv* mutants is compensated at first by the modification of the 3D architecture of the embryo.

To test whether the collapse of the embryo stems from defects of amnioserosa contraction over time, we decided to quantify the dynamics of its contraction. Control (Figure 2B and Movie2B), *tkv* homozygous mutant (Figure 2B' and Movie2B') and *tkv/+* (data not shown) expressing the shg::GFP marker were simultaneously imaged in order to visualize their amnioserosa dynamics. We noticed that Wild-type and *tkv/+* embryos close with specific dynamics and therefore analyzed them separately hereafter. Experiments were performed in three different batches with the different genotypes and no batch effect was detected. We quantified the area of the AS with a 10 minutes time resolution for the complete DC process of control and heterozygous *tkv* mutant and stopped as evisceration occurred in *tkv* homozygous mutants. Quantification of the amnioserosa area over time of control embryos revealed a sigmoid-like dynamic of closure of the amnioserosa (Figure 2C). At first, the amnioserosa area reduction is slow, then accelerates by 50 minutes post DC onset before slowing down again at mid closure. The same pattern is observed in *tkv/+* embryos, the sole difference being that the fast closure phase of the AS is initiated earlier, few minutes after DC onset. In *tkv* mutants, we observed a similar decrease of amnioserosa area prior to evisceration. The AS contraction having been identified as the main source of force during DC, we could expect that DC failure correlates with defects in AS morphogenesis. However, the area of the amnioserosa at the time of evisceration of *tkv* mutant embryos overlaps with the amnioserosa areas of control and *tkv/+* embryos. As the two latter manage to close, those results indicate that the evisceration of *tkv* mutants does not result from an absence of amnioserosa contraction. In order to

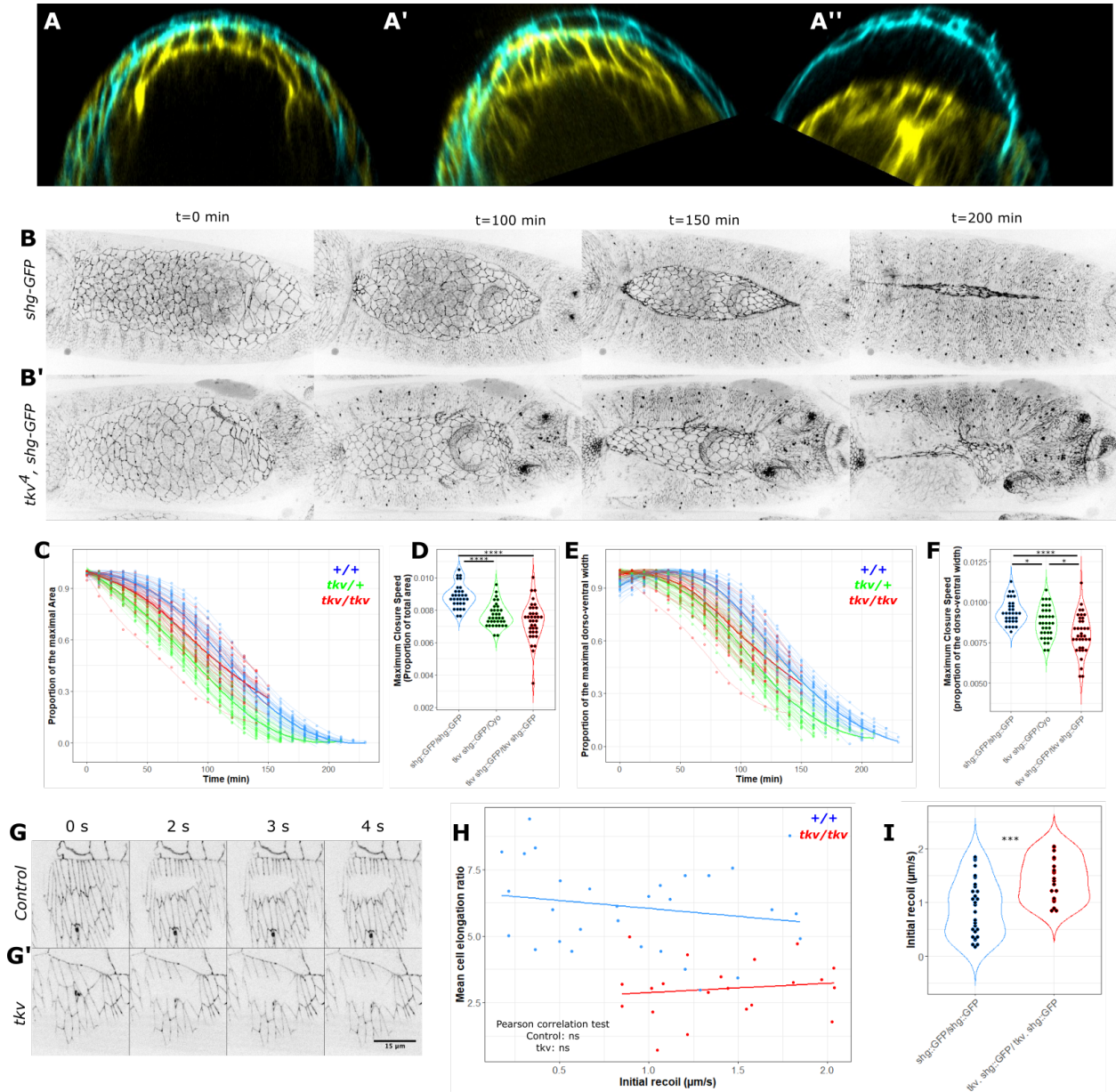


Figure 2: Amnioserosa contraction and traction functions are not impaired in *tkv* mutants:
A: Transversal cuts of time-lapse imaging of *CAAX::GFP* (**A**), *jra/jra; CAAX::GFP* (**A'**) and *tkv4/tkv4; CAAX::GFP* embryos. Time is color-coded: cyan is DC initiation, yellow mid-DC. **B:** Maximum projection of time-lapse imaging of *shg::GFP* (**B**) and *tkv4/tkv4; shg::GFP* embryos (**B'**) from the onset of DC.

C: Quantification of the amnioserosa area in function of time from the onset of DC for *shg::GFP* (n=31), *tkv4/+; shg::GFP* (n=35) and *tkv4/tkv4; shg::GFP* (n=36) embryos. Loess regressions are performed for each embryos and displayed as lines. Mean loess regressions for each genotype are displayed as bold lines **D:** Comparison of the maximum area closure speed extracted from a 5-parameter logistic regression fit for each amnioserosa closure of *shg::GFP* (n=31), *tkv4/+; shg::GFP* (n=35) and *tkv4/tkv4; shg::GFP* (n=36) embryos. Comparison using ANOVA followed by Tukey HSD tests. **E:** Quantification of the amnioserosa dorso-ventral width (extracted from ellipsoid fit) in function of time from the onset of DC for *shg::GFP* (n=31), *tkv4/+; shg::GFP* (n=35) and *tkv4/tkv4; shg::GFP* (n=36) embryos. Mean loess regressions for each genotype are displayed as bold lines **F:** Comparison of the Maximum dorso-ventral closure speed extracted from a 5-parameter logistic regression fit for each amnioserosa closure of *shg::GFP* (n=31), *tkv4/+; shg::GFP* (n=35) and *tkv4/tkv4; shg::GFP* (n=36) embryos. Comparison using ANOVA followed by Tukey HSD tests. **G:** Maximum projection of time-lapse imaging of *shg::GFP* (H) and (H') *tkv4/tkv4; shg::GFP* embryos showing results of leading-edge laser ablation **H:** Mean cell elongation of ablated cells as a function of initial recoil for *shg::GFP* (n=30) and *tkv4/tkv4; shg::GFP* (n=22). Result of linear regressions performed for each genotype are displayed as lines. **I:** Comparison of the initial recoil speed between *shg::GFP* (n=30) and *tkv4/tkv4; shg::GFP* (n=22) embryos by Wilcoxon ranks-sum test.

* : p - values < 0.05, ** : p - values < 0.01, *** : p - values < 0.001, **** : p - values < 0.0001

further analyze potential differences of amnioserosa contraction dynamics between genotypes, we extracted the overall maximum speed of amnioserosa closure of each embryo by performing 5-parameter logistic regression fits (Figure 2D). Maximum speeds were compared by ANOVA followed by a Tukey HSD test. We found significant differences of area maximal closure speed between control versus *tkv/+* and control versus *tkv/tkv* mutants, but no significant differences *tkv/+* and *tkv/tkv* mutants. Moreover, we observed a strong overlap between the closure speed distribution of all genotypes. Altogether, these results show that the amnioserosa contracts in a similar manner in *tkv* and wild-type embryos, and that the slight variations in their dynamics cannot account for the evisceration.

In order to verify if the the amnioserosa contraction towards the midline, hence in the direction of migration of the dorsal epidermis, is impaired in *tkv* mutants, we performed an ellipsoid fit of the previously quantified area. We extracted the small axis length, orthogonal to the midline, and performed the same analysis as in Figure 2C-D. We observed the same dynamics of closure as for the general area, for every genotype. Reduction of the amnioserosa width towards the midline behaves as a sigmoid like curve for every embryo (Figure 2E). Duration of the slow phase is also reduced in *tkv/+*

embryos compared to control. Furthermore, by the time of evisceration the width of the amnioserosa of *tkv/tkv* mutants strongly overlaps with those of *+/+* and *tkv/+* embryos. Hence, the evisceration phenotype does not stem from a lack of amnioserosa contraction. We applied the same analysis as in Figure 2D on the amnioserosa width. We observed a significant difference of maximal closure speed between each genotype but also a strong overlap of their distribution (Fig2F). Therefore, the amnioserosa contraction dynamics cannot account for *tkv* mutant eviscerations.

Forces exerted by the contracting amnioserosa must be transmitted to the dorsal epidermis in order to drive its elongation. In order to verify if this transmission of traction is affected in *tkv* mutants, we performed laser ablations on control and *tkv* mutant embryos. Ablations were performed on the first two rows of cells of the leading edge, parallel to the dorsal epidermis / amnioserosa interface (Figure 2G-G'). We measured the initial recoil post ablation as a read-out of the tension in a visco-elastic material. As the cut is performed parallel to the amnioserosa interface, it acts as a read-out of the tension exerted on the epidermis towards the midline. In order to test whether the tension applied on these cells correlates with their elongation we also measured the mean elongation of the cells along the cut for

each genotype. Quantification of cell elongation as a function of tension is presented in Figure 2H. Interestingly, we found no significant correlation between cell elongation and applied tension for control and *tkv* embryos (Pearson correlation tests). As cells progressively elongate through time, at least in control embryos, these results suggest that the tension exerted by the amnioserosa on the dorsal epidermis does not increase during DC. Moreover, comparison of the recoil initial speed between control and *tkv* mutants using a Wilcoxon rank-sum test showed a significantly higher recoil speed in the mutants (Figure 2I). The fact that the distribution of the speed overlaps between the two genotypes while staying in the same order of magnitude indicates that the amnioserosa is actively pulling on the dorsal epidermis of *tkv* mutant embryos.

Altogether, these results demonstrate that the force provided by the amnioserosa on the epidermis in order to drive its elongation is intact in *tkv* mutants. Furthermore, these results suggest that in *tkv* embryos, the failure of epidermal elongation together with a normal amnioserosa contraction yields to embryonic collapse.

2.3 DPP turns the dorsal epidermis into a visco-plastic tissue

Next, we quantified the elongation of the epidermis in a dynamic manner. We focused on the first abdominal segment as it is not compressed in *tkv* mutants. Three neurons are present at stereotyped positions within the dorsal epidermis of each abdominal segment and can be used as landmarks. These dorsal bipolar neurons are easy to locate thanks to their high level of cadherin expression. We observed that the first neuron borders the leading edge and that the third one sits on the boundary of the *pnr* domain (Figure 3A, white arrowheads). Therefore, we used these 2 neurons to pinpoint the location of the leading edge and dorsal epidermis domains respectively. We first measured the first abdominal segment elongation pattern of 9 control and 7 *tkv* embryos expressing *shg::GFP* by measuring the 3D distance between the amnioserosa/epidermis bound-

ary and the third dorsal bipolar neuron (Figure 3B). The control embryos display a conserved pattern of linear elongation during DC, from 60 to 90 μ m. However, *tkv* mutants show little elongation until evisceration interrupts closure. Furthermore, comparison of the dorsal epidermis length at the onset of closure the dorsal epidermis showed that *tkv* dorsal epidermis is significantly less elongated from the onset of DC (mean elongation = 41 μ m, p-value = 0.0004, Wilcoxon rank-sum test). We performed individual linear regression for each elongation profile to estimate their speed (Figure 3C). We found a significant difference of elongation speed between control and *tkv* embryos. Control embryos elongated at a mean rate of 0.2 μ m/min. However, mean elongation was reduced 5-fold in *tkv* embryos, with 5 out of 7 *tkv* embryos barely showing any elongation at all. We then subdivided the dorsal epidermis domain in two subdomains: leading-edge and dorso-lateral - based on the neurons described in Figure 3A. We observed that elongation defects are present in the leading edge as shown in previous publications ref (Figure 3D). However, we also observed a constant elongation from the onset of DC of the dorso-lateral epidermis of control embryos that is absent in *tkv* mutants (Figure 3E). Altogether, these results show that the elongation of the whole dorsal epidermis is dramatically affected in *tkv* mutants, even prior to DC.

To understand the role of DPP signaling in tissue elongation of the dorsal epidermis, we first documented cell elongation in the wild-type dorsal epidermis. This elongation could result from the stretching induced by amnioserosa traction, then fitting a purely visco-elastic model of elongation. Alternatively, elongation could result from both stretching and permanent deformation, hence fitting a visco-plastic model. In order to discriminate between these two models, we analyzed the physical properties of the epidermis by performing a series of laser ablations (Figure 3F). First, two ablations were performed orthogonally to the leading edge to individualize a single epidermal segment and to remove border effects. Then, a third ablation was performed parallel to the leading-edge interface in order to detach the individualized epidermis segment from the amnioserosa. The retraction of this stripe of tissue provides an estimate of the char-

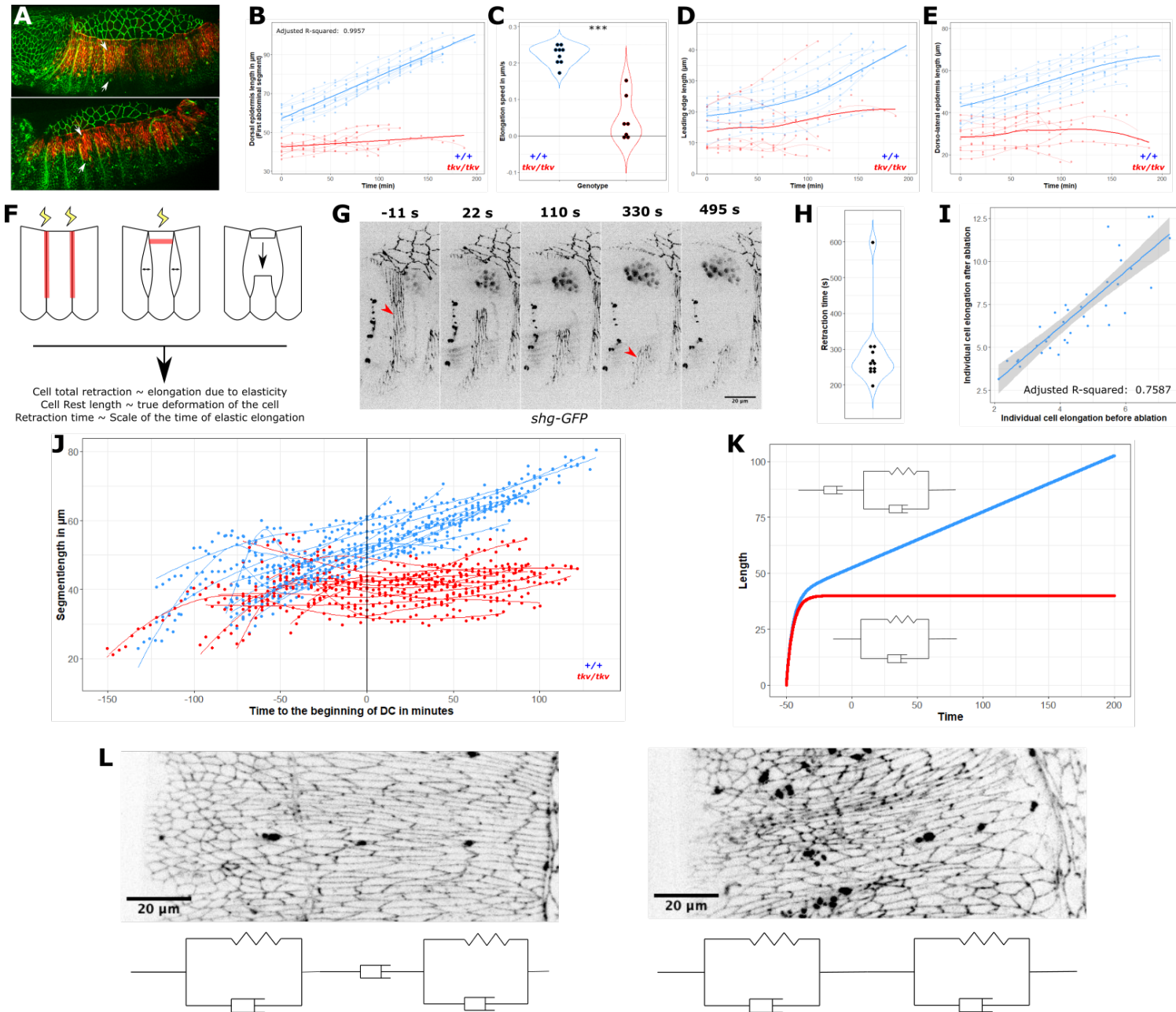


Figure 3: DPP turns the dorsal epidermis into a visco-plastic tissue:

A: Maximum projection of *shg::mKate2*; *pnr Gal4 UAS-APC2::GFP* and *tkv4/tkv4 shg::mKate2*; *pnr Gal4 UAS-APC2::GFP*. White arrows indicate the *shg::mKate2* expressing neurons used to indicate the limits of the leading edge and *pnr* domains for both genotypes. **B:** Quantification of the elongation as a function of time of the first abdominal segment dorsal epidermis during DC for *shg::GFP* (n=9) and *tkv4 shg GFP/tkv4 shg::GFP* (n=7) embryos. Loess regression for each embryo is displayed as line. Bold lines indicate linear regressions performed for each genotype.

C: Comparison of the elongation speed between *shg::GFP* (n=9) and *tkv4 shg GFP/tkv4 shg::GFP* (n=7) extracted by linear regression for each embryo (Adjusted R-squared: 0.9352). Comparison is carried by Wilcoxon test. **D:** Quantification of the elongation as a function of time of the first abdominal segment leading-edge epidermis during DC for *shg::GFP* (n=9) and *tkv4 shg GFP/tkv4 shg::GFP* (n=7) embryos. Loess regression for each embryo is displayed as line. Bold lines indicate mean loess regressions performed for each genotype. **E:** Quantification of the elongation as a function of time of the first abdominal segment dorso-lateral epidermis during DC for *shg::GFP* (n=9) and *tkv4 shg GFP/tkv4 shg::GFP* (n=7) embryos. Loess regression for each embryo is displayed as line. Bold lines indicate mean loess regressions performed for each genotype. **F:** Explanatory scheme of the experiment allowing to estimate the visco-elastic and visco-plastic properties (visco-elastic characteristic time and proportion of elastic and plastic deformation during DC). Thunderbolts indicate laser ablation pulses. **G:** Maximum projection of time-lapse imaging of a *shg::mKate2* embryo during the experimental procedure described in **F**. Red arrowheads indicate a cell from which properties were extracted prior and after retraction. **H:** Quantification of the retraction time of n= 12 stripes from *shg::mKate2* embryos **I:** Quantification of the elongation of cells after retraction as a function of their elongation prior to ablation (37 cells from 7 stripes). Linear regression is performed and displayed as a blue line. 95% confidence interval is displayed in grey. **J:** Quantification of the elongation of the dorsal epidermis of abdominal dorsal epidermis segments of *shg::GFP; Jupiter::GFP* (n=12 segments from 6 embryos) and *tkv4/tkv4 shg::GFP; Jupiter::GFP* (n=12 segments from 4 different embryos) as a function of time at the transition between GBR and DC. Lines show loess regression performed for each abdominal dorsal epidermis segment. **K:** Result from simulation of elongation under constant force of a visco-elastic (red) and visco-plastic material (blue). Visco-elastic characteristic time is estimated from the result of H (5 minutes), maximal visco-elastic elongation is estimated from data displayed in J (40 μ m), and plastic elongation rate is estimated from the results displayed in B (0.2 μ m/min). **L:** Maximum projections of *shg::GFP* and *tkv shg::GFP* illustrating the hypothesis of a transition from visco-elastic to visco-plastic in the dorsal epidermis that requires *tkv*. * : *p* - values < 0.05, ** : *p* - values < 0.01, *** : *p* - values < 0.001, * * * * : *p* - values < 0.0001

acteristic time of the visco-elastic system and quantifies the implication of elastic deformation in the elongation process. An example of such experiment is shown on Figure 3G. By 330 seconds, the retraction stops, and the elongation prior ablation and after retraction is measured for the cell indicated by red arrowheads. Quantification of the retraction time of n= 12 stripes is displayed in Figure 3H. It shows that the characteristic time of the visco-elastic deformation of the dorsal epidermis is inferior to 300 seconds, about 40 time less than the duration of DC. We previously showed in Figure 2I that the force exerted on the dorsal epidermis does not vary during DC, which is coherent with observations performed by Saias et al [10]. Therefore, under those assumptions, DC should not last more than 300 seconds in a purely visco-elastic model. Furthermore, we measured a strong correlation between cell elongation prior to ablation and after retraction (Pearson rho = 0.87, p-value = 1.5e-12, Figure 3I). We performed a linear model regression and found that the cell elongation before ab-

lation is equal to approximately 1.6 times the elongation after retraction (Adjusted R-squared: 0.7587). This indicates that cell elongation during DC is due both to stretching caused by tension and permanent cell deformation, as no correlation should be observed in a purely visco-elastic model.

Thus, the elongation of the dorsal epidermis could be a combination between a rapid visco-elastic elongation followed by a slow plastic cell deformation. To verify this hypothesis, we observed the elongation profiles of multiple abdominal segments in control and *tkv* embryos at the time of transition between GBR and DC (Figure 3J). We observed two phases of elongation in control abdominal segments. First, a fast phase, that ends when the dorsal epidermis length is approximately 40 μ m. Next, a slow phase that occurs during DC. The transition between the slow/fast phases of elongation occurs during GBR, prior to DC initiation. However, in *tkv* mutants the elongation is stopped after the fast phase. Once the dorsal epidermis length reaches 40 μ m, elongation

reaches the plateau we observe during DC (Figure 3A). These observations fit a model of visco-plastic deformation of the dorsal epidermis (Figure 3K). The model considers the epidermis as a Kelvin-Voigt material, behaving as a spring and dashpot in parallel. The permanent deformation is brought by an additional dashpot, that appears missing in *tkv* mutants. We estimated the parameters of the model from previous experiments: The visco-elastic characteristic time was estimated from the results displayed in Figure 3H (5 minutes), maximal visco-elastic elongation was estimated from data displayed in Figure 3J (40 μm), and plastic elongation rate was estimated from the results displayed in Figure 3B (0.2 $\mu\text{m}/\text{min}$). Strikingly, this rather simple model recapitulates both phases of elongation observed in control and *tkv* mutants. Interestingly, the fast phases of elongation are slower than predicted by the model for both genotypes. This might indicate that the forces exerted on the dorsal epidermis during GBR are increasing continuously within that time-frame, instead of being constant from the onset of GBR as stated by the model.

To observe the effects of DPP on cellular elongation behavior, we compared the elongation profiles of cells in the dorsal epidermis domain of control and *tkv* embryos inside and outside of the *pnr* domain (delimited by the bipolar dorsal neurons, Figure 3L). We observed that plastic elongation is confined to the dorsal epidermis domain of control embryos, thus creating a limit between the lateral and dorsal domains. However, as plastic elongation is lost in *tkv* mutants, no limit is observed. Therefore, DPP signaling is required for the selective cell elongation of the dorsal epidermis to accommodate the traction provided by the amnioserosa. In absence of DPP signaling, the epidermis does not respond to the traction exerted by the amnioserosa and resists elongation, thus preventing the appropriate scaling of the tissue necessary for the correct morphogenesis of the embryo: The diameter of *tkv* embryos is therefore out of proportions with the vitelline membrane and the eggshell.

2.4 The morphogenesis potential of the dorsal epidermis directly stems from DPP signaling

Next, we sought to ascertain the impact of adhesion and elongation on global morphogenesis. Indeed whereas DPP provides this morphogenetic potential at once to all dorsal cells in their early development, the mechanics of dorsal closure occur in a stepwise manner hours later. The keystone of this intricate choreography is the formation of the canthi, that are absent in *tkv* mutants. It is hard to predict what would happen in a case where the absence of DPP signaling prevents canthi formation but where the central cells of the embryo keep the competence to maintain their adhesion to AS and to elongate. In order to investigate such a situation, we performed localized rescue of *tkv* function.

First, we tested whether rescuing *tkv* with a UAS construct constitutes a valid approach. Thus we rescued the whole dorsal epidermis domain of *tkv* mutant embryos by inducing a *tkv::GFP* construct in the *pnr* expression domain (Figure 4A, Movie4A). This resulted in the complete rescue of the 17 embryos we observed with time-lapse. Analysis at the cell level shows that rescued dorsal epidermis cells elongate and manage to reach their counterparts at the midline (Figure 4A'). No tearing between the amnioserosa and the dorsal epidermis was observed. Therefore, the *UAS-tkv* construct rescues both the adhesion to the amnioserosa and the cell elongation, thus resulting in closure.

In order to monitor the morphogenetic potential of central cells in a context where canthi did not form, we rescued *tkv* mutants in the *ubx* expression domain (Figure 4B, Movie4B). Indeed, *ubx* is expressed from the second thoracic to the 7th abdominal segment of the embryo but not in the first thoracic nor the last abdominal segment. Thus, the segments where the canthi form in wild-type are not rescued. Strikingly, DC was completed in the 18 embryos we observed. As head involution is impaired in these embryos, we performed a close-up analysis at the junction of the head, *tkv*- dorsal epidermis and rescued epidermis domains (Figure 4B'). We observed that the *tkv*-epidermis fails to elongate as in *tkv* mutants, associated with tearing from the amnioserosa (see the red arrow-

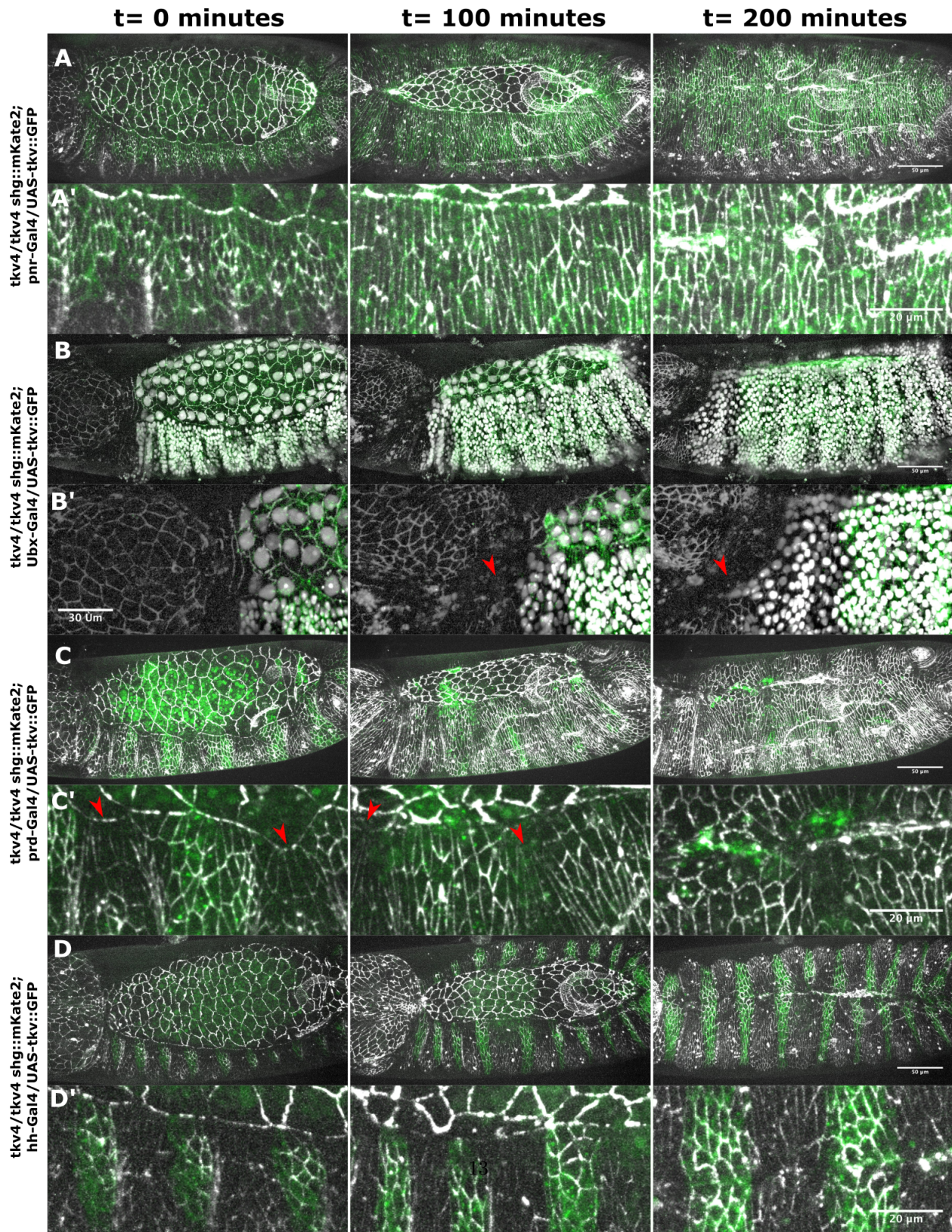


Figure 4: The morphogenesis potential of the dorsal epidermis directly stems from DPP signaling

A: Maximum projection of time-lapse imaging of *tkv4 shg::mKate2/tkv4; pnr-Gal4/UAS-tkv::GFP* from the onset of DC (n=17 completion of DC). **A':** Associated close-ups on leading edge cells. **B:** Maximum projection of time-lapse imaging of *tkv4 shg::mKate2/tkv4; Ubx-Gal4, UAS-RFP::NLS/UAS-tkv::GFP* from the onset of DC (n=18 completion of DC with anterior-open phenotype). **B':** Associated close-ups on leading edge cells. Red arrowheads indicate the unrescued dorsal epidermis that did not fulfil closure. **C:** Maximum projection of time-lapse imaging of *tkv4 shg::mKate2/tkv4; prd-Gal4/UAS-tkv::GFP* from the onset of DC (n=7 completion of DC including 3 with anterior-open phenotype). **C':** Associated close-ups on leading edge cells. Red arrowheads indicate the unrescued epidermis bands that fail to elongate and finally fail to fulfil closure. **D:** Maximum projection of time-lapse imaging of *tkv4 shg::mKate2/tkv4; hh-Gal4/UAS-tkv::GFP* from the onset of DC (n=7 completion of DC and n=10 dorsal open phenotype). **D':** Associated close-ups on leading edge cells.

head) as in not-rescued *tkv* embryos. However, the tear between both tissues does not propagate within the rescued *ubx* domain. The dorsal epidermis cells within the rescued *ubx* domain maintain their adhesion to the amnioserosa and elongate towards the midline, independently of the anterior and posterior eviscerated parts of the embryo. Therefore, the DPP-induced morphogenetic potential is powerful enough to close the central part of the tissue in the absence of canthi, indicating that the system is quite resilient. Next, we wondered to what extent the system is robust by unleashing the morphogenetic potential in fewer cells. We therefore rescued *tkv* expression in domains of different sizes. First, we rescued *tkv* embryos within the alternate pattern of the *prd* expression domain (Figure 4C, Movie4C). The pair rule gene *prd* is expressed in large repeated bands, encompassing segmental boundaries. This resulted in the rescue of DC of the 7 embryos we observed, including 3 with anterior open-like phenotypes. Close up analysis revealed that the cells within the rescued bands manage to elongate, whereas the cells outside the *prd* domain failed to do so (see the red arrowheads, Figure 4C'). We observed that the rescued bands express higher levels of Cadherin. As adherent junctions need to elongate during DC, this might indicate that DPP signaling must upregulate adherent junction components to allow cell elongation. Moreover, leading edge cells of the rescued bands manage to maintain and even increase their interface with the amnioserosa thus replacing the cells lacking DPP signaling at the tissues junction. This uneven elongation and adhesion pattern results in a wave like phenotype of the leading edge, the rescued bands being

dragged ventrally by the cells lacking DPP signaling. As cells cannot exchange neighbors during DC, excepted for the stereotyped insertion of the mixer cell at the leading edge, rescued cells at the boundary adapted their orientation to the constraints from both the amnioserosa and their unrescued neighbors. Interestingly, the combination of the increase of both length and width of the rescued bands leads to a total elongation of the rescued bands that is intermediate between wild type and mutant. Nonetheless, it confirms that DPP signaling provides elongation and adhesion to the amnioserosa in a cell autonomous manner. Interestingly, this intermediate phenotype of elongation/adhesion does not result in evisceration as observed in *tkv* mutant, suggesting that closure is robust enough to occur even when a fraction of the cells acquired DPP morphogenetic potential.

To test whether fewer cells owning DPP morphogenetic potential still prevent evisceration, we rescued *tkv* mutants in thinner bands of their dorsal epidermis by inducing *tkv::GFP* in the *hh* domain (Figure 4D, Movie4), that is the posterior part of each segment. The rescued bands provide regular and discrete anchorage points between at the dorsal epidermis interface but could not elongate properly or form "waves" as observed in the *prd* rescue experiment. Interestingly, despite the narrowness of the band, 7 out of 17 of the rescued embryos managed to complete DC. Again, rescued bands are associated with higher levels of Cadherin expression, as witnessed in rescue experiments involving the *prd* domain. Failure of closure is associated with fusion of rescued neighboring bands during closure. We hypothesized that these events of ipsilateral fusion between *hh* rescued

bands are artefacts resulting from our experimental design. In fact, it has been shown that the zipping of the contralateral cells depends on their segment polarity identity, and is mediated by filopodia [28]. As DPP signaling is required for filopodia production at the leading-edge [6], it is possible that two ipsilateral *hh* positive bands recognize each other, thus resulting in ipsilateral fusion. These ectopic leading edge fusion result in abnormal detachment from the amnioserosa, leading to embryo evisceration. However, among embryos that complete DC, *tkv*- bands participate to the final fusion at the midline despite lacking cell elongation and correct pairing with their counterparts from the opposite side (Figure 4D').

Altogether, these results indicate that DPP provides a morphogenetic potential that allows cells to maintain their adhesion to the AS and also to respond to the mechanical induction by the AS by elongating. This morphogenetic potential is powerful enough so even a partial induction of well localized cells prevents evisceration and foster closure, revealing an amazing robustness potential.

3 Discussion

Our data point to an indirect function of the BMP homologue DPP in the morphogenesis of the dorsal epidermis. Indeed, it is not the DPP secreted during the collective cell migration that controls cell elongation, but a wave of signal that occurs hours before. Importantly this earlier wave determines the cellular field that will possess the potential to elongate. Thus DPP patterns tissues to provide them with a morphogenetic potential. This potential endows cells with the unique capability to elongate upon the mechanical stimulation orchestrated by the amnioserosa, hours later. A surprising finding is that loss of DPP does not prevent amnioserosa contraction, that occurs at a near wild-type rate. Thus DPP patterns both tissues but does not directly trigger their contraction nor their elongation.

The difference between JNK and DPP phenotypes is unsettling at first because JNK has been proposed to work together with DPP in a Feed-Forward motif [6]. An attractive model is that both signals would

control morphogenesis together. Still, the lack of DPP signaling has a wider impact as tissues wrinkle and form self-adhesion on a given side of the embryo, which is never the case in *jra* mutants. Interestingly our data indicate that this wrinkling is JNK dependent as it disappears upon inhibition of JNK activity. Thus JNK is able to induce adhesion between cells of the dorsal epidermis in a DPP independent manner. This indicates that JNK controls a DPP independent program that may be involved in its fast and reliable action during wound healing [29].

Still, *jra* and *tkv* phenotypes share some common features: the loss of function of either pathway allows a near wild-type contraction of the amnioserosa. The splitting between the epidermis and the amnioserosa slightly differs from JNK and DPP, and could stem from an insufficient adhesion, an increased tension or both. We favor a model where a defective adhesion constitutes the primary defect of dorsal open embryos as both pathways have been shown to upregulate key factors of cellular adhesion [20, 21, 30, 31, 6].

The fact that *tkv* phenotype is distinct from *jra* phenotype points out that DPP has a wider, and then earlier function. This is shown by the analysis of Dad-GFP, a target of DPP signaling that we could not detect in *tkv* embryos but that is still present in *jra* mutants. Thus *tkv* embryos lack the second and third wave of DPP signaling. The first wave is still present, as the amnioserosa forms. Furthermore, as the amnioserosa contracts in *tkv* embryos, we can conclude that the first wave DPP solely patterns the amnioserosa and does not influence its morphogenesis once this pattern is achieved. Thus the function of the first wave of DPP is to provide the morphogenetic potential towards contraction to the dorsal-most cells of the embryo.

Moreover, we identify the second wave of DPP as the one responsible for the elongation capacity of the dorsal epidermis in response to the traction exerted by the amnioserosa. Indeed, these cells have the unique capability to respond in a visco-plastic manner: First, they elongate linearly across time when subjected to a constant stress and second upon laser ablation they conserve their resulting deformation. While tissue plasticity involving cell rearrangements is a common feature of animal development, we do not detect any

cell rearrangement during the elongation of the dorsal epidermis. Rather, we witness only the emergence of a plastic behavior at the cellular scale.

The absence of visco-plastic behavior and therefore the lack of elongation leads, in the context of a constricting amnioserosa, to the collapse of the embryo. This brings forward the special ability of DPP to set the tissues and their specific properties so they adapt to the volume and shape of the egg in a smooth manner. Indeed, the dorsal epidermis stretches according to the available space left by the amnioserosa. No signal other than the constant traction of the amnioserosa needs to be tweaked in order to fill this dimension.

Still the former perspective was that DPP would have two mode of action: First to pattern the tissues, then to actively act on them to induce their morphogenesis [5, 18]. Our data rather point to a scenario where DPP only acts through patterning, setting layers of tissues holding distinct physical properties: First the amnioserosa, then the dorsal epidermis and at the end their interface with the leading edge. Then the amnioserosa contracts in a DPP independent manner, pulling on the dorsal epidermis that responds to its traction. It is this traction and not the DPP ligand that lead the dorsal cells to elongate. Thus, dorsal closure had been for a long time considered as a rare example of a direct morphogenetic control, but our model proposes that DPP patterning conveys a morphogenetic potential rather than a morphogenetic signal.

4 Material & Methods

4.1 Fly strains:

Fly strains used were *tkv*⁴ [32], *jra*⁷⁶⁻¹⁹ (BL #9880), *shg::GFP* (BL #60584), *shg::mKate2* (gift from S. Noselli), *CAAX::GFP* (on II: Kyoto #109-824; on III: Kyoto #109-823), *Jupiter::GFP* (BL #6836), *TRE::GFP* (BL #59010), *Dad::GFP::NLS* [33], *UAS-APC2::GFP*, *UAS - Bsk^{DN}* (BL #6409), *UAS-tkv::GFP* (BL #51653), *Ubx-Gal4 UAS RFP::NLS* (gift from S. Merabet), *pnr-Gal4* (BL #3039), *hh-Gal4*, *prd-Gal4* (BL #1947).

4.2 Imaging and laser ablation:

Crosses are kept at 25°C for at least 8 hours. Embryos are collected and dechorionated in 70% bleach then washed and aligned in Halocarbon oil 27 from Sigma-Aldrich.

Live imaging is performed at 25°C with a home-built spinning disk microscope built from an inverted DMI 4000B Leica stand, a spinning disk system CSU-W1-T1 Yokogawa. We used the dry 20X (Leica #11506309), oil immersed 40X (Leica #11506261), water immersed 63X (Leica #11506281) and oil immersed (Leica #11506210). Temperature was controlled by a Heating Unit Pecon. Imaging was controlled using the Metamorph software.

Laser ablations were performed using a Diode 355 nm: SFV-08E-0S0-BETA teem photonics from a MAG Biosystem Laser remote V1, controlled by a teem photonics Microchip Controller and a Smar act HCU 1D box allowing power specification. Control was performed using the Ilas2 software.

4.3 Image analysis:

Image analysis and measurements were performed using the Fiji software. Areas were measured in 2D from maximum projections and the ellipsoid fit performed in Fiji. Lengths were obtained from 3D measurements neuron and leading edge 3D positions in Fiji and calculated in R. Unless indicated otherwise, images displayed in the figures are maximum projections.

4.4 Statistical analysis

All statistical tests were performed using R. Each test performed is indicated within the figure's legend. Normality of the data and homoscedasticity were assessed using Kolmogorov-Smirnov and Fisher tests respectively.

Speeds were extracted from linear and logistic regressions, one regression is performed per embryo. 5-parameter logistic regression were performed using the *nplr* R package.

Plots were generated using the *ggplot2* R package.

4.5 Visco-plastic model:

The visco-plastic model was made from the combination of a Kelvin-Voigt visco-elastic model in series with a dashpot. The equation dictating the deformation of the system can be dictated as:

$$\epsilon_{tot}(t) = \frac{\sigma_{AS}}{\eta_{pl}}t + \frac{\sigma_{AS}}{k_{el}}(1 - e^{-\frac{t}{\tau}}) \quad (1)$$

Where:

$\epsilon_{tot}(t)$ is the epidermis deformation as a function of time

σ_{AS} the constant stress emanating from the amnioserosa

η_{pl} the viscosity constant of the plastic dashpot

k_{el} the elasticity constant of the Kelvin Voigt model

$\tau = \frac{\eta_{el}}{k_{el}}$ with η_{el} the viscosity constant of the Kelvin Voigt model

Estimation for each parameters is done as follows:

$\frac{\sigma_{AS}}{\eta_{pl}}$ is estimated from the linear elongation speed in wild-type

$\frac{\sigma_{AS}}{k_{el}}$ is estimated from the elongation of tkv mutants at the onset of DC

τ is estimated from the retraction time of wild-type epidermis stripes

References

- [1] B. Glise and S. Noselli. Coupling of Jun amino-terminal kinase and Decapentaplegic signaling pathways in *Drosophila* morphogenesis. *Genes & Development*, 11(13):1738–1747, July 1997. Company: Cold Spring Harbor Laboratory Press Distributor: Cold Spring Harbor Laboratory Press Institution: Cold Spring Harbor Laboratory Press Label: Cold Spring Harbor Laboratory Press Publisher: Cold Spring Harbor Lab.
- [2] X. S. Hou, E. S. Goldstein, and N. Perrimon. *Drosophila* Jun relays the Jun amino-terminal kinase signal transduction pathway to the Decapentaplegic signal transduction pathway in regulating epithelial cell sheet movement. *Genes & Development*, 11(13):1728–1737, July 1997.
- [3] L. Kockel, J. Zeitlinger, L. M. Staszewski, M. Mlodzik, and D. Bohmann. Jun in *Drosophila* development: redundant and nonredundant functions and regulation by two MAPK signal transduction pathways. *Genes & Development*, 11(13):1748–1758, July 1997. Company: Cold Spring Harbor Laboratory Press Distributor: Cold Spring Harbor Laboratory Press Institution: Cold Spring Harbor Laboratory Press Label: Cold Spring Harbor Laboratory Press Publisher: Cold Spring Harbor Lab.
- [4] J. R. Riesgo-Escovar and E. Hafen. *Drosophila* Jun kinase regulates expression of decapentaplegic via the ETS-domain protein Aop and the AP-1 transcription factor DJun during dorsal closure. *Genes & Development*, 11(13):1717–1727, July 1997.
- [5] Beatriz García Fernández, Alfonso Martínez Arias, and Antonio Jacinto. Dpp signalling orchestrates dorsal closure by regulating cell shape changes both in the amnioserosa and in the epidermis. *Mechanisms of Development*, 124(11):884–897, November 2007.
- [6] Antoine Ducuing, Charlotte Keeley, Bertrand Mollereau, and Stéphane Vincent. A DPP-mediated feed-forward loop canalizes morphogenesis during *Drosophila* dorsal closure. *The Journal of Cell Biology*, 208(2):239–248, January 2015.
- [7] Jose A. Campos-Ortega and Volker Hartenstein. *The Embryonic Development of Drosophila melanogaster*. Springer-Verlag, Berlin Heidelberg, 2 edition, 1997.
- [8] Yusuke Toyama, Xomalin G. Peralta, Adrienne R. Wells, Daniel P. Kiehart, and Glenn S. Edwards. Apoptotic Force and Tissue Dynamics During *Drosophila* Embryogenesis. *Science (New York, N.Y.)*, 321(5896):1683–1686, September 2008.
- [9] J. Solon, A. Kaya-Copur, J. Colombelli, and D. Brunner. Pulsed forces timed by a ratchet-like mechanism drive directed tissue movement during dorsal closure. *Cell*, 137, 2009.

- [10] Laure Saias, Jim Swoger, Arturo D'Angelo, Peran Hayes, Julien Colombelli, James Sharpe, Guillaume Salbreux, and Jérôme Solon. Decrease in Cell Volume Generates Contractile Forces Driving Dorsal Closure. *Developmental Cell*, 33(5):611–621, June 2015.
- [11] D. P. Kiehart, C. G. Galbraith, K. A. Edwards, W. L. Rickoll, and R. A. Montague. Multiple forces contribute to cell sheet morphogenesis for dorsal closure in *Drosophila*. *The Journal of Cell Biology*, 149(2):471–490, April 2000.
- [12] M. Shane Hutson, Yoichiro Tokutake, Ming-Shien Chang, James W. Bloor, Stephanos Venakides, Daniel P. Kiehart, and Glenn S. Edwards. Forces for morphogenesis investigated with laser microsurgery and quantitative modeling. *Science (New York, N.Y.)*, 300(5616):145–149, April 2003.
- [13] Laurynas Pasakarnis, Erich Frei, Emmanuel Caussinus, Markus Affolter, and Damian Brunner. Amnioserosa cell constriction but not epidermal actin cable tension autonomously drives dorsal closure. *Nature Cell Biology*, 18(11):1161–1172, November 2016.
- [14] V. F. Irish and W. M. Gelbart. The decapentaplegic gene is required for dorsal-ventral patterning of the *Drosophila* embryo. *Genes & Development*, 1(8):868–879, October 1987.
- [15] K.A. Wharton, R.P. Ray, and W.M. Gelbart. An activity gradient of decapentaplegic is necessary for the specification of dorsal pattern elements in the *Drosophila* embryo. *Development*, 117(2):807–822, February 1993.
- [16] Minh Nguyen, Sangbin Park, Guillermo Marqués, and Kavita Arora. Interpretation of a BMP Activity Gradient in *Drosophila* Embryos Depends on Synergistic Signaling by Two Type I Receptors, SAX and TKV. *Cell*, 95(4):495–506, November 1998. Publisher: Elsevier.
- [17] R. Dorfman and B.Z. Shilo. Biphasic activation of the BMP pathway patterns the *Drosophila* embryonic dorsal region. *Development*, 128(6):965–972, March 2001.
- [18] Karolina Lada, Nicole Gorfinkiel, and Alfonso Martinez Arias. Interactions between the amnioserosa and the epidermis revealed by the function of the *u-shaped* gene. *Biology Open*, 1(4):353–361, April 2012.
- [19] P. David Jackson and F. Michael Hoffmann. Embryonic expression patterns of the *Drosophila* decapentaplegic gene: Separate regulatory elements control blastoderm expression and lateral ectodermal expression. *Developmental Dynamics*, 199(1):28–44, 1994. eprint: <https://onlinelibrary.wiley.com/doi/pdf/10.1002/aja.10019>
- [20] Maithreyi Narasimha and Nicholas H. Brown. Novel functions for integrins in epithelial morphogenesis. *Current biology: CB*, 14(5):381–385, March 2004.
- [21] Atsushi Wada, Kagayaki Kato, Makiko F. Uwo, Shigenobu Yonemura, and Shigeo Hayashi. Specialized extraembryonic cells connect embryonic and extraembryonic epidermis in response to Dpp during dorsal closure in *Drosophila*. *Developmental Biology*, 301(2):340–349, January 2007.
- [22] Nicole Gorfinkiel and Alfonso Martinez Arias. Requirements for adherens junction components in the interaction between epithelial tissues during dorsal closure in *Drosophila*. *Journal of Cell Science*, 120(18):3289–3298, September 2007.
- [23] D. Nellen, M. Affolter, and K. Basler. Receptor serine/threonine kinases implicated in the control of *Drosophila* body pattern by decapentaplegic. *Cell*, 78(2):225–237, July 1994.
- [24] M. Affolter, D. Nellen, U. Nussbaumer, and K. Basler. Multiple requirements for the receptor serine/threonine kinase thick veins reveal novel functions of TGF beta homologs during *Drosophila* embryogenesis. *Development (Cambridge, England)*, 120(11):3105–3117, November 1994.

- [25] Marie A. Bogoyevitch and Bostjan Kobe. Uses for JNK: the Many and Varied Substrates of the c-Jun N-Terminal Kinases. *Microbiology and Molecular Biology Reviews*, 70(4):1061–1095, December 2006.
- [26] K. Tsuneizumi, T. Nakayama, Y. Kamoshida, T. B. Kornberg, J. L. Christian, and T. Tabata. Daughters against dpp modulates dpp organizing activity in *Drosophila* wing development. *Nature*, 389(6651):627–631, October 1997.
- [27] H. Inoue, T. Imamura, Y. Ishidou, M. Takase, Y. Udagawa, Y. Oka, K. Tsuneizumi, T. Tabata, K. Miyazono, and M. Kawabata. Interplay of signal mediators of decapentaplegic (Dpp): molecular characterization of mothers against dpp, Medea, and daughters against dpp. *Molecular Biology of the Cell*, 9(8):2145–2156, August 1998.
- [28] Thomas H. Millard and Paul Martin. Dynamic analysis of filopodial interactions during the zippering phase of *Drosophila* dorsal closure. *Development*, 135(4):621–626, February 2008.
- [29] Luis Daniel Ríos-Barrera and Juan Rafael Riesgo-Escovar. Regulating cell morphogenesis: The *drosophila* jun N-terminal kinase pathway. *genesis*, 51(3):147–162, 2013. _eprint: <https://onlinelibrary.wiley.com/doi/pdf/10.1002/dvg.22354>.
- [30] Georgina Sorrosal, Lidia Pérez, Héctor Herranz, and Marco Milán. Scarface, a secreted serine protease-like protein, regulates polarized localization of laminin A at the basement membrane of the *Drosophila* embryo. *EMBO reports*, 11(5):373–379, May 2010.
- [31] Jason G. Homsy, Heinrich Jasper, Xomalin G. Peralta, Hai Wu, Daniel P. Kiehart, and Dirk Bohmann. JNK signaling coordinates integrin and actin functions during *Drosophila* embryogenesis. *Developmental Dynamics*, 235(2):427–434, 2006. _eprint: <https://onlinelibrary.wiley.com/doi/pdf/10.1002/dvdy.20649>.
- [32] J Szidonya and G Reuter. Cytogenetics of the 24D4-25F2 region of the *Drosophila melanogaster* 2L chromosome. *Drosoph. Inf. Serv*, 67:77–79, 1988.
- [33] Nikolay Ninov, Sofia Menezes-Cabral, Carla Prat-Rojo, Cristina Manjón, Alexander Weiss, George Pyrowolakis, Markus Affolter, and Enrique Martín-Blanco. Dpp signaling directs cell motility and invasiveness during epithelial morphogenesis. *Current Biology*, 20(6):513–520, 2010. Publisher: Elsevier.

II) DPP signaling and apoptosis during dorsal closure

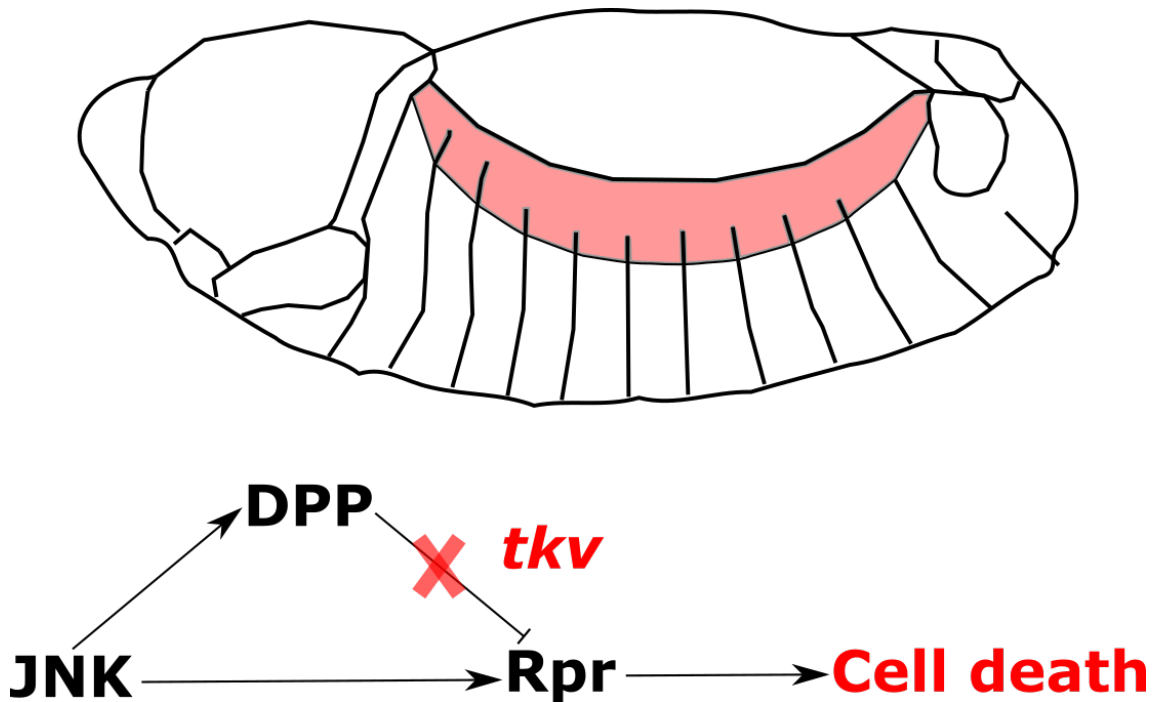


Figure II.1: The leading-edge is supposed to undergo JNK induced apoptosis according to *Beira et al.*:

In order to identify the mechanisms at the origin of the evisceration of embryos lacking DPP signaling, I investigated the potential role of apoptosis. In 2014, *Beira et al.* hypothesized that JNK mediated apoptosis in the absence of DPP signaling would induce apoptosis of leading-edge cells through *rpr* induction [Beira et al., 2014]. They identified two putative binding sites for the AP-1 transcription factor and one binding site of Shn. They found that AP-1 would enhance *rpr* expression whereas Shn would prevent it. Therefore they concluded that during dorsal closure, the induction of DPP by JNK would prevent the apoptosis of the leading edge-cells through an incoherent feed-forward loop, in which JNK would induce both *dpp* and *rpr*, the latter being inhibited by the first. Moreover, they proposed that the dorsal-open phenotype and associated epidermis shrinkage in mutants of the DPP pathway is the direct consequence of apoptosis of the leading-edge cells.

These findings are in contradiction with most of the observation I performed during my thesis. First, I showed in the first part of the Results section that the lack of epidermis elongation in embryos deficient for DPP signaling is not restricted to the JNK activation domain. Moreover, I did not observe apoptosis at the leading-edge in *tkv*, *put* or *shn* mutants.

However, in order to discard the hypothesis of an important role of apoptosis in the evisceration of *tkv* mutants, I performed the series of experiments that I display in this section.

A) *rpr* induction in the dorsal epidermis induces apoptosis events invisible in *tkv* mutants

According to *Beira et al*, the *rpr* gene should be induced in the dorsal epidermis of *tkv* mutants. In order to check for similitudes between the induction of *rpr* in the dorsal-epidermis and *tkv* mutants, I performed induction of *rpr* in the *pnr* domain using the UAS/Gal4 system. I performed live-imaging of these embryos in order to observe their dorsal closure, using the APC2::GFP construct as a marker for visualization. Induction of *rpr* resulted in the evisceration of the 9/9 embryos observed during dorsal closure. This evisceration was associated with defects in dorsal epidermis elongation and amnioserosa adhesion compared to control. However, I observed that this phenomenon correlated with a large number of cells undergoing apoptosis (red arrowheads), from both the leading edge and the dorso-lateral epidermis. Interestingly, I did not observe such apoptotic events in *tkv* mutants filmed during dorsal closure using the same APC2::GFP marker. Altogether, these results demonstrate that the induction of *rpr* in the dorsal epidermis is sufficient to induce the evisceration of embryos during dorsal closure as stated by *Beira et al*. However, it occurs in a different way compared to *tkv* mutants.

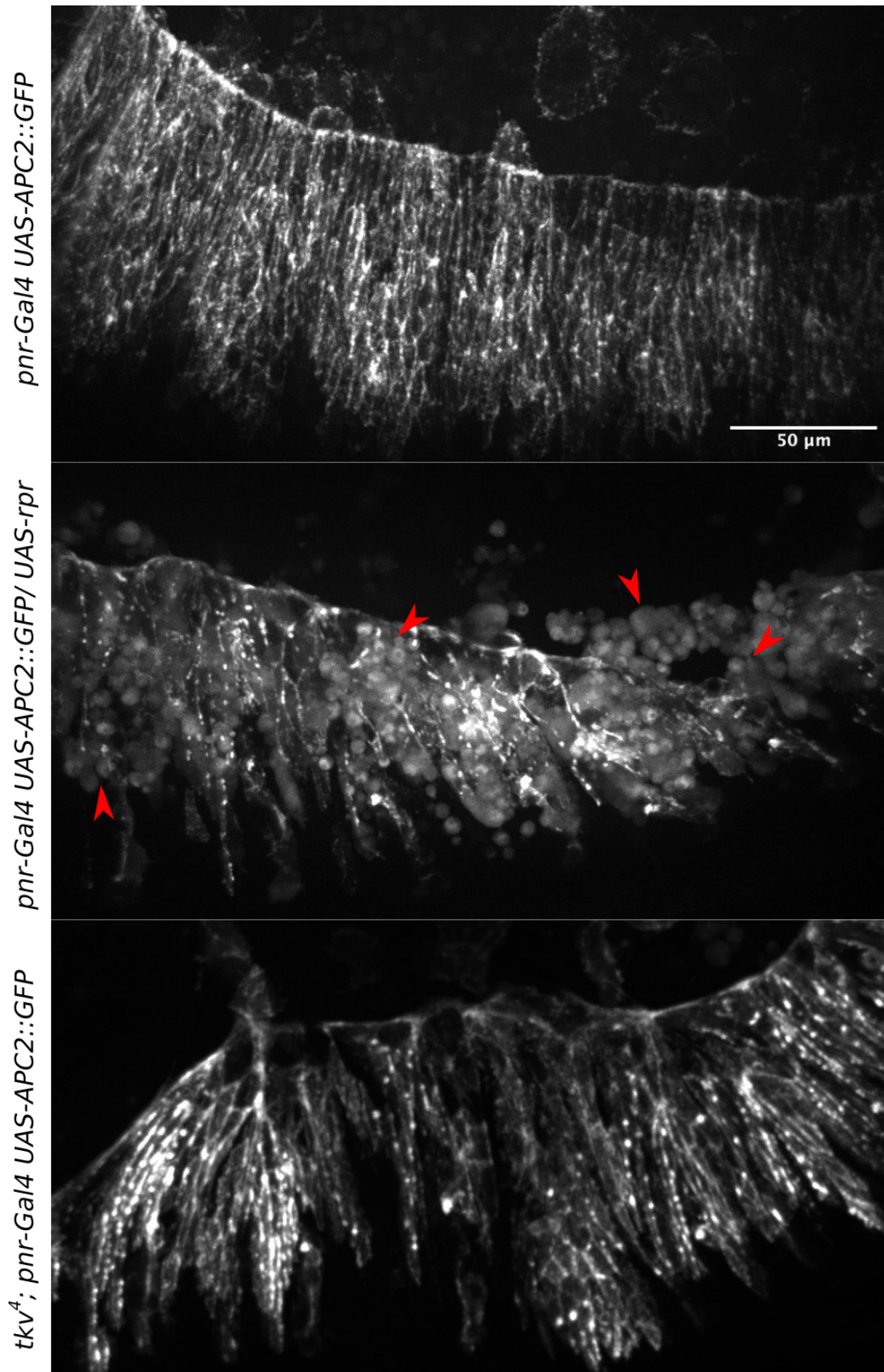


Figure II.2: *rpr* induction in the *pnr* domain does not phenocopy *tkv* mutants: Dorsal epidermis of *pnr-Gal4 UAS-APC2::GFP*, *pnr-Gal4 UAS-APC2::GFP/ UAS-rpr* and *tkv; pnr-Gal4 UAS-APC2::GFP* embryos during dorsal closure. Red arrowheads indicate dying cells

B) JNK+ leading-edge cells do not undergo apoptosis during dorsal closure in *tkv* mutants

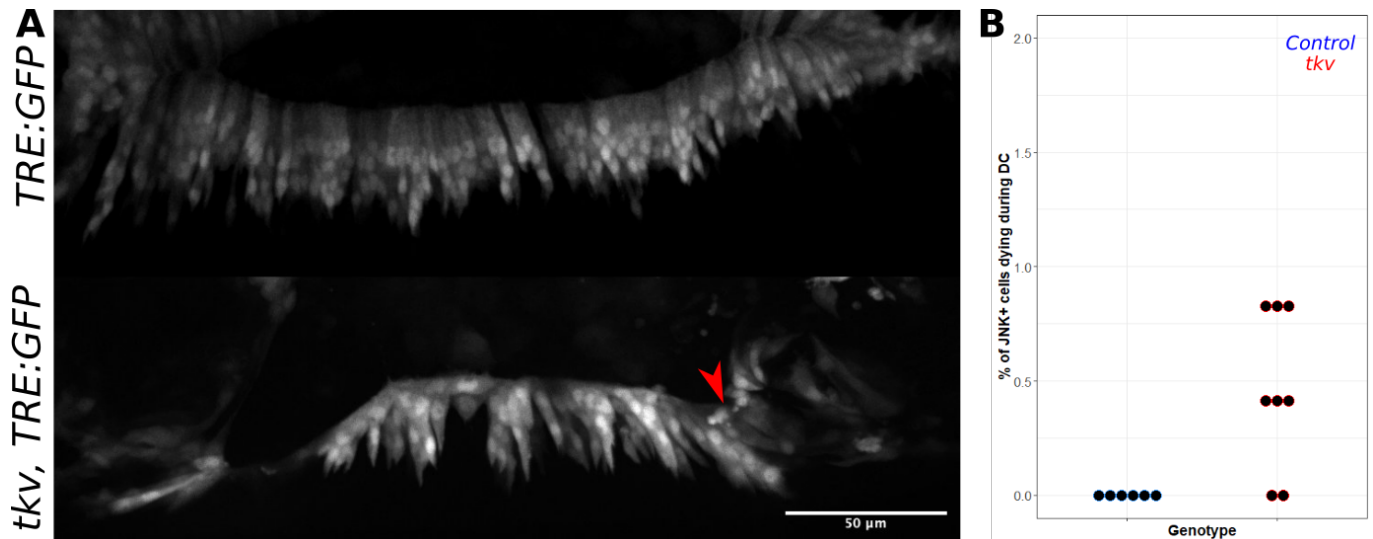


Figure II.3: JNK+ cells of *tkv* mutants do not undergo apoptosis during dorsal closure: **A:** Dorsal epidermis of *TRE:GFP* and *tkv, TRE:GFP* embryos during dorsal closure. Red arrowheads indicate dying cells. **B:** Quantification of cell death observed in *TRE:GFP* and *tkv, TRE:GFP* embryos during dorsal closure

In order to monitor precisely cell death in the leading-edge as a consequence of JNK activation, I performed live imaging of control and *tkv* mutants carrying the *TRE:GFP* construct during dorsal closure, thus marking JNK + cells (Figure II.3 A). As hypothesized by *Beira et al*, no cell death is detected in control embryos. However, in *tkv* mutants, cells in the leading-edges survive during the whole dorsal closure initiation/evisceration process. Nonetheless, rare events were spotted as indicated in Figure II.3 A (red arrowhead). In order to estimate the percentage of cell death in the leading-edge JNK + positive cells, I first quantified the number of cell death events observed per leading-edge per embryo (Figure II.3 B). Then, I approximated the total number of cells per leading-edge as the product of the number of cells per segment at the leading-edge at the onset of dorsal closure (11), times the number of segments (from the thoracic 1 to the abdominal 8, 11 segments), time the number of rows of JNK + cells per leading-edge (2). Counts were performed on n=6 control embryos and n=8 *tkv* embryos. No cell death is observed in control

embryos. I estimated the percentage of cell death to be approximately 0.46% in *tkv* mutants. Moreover, cell death is associated with dramatic cell stretching due to the evisceration process. Therefore, the shrinkage of the dorsal epidermis observed in *tkv* mutants is not the consequence of cell death in the LE.

C) Apoptosis is not involved in the *tkv* mutant evisceration phenotype

Even if cell death does not occur in the leading-edge of *tkv* mutants during dorsal closure, it remains possible that the activation of the apoptotic program in the leading-edge would be responsible for defects leading to evisceration. In order to test this hypothesis, I analyzed the dorsal closure in *tkv* mutant carrying the *H99* deletion (Figure II.4 A). I used *shg::mKate2* to mark the adherent junctions. The *H99* deficiency removes the genes *hid*, *grim* and *rpr* from the genome, thus impairing apoptosis. In *H99* mutant embryos, I observed the characteristic oversized head due to the absence of apoptosis in the CNS that leads to head-involution defects. Moreover, the deficiency also prevents the delamination of AS cells during the bulk of closure and delays the final elimination of the tissue, thus leading to scarring of the trunk by the end of the dorsal closure process (blue arrowhead). During this experiment, *tkv* mutants also failed their dorsal closure, as already described in the previous result part of this thesis. Interestingly, the *tkv H99* double-mutants display the combination of the two phenotypes: an oversized head, an absence of individual AS cell delamination, but also an absence of dorsal epidermis elongation and defects of adhesion to the AS leading to evisceration. I performed a close-up analysis of the leading-edge phenotypes of the same embryos (Figure II.4 B). It showed that defects of cell shape at the leading-edge observed in *tkv* mutants are still observed in *tkv H99* double mutants (blue arrowheads), associated with the characteristic down-regulation of cadherin expression. Therefore, the phenotype of *tkv* mutants is not the consequence of induced apoptosis in the LE.

Altogether, my work demonstrates that the evisceration and shrinkage of the epidermis in embryos deficient for DPP signaling is not the consequence of leading-edge apoptosis. Only rare events of apoptosis are spotted during evisceration, and preventing apoptosis does not influence the overall phenotype of the mutants. These results reinforce the analysis of the *tkv* mutant phenotype I made earlier, as a con-

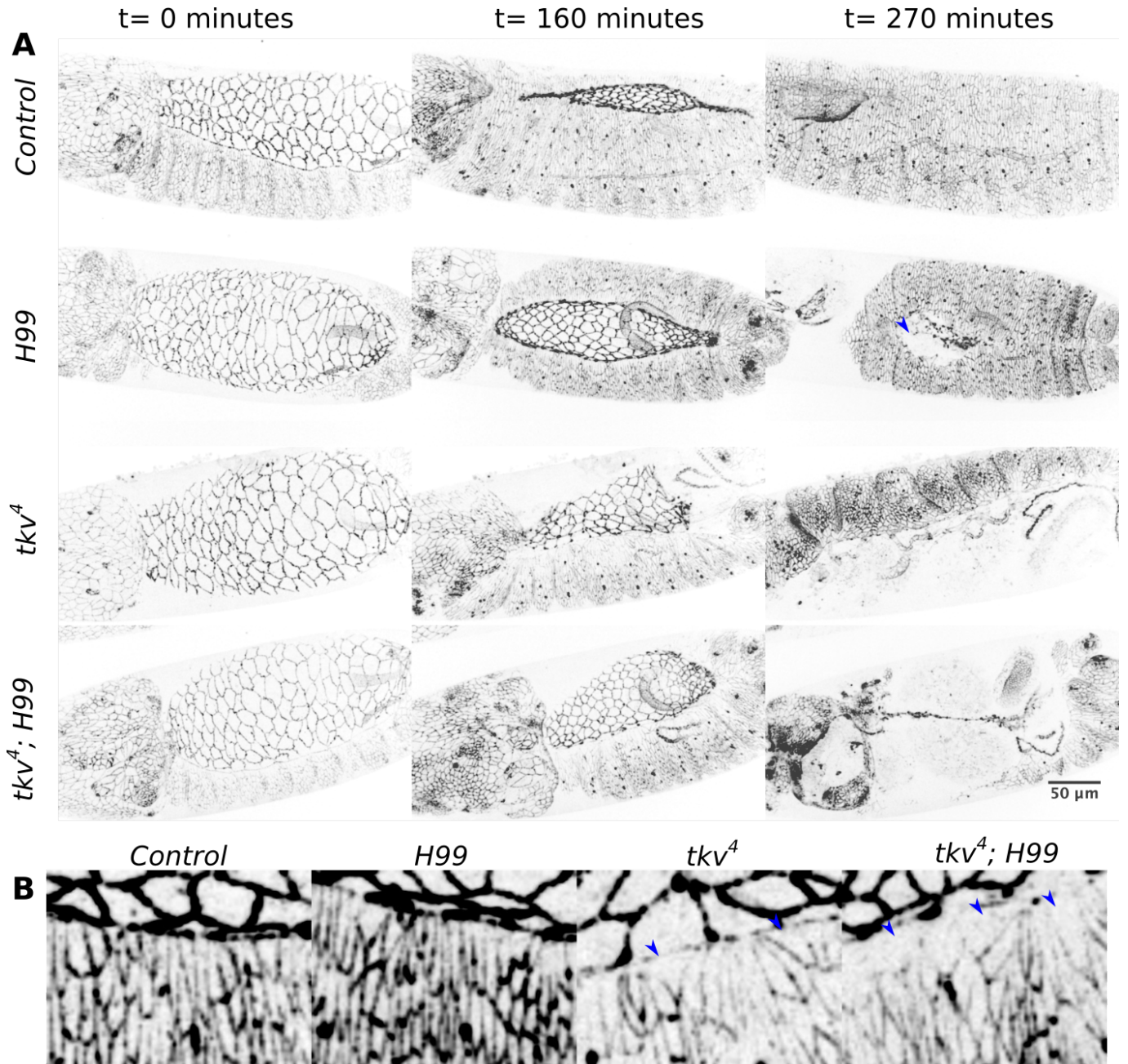


Figure II.4: Preventing apoptosis does not rescue *tkv* mutants: **A:** Time-lapse imaging of *shg::mKate2, shg::mKate2; H99, tkv shg::mKate2, tkv shg::mKate2; H99* embryos. Blue arrowhead indicates scarring observed in the H99 mutant. **B:** Close-up analysis of the leading-edge of the embryos displayed in **A**. Blue arrowheads show leading-edge cells with aberrant shape characteristic of *tkv* mutants

sequence of defects in cell elongation and adhesion, independently of JNK related cell death.

III) Contribution of internal organs morphogenesis during *tkv* mutant evisceration

The dorsal closure study field has mainly focused on the dorsal epidermis, independently of the other morphogenetic events occurring concomitantly in the embryo. I showed previously that rescuing the dorsal epidermis of *tkv* mutants was sufficient to rescue dorsal closure. However, early in my thesis, based on the fact that all organs are in close contact during embryogenesis, I hypothesised that defects in organization of the internal organ could trigger the evisceration of *tkv* mutants. Indeed, morphological defects of the internal organs could generate forces that would propagate to the epidermis layer and trigger the evisceration of *tkv* embryos.

I described in the introduction how DPP signaling is required for both visceral mesoderm and heart differentiation prior to dorsal closure. In *tkv* mutant embryos, the visceral mesoderm fails to form a continuous layer by the start of GBR [Bradley et al., 2003]. Moreover, DPP signaling in both the visceral mesoderm and midgut has been shown to be required for their constriction after dorsal closure. Nonetheless, the patterning information for the constriction is defined prior to dorsal closure, thus it remains possible that it influences morphogenesis during dorsal closure.

In this section I show how internal organs get eviscerated in *tkv* mutants and how their impaired morphogenesis worsens such phenotype.

A) Internal organ rather than amnioserosa contraction induces evisceration of *tkv* mutants

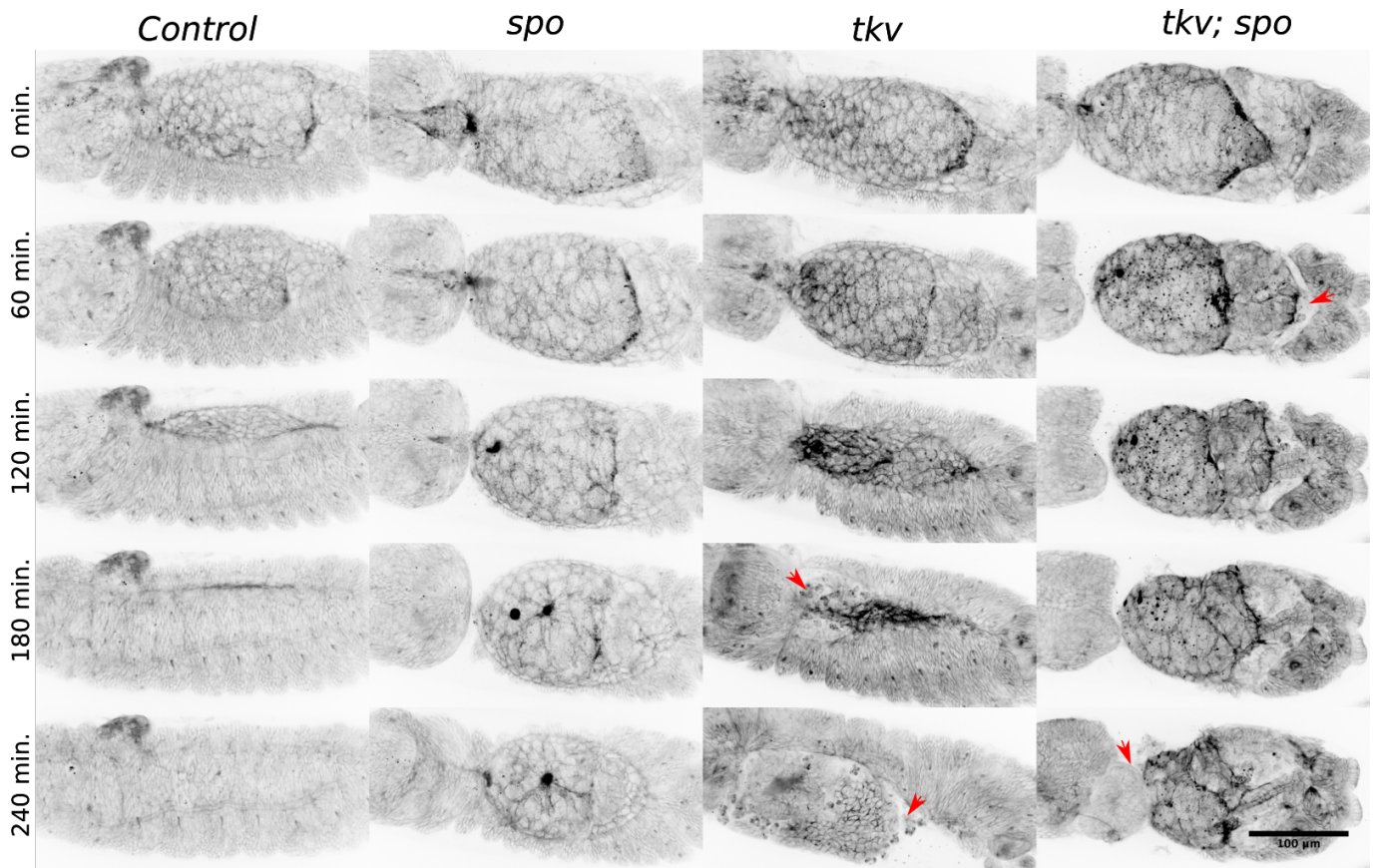


Figure II.5: Internal organ rather than amnioserosa contraction induces evisceration of *tkv* mutants: Maximum projection of time-lapse imaging of Control, *spo*, *tkv*, and *tkv; spo* embryos expressing the *CAAX::GFP* marker. Red arrowheads indicate the origin of ripping between the dorsal epidermis and the amnioserosa.

In the first section of the Results chapter of this thesis, I showed how amnioserosa/dorsal epidermis adherence strength is affected in *tkv* mutants while amnioserosa contraction is maintained. Therefore, one could hypothesize that the amnioserosa simply detaches as the epidermis resists elongation. Hence, inhibiting amnioserosa contraction should prevent the evisceration of *tkv* mutant embryos.

In order to test this hypothesis, I used a mutant of the ecdysone pathway: *spo*. A recent study demonstrated that in *spo* mutants, the amnioserosa fails to contract thus leading to the arrest of the dorsal closure process [Yoo et al., 2021]. Therefore, I performed the simultaneous time-lapse imaging of *tkv* and *spo* simple and double

mutants marked with the CAAX::GFP membrane marker and compared their dorsal closure phenotype (Figure II.5).

As predicted by both my previous results and the literature, amnioserosa contraction occurs at a similar rate in control and *tkv* mutants, whereas it is dramatically slowed down in *spo* and *tkv; spo* double mutants. However, contrary to the initial hypothesis, the ripping phenotype of *tkv; spo* mutants still occurs as in simple *tkv* mutants. Indeed, for both genotypes, the detachment occur at the anterior pole of the amnioserosa where it correlates spatio-temporally with the head-involution process and at the posterior pole of the amnioserosa where it correlates with the underlying hindgut elongation (see the red arrowheads).

Therefore, it is not the contraction of the amnioserosa combined with the resistance to elongation of the dorsal epidermis that induces the evisceration of *tkv* mutants. Interestingly, DPP is also known to be involved in internal organ development. Thus, I decided to investigate the dynamics of the morphogenetic defects in *tkv* mutants and tested the influence of such defects on *tkv* mutants evisceration.

B) Both heart and midgut morphogenesis are affected in *tkv* mutants

In order to inspect the morphogenesis of mesodermal derived tissues, I performed time-lapse imaging of control and *tkv* embryos expressing the APC2::GFP construct in the twist domain -that encompasses the mesoderm and early midgut anlage- using the UAS/Gal4 tool (Figure II.6 A). As seen in the control embryo and thoroughly described in the literature, the heart tissue (cyan arrowhead), followed by the somatic musculature, migrates dorsally underneath the epidermis during dorsal closure. However, in *tkv* mutants the heart is absent and only the somatic musculature is observed. Therefore, a whole tissue is missing in the vicinity of the epidermis leading-edge during dorsal closure.

Furthermore, I monitored the dynamics of midgut migration using the *Syb-QF2 QUAS-mCD8::GFP* system in control and *tkv* embryos (Figure II.6 B). This construct, engineered to mark neurons has the advantage to mark the yolk sac during dorsal closure. The mCD8::GFP marker accumulates at the interface between the yolk and the midgut leading-edge (dashed red lines). This has been assessed by careful visualization of the 3D stack, because the mCD8::GFP faintly marks the midgut (data not shown). In control embryos, the midgut migrates dorsally and finally fuses with its contralateral counterpart at the midline. Interestingly the anterior and posterior midgut migration front can be distinguished as both tissues fuse and compress the yolk dorso-laterally during the process (white arrowheads). However in *tkv* mutants, the direction of midgut migration is affected. Both midgut tissues migrate towards a single point in the dorsal part of the yolk where the anterior and posterior midgut fuse (see the migration leading edge and anterior/posterior fusion point). Moreover, fusion rather happens between the anterior to posterior midgut instead of contralaterally. I formulated the hypothesis that DPP signaling promotes contralateral fusion or inhibits fusion of the anterior and posterior midgut at the dorsal leading-edge. Sadly, I did not have the time to test it. Yet, these observations

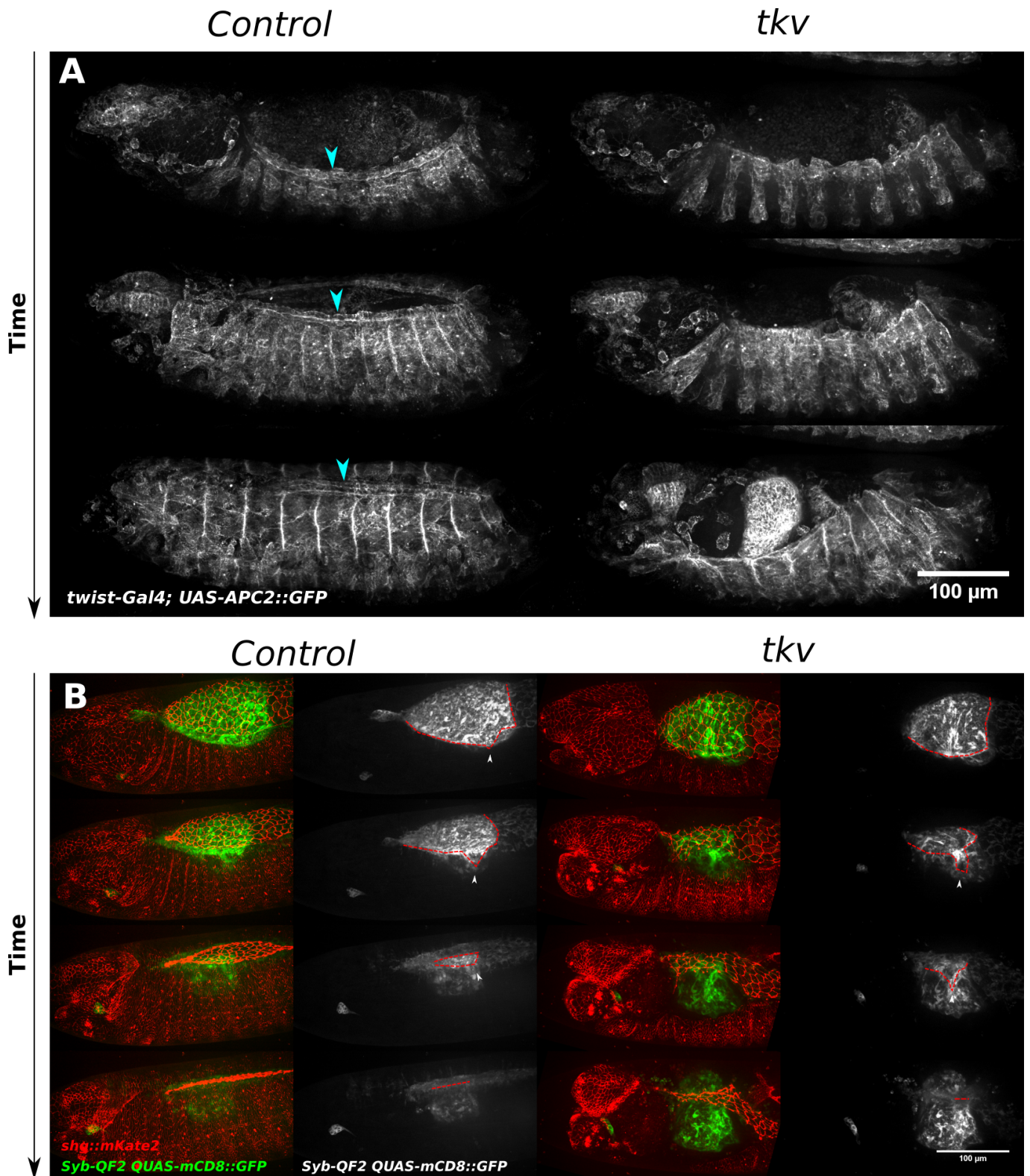


Figure II.6: Both heart and midgut morphogenesis are affected in *tkv* mutants:

A: Maximum projections of time-lapses from a *twist-Gal4; UAS-APC2::GFP* and a *twist-Gal4; tkv/tkv; UAS-APC2::GFP* embryos during dorsal closure. Cyan arrowheads indicate the heart tube in the control embryo, absent in the *tkv* mutant. **B:** Maximum projections of time-lapses from a *shg::mKate2; Syb-QF2 QUAS-mCD8::GFP* and a *tkv/tkv shg::mKate2; Syb-QF2 QUAS-mCD8::GFP* embryos during dorsal closure. Dashed lines indicate the migration front of the midgut on the yolk on the GFP channel, white arrowheads je junction between the anterior and posterior midgut.

demonstrate that the endoderm and yolk morphogenesis are dramatically impaired in *tkv* mutants during dorsal closure.

Thus, the morphogenesis of internal organs is also impaired in *tkv* mutants during dorsal closure and can be considered as a factor involved in their evisceration.

C) Impairment of DPP signaling in both the dorsal epidermis and the internal organs increases the risks of evisceration

One of the first experiments I performed as a PhD student was to selectively inhibit DPP signaling in the dorsal epidermis in order to mimic the effects observed in *tkv* mutants. To do so, I used the *pnr-Gal4* driver to express the *UAS-Brk* construct. Interestingly, the induced embryos were not eviscerated but scarred instead. Intrigued by this intermediate phenotype, I decided to inhibit DPP signaling in both the dorsal epidermis and internal organs. To target the internal organs I used the *twist-Gal4* inducer. To test the interaction, I performed time lapse imaging of *pnr-Gal4 UAS-APC2:: GFP, twist-Gal4; pnr-Gal4 UAS-APC2:: GFP, pnr-Gal4 UAS-APC2:: GFP/ UAS-Brk, twist-Gal4; UAS-APC2:: GFP/UAS-Brk* and *twist-Gal4; pnr-Gal4 UAS-APC2::GFP/UAS-Brk* embryos during their dorsal closure (Figure II.7 A). All control embryos -which were not induced with Brk- performed dorsal closure without closure defects. Interestingly, 5/5 embryos in which Brk was induced in the *twist* domain failed to form a heart and displayed endoderm migration defects but still managed to fulfil dorsal closure. Brk induction in the dorsal epidermis resulted in 21 scarred, 2 anterior open and one dorsal-open out of 24 embryos. However, Brk induction in both the internal organs and dorsal epidermis resulted in 11 scarred and 7 dorsal open out of 18 embryos. Statistical analysis carried using independence Fisher test adjusted by Bonferonni hypothesis showed a significant effect of Brk induction in the epidermis in producing scars compared to control (Figure II.7 B). Moreover, I observed significant contribution of coordinated Brk induction in both the internal organs and dorsal epidermis in producing dorsal open embryos compared to induction in the dorsal epidermis alone.

First, these results demonstrate thatdorsal closure is robust enough to succeed independently of the morphogenetic defects of the internal organs that lacked DPP signaling. However, these defects contribute to the evisceration of embryos when

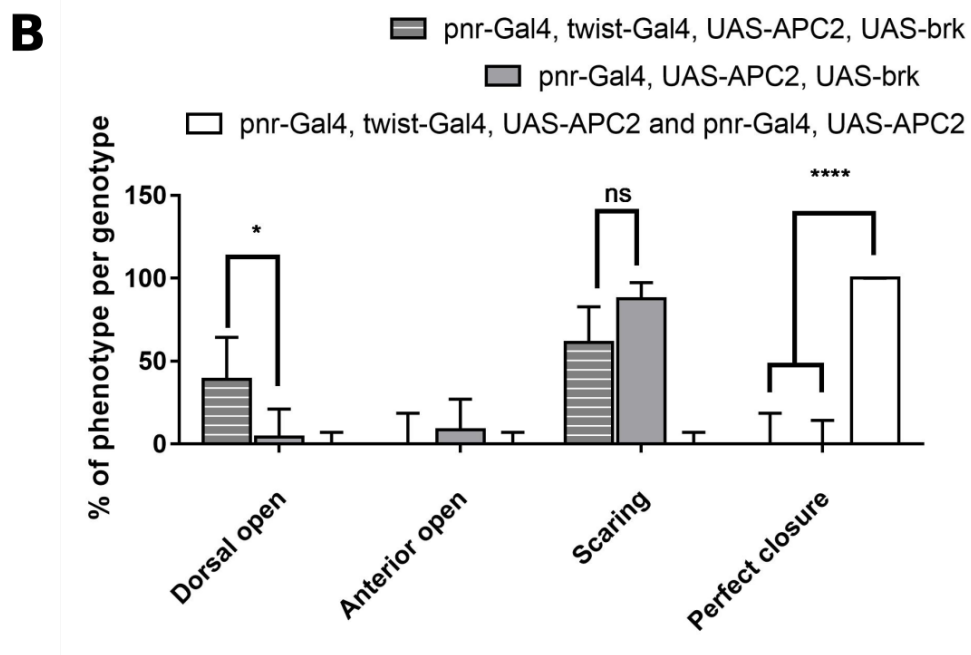
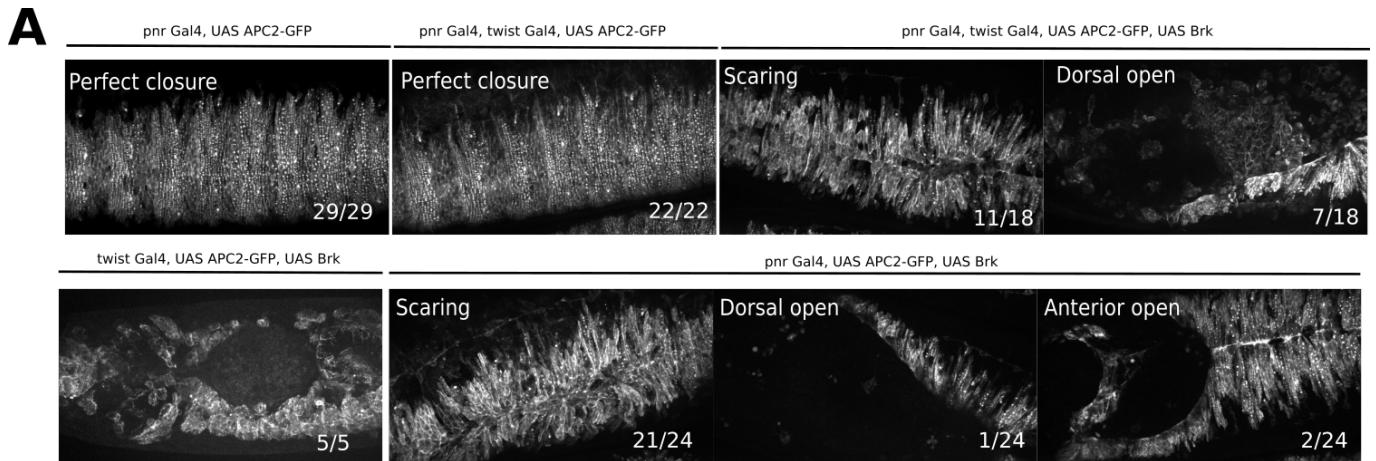


Figure II.7: Impairment of DPP signaling in both the dorsal epidermis and the internal organs increases the risks of evisceration: **A:** Phenotypical variations post Dorsal closure after induction of Brk in the dorsal epidermis, mesoderm or both are displayed. Genotypes and proportions of each phenotype are indicated. **B:** Comparison of the proportion of each phenotype per genotype. 95% confidence interval were calculated using the Wilson Brown method and statistical comparison were carried using 3 separated Fisher tests. p-value were adjusted using the Bonferonni method.

DPP signaling is also impaired in the dorsal epidermis. Therefore, internal organ morphogenesis could contribute to the evisceration process of *tkv* mutant embryos.

D) Rescue of internal organ morphogenesis delays evisceration in *tkv* mutants

In order to test whether the defects in mesoderm and midgut morphogenesis affect the evisceration of *tkv* mutants, I performed a selective rescue of the midgut and musculature using the *twist-Gal4* inducer driving the expression of *UAS-tkv::GFP* in *tkv* mutants (Fig II.8 A). The rescue was a success as heart development occurs in these mutants, and midgut constriction is observed by the end of development. However, rescued embryos all failed to close. Rescued embryos display the characteristic failure of dorsal epidermis elongation of *tkv* mutants (mean abdominal 1 elongation = 37 μ m, n=16). However, amnioserosa tearing occurs substantially later in these embryos compared to non-rescued *tkv* mutants (Figure II.8 B). The ripping occurs as the heart cells pass under leading edge cells while migrating towards the midline (red arrowhead).

Thus, defects in internal organ morphogenesis do contribute to the evisceration of *tkv* mutants. Therefore, this evisceration is the combination of both a lack of cell elongation in the epidermis, a lack of adherence to the amnioserosa and increased physical constraints from the internal organs. Moreover, this demonstrates that wild-type dorsal closure is robust enough to resist major disruptions in internal organ morphogenesis.

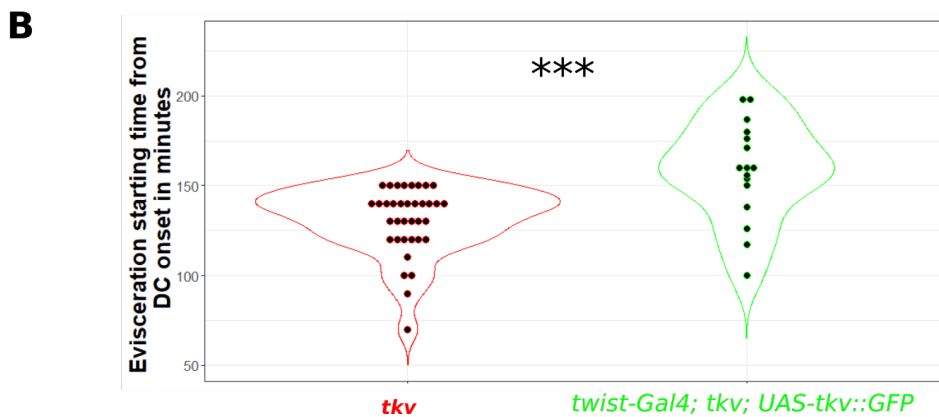
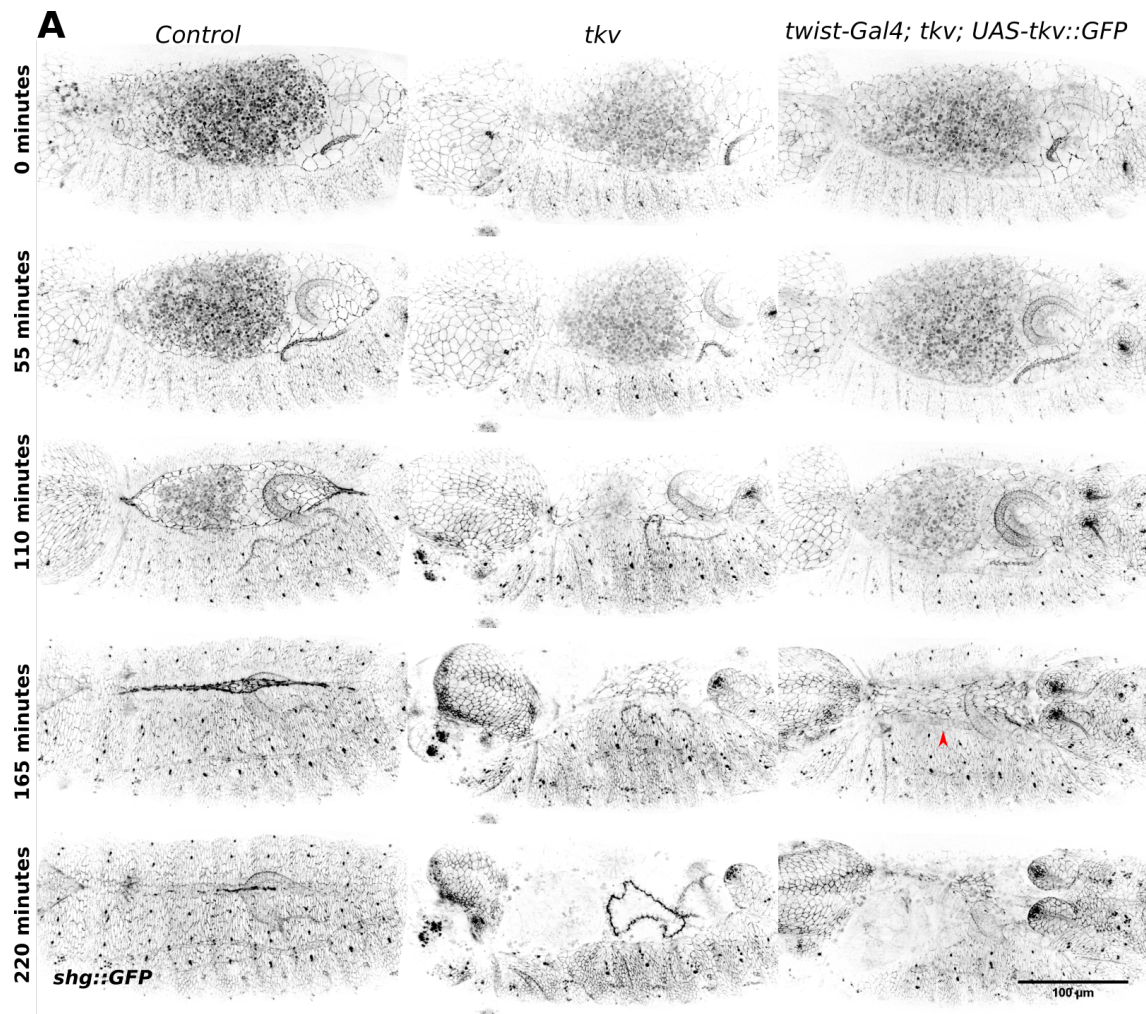


Figure II.8: Rescue of internal organ morphogenesis delays evisceration of *tkv* mutants: **A:** Maximum projections of time-lapses from a Control, *tkv/tkv* and a *twist-Gal4; tkv/tkv; UAS-tkv::GFP* embryos during dorsal closure. Red arrowhead indicates the heart tube in the rescued mutant. **B:** Quantification of the evisceration starting time between *tkv* mutants and *tkv* mutants rescued in the twist domain. Comparison carried using a Wilcoxon test.

IV) **Contraction of a band of head epidermis cells promotes the head-involution process**

As described in the introduction, it is today commonly accepted that forces driving the head-involution process come from the contraction of circumferential actin cables in the *hh* domain of the dorsal ridge and thoracic segments [Czerniak et al., 2016]. As these cables only become circumferential after dorsal closure, the anterior movement of the thoracic epidermis should absolutely require dorsal closure. In fact, in the wild-type, head-involution and dorsal closure are perfectly synchronized and head-involution initiation coincides with dorsal ridge fusion and anterior canthus formation [VanHook and Letsou, 2008].

During my thesis, while searching for physical cues at the origin of *tkv* embryos eversion, I observed that the head-involution process is initiated in these mutants. In the absence of dorsal closure, the process fails dorsally, but forces pulling the epidermis towards the anterior direction are still present. Careful observations of the phenomenon allowed me to identify a stripe of head epidermis cells that undergoes antero-posterior contraction during head-involution and dorsal closure which correlates with anterior movement of the epidermis independently of dorsal closure completion.

A) Head-involution initiation does not require dorsal ridge or dorsal closure in *tkv* mutants

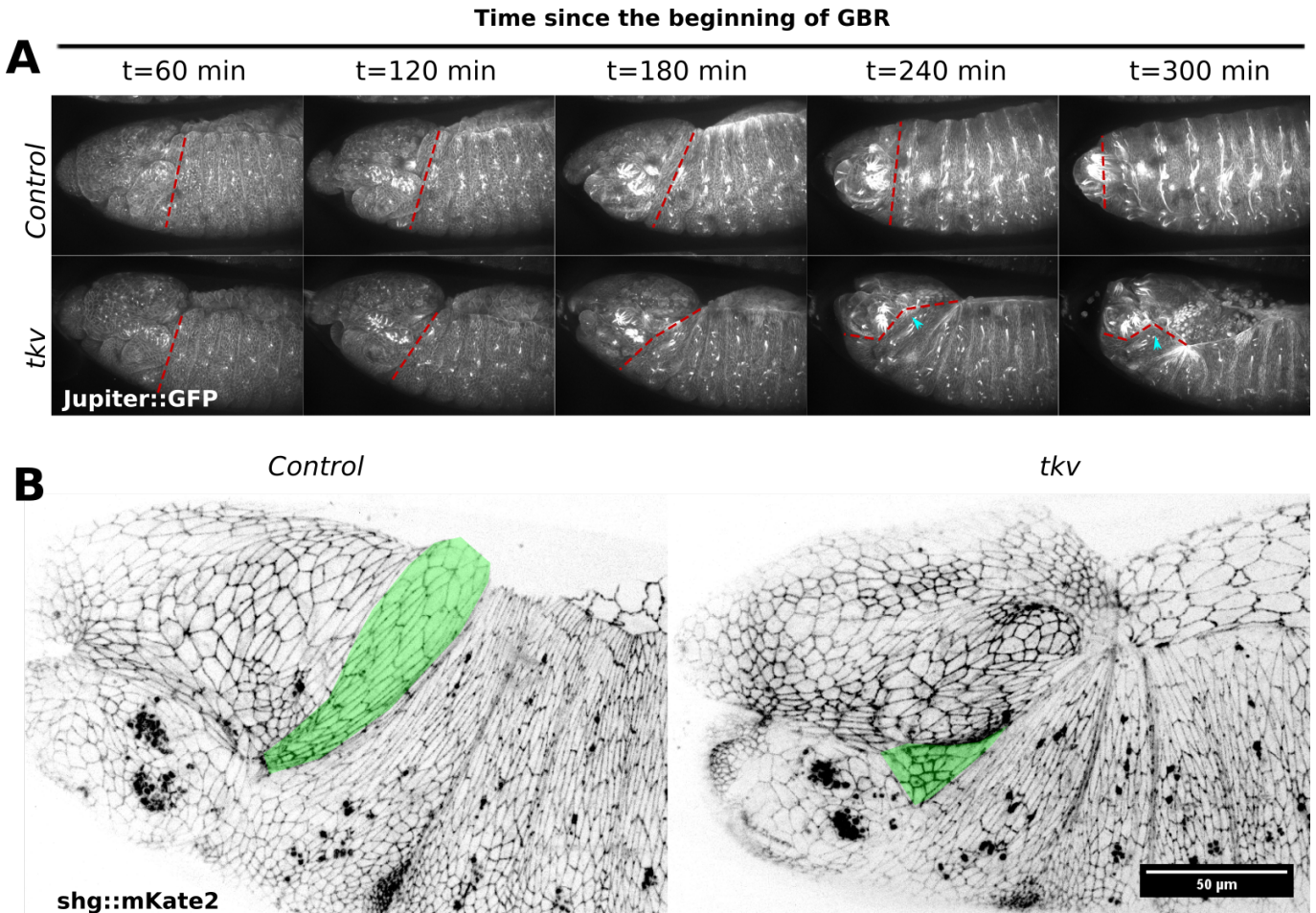


Figure II.9: Head-involution initiation does not require dorsal ridge or dorsal closure in *tkv* mutants: **A:** Maximum projections of time-lapses from a Control and *tkv* embryos expressing the Jupiter::GFP marker embryos during dorsal closure. Red dashed lines indicate the leading edge of the first thoracic segment migrating over the head. **B:** Maximum projection of the head of a Control and a *tkv* mutant embryo expressing the *shg::mKate2* marker. The dorsal ridge domain is highlighted in green.

To observe head-involution in *tkv* mutant, I performed time-lapse imaging of control and *tkv* mutant embryos, oriented laterally and expressing the Jupiter::GFP marker (Figure II.9 A). In control embryos, I observed that the leading edge of the thoracic segments advances anteriorly in a dorso-ventrally coordinated manner (red dashed line). Surprisingly, despite the failure of dorsal closure, anterior migration occurs on the ventral side of the embryo. However, dorsal-most cells do not migrate

anteriorly as their adhesion with the amnioserosa is kept in the absence of contralateral fusion. Interestingly, the leading edge forms an angle dorso-laterally at the junction between the ventral-most part of the dorsal ridge and the head-epidermis, thus suggesting that a traction force is also exerted on the dorsal epidermis at this location (cyan arrowhead).

As the dorsal ridge has been shown to promote head-involution by *Czerniak et al*, I analyzed the dorsal ridge behavior in control and *tkv* mutant embryos (Figure II.9 B). In control embryos, the ridge (highlighted in green) forms a tubular structure that grows and migrates dorsally until it reaches and fuses with its contralateral counterpart at the dorsal midline. However, *tkv* mutants display an atrophied dorsal ridge that fails to migrate towards the midline as dorsal closure fails.

Therefore, head-involution proceeds in *tkv* mutant embryos independently of dorsal ridge formation and dorsal closure completion. This demonstrates that another force drives head-involution in these mutants, in addition to the circumferential actin-cables contraction described in the literature.

B) The contraction of a stripe of head epidermis cells tracts the dorsal ridge towards the anterior of the embryo

To identify the cellular structures that generate the forces required for head-involution, I performed time-lapse imaging of the head of control and *tkv* embryos expressing the *shg::mKate2* marker during head-involution (Figure II.10 A). In control embryos, I first identified a stripe of cells (highlighted in red) linking the dorsal ridge (highlighted in green) ventral-most part to the anterior most part of the head. During head-involution, the stripe length decreases as the dorsal ridge migrates towards the anterior of the embryo. Interestingly, the *shg::mKate2* signal increases gradually in these cells, thus suggesting a reduction of the adherent junction perimeter during the process. Therefore, I hypothesized that the contraction of this cell stripes, situated on each side of the head, could generate the forces required for head-involution. I decided to name these cells Suspender Cells for reasons that will be further explained in the light of the following results. Suspender cells are also observed in *tkv* embryos. As in control conditions, their contraction correlates with the anterior migration of the dorsal ridge, despite the absence of fusion at the dorsal midline. Therefore the initiation of the anterior migration of the epidermis over the head does not depend on the formation of a dorsal ridge nor on the completion of dorsal closure. Nonetheless, this migration remains strongly correlated to Suspender cells domain shrinking. However, the dramatic failure of dorsal closure in *tkv* mutants does not allow to verify if head-involution could be achieved by Suspender cells stripe contraction alone in the absence of circumferential actin cables, as the evisceration of the embryos prevents the whole head-involution process.

Circumferential actin-cables have been identified in the dorsal ridge and the dorsal part of the Hh stripes. Hence, I hypothesized that their production requires DPP signaling, as already observed for the dorsal ridge. Therefore, to impair their production without impacting the dorsal closure process, I performed DPP signaling inhibition in the epidermis posterior cells of all segments using the *UAS-Brk*

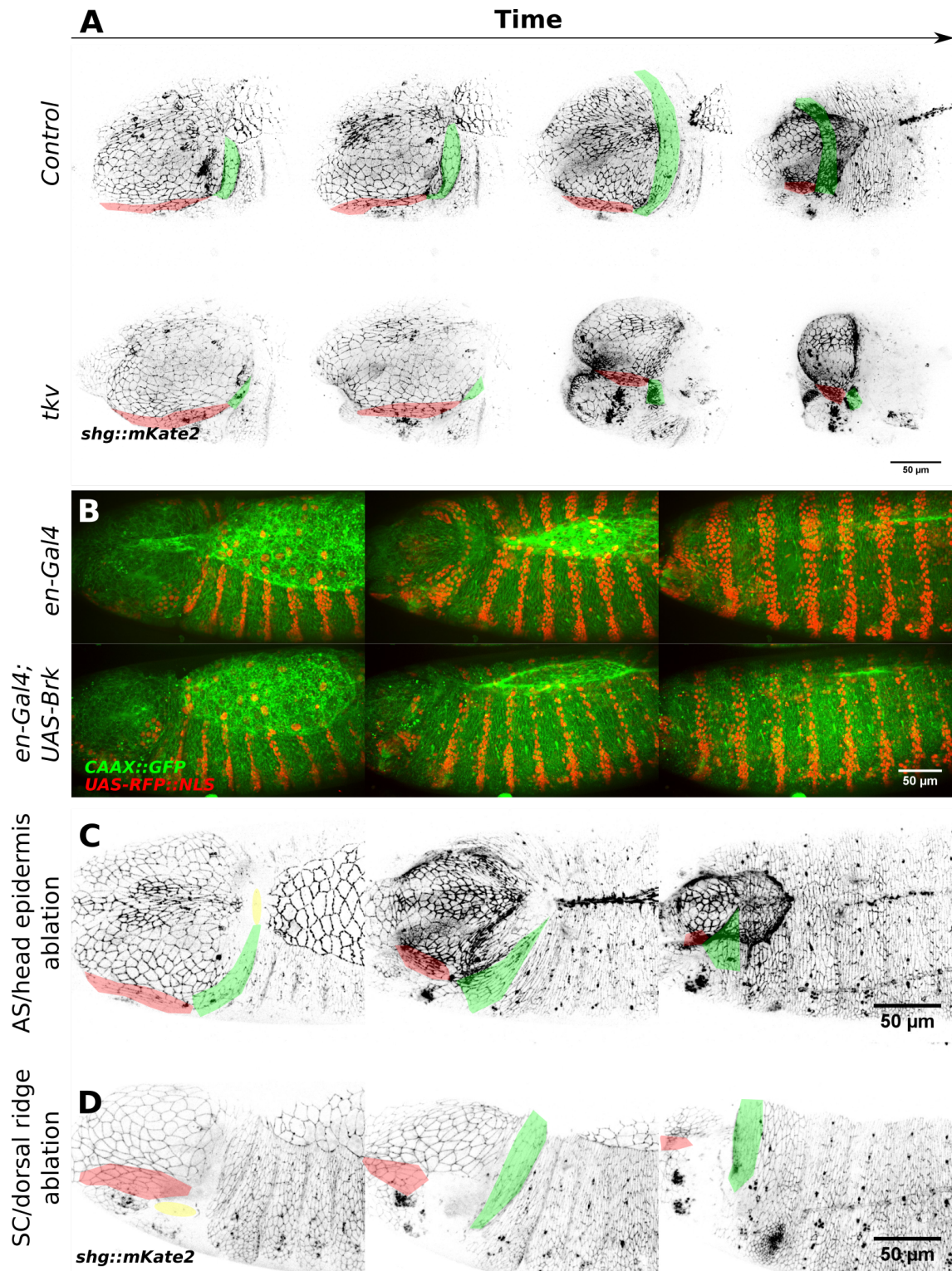


Figure II.10: The contraction of a stripe of head epidermis cells tracts the dorsal ridge towards the anterior of the embryo

A: Maximum projections of time-lapses from a control and *tkv* mutant during dorsal closure. The dorsal ridge is highlighted in green and Suspender Cells in red. **B:** Maximum projections of time-lapses from a *en-Gal4, UAS-RFP::NLS; Jupiter::GFP* and a *en-Gal4, UAS-RFP::NLS; Jupiter::GFP/UAS-Brk* embryos during dorsal closure. **C:** Maximum projections of time-lapses from a *shg::mKate2* embryo following laser ablation of the junction between the head epidermis and the amnioserosa. Dorsal ridge highlighted in green, Suspender Cells in red and ablated region highlighted in yellow. **D:** Maximum projections of time-lapses from a *shg::mKate2* embryo following laser ablation of the junction between the Suspender cells and the dorsal-ridge. Dorsal ridge highlighted in green, Suspender Cells in red and ablated region highlighted in yellow.

construct under the control of the *en-Gal4* driver (*en* and *hh* have the same pattern of expression at the dorsal closure stage). The embryos were expressing the *CAAX::GFP* and *UAS-RFP::NLS* as reporters for visualization (Figure II.10 B). In control embryos, I observed that the *en-Gal4* driver successfully induces the *UAS-RFP::NLS* construct in the posterior cells of the dorsal ridge and of the segments. Induction of *Brk* in this subset of cells impaired dorsal ridge development and surprisingly decreased the number of dorsal *en* + cells in the epidermis domain. Thus, *Brk* induction led to the impairment of dorsal patterning. However in these embryos, dorsal closure and head-involution are completed. Moreover, Suspender cells contraction occurs and correlates with head-involution initiation in the absence of dorsal ridge fusion. Therefore, these results suggest that in these conditions circumferential actin-cables are not required for head-involution, whose completion still correlates with Suspender cells stripe contraction.

In order to physically decorrelate circumferential actin-cables formation and head-involution in wild-type conditions I performed laser ablation of the region at the interface between the head epidermis and AS anterior most cells, including some of the AS cells (Figure II.10 C, ablated region highlighted in yellow). Time-lapse imaging of such embryos expressing the *shg::mKate2* marker reveals that the ablation impairs dorsal ridge fusion (highlighted in green) and delays dorsal closure anterior canthus formation. In such conditions, head-involution initiates independently of the fusion of the dorsal epidermis at the midline. Suspender cells stripes

(highlighted in red) contraction and dorsal ridge anterior migration occur prior to canthus formation, thus prior circumferential actin-cables formation. Therefore, it is confirmed that head-involution initiation does not physically depend on circumferential actin-cables contraction in wild-type conditions.

However, it remained unclear whether the Suspender cell stripes contraction correlates with dorsal ridge anterior migration because Suspender cells exert traction on the dorsal ridge or because the dorsal ridge actively compresses the stripes while migrating towards the anterior of the embryo. To test this hypothesis I performed laser ablations of the Suspender cells/dorsal-ridge interface (Figure II.10 D, ablated region highlighted in yellow). In such conditions Suspender cells (highlighted in red) contraction is conserved whereas dorsal ridge (highlighted in green) anterior migration is affected. Therefore Suspender cells stripes contraction is active and does not result from a compression initiated by the dorsal ridge. I hypothesize that dorsal ridge anterior migration occurs after a delay because it remains linked to the other side of the embryo where Suspender cells are intact. In the other side, the Suspender cells stripe contracts and therefore exerts an anterior traction on the epidermis that drives anterior migration.

Altogether, my results show that circumferential actin-cables are not required to initiate head-involution. However, Suspender cells contraction is able to drive anterior migration of the dorsal epidermis over the head, thus allowing head-involution.

C) Contraction of a supra cellular actin web is associated with cellular contraction and convergent extension in the head epidermis

In order to understand the molecular origin of the forces leading to Suspender cells contraction, I analyzed the pattern of the Zasp52 protein. Zasp52 is involved in supra-cellular actin structures formation, such as the muscles and the actin cable during dorsal closure [Ducuing and Vincent, 2016]. I performed time-lapse imaging of embryos expressing the *zasp52::GFP* reporter during head-involution and observed that Suspender cells display an elevated expression of *zasp52* (Figure II.11 A). Moreover, the protein is organized in a vast supra-cellular web, polarized from anterior to posterior. During head-involution, the supra-cellular actin web contracts simultaneously with Suspender cells. Therefore, I hypothesized that supra-cellular actin web contraction could power the contraction of the whole Suspender cells domain.

To understand the cellular mechanisms underlying the contraction of the Suspender cells domain, I turned again to time-lapse imaging of Suspender cells cells expressing the *shg::mKate2* marker, but this time using a higher time resolution (Figure II.11 B). This allowed me to perform single cell tracking of Suspender cells cells through the course of head-involution. This analysis allowed me to observe a succession of T1 cell intercalation events (four cells vertex formations are indicated by red arrow-heads). Tracking of the four cells displayed in Figure II.11 B shows that Suspender cells operate a convergent extension rearrangement contributing to the shrinking of the Suspender cells stripe. Moreover, quantification of the apical area of these cells through time shows that these cells also undergo apical contraction (Figure II.11 C). Therefore, convergent extension and cell contraction cooperate to achieve the active and fast shrinking of suspender cells stripes.

Altogether, I identified a new sub-region of the head epidermis that acts as a motor

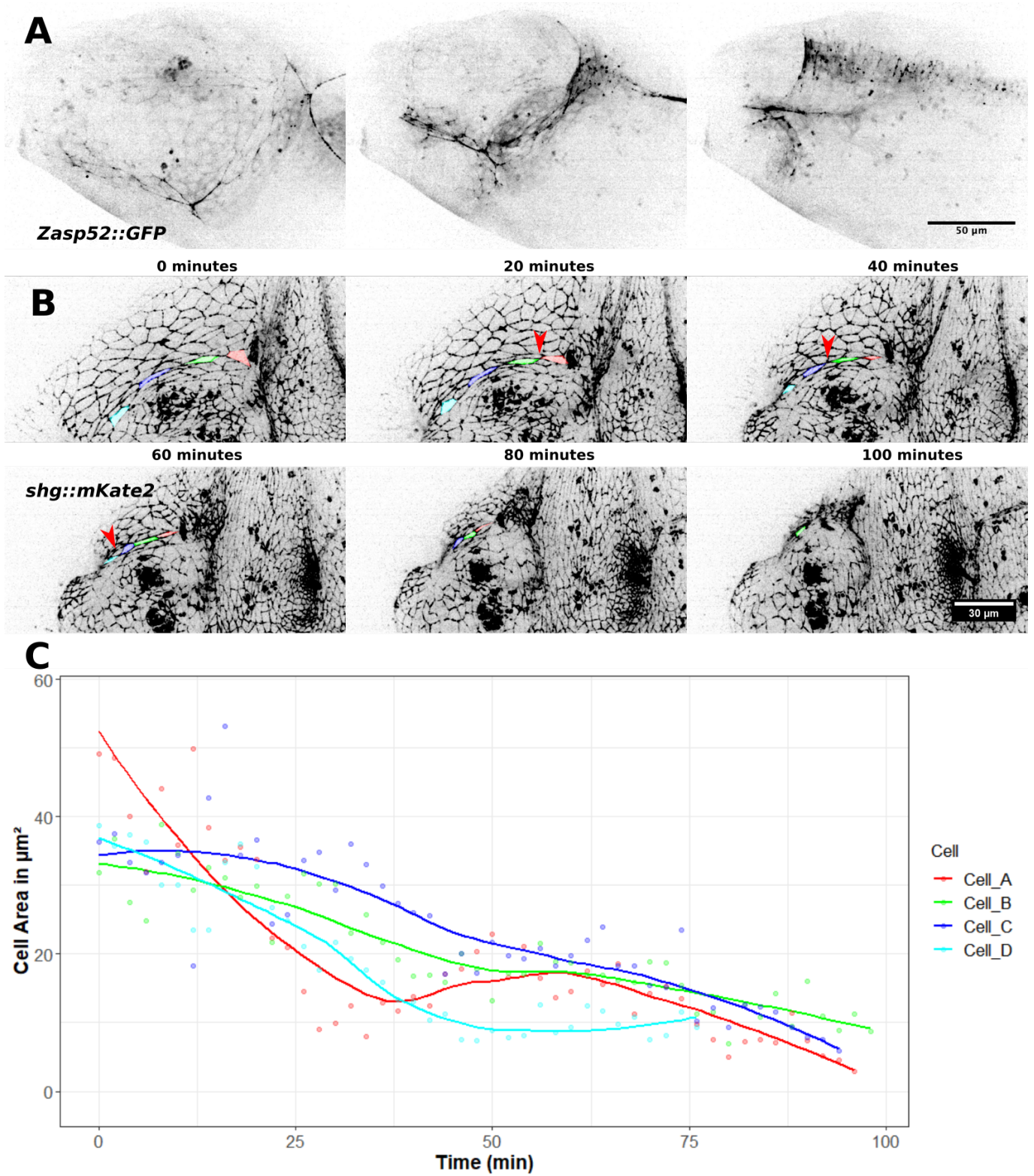


Figure II.11: Contraction of a supra-cellular actin web is associated with cellular contraction and convergent extension in the head epidermis

A: Maximum projections of time-lapse from a *zasp52::GFP* embryo displaying a supra-cellular actin web within its Suspender Cells. **B:** Maximum projections of time-lapse from a *shg::mKate2* embryo during the head-involution. 4 Suspender cells are tracked and highlighted in red, green, blue and cyan respectively. Red arrowheads indicate T1 neighbor exchanges. **C:** Quantification of the apical area of the 4 tracked cells as a function of time.

for head-involution. I coined the name "suspender cells" because their contraction acts as suspenders whose contraction would pull up pants. Interestingly in this model the circumferential actin-cables do not act as the motor, but much more as belts that allows the coordinated migration of the epidermis perpendicular to the two unique traction points created by Suspender cells.

Chapter III

Discussion

My thesis work is mostly dedicated to the understanding of dorsal closure. I used the classical approach of genetic mutation and gene induction in order to disrupt the process, thus revealing the properties of the system. However, my work can be distinguished from others as it focused mainly on the morphogenesis of distinct tissues and on their dynamic interaction instead of considering them as independent entities. Few have chosen this approach to describe late *D. melanogaster* embryogenesis. I found only one exception: the work of Doctors VanHook and Letsou that tried to link together the dorsal closure and head-involution processes more than a decade ago [VanHook and Letsou, 2008]. This approach led me to investigate a broader morphogenetic field than dorsal closure alone, and allowed me to propose an innovative vision of both dorsal closure and other simultaneous morphogenetic processes.

I) A fresh look on the dorsal closure process

At first, my thesis goal was to understand the dorsal-open phenotype at the origin of the evisceration of mutants for components of the JNK and DPP pathways. Through this work I shed light on several new aspects of the dorsal-open phenotype, but also on the roles of these two signaling pathways and properties of the dorsal closure process in wild-type conditions.

A) The dorsal closure fails after its initiation in dorsal-open embryos

The first key point that I identified during my thesis is that embryos mutated for the DPP and JNK pathways initiate dorsal closure prior to evisceration. In contrary of what was proposed by Fernandez et al [Fernández et al., 2007], AS contraction occurs during dorsal closure of these embryos. Surprisingly, our data strongly diverge on this specific aspect of dorsal closure in *tkv* mutants. My results, obtained from a high number of embryos demonstrate that amnioserosa contraction occurs in these mutants. Therefore, the dorsal open phenotype of *tkv* mutants is not the consequence of an arrest of the development of the epidermis layer at the dorsal closure stage.

However, from this point on, dorsal open phenotypes of mutants of the JNK and DPP pathways diverge in their proceeding. While AS contraction correlates with epidermis elongation in *jra* mutants, elongation fails in *tkv* mutants. The fact that AS contraction can be uncoupled from epidermis elongation in *tkv* mutants is intriguing. As the amnioserosa contracts, it reduces the size of the dorsal hole of the embryo. Therefore, if dorsal closure is considered as a 2.5D phenomenon, thus implying that the dorsal epidermis and amnioserosa accomplish there morphogenesis on a folded plane, reduction of the area of the first must lead to the increase of the area of the second. However, these two processes can be uncoupled in 3D. In *tkv*

mutant embryos, AS contraction is able to reduce the area of the dorsal hole, but in the absence of epidermis elongation the AS and dorsal epidermis both collapse towards the center of the embryo. Moreover, in *tkv* mutant embryos rescued with a functional *tkv* construct in the posterior compartment of each segment, dorsal closure is fulfilled in the absence of epidermis elongation and while the collapse occurs. Therefore, dorsal epidermis elongation is not necessary to close the hole. Hence, dorsal closure must be considered as a 3D morphogenetic event that does not obey the same physical laws that are expected in 2D. However, some parts in this collapse phenomenon remain unclear. Indeed, I could not test if the origin of the collapse of both tissues in *tkv* mutants is the consequence of the AS contraction alone.

As AS contraction is observed in dorsal-open embryos and epidermis elongation is not required for the process, the cause of the dorsal open phenotypes observed in *jra* and *tkv* embryos lies elsewhere. By describing carefully the dynamics of evisceration of both mutants, I showed that evisceration always initiates as a detachment of the epidermis from the AS. In *jra* embryos, these events occur throughout the LE/AS interface and trigger the instantaneous retraction of the epidermis whereas in *tkv* mutants, the activation of the JNK pathway delays the phenomenon as sutures are formed at the detachment site. Strikingly, the phenotype of *jra* mutants highly resembles the evisceration observed in *shg* mutants described by *Grofinkiel et al* [Gorfinkiel and Arias, 2007], and both pathways regulate the attachment between the two tissues at the adherent junction and basal membrane level. Interestingly, rescue of *tkv* mutants with up-regulation of *shg* in their dorsal epidermis were not successful (data not shown in this manuscript), suggesting that these pathways indeed regulate the AS/dorsal epidermis adhesion in a complex multi-faceted process. However, the common parameter present in the successful *tkv* rescues is the preservation of this interface. Therefore, the dorsal open phenotype can be recapitulated as the loss of adhesion strength between the AS and the dorsal epidermis, that leads to the evisceration of the embryos as the rest of embryogenesis proceeds.

B) DPP and JNK cooperate during dorsal closure while assuming non-overlapping functions

For decades now, the functions of DPP and JNK signaling have been linked together, as JNK induces DPP expression and mutants from both pathways lead to dorsal-open embryos. Moreover, our team demonstrated the presence of a feed-forward motif involving the two pathways, thus strengthening the hypothesis that the two pathways need to cooperate in order to assume their functions during dorsal closure. However, early in my thesis, I observed and started to characterize strong phenotypic differences between mutants of the two pathways, thus uncovering a more complex mechanism through which both pathways contribute to the dorsal closure process.

a) Early DPP signaling determines the properties of dorsal closure actors

As JNK is upstream of DPP during dorsal closure, one could easily explain that the phenotypes from these pathways diverge because JNK would have DPP independent targets. However, this hypothesis implies that JNK phenotype encompasses the one of DPP pathway mutants. Therefore, the fact that *jra* mutants do not display the lack of epidermis elongation observed in *tkv* mutants during dorsal closure discards this hypothesis. More, this demonstrates that another earlier source of DPP is required to allow epidermis elongation during dorsal closure. My thesis work does not allow to have a precise understanding of the precise spatio-temporal requirement of DPP signaling allowing dorsal epidermis elongation, but the analysis of *tkv* phenotype can be used to clear this matter. Thanks to the *tkv* mRNA deposited within the egg by their mother, *tkv* mutants are receptive to DPP up to a certain point of their embryogenesis. Therefore, the requirement of DPP signaling for dorsal epidermis elongation can be narrowed down to the period of time between the arrest of DPP signaling in *tkv* mutants and the activation of DPP by JNK signaling later on in embryogenesis. First, *tkv* mutants manage to develop a functional amnioserosa,

which requires *zen* activation by DPP at stage 5-7 of development, prior to GBE [Rushlow et al., 2001]. However, the heart tube differentiation is absent in *tkv* mutants, indicating that DPP dependent maintenance of *tinman* is absent. Lockwood et al performed a careful analysis of the requirement of DPP signaling for *tinman* expression and found that DPP signaling emanating from the epidermis is required at stage 9 and 11 [Lockwood and Bodmer, 2002]. Therefore, DPP signaling is lost in *tkv* mutants by stage 11 at the latest. Moreover, in *tkv* mutants, the tracheal dorsal branches are absent. This cell subpopulation emerges from the epidermis derived tracheal placodes that receive DPP signaling, which in turn drives *knirps* expression, concomitantly with their invagination at stage 10 [Vincent et al., 1997b]. Altogether, these observations suggest that DPP signaling is maintained in *tkv* mutants until stage 7-8 but is lost from stage 10 and onward.

One should also cross these observations with the DPP signaling activity during the early embryogenesis process. The dynamics of DPP signaling have been precisely reviewed by Rafterly and Sutherland in 2003 [Rafterly and Sutherland, 2003]. In their review, the authors describe how DPP signaling is at first broadly active in the dorsal region at cellularization, thus leading to the expression of *zen* and *pnr* in the whole dorsal part of the embryo. However, by stage 7, only the presumptive amnioserosa receives DPP, as *zen* expression pattern narrows down to this specific area. By stage 9 and GBE, DPP signaling is lost in the amnioserosa but rises in the whole dorsal epidermis region as its cells express DPP [Dorfman and Shilo, 2001]. Therefore, as JNK dependent DPP expression from stage 11 is not required for elongation, this would imply that autocrine DPP signaling emanating from the dorsal epidermis cells between stage 9 to 10 determines their ability to elongate during dorsal closure.

Altogether, I show that DPP determines the amnioserosa and dorsal epidermis several stages prior dorsal closure, thus unlocking their morphogenetic potential. Tissues then continue their morphogenesis independently of DPP, thus allowing its contractile behavior of the amnioserosa and promoting the elongation potential of

the dorsal epidermis. Much is known about the morphogenesis and properties of the amnioserosa during dorsal closure. In the next part, I will discuss my findings about the physical properties of the dorsal epidermis.

b) DPP signaling turns the dorsal epidermis from a visco-elastic into a visco-plastic tissue

Following the characterization of the spatio-temporal aspect of DPP signaling required for dorsal epidermis elongation during dorsal closure, I managed to unveil its mechanistic action. The physical mechanism and properties responsible for dorsal epidermis elongation have divided the scientific community for many years. Prior to the early 2000's, the dorsal epidermis was thought to migrate over the amnioserosa, thus leading to its elongation. Thanks to the work of Doctors Brown and Hayashi's teams, it was then demonstrated that the dorsal epidermis remains attached to the same pool of AS cells and therefore could not migrate over it [Narasimha and Brown, 2004, Wada et al., 2007]. Then, the forces driving dorsal epidermis elongation were thought to be a combination of AS and leading-edge emanating forces [Kiehart et al., 2000, Jacinto et al., 2000, Hutson et al., 2003, Toyama et al., 2008, Saias et al., 2015]. Finally, the AS alone has been shown to provide the forces necessary for epidermis elongation [Ducuing and Vincent, 2016, Pasakarnis et al., 2016]. However, all these hypotheses failed to focus on the properties allowing the dorsal epidermis to elongate in response to these applied forces. This question starts to emerge in the dorsal closure field, but has for now only raised interrogations. In their review, *Keihart et al* mention that it remains unclear whether the dorsal epidermis cells are only stretched or if they elongate [Kiehart et al., 2017]. Additionally, a recent review from *Trubuil et al* suggests that the epidermis stretches continuously under constant exerted forces by gradually decreasing its stiffness over time [Trubuil et al., 2021].

However, my thesis work demonstrates that a different mechanism, which is DPP dependent, allows the dorsal epidermis cell elongation. I showed that each individual

cell of the dorsal epidermis acquire plastic properties, thus allowing their continuous elongation at a constant rate under constant applied tension. These cells keep the visco-elastic behavior characteristics of all epithelia, but acquire the ability to semi-permanently deform as shown by ablation experiments. This allows the dorsal epidermis to accommodate to the tension exerted by the amnioserosa. Moreover, I demonstrated that this behavior is directly under the control of DPP signaling, as only the visco-elastic behavior of the dorsal epidermis is kept in *tkv* mutants. This leads to an arrest of the increase of the dorsal epidermis length during GBR, that is required later-on in wild-type to ensure the proper morphogenesis of the tissue. Two major questions arise from these observations: how do cells specifically acquire plastic properties and why is this mechanism chosen over classic intercalation/stretching processes. Unfortunately, I did not have the time to perform experiments to investigate these questions during my thesis. Regarding the molecular mechanism at the origin of plasticity, my main hypothesis is that it is driven by microtubule rearrangements. Indeed, *Jankovics et al* showed how microtubule transiently polymerize and align in the dorso-ventral direction during dorsal closure [Jankovics and Brunner, 2006]. Moreover, a similar behavior that I described in the introduction has been shown to promote cell elongation in the pupal wing. In these cells, microtubules grow and buckle against the membrane in order to elongate the cells, therefore indicating that microtubule alignment can promote permanent cell shape changes during morphogenesis [Singh et al., 2018].

The second interrogation, why is such cell plasticity promoted during dorsal closure, is more open and gives more room for hypotheses. At first, one could ask why cells in all epithelia do not present a similar plastic behavior. I would hypothesize that in an epithelium at equilibrium, such properties would prevent the tissue from keeping a permanent shape. Indeed, any disturbance would permanently deform it. Then, why choose cell plasticity over cell visco-elasticity or tissue fluidization through cell intercalation for an event such as dorsal closure? I will address both matters in

the next two paragraphs.

In the hypothesis of pure stretching, implying that the dorsal epidermis behaves as a visco-elastic material, the amnioserosa would need to provide significantly higher forces to generate , the same amount of epidermis elongation. I showed that the maximal elongation of the dorsal epidermis reaches approximately 90 μm whereas the non-plastic dorsal epidermis of *tkv* mutants reaches approximately 40 μm under similar traction. Therefore if the dorsal epidermis of wild-type embryos behaved as a visco-elastic tissue, the amnioserosa would need to exert twice as much forces in order to reach the same dorsal epidermis elongation. Exerting more forces on the dorsal epidermis/amnioserosa interface could therefore become a source of ripping between the two tissues, thus becoming a source of dorsal closure failure. Moreover, in order to perform the closure in a time range that is compatible with the morphogenesis of the neighboring organs, the force exerted by the amnioserosa would need to increase gradually. Indeed, I showed that the elongation characteristic time of the dorsal epidermis is close to 3 minutes. Therefore, exactly as the hypothesis of stiffness decrease from *Trubuil et al*, the physical properties of the system would need to change during the dorsal closure process, whereas under the plasticity hypothesis the properties of the system are determined prior to dorsal closure initiation. In such context, the dynamics of dorsal closure do not need precise regulations and its duration and morphogenesis is the consequence of initial conditions alone. Thus, under the principle of parsimony stated by the Ockham razor model, plasticity should be preferred as it provides a similar result through a simpler process.

By promoting cell plasticity, the dorsal epidermis acquires properties at the tissue scale that resembles the properties of a fluidized tissue through neighbor exchange. However, in most animal tissues plasticity almost always correlates with fluidization [Guillot and Lecuit, 2013, Collinet and Lecuit, 2021]. Then why is such mechanism, at the cell instead of tissue scale, promoted during the germband re-

traction and dorsal closure? I draw two hypothesis to answer such interrogation. First, I hypothesize that the answer could lie in the transitory aspect of the elongation of the dorsal epidermis during both processes. Indeed, the dorsal epidermis dorso-ventral length decreases almost immediately once dorsal closure is over. Therefore, the dorsal epidermis goes through a rapid cycle of elongation/shortening, thus not requiring the permanent aspect of deformation promoted by tissue fluidization. Moreover, by the stage 11 preceding germband retraction, the embryo segmentation is already defined with a precision going to the single cell. Therefore, morphogenetic processes leading to neighbor exchange would perturb the segmentation pattern of the embryo. Thus, tissue fluidization cannot be used for *D. melanogaster* morphogenesis after stage 11.

To go further, another conclusion can be drawn from these results. DPP, well known as a morphogen for its contribution as a pattern creator in the wing disc, acts also as a morphogen during dorsal closure, but in a different way. The name morphogen has the same origin as morphogenesis that I thoroughly described in the introduction part of this thesis. During dorsal closure, DPP allows the generation of a new shape of the dorsal epidermis, not by simply creating a pattern of several classes of cells, but by changing their mechanical properties in order to achieve morphogenesis. Interestingly, a parallel with the role of DPP during oogenesis in *Drosophila* can be made. As its secretion drives the change of physical properties of follicular cells, it leads to their flattening in response to nurse cells internal pressure. Therefore, the role of DPP as a morphogen acting as a modulator of cells mechanical properties seems to be generalizable to multiple morphogenesis events in *D. melanogaster*.

c) JNK signaling: the wound-healer

As described earlier, I characterized the role of DPP signaling independently of JNK signaling by comparing the similitudes and differences between control, *jra* and *tkv* mutants during dorsal closure. The reverse approach can be performed to

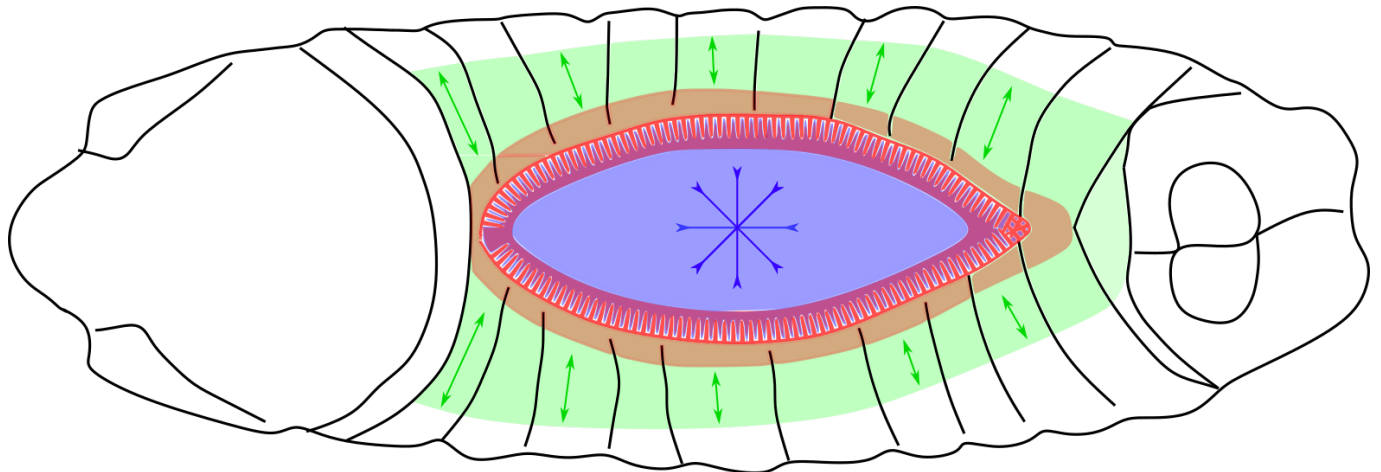
understand the role of JNK signaling independently of DPP. In *tkv* mutants, when the adhesion with the amnioserosa is lost, the leading-edge cells that receive high JNK signaling perform a closure of the wound and fuse with their neighbors, thus delaying evisceration. Therefore, the leading edge of *tkv* mutants behave as a giant wound on the brink of opening. In this wound, individual sutures immediately start whenever a tearing appears. On the contrary, *jra* embryos are unable to perform such sutures and any loss of adhesion between the dorsal epidermis and the amnioserosa leads to the immediate retraction of the epidermis. Thus, these conditions reveal the role of JNK signaling as the master regulator of wound healing. JNK signaling is absolutely required to perform the suture between two tissues in reaction to hole opening. Interestingly, this role is conserved throughout the life of the flies as it has already been described abundantly in the literature [Ríos-Barrera and Riesgo-Escovar, 2013]. The reiterative use of such tool, normally used for the response to non-physiological stress, provides an elegant example of how evolution combines different mechanisms to produce new shapes during embryogenesis. In the case of dorsal closure, only the zipping phase resembles the classic wound-healing process in which JNK signaling is usually involved - a point that I will discuss in a subsequent section of this discussion. Moreover, the use of JNK in cooperation with DPP signaling for the whole dorsal closure process might be the source of the perfect suture observed in embryos once the process is completed.

d) DPP and JNK signaling cooperate to promote dorsal epidermis/amnioserosa adhesion

The common points between mutants of both pathways is that they end up being dorsally open by the end of dorsal closure. Interestingly, this similarity between *tkv* and *jra* mutants is that both fail to ensure a proper adhesion between the amnioserosa and the dorsal epidermis. Therefore, one could formulate the hypothesis that the interaction between both pathways enables adhesion. Our team showed previously that the two pathways are involved in a feed-forward loop, thus ensuring

the robustness of the seamless aspect of dorsal closure zipping [Ducuing et al., 2015]. However, the reason why it relies on a diffusible protein, DPP, remained elusive. A possibility is that the interface between the dorsal epidermis and the amnioserosa involves the peripheral amnioserosa cells that are JNK negative. Therefore, JNK and DPP signaling would create an interface at the boundary of both tissues: the JNK/DPP positive cells of the leading edge and the DPP positive peripheral AS cells. These specific identities would then allow to develop an interface in which cells behave differently from their counterparts of the same tissue. However, experiments allowing to selectively remove the DPP induced by JNK in the leading-edge would be required to test such hypotheses. Alas, this specific experiment is difficult to perform with conventional tools already available with the UAS/Gal4 system. Indeed, Gal4s that encompass the precise spatio-temporal window required to perform the specific inhibition of DPP provided by JNK do not exist as for now. The different lines that I tested produce spatio-temporal patterns of expression that were either too early or too late to obtain a clear understanding of the process. However, one could get around this issue by performing targeted mutagenesis using the CRISPR/CAS9 system. The site of fixation of the Jra/Fos transcription factor would have to be removed from the *dpp* promoter, therefore removing only the last wave of DPP signaling that is JNK dependent. Such mutants would be crucial to finally understand the role of JNK/DPP interaction during dorsal closure.

Altogether, my findings about the role of DPP and JNK signaling during dorsal closure as a morphogenetic event are recapitulated here in Figure III.1.



3 waves of DPP signaling define tissue properties required for Dorsal Closure

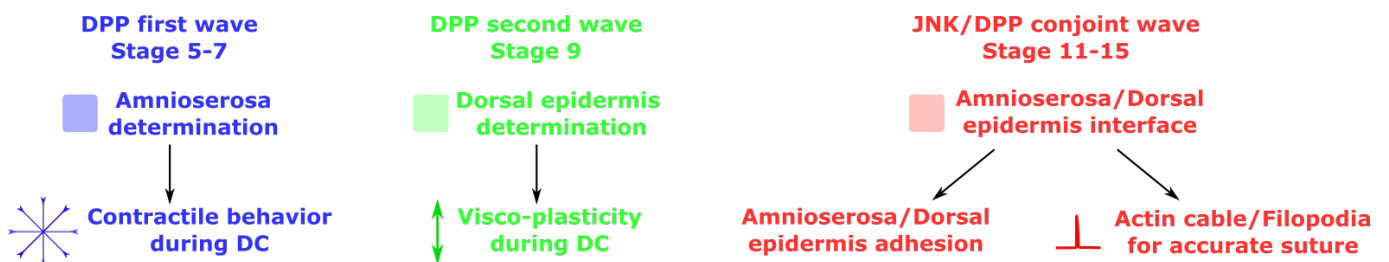


Figure III.1

C) Is dorsal closure a great model for wound-healing?

As of today, dorsal closure is used as a proficient and rather easy model for wound-healing. Indeed, dorsal closure shares similarities with the wound-healing process. These include the formation of an actin cable and filopodia protrusions at the leading-edge of the wound [Rothenberg and Fernandez-Gonzalez, 2019]. However, several aspects of dorsal closure should disqualify this complex morphogenetic event as a simple wound-healing model.

The first one would be the scale of the process. The tissue movements required for dorsal closure completion are within the whole embryo scale. Wounds that scale are not able to repair, even in embryos in any other conditions. This aspect is exemplified by the behavior of the leading-edge of *tkv* mutants. In these embryos, I observed functional wound-healing at the leading-edge. Indeed, the opening between the dorsal epidermis and the amnioserosa leads to ipsilateral fusion events, rather than contralateral fusion with the other flank of the epidermis. This phenomenon has also been identified using laser ablation in wild-type, where ablation of the leading-edge results in ipsilateral suture [Kiehart et al., 2000]. Therefore, dorsal closure does not recapitulate classical wound-healing as it allows the contralateral fusion of two flanks of the epidermis separated by half the circumference of the embryo.

This point underlines the second limitation regarding dorsal closure potential as a wound healing-model: dorsal closure involves other organs. Chief among them is the amnioserosa that is absolutely required for the process. Forces generated by the amnioserosa have been shown to be the driver of dorsal closure [Pasakarnis et al., 2016]. Moreover, my work demonstrates that failure of the process is the consequence of loss of adhesion between the amnioserosa and dorsal epidermis in classical dorsal open mutants. During physiological wound-healing, the wound is not covered by a short-lived tissue that brings the flanks of the wound together. Interestingly, in mammals, a small population of fibroblasts has been shown to differentiate at the wound site, therefore becoming specialized cells known as myo-fibroblasts [Chitturi et al., 2015]. These cells lie in the middle of the wound and contract. However, the

role of the myo-fibroblasts cannot be compared to the one of the amnioserosa, as they are thought to only facilitate the migration of the leading edge rather than generate the whole necessary pulling force necessary for wound closure. Additionally, my work demonstrates the involvement of the morphogenesis of internal organs and head-involution during dorsal closure, both generating supplementary constraints. Such conditions are not found in any wound closure events.

Therefore, the only step of dorsal closure that resembles wound healing is the very last one: the zipping phase. Once the two sides of the epidermis fuse together, the bulk of tissue morphogenesis is achieved and the "real closure" starts. However, even at that step, dorsal closure diverges from embryonic wound healing. Indeed, it has been shown that the fusion of the flanks of the epidermis is regulated by segment polarity genes. Indeed, cells use their filopodia in order to recognize the cells that they adhere to [Millard and Martin, 2008]. However, in embryonic epidermis wound healing of *D. melanogaster* and *D. rerio*, it can be clearly observed that cells from the leading-edge fuse at the center of the wound, with no preferences for their contralateral counterparts as in dorsal closure [Hunter et al., 2018].

Finally, the use of JNK signaling as the regulator of both wound-healing and adhesion to the amnioserosa complicates the genetic study of wound-healing during dorsal closure. Indeed, this dual requirement of JNK signaling illustrates that the regulation of the wound closure signaling during dorsal closure can also interfere with the bulk of dorsal closure morphogenesis. Thus, defects of wound closure observed during dorsal closure can also stem from morphogenesis defects and *vice-versa*. Therefore, interpreting the results of wound-healing experiment performed on dorsal closure increases the risks of biases induced by morphogenesis.

Taken altogether, these arguments converge into one simple explanation: dorsal closure is a morphogenetic event pre-programmed during embryogenesis of *D. melanogaster*. Therefore, it possesses all the properties and robustness characteristic of such events. Indeed, if dorsal closure is to be compared to a wound healing event, it would be a wound from which the borders would have been prepared for hours for its healing,

with a precision as thin as the single-cell scale. This is of course impossible, therefore I advocate that dorsal closure is not an adequate model for wound-healing.

II) From now on, you pull the strings: inter-organ cooperation drives epidermis morphogenesis

In the introduction of this manuscript, I mentioned that forces required for the morphogenesis of an organ could stem from endogenous or exogenous origin. However, in most of the morphogenetic events of early *D. melanogaster* embryogenesis, most of the forces are from endogenous origin. Surprisingly, I observed that late epidermis morphogenesis operates differently as it relies entirely on forces produced by external organs that are specialized in this process.

A) Amnioserosa and Suspender cells: the motors of dorsal epidermis morphogenesis

Dorsal closure and head-involution both rely on external forces. These are provided by specialized tissues that undergo contraction, the amnioserosa or the suspender cells. Interestingly, both tissues either disappear or have no known functions following embryogenesis. Indeed, all amnioserosa cells undergo apoptosis after dorsal closure, and so far nothing is known about the precise function of the three lateral rows of the procephalic epidermis later-on during larval life. This suggests that the conservation of both tissues morphogenesis through evolution occurred due to their role as motors providing the forces necessary for proper epidermis morphogenesis. However, both tissues perform contraction using different molecular and cellular processes. On one hand, the contraction of the amnioserosa relies on a complex interplay between acto-myosin dependent apical contraction, cell death and volume loss. It results in an isotropic contraction of the tissue, enclosing the hole on the dorsal part of the embryo. On the other hand, the Suspender cells, present on the lateral part of the procephalic epidermis, contract in the anterior to posterior direction. Therefore, they drag the dorsal epidermis over the procephalon. The directionality of the contraction is given both by the antero-posterior intercalation of the

Suspender cells and their initial shape prior to contraction. Indeed, prior to dorsal closure, Suspender cells are elongated towards the antero-posterior axis. Therefore, there uniform contraction generates more traction in the antero-posterior axis than in the lateral one. It is likely that both intercalation and contraction mechanisms are mediated by a supra-cellular acto-myosin web, a phenomenon already described during chicken neural plate development [Nishimura et al., 2012]. Another similitude with this phenomenon is the requirement of Rho GTPases, which mutation blocks head-involution in flies [Magie et al., , Jacinto et al., 2002].

Therefore, dorsal closure and head involution are morphogenetic movements that rely on two different external tissues that act as motors for their completion.

B) The dorsal epidermis is directionally predetermined for massive morphological changes

Forces responsible for dorsal closure and head involution do not come from the epidermis. However, several morphological aspects of the epidermis that are implemented prior both events and allow the directional changes observed during dorsal closure and head-involution are observed.

First, the dorsal epidermis undergoes two rounds of cell divisions before the onset of germ-band retraction [Foe, 1989]. By providing more cells to the tissues, these divisions allow for the necessary increase of the surface of the epidermis during germ-band retraction, dorsal closure and head involution.

Moreover, the germ-band retraction unfolds the U-shape of the dorsal epidermis. Therefore, the dorsal epidermis linear length is divided by two. This results in the folding of each segment separated by furrows. These folds can therefore act as area reservoirs for antero-posterior movements, which occur during the head involution process. However, these folds disappear during dorsal closure prior to head involution in the dorsal epidermis, suggesting that dorsal epidermis elongation on the antero-posterior axis relies on a different mechanism.

Additionally, my work demonstrates that the dorsal epidermis is able to adapt and

deform in the dorso-ventral axis in order to complete dorsal closure. This ability is predetermined by an earlier event: the DPP signaling from stage 9 and 10. However, my work encounters limitations in the sense that it cannot absolutely determine if this deformation is passive. Indeed, traction from the amnioserosa is absolutely required for the elongation as demonstrated by the series of ablations I performed. Moreover, the elongation of the tissues follows the same law as a visco-plastic material undergoing deformation under a constant stress. However, these are only clues converging with the passive deformation hypothesis. It remains possible that dorsal epidermis cells elongate actively in the direction of maximal tension and at a constant rate. The overgrowth of rescued *hh* bands in *tkv* mutant embryos would go in that direction. In order to test this hypothesis, I would need to increase the traction generated by the amnioserosa on the dorsal epidermis. If the linear elongation speed increases proportionally with the tension -that could be measured with laser ablations- then it would indicate that the deformation is passive. On the contrary, if the linear elongation remains unchanged, that would indicate that cells actively grow towards the midline, using the traction provided by the amnioserosa as a directional information. However, the complex origin of amnioserosa traction prevented me from modulating it, thus preventing me from drawing any conclusions regarding the nature of the dorsal epidermis deformation.

Additionally, the permanent elongation of the dorsal epidermis during dorsal closure could also be beneficial to head involution. Indeed, following zipping, dorsal epidermis cells are elongated towards the dorso-ventral direction. However, as head involution proceeds, this elongation diminishes and cells get wider along the antero-posterior axis. Therefore, elongation during dorsal closure could act as a reservoir of area for the antero-posterior head involution movement.

Altogether, these observations bring a new vision of the late epidermis morphogenesis. Despite being entirely dependent on external sources of force for its own morphogenesis, the dorsal epidermis is pre-patterned for the morphogenetic movements that it must accomplish.

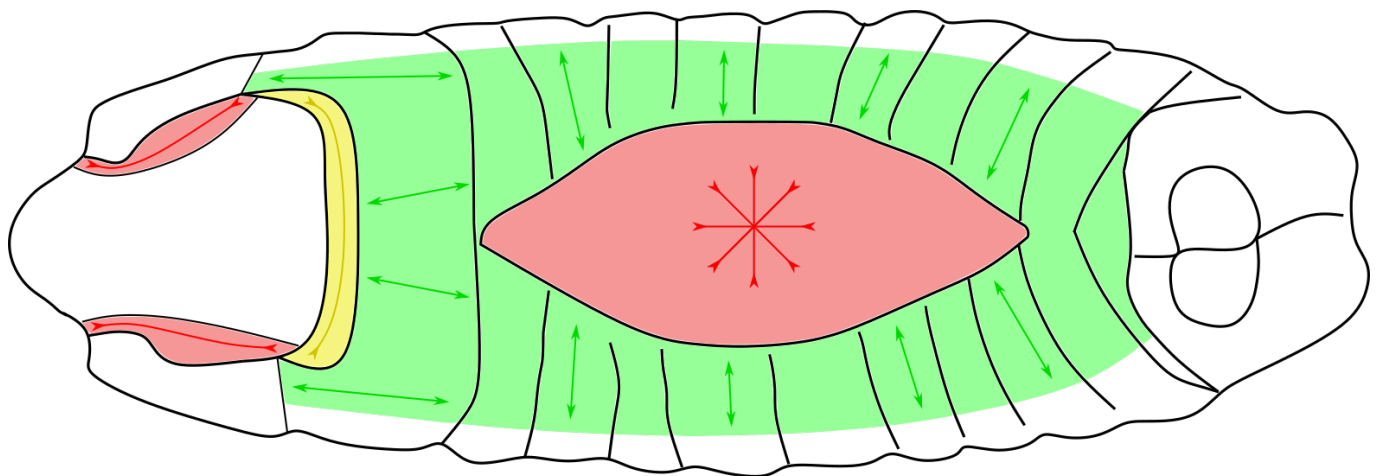
C) The synchronization of independent motors

So far, I highlighted two classes of actors during dorsal closure and head involution: the motors and the deformable recipient of the forces they generate. However, the study of *tkv* mutants enlightened a particular feature of their relation: their independence. Indeed, in *tkv* mutants, I observe that suspender cells contract independently of dorsal closure completion. Therefore, despite the fact that epidermis fusion at the midline is required for proper head involution, suspender cells initiate their developmental program. Similarly, in *tkv* mutants, the amnioserosa is able to contract independently of dorsal epidermis elongation and proper morphogenesis of the internal organs, which are also required for proper embryogenesis. Moreover, regarding dorsal closure, rescue of the *hh* bands in *tkv* mutants even show that it can be completed by amnioserosa contraction alone as long as the dorsal epidermis remains attached. In this particular case, the epidermis elongation is not even required. Thus, these two tissues act on the epidermis morphogenesis as independent entities without any retro-control loop.

However, the dorsal closure and head involution processes need to be synchronized in order to be successful. Therefore, the existence of two organs whose independent morphogenesis are not linked together might alter the whole embryogenesis process. I hypothesize that the dorsal ridge is instrumental to synchronize dorsal closure and head involution. Indeed, this structure is located between the head and the dorsal epidermis. Furthermore, it is involved in both processes as it migrates towards the midline during dorsal closure and forms the dorsal leading edge of head involution. In wild-type conditions, head-involution starts as it fuses at the midline. Interestingly, its contractile behavior identified by *Czerniak et al* could lead to the synchronization of the two morphogenetic processes [Czerniak et al., 2016]. The laser ablation of the dorsal ridge fusion point and anterior canthus formation that I performed resulted in the delay of dorsal closure zipping initiation. Therefore, it led to an artificial desynchronization of the two processes. In this case, the dorsal ridge ventral-most part is pulled anteriorly by the suspender cells but is still attached to

the dorsal epidermis dorsally. Therefore, the dorsal ridge is no longer orthogonal to the midline. When the dorsal ridge finally fuses at the midline, it begins to contract. Hence, the force generated participates to the anterior migration of the dorsal epidermis as it is not orthogonal to the midline. This behavior is associated with a temporally limited acceleration of the head involution process, thus resynchronizing head involution and dorsal closure. This way, the *Drosophila* embryo might manage to robustly synchronize two otherwise independent morphogenetic events, thus preventing developmental failure if a dorsal closure delay incidentally appears.

Altogether, my findings about the inter-organ cooperation responsible for epidermis morphogenesis are recapitulated here in Figure III.2.



Inter-organ cooperation in epidermis morphogenesis during late *D. melanogaster* embryogenesis

The independent motors



The Amnioserosa powers Dorsal Closure



The Suspenders power Head-Involution

The deformation acceptor



The dorsal epidermis covers the back and head of the embryo

The synchronizer



The Dorsal-ridge synchronizes Dorsal Closure and Head Involution

Figure III.2

Chapter IV

Material and Methods

I) Fly stocks

In order to generate the results displayed in this thesis, I used the following stable lines.

A) Gal4 lines

Lines	Genotype	Drives Gal4 expression in the following domains
Prd-Gal4	<i>w ; + ; Prd-Gal4 / TM6, Sb, Tb, Hu, Dfd::YFP</i>	Epidermal <i>prd</i> domain
Pnr-Gal4	<i>w ; + ; Pnr-Gal4 / TM6, Sb, Tb, Hu, Dfd::YFP</i>	Dorsal epidermis
hh-Gal4	<i>w ; + ; Hh-Gal4</i>	Epidermal <i>hh</i> domain
Ubx-Gal4	<i>w, +, Ubx-Gal4, UAS-RFP::NLS/TM3, Sb</i>	<i>Ubx</i> domain associated with a RFP::NLS construct
en-Gal4	<i>w ; En-Gal4, UAS-RFP::NLS/Cyo</i>	Epidermal <i>en</i> domain associated with a RFP::NLS construct
twist-Gal4	<i>w, twi-Gal4; +</i>	<i>twi</i> domain (mesoderm plus early midgut)

B) UAS lines

Lines	Genotype	Gal4 dependent induction of the following constructs
UAS-Brk	<i>w ; UAS-Brk / TM3, Sb, Ubx::lacZ</i>	inhibitor of the DPP pathway Brk
UAS-BskDN	<i>yw, UAS-bskDN ; +</i>	inhibitor of the JNK pathway
UAS-Rpr	<i>w ; + ; UAS-rpr / TM6B</i>	pro-apoptotic gene <i>rpr</i>
UAS-tkv::GFP	<i>w ; + ; UAS-tkv::GFP</i>	receptor of the DPP pathway <i>tkv</i> fused with a GFP
UAS-APC2::GFP	<i>w ; + ; UAS-APC2::GFP</i>	the actin binding site of APC2 fused with GFP

C) Mutant lines

Lines	Genotype	Description
<i>tkv</i>	<i>yw ; tkv⁴ / Cyo, w+</i>	Amorphic <i>tkv</i> allele
<i>jra</i>	<i>w ; jra⁷⁶⁻¹⁹ / Cyo, Wg::lacZ</i>	Amorphic <i>jra</i> allele
H99	<i>Df(3L)H99/TM3, Sb</i>	Deletion removing <i>D. melanogaster</i> pro-apoptotic genes

D) Lines used as live-markers

Lines	Genotype	Description
shg::GFP	<i>yw; shg::GFP</i>	endogenous E-cadherin <i>shg</i> fused with GFP
shg::mKate2	<i>yw, shg::mKate2</i>	endogenous E-cadherin <i>shg</i> fused with mKate2
CAAX::GFP	<i>yw; CAAX::GFP</i>	GFP fused with a CAAX peptide for membrane staining
CAAX::GFP	<i>yw ; + ; CAAX::GFP</i>	GFP fused with a CAAX peptide for membrane staining
Jupiter::GFP	<i>w ; + ; Jupiter::GFP</i>	endogenous microtubule binding protein Jupiter fused with GFP
Syb-QF2 QUAS-mCD8::GFP	<i>yw; + ; Syb-QF2, QUAS-mCD8::GFP/TM6B</i>	the QF2 transcription factor is driven by the <i>syb</i> promoter which leaks in the yolk cell, thus driving the expression of mCD8::GFP
TRE::GFP	<i>w ; TRE:GFP ; +</i>	AP1 (Jra-Fos) binding sites drive the expression of GFP, used as a JNK pathway sensor
Dad:GFP::NLS	<i>w ; If/Cyo; Dad:GFP::NLS</i>	Dad promoter drives the expression of GFP::NLS, used as a DPP pathway sensor
Zasp52::GFP	<i>w ; Zasp52::GFP ; +</i>	endogenous actin cables binding protein Zasp52 fused with GFP

E) Additional stable lines from combination of the previous lines

Lines	Genotype
<i>tkv</i> , <i>shg::GFP</i>	<i>tkv</i> ⁴ , <i>shg::GFP/Cyo</i> , <i>Dfd::YFP</i>
<i>tkv</i> , <i>shg::mKate2</i>	<i>w; tkv</i> ⁴ , <i>shg::mKate2/Cyo</i> , <i>Dfd::YFP</i>
<i>tkv</i> , <i>CAAX::GFP</i>	<i>w; tkv</i> ⁴ , <i>CAAX::GFP/Cyo</i> , <i>Dfd::YFP</i>
<i>tkv</i> ; <i>UAS-tkv::GFP</i>	<i>w; tkv</i> ⁴ ; <i>UAS-tkv::GFP/ST</i>
<i>tkv</i> ; <i>Pnr-Gal4</i> , <i>UAS-APC2::GFP</i>	<i>w; tkv</i> ⁴ , <i>Pnr-Gal4</i> , <i>UAS-APC2::GFP /ST</i>
<i>tkv</i> , <i>shg::mKate2</i> , <i>Dad:GFP::NLS</i>	<i>w; tkv</i> ⁴ , <i>shg::mKate2/Cyo</i> , <i>Dfd::YFP</i> ; <i>Dad:GFP::NLS</i>
<i>tkv</i> , <i>TRE::GFP</i>	<i>w; tkv</i> ⁴ , <i>TRE::GFP/Cyo</i>
<i>Pnr-Gal4</i> , <i>UAS-APC2::GFP</i>	<i>w; +; Pnr-Gal4, UAS-APC2::GFP/TM6, Sb, Tb, Hu, Dfd::YFP</i>

All other genotypes displayed in this thesis were generated from crosses that were not stabilized afterwards.

II) Live microscopy and image analysis

A) Embryo collection and preparation for live microscopy

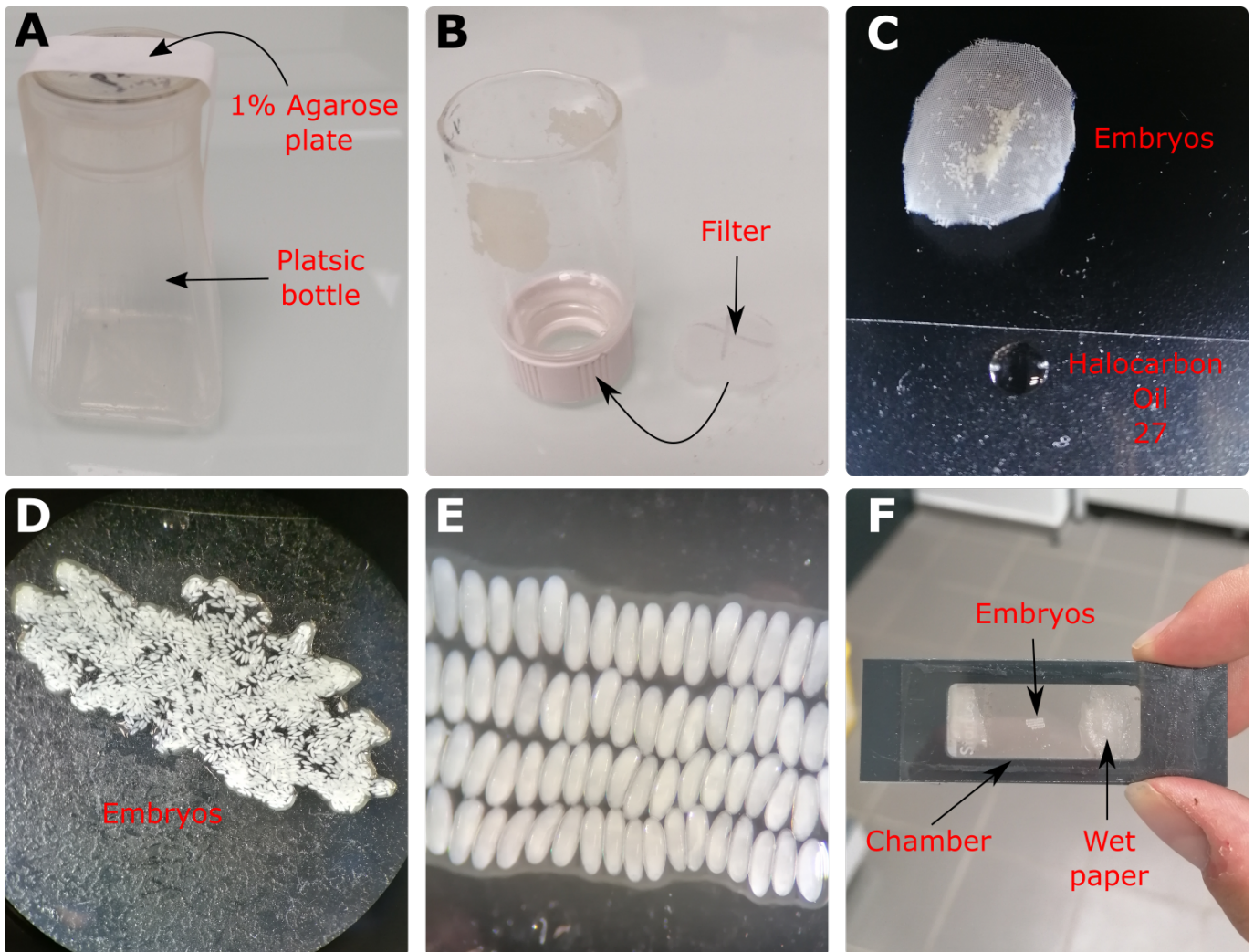


Figure IV.1: Embryo collection and preparation: **A:** Laying pot; **B:** Collection device; **C:** Embryos retrieval; **D:** Embryos spread in halocarbon oil 27; **E:** Embryo alignment; **F:** Embryos ready for imaging.

Crossed flies are kept in a bottle capped by a small 1% agarose plate (Figure IV.1 A). The egg-laying phase lasts at least 8 hours at 25°C.

The agarose plate is then retrieved, and 70% bleach is added for 3 minutes in order to digest the chorion of the embryos.

The dechorionated embryos are then retrieved on a small filter and washed using tap water (Figure IV.1 B). Then, embryos are quickly dried and immersed in halocarbon

oil 27 from Sigma on a microscopy coverslip (Figure IV.1 C).

Dechorionated embryos in oil then become transparent (Figure IV.1 D). Each embryo is then carefully staged and selected or not for the experiment. Selected embryos are then aligned in the middle of the slide (Figure IV.1 E).

Aligned embryos are then placed on a special chamber built from a microscopy slide. Wet paper is disposed in the chamber in order to avoid desiccation. The chamber is then sealed hermetically from both sides with tape (Figure IV.1 F).

B) Spinning disk microscopy

During my thesis I mainly used spinning disk microscopy. Spinning disks microscopy combines the use of a camera, as in epifluorescence or light-sheet microscopy, and the use of pin-holes as in conventional scanning confocal microscopy. Compared to the latter, spinning disk microscopy uses hundreds of pinholes disposed on a turning wheel. Combined with the use of a camera, this allows the simultaneous imaging of hundreds of point while keeping the 3D accuracy characteristic of confocal microscopy. The whole field of view is imaged as the wheel and pinholes turn, compared to one laser scanning the sample alone in classical scanning confocal microscopy. Therefore, spinning disk microscopy is a useful tool to perform 4D imaging on a high number of embryos as it allows an imaging that is manifold faster than scanning confocal microscopy.

a) Spinning disk specifications

The spinning disk I used during my thesis was built by the PLATIM imaging facility (Figure IV.2). It is built from an inverted DMI 4000B Leica stand, a spinning disk system CSU-W1-T1 Yokogawa, a Photometrics PRIME 95B camera and a Märzhäuser A8 (stage IM 123X87) stage combined with an additional piezo stage (P-737 PI piloted by Piezo Amplifier / Servo-Controller LVPZT PI). Illumination is generated by diodes from a MAG Biosystem Laser remote V1. I used these ones in this thesis: Diode 491 nm : Cobolt Calypso 50 mW serial number 5279 and Diode

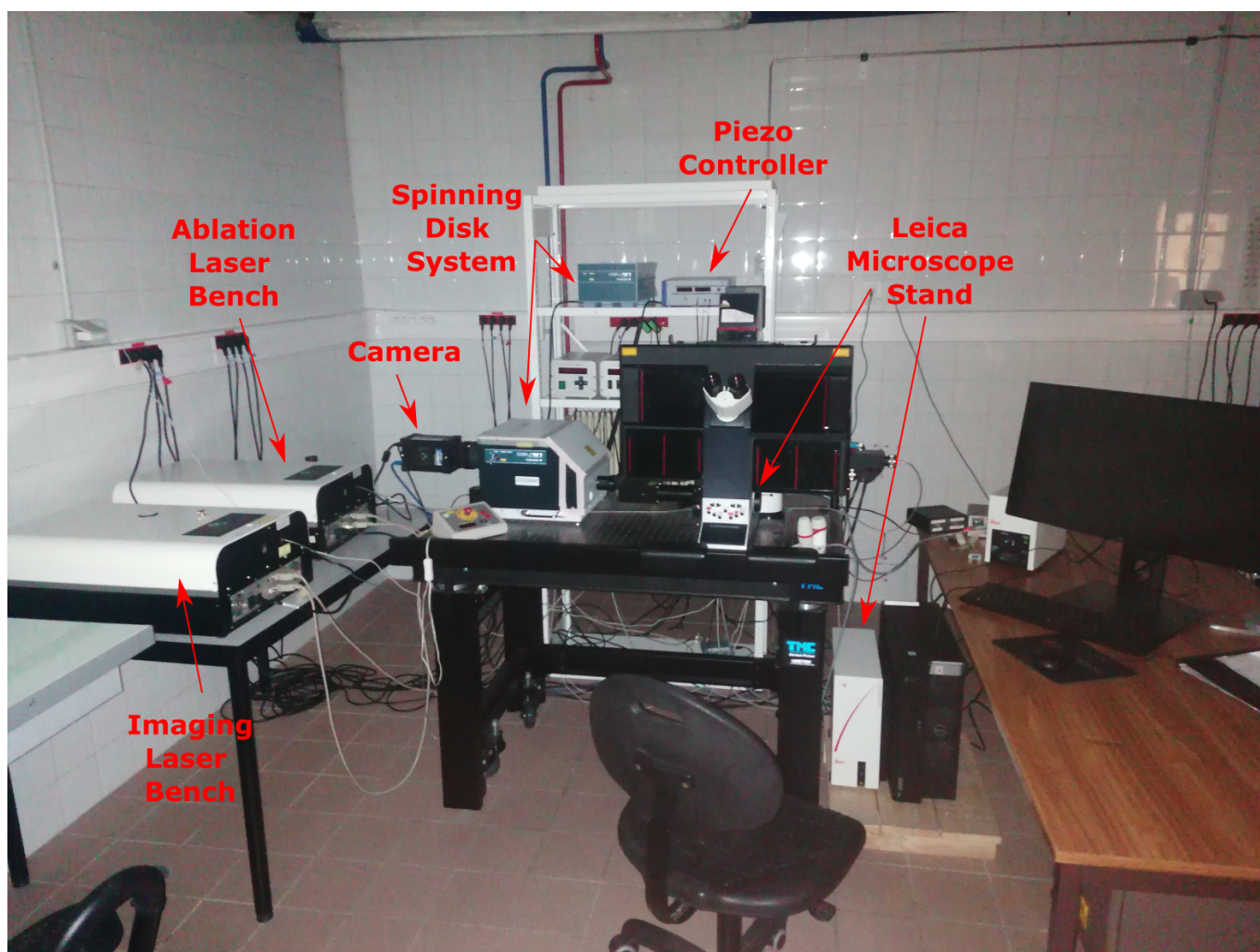


Figure IV.2: The PLATIM home-built spinning-disk microscope

561 nm : Cobolt-Jive 561 nm 50 mW serial number 8351. In this thesis I used the dry 20X (Leica #11506309), oil immersed 40X (Leica #11506261), water immersed 63X (Leica #11506281) and oil immersed (Leica #11506210). Additionally a chamber is built around the stage allowing the control of the imaging temperature by a Heating Unit Pecon.

The microscope also comprises a laser ablation device, composed of a Diode 355 nm: SFV-08E-0S0-BETA teem photonics from a MAG Biosystem Laser remote V1, controlled by a teem photonics Microchip Controller and a Smar act HCU 1D box allowing power specification.

b) Imaging and laser ablation

All experiments in this thesis were performed at 25°C. The microscope is controlled from the Metamorph software. Aligned embryos are localized on the slip directly from the live camera images. Embryos are selected for imaging are selected according to their stage and genotype (deducible from the fluorophores expressed by the embryo). The Metamorph software allows to perform the 4D imaging of each selected embryo when given the x,y,z position of each embryo, the desired z and time resolution and the number of z-slice desired. As an example, for 40X, imaging conditions usually chosen were: 2 μm z resolution, 41 slices and 10 minutes time-step. Laser ablations are performed using the Ilas2 control software. I always used less than a hundred repetitions of the pulsed laser at full power, using the 100X objective in order to increase precision and power (this objective has the highest numerical aperture). Imaging is then performed at 40, 63 or 100X.

C) Image analysis

4D stacks are processed using the FIJI software [Schindelin et al., 2012]. A first overview of the data is obtained by processing the data with the ".nd stack builder from Fiji", which can produce maximum projection movies of the data for each embryo.

Individual 4D stacks are then observed. Properties for each 4D stack are implemented manually by tacking into account the objective used during the experiment, the size of the camera captor, the z and time resolution of the experiment using the "Properties command".

Measures of 2D length, 2D area, cell count or time are then performed directly on the x,y,t or x,y,z,t stacks using the built in functions in Fiji. Ellipsoid fits of areas are performed automatically by the Fiji software. For 3D distances, only positions are recorded and length are calculated afterward in R during the post processing phase.

III) Statistical analysis and model fitting

Most of the statistical analysis were performed using R [R Core Team, 2022], via the RStudio interface [RStudio Team, 2020]. Unless indicated otherwise, the tests performed and modelization tools used come from the stats package of R. Plots were obtain using the ggplot2 package from R [Wickham, 2016]. A small subset of the analysis was also performed using GraphPad Prism.

A) Statistical analysis

Comparison between two means were performed using Welch's tests or Wilcoxon tests. Normality of the data was verified using Kolmogorov-Smirnov tests and Fisher tests were performed to assess for homoscedasticity. If both tests were non significant and the number of samples were judged sufficient, the parametric Welch's test was chosen. Otherwise, Wilcoxon tests were performed.

Comparison between multiple means were performed using ANOVA or Kruskal Wallis tests. Normality of the data was verified using Kolmogorov-Smirnov tests and Fisher tests were performed to assess for homoscedasticity. If both tests were non significant and the number of samples were judged sufficient, the parametric ANOVA followed by Tukey HSD post-hoc tests were chosen. Otherwise, Wilcoxon followed by Dunn's tests were performed.

Independence was assessed using Fishers exact tests for independence.

No ANOVA2 were performed on the results displayed in this manuscript.

B) Model fitting for speed extraction

Most of the analysis that I carried were performed in order to compare measures from individual embryos of different genotypes across multiple time-points. Therefore, measures obtained across time-points could not be considered as independent repetitions. Thus, even if many studies from the literature seem to be less sensitive regarding this matter, I could not perform conventional statistical tests such as

two-way ANOVA to perform comparisons over time. To get around this problem, I turned to the analysis of overall or maximum speeds, that are not time dependent. Speeds of individual embryos can then be compared between genotypes as embryos can be considered as independent.

To obtain the overall speed or maximum speed per embryo, one could calculate these results directly from the discrete variation of the measured feature over each time-point. However, this method happens to be extremely sensitive to outliers. Therefore, a proper fit of the data across time need to be performed in order to extract such values reliably.

If the feature measured evolves linearly with time, such as the case of the elongation of the dorsal epidermis, such linear model can be built:

$$\sum_{i=1}^{n_e} \sum_{j=0}^{n_t-1} l_{i,j} \vec{u}_{i,j} = \sum_{i=1}^{n_e} \sum_{j=0}^{n_t-1} (v_i t_j + l_{oi} + \epsilon_{i,j}) \vec{u}_{i,j} \quad (\text{IV.1})$$

where:

n_e is the number of embryos

n_t is the number of time-points

$l_{i,j}$ is the measured feature of the i^{th} embryo at the j^{th} time-point

v_i is the estimated speed of the i^{th} embryo

t_j is the time at the j^{th} time-point

l_{oi} is the estimated feature at $t = 0$

$\epsilon_{i,j}$ is the residual error of the fitted feature of the i^{th} embryo at the j^{th} time-point

$\vec{u}_{i,j}$ a unit vector setting the dimension

Therefore, the overall goodness of the fit can be evaluated and the mean speed of evolution of the measured feature for each embryo are extracted. Such speeds can then be compared using conventional tests.

However, the evolution through time of the area and width of the amnioserosa is not linear and such approach cannot be used. Nevertheless, I observed that they follow a

sigmoid function of time. Hence, for each embryo, I performed a 5-parameter logistic regression of the feature measured across time using the `nplr` R package [Commo and Bot, 2016]. Then, I obtained this fit for each embryo:

$$l(t) = l_{min} + \frac{l_{max} - l_{min}}{(1 + 10^{b(t_{inf}-t)})^s} + \epsilon(t) \quad (\text{IV.2})$$

where :

$l(t)$ is the measured feature at time t

l_{min} is the estimated bottom of the sigmoid

l_{max} is the estimated top of the sigmoid

b controls the stiffness of the estimated sigmoid

t_{inf} is the time at the inflexion point of the estimated sigmoid

s controls the potential asymmetry of the estimated sigmoid

$\epsilon(t)$ is the residual error of the model at time t

The goodness of such fit can then be evaluated for each embryo. If the fit is correct, the maximum speed of evolution of the measured feature for each embryo is extracted. Such speeds can then be compared using conventional tests.

IV) Modelling the physical behavior of the dorsal epidermis

A) Building of the visco-plastic model

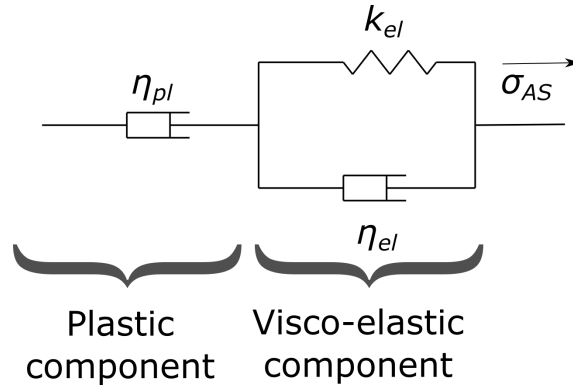


Figure IV.3: The simplified visco-plastic model

While characterizing the properties of the dorsal epidermis during dorsal closure, I observed that the dorsal epidermis behaves both as a visco-elastic and a plastic tissue. Therefore, I built a model of the dorsal epidermis elongation can be separated in two distinct parts (Figure IV.3). First, the visco-elastic component of the model is composed of a spring of stiffness constant k_{el} in parallel of a dash-pot of viscosity constant η_{el} . I added the plastic component of the tissue in a series, as a dash-pot of viscosity η_{pl} . Thus, I refer as this combination as a visco-plastic model.

On this dorsal epidermis model, a stress σ_{AS} , constant over time, is applied by the amnioserosa. I was allowed to consider this constraint as constant thanks to its estimation by laser ablation, as explained in the next result sections.

To study the total deformation over time of this system $\epsilon_{tot}(t)$, we first use the fact that the plastic and visco-elastic part of the system are in series, therefore:

$$\epsilon_{tot}(t) = \epsilon_{pl}(t) + \epsilon_{el}(t) \quad (\text{IV.3})$$

where $\epsilon_{pl}(t)$ is the deformation of the plastic component over time and $\epsilon_{el}(t)$ the visco-elastic deformation over time. Both values are fixed at 0 for $t = 0$.

Moreover, as both system are in series, it verifies:

$$\sigma_{pl} = \sigma_{el} = \sigma_{AS} \quad (\text{IV.4})$$

where σ_{pl} and σ_{el} are the stress experienced by the plastic and visco-elastic components respectively.

Hence, both systems can be easily studied separately.

The plastic deformation

From the first equations, we obtain:

$$\sigma_{AS} = \eta_{pl} \frac{d\epsilon_{pl}(t)}{dt} \quad (\text{IV.5})$$

wich can be resolved as:

$$\epsilon_{pl}(t) = \frac{\sigma_{AS}}{\eta_{pl}} t \quad (\text{IV.6})$$

The visco-elastic deformation

In the visco-elastic part of the model, the dash-pot and the spring are in parallel.

Given s and d as abbreviation for spring and dash-pot respectively, we obtain:

$$\sigma_{AS} = \sigma_s(t) + \sigma_d(t) \quad (\text{IV.7})$$

and

$$\epsilon_{el}(t) = \epsilon_s(t) = \epsilon_d(t) \quad (\text{IV.8})$$

Therefore, by using the formulae of the stress exerted on a spring or dash-pot we obtain:

$$\sigma_{AS} = \eta_{el} \frac{d\epsilon_{el}(t)}{dt} + k_{el}\epsilon_{el}(t) \quad (\text{IV.9})$$

Which can be resolved given the initial conditions as:

$$\epsilon_{el}(t) = \frac{\sigma_{AS}}{k_{el}}(1 - e^{-\frac{t}{\tau}}) \quad (IV.10)$$

with $\tau = \frac{\eta_{el}}{k_{el}}$

Therefore, the total deformation of the system becomes:

$$\epsilon_{tot}(t) = \frac{\sigma_{AS}}{\eta_{pl}}t + \frac{\sigma_{AS}}{k_{el}}(1 - e^{-\frac{t}{\tau}}) \quad (IV.11)$$

Then, it is possible to simulate the output of the model. An example is given in Figure IV.4.

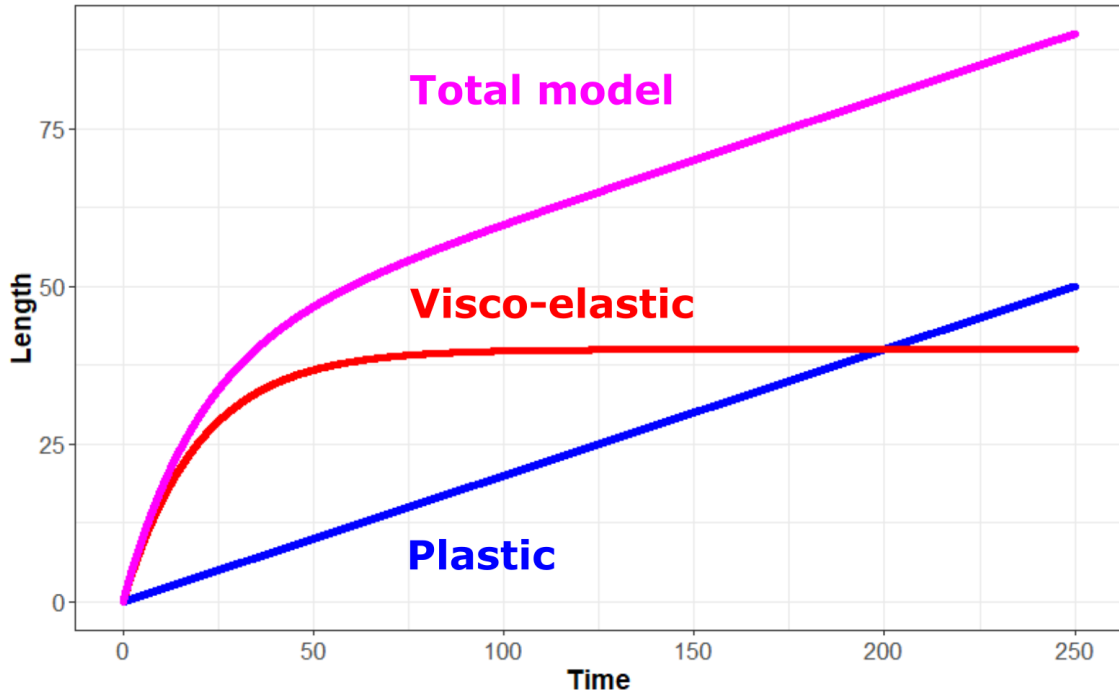


Figure IV.4: The output of the model

B) Stress estimation using laser ablation

In order to obtain an estimate of the stress applied to a tissue, we can combine laser ablation with the visco-elastic properties of the tissue. As plastic deformation are supposed to be permanent, they are not affected by the laser ablation. Two other hypothesis are required for this estimation: the tissue under stress is at equilibrium

and border effects can be neglected. We supposed that the first hypothesis is verified as the visco-elastic deformation of the tissue occurs during germband retraction and ablations were performed during dorsal closure. I will explain how the second hypothesis is verified later in the demonstration.

In these conditions, prior to ablation ($t = 0$), we have:

$$\epsilon_{el}(0) = \frac{\sigma_{AS}}{k_{el}} \quad (\text{IV.12})$$

However, after ablation the amnioserosa is detached from the epidermis, therefore σ_{AS} goes to 0. We can then re-use the equation of the deformation of a visco-elastic tissue defined earlier which gives:

$$0 = \eta_{el} \frac{d\epsilon_{el}(t)}{dt} + k_{el}\epsilon_{el}(t) \quad (\text{IV.13})$$

This ODE can be resolved given the initial conditions of the system and we obtain:

$$\epsilon_{el}(t) = \frac{\sigma_{AS}}{k_{el}} e^{-\frac{t}{\tau}} \quad (\text{IV.14})$$

It is then possible to calculate the derivative of this functions which gives:

$$\frac{d\epsilon_{el}(t)}{dt} = -\frac{\sigma_{AS}}{\eta_{el}} e^{-\frac{t}{\tau}} \quad (\text{IV.15})$$

and

$$\frac{d\epsilon_{el}(0)}{dt} = -\frac{\sigma_{AS}}{\eta_{el}} \quad (\text{IV.16})$$

Therefore, calculating the initial recoil after laser ablation gives an estimate of $\frac{\sigma_{AS}}{\eta_{el}}$. Under such conditions, at $t = 0$, the variation of ϵ_{el} are very small and border effects can therefore be neglected.

Finally, by making the hypothesis that η_{el} is the same for every embryo, we can conclude that the initial recoil measured after laser ablation is proportional to σ_{AS} . Therefore the initial recoil can be used to compare σ_{AS} between embryos.

C) Stretching time estimation using laser ablation

This precise estimation requires the same hypothesis as for stress estimation. However, border effects cannot normally be neglected in this case as we are observing the system for longer ($t \gg 0$). Here, border effects can be neglected as I individualized the segments by laser ablations prior to the measurements. Hence, when a third ablation separates the amnioserosa from the dorsal epidermis, there are no border effects remaining.

By comparing these two equations:

Visco-elastic stretching:

$$\epsilon_{el}(t) = \frac{\sigma_{AS}}{k_{el}}(1 - e^{-\frac{t}{\tau}}) \quad (\text{IV.17})$$

and visco-elastic relaxation:

$$\epsilon_{el}(t) = \frac{\sigma_{AS}}{k_{el}}e^{-\frac{t}{\tau}} \quad (\text{IV.18})$$

it can be observed that stretching and relaxation time are determined by the same variable: τ . Therefore it takes the same time for a visco-elastic tissue to be stretched, or to relax (Figure IV.5). Therefore, the time of relaxation measured from individualized epidermis stripes by laser ablation is a direct estimate of the visco-elastic stretching time of the same epidermis during dorsal closure.

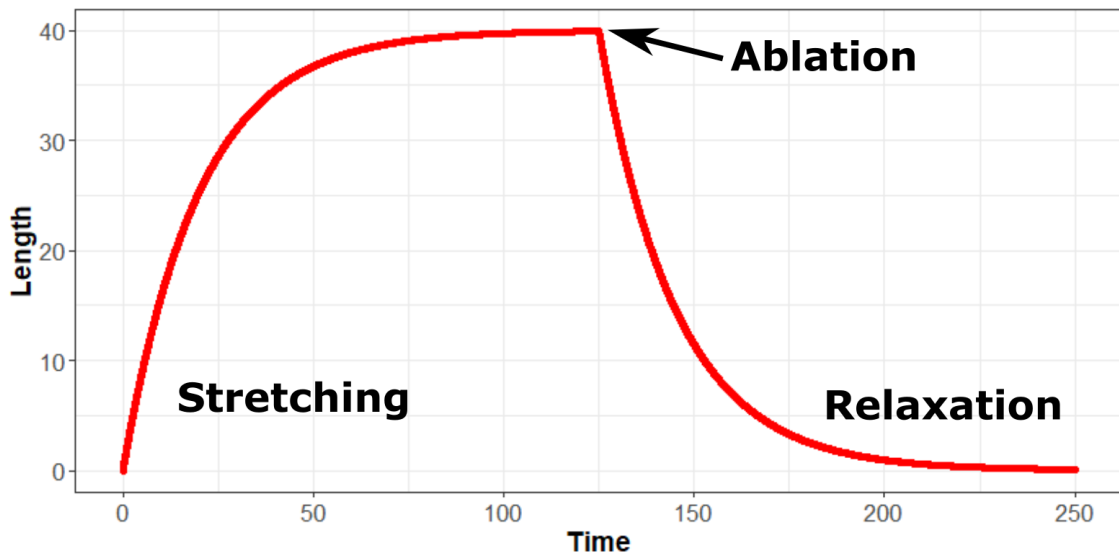


Figure IV.5: Simulation of the stretching and relaxation of a visco-elastic tissue undergoing laser ablation

Bibliography

- [Abbott and Lengyel, 1991] Abbott, M. K. and Lengyel, J. A. (1991). Embryonic head involution and rotation of male terminalia require the *Drosophila* locus head involution defective. *Genetics*, 129(3):783–789. Publisher: Oxford University Press.
- [Acot et al., 1998] Acot, P., Blandin, P., Hamm, B. P., Drouin, J.-M., Acot, P., Blondel-Mégrelis, M., Matagne, P., Bergandi, D., and Müller, G. (1998). Ernst Haeckel (1866): Generelle Morphologie der Organismen, Berlin, Reimer, 1866. Vol. i, pp. 2–21. Vol. ii, pp. 286–289. In *The European Origins of Scientific Ecology (1800-1901)*. Routledge. Num Pages: 26.
- [Affolter and Basler, 2007] Affolter, M. and Basler, K. (2007). The Decapentaplegic morphogen gradient: from pattern formation to growth regulation. *Nature Reviews. Genetics*, 8(9):663–674.
- [Almeida et al., 2011] Almeida, L., Bagnerini, P., Habbal, A., Noselli, S., and Serman, F. (2011). A mathematical model for dorsal closure. *Journal of theoretical biology*, 268(1):105–119. Publisher: Elsevier.
- [Arefin et al., 2019] Arefin, B., Parvin, F., Bahrapour, S., Stadler, C. B., and Thor, S. (2019). *Drosophila* Neuroblast Selection Is Gated by Notch, Snail, SoxB, and EMT Gene Interplay. *Cell Reports*, 29(11):3636–3651.e3.
- [Arora et al., 1995] Arora, K., Dai, H., Kazuko, S. G., Jamal, J., O’Connor, M. B., Letsou, A., and Warrior, R. (1995). The *Drosophila* *schnurri* gene acts in the

- Dpp/TGF beta signaling pathway and encodes a transcription factor homologous to the human MBP family. *Cell*, 81(5):781–790.
- [Ashe et al., 2000] Ashe, H. L., Mannervik, M., and Levine, M. (2000). Dpp signaling thresholds in the dorsal ectoderm of the *Drosophila* embryo. *Development (Cambridge, England)*, 127(15):3305–3312.
- [Bahri et al., 2010] Bahri, S., Wang, S., Conder, R., Choy, J., Vlachos, S., Dong, K., Merino, C., Sigrist, S., Molnar, C., Yang, X., Manser, E., and Harden, N. (2010). The leading edge during dorsal closure as a model for epithelial plasticity: Pak is required for recruitment of the Scribble complex and septate junction formation. *Development*, 137(12):2023–2032.
- [Bailles et al., 2019] Bailles, A., Collinet, C., Philippe, J.-M., Lenne, P.-F., Munro, E., and Lecuit, T. (2019). Genetic induction and mechanochemical propagation of a morphogenetic wave. *Nature*, 572(7770):467–473. Number: 7770 Publisher: Nature Publishing Group.
- [Baker et al., 1993] Baker, J., Theurkauf, W., and Schubiger, G. (1993). Dynamic changes in microtubule configuration correlate with nuclear migration in the pre-blastoderm *Drosophila* embryo. *Journal of Cell Biology*, 122(1):113–121.
- [Bates et al., 2008] Bates, K. L., Higley, M., and Letsou, A. (2008). Raw mediates antagonism of AP-1 activity in *Drosophila*. *Genetics*, 178(4):1989–2002.
- [Beira et al., 2014] Beira, J. V., Springhorn, A., Gunther, S., Hufnagel, L., Pyrowolakis, G., and Vincent, J.-P. (2014). The Dpp/TGF-dependent corepressor Schnurri protects epithelial cells from JNK-induced apoptosis in *Drosophila* embryos. *Developmental cell*, 31(2):240–247. Publisher: Elsevier.
- [Bertet et al., 2004] Bertet, C., Sulak, L., and Lecuit, T. (2004). Myosin-dependent junction remodelling controls planar cell intercalation and axis elongation. *Nature*, 429(6992):667–671. Number: 6992 Publisher: Nature Publishing Group.

- [Bhat, 1999] Bhat, K. M. (1999). Segment polarity genes in neuroblast formation and identity specification during *Drosophila* neurogenesis. *Bioessays*, 21(6):472–485. Publisher: Wiley Online Library.
- [Blanchard et al., 2010] Blanchard, G. B., Murugesu, S., Adams, R. J., Martinez-Arias, A., and Gorfinkiel, N. (2010). Cytoskeletal dynamics and supracellular organisation of cell shape fluctuations during dorsal closure. *Development*, 137(16):2743–2752.
- [Blankenship et al., 2006] Blankenship, J. T., Backovic, S. T., Sanny, J. S. P., Weitz, O., and Zallen, J. A. (2006). Multicellular Rosette Formation Links Planar Cell Polarity to Tissue Morphogenesis. *Developmental Cell*, 11(4):459–470.
- [Bogoyevitch and Kobe, 2006] Bogoyevitch, M. A. and Kobe, B. (2006). Uses for JNK: the Many and Varied Substrates of the c-Jun N-Terminal Kinases. *Microbiology and Molecular Biology Reviews*, 70(4):1061–1095.
- [Bradley et al., 2003] Bradley, P. L., Myat, M. M., Comeaux, C. A., and Andrew, D. J. (2003). Posterior migration of the salivary gland requires an intact visceral mesoderm and integrin function. *Developmental Biology*, 257(2):249–262.
- [Brigaud et al., 2015] Brigaud, I., Duteyrat, J.-L., Chlasta, J., Le Bail, S., Couderc, J.-L., and Grammont, M. (2015). Transforming Growth Factor β /activin signalling induces epithelial cell flattening during *Drosophila* oogenesis. *Biology Open*, 4(3):345–354.
- [Brummel et al., 1994] Brummel, T. J., Twombly, V., Marqués, G., Wrana, J. L., Newfeld, S. J., Attisano, L., Massagué, J., O’Connor, M. B., and Gelbart, W. M. (1994). Characterization and relationship of Dpp receptors encoded by the saxophone and thick veins genes in *Drosophila*. *Cell*, 78(2):251–261.
- [Bufi et al., 2015] Bufi, N., Durand-Smet, P., and Asnacios, A. (2015). Single-cell mechanics: the parallel plates technique. In *Methods in cell biology*, volume 125, pages 187–209. Elsevier.

- [Campbell et al., 2011] Campbell, K., Whissell, G., Franch-Marro, X., Batlle, E., and Casanova, J. (2011). Specific GATA Factors Act as Conserved Inducers of an Endodermal-EMT. *Developmental Cell*, 21(6):1051–1061. Publisher: Elsevier.
- [Campos-Ortega and Hartenstein, 1997] Campos-Ortega, J. A. and Hartenstein, V. (1997). *The Embryonic Development of Drosophila melanogaster*. Springer-Verlag, Berlin Heidelberg, 2 edition.
- [Catala et al., 1996] Catala, M., Teillet, M., De Robertis, E., and Le Douarin, M. (1996). A spinal cord fate map in the avian embryo: while regressing, Hensen's node lays down the notochord and floor plate thus joining the spinal cord lateral walls. *Development*, 122(9):2599–2610.
- [Caussinus et al., 2008] Caussinus, E., Colombelli, J., and Affolter, M. (2008). Tip-cell migration controls stalk-cell intercalation during Drosophila tracheal tube elongation. *Current biology*, 18(22):1727–1734. Publisher: Elsevier.
- [Chen et al., 1998] Chen, C.-K., Kuhnlein, R., Eulenberg, K. G., Vincent, S., Affolter, M., and Schuh, R. (1998). The transcription factors KNIRPS and KNIRPS RELATED control cell migration and branch morphogenesis during Drosophila tracheal development. *Development*, 125(24):4959–4968. Publisher: Company of Biologists The Company of Biologists, Bidder Building, 140 Cowley
- [Chen et al., 2009] Chen, Y.-C., Lin, S. I., Chen, Y.-K., Chiang, C.-S., and Liaw, G.-J. (2009). The Torso signaling pathway modulates a dual transcriptional switch to regulate tailless expression. *Nucleic Acids Research*, 37(4):1061–1072.
- [Chitturi et al., 2015] Chitturi, R. T., Balasubramaniam, A. M., Parameswar, R. A., Kesavan, G., Haris, K. T. M., and Mohideen, K. (2015). The role of myofibroblasts in wound healing, contraction and its clinical implications in cleft palate repair. *Journal of international oral health: JIOH*, 7(3):75–80.

- [Cho et al., 2012] Cho, Y. S., Stevens, L. M., Sieverman, K. J., Nguyen, J., and Stein, D. (2012). A Ventrally Localized Protease in the *Drosophila* Egg Controls Embryo Dorsoventral Polarity. *Current Biology*, 22(11):1013–1018.
- [Chopra and Levine, 2009] Chopra, V. S. and Levine, M. (2009). Combinatorial patterning mechanisms in the *Drosophila* embryo. *Briefings in Functional Genomics*, 8(4):243–249.
- [Chu et al., 2006] Chu, Y.-S., Eder, O., Thomas, W. A., Simcha, I., Pincet, F., Ben-Ze'ev, A., Perez, E., Thiery, J. P., and Dufour, S. (2006). Prototypical type I E-cadherin and type II cadherin-7 mediate very distinct adhesiveness through their extracellular domains. *Journal of Biological Chemistry*, 281(5):2901–2910. Publisher: ASBMB.
- [Clark et al., 2011] Clark, I. B. N., Muha, V., Klingseisen, A., Leptin, M., and Müller, H.-A. J. (2011). Fibroblast growth factor signalling controls successive cell behaviours during mesoderm layer formation in *Drosophila*. *Development*, 138(13):2705–2715.
- [Cleaver and Krieg, 1998] Cleaver, O. and Krieg, P. (1998). VEGF mediates angioblast migration during development of the dorsal aorta in *Xenopus*. *Development*, 125(19):3905–3914.
- [Clément et al., 2017] Clément, R., Dehapiot, B., Collinet, C., Lecuit, T., and Lenne, P.-F. (2017). Viscoelastic Dissipation Stabilizes Cell Shape Changes during Tissue Morphogenesis. *Current Biology*, 27(20):3132–3142.e4.
- [Collinet and Lecuit, 2021] Collinet, C. and Lecuit, T. (2021). Programmed and self-organized flow of information during morphogenesis. *Nature Reviews Molecular Cell Biology*, 22(4):245–265.
- [Commo and Bot, 2016] Commo, F. and Bot, B. M. (2016). *nplr: N-Parameter Logistic Regression*.

- [Costa et al., 1994] Costa, M., Wilson, E. T., and Wieschaus, E. (1994). A putative cell signal encoded by the folded gastrulation gene coordinates cell shape changes during *Drosophila* gastrulation. *Cell*, 76(6):1075–1089.
- [Czerniak et al., 2016] Czerniak, N. D., Dierkes, K., D’Angelo, A., Colombelli, J., and Solon, J. (2016). Patterned Contractile Forces Promote Epidermal Spreading and Regulate Segment Positioning during *Drosophila* Head Involution. *Current biology: CB*, 26(14):1895–1901.
- [da Silva and Vincent, 2007] da Silva, S. M. and Vincent, J.-P. (2007). Oriented cell divisions in the extending germband of *Drosophila*. *Development*, 134(17):3049–3054.
- [De Pascalis and Etienne-Manneville, 2017] De Pascalis, C. and Etienne-Manneville, S. (2017). Single and collective cell migration: the mechanics of adhesions. *Molecular Biology of the Cell*, 28(14):1833–1846. Publisher: American Society for Cell Biology (mboc).
- [Deng and Bownes, 1998] Deng, W. M. and Bownes, M. (1998). Patterning and morphogenesis of the follicle cell epithelium during *Drosophila* oogenesis. *The International Journal of Developmental Biology*, 42(4):541–552.
- [Desprat et al., 2005] Desprat, N., Richert, A., Simeon, J., and Asnacios, A. (2005). Creep function of a single living cell. *Biophysical journal*, 88(3):2224–2233. Publisher: Elsevier.
- [Doe, 2017] Doe, C. Q. (2017). Temporal patterning in the *Drosophila* CNS. *Annu. Rev. Cell Dev. Biol*, 33(219-240):776.
- [Dorfman and Shilo, 2001] Dorfman, R. and Shilo, B. (2001). Biphasic activation of the BMP pathway patterns the *Drosophila* embryonic dorsal region. *Development*, 128(6):965–972.
- [Driesch, 1892] Driesch, H. (1892). The potency of the first two cleavage cells in echinoderm development. Experimental production of partial and double forma-

- tions. *Foundations of experimental embryology*, pages 38–55. Publisher: Hafner: New York, NY, USA.
- [Ducuing et al., 2015] Ducuing, A., Keeley, C., Mollereau, B., and Vincent, S. (2015). A DPP-mediated feed-forward loop canalizes morphogenesis during *Drosophila* dorsal closure. *The Journal of Cell Biology*, 208(2):239–248.
- [Ducuing and Vincent, 2016] Ducuing, A. and Vincent, S. (2016). The actin cable is dispensable in directing dorsal closure dynamics but neutralizes mechanical stress to prevent scarring in the *Drosophila* embryo. *Nature Cell Biology*, 18(11):1149–1160.
- [Esteves et al., 2014] Esteves, F. F., Springhorn, A., Kague, E., Taylor, E., Pyrowolakis, G., Fisher, S., and Bier, E. (2014). BMPs regulate *msx* gene expression in the dorsal neuroectoderm of *Drosophila* and vertebrates by distinct mechanisms. *PLoS Genetics*, 10(9):e1004625. Publisher: Public Library of Science San Francisco, USA.
- [Fernandez-Gonzalez et al., 2009] Fernandez-Gonzalez, R., Simoes, S. d. M., Röper, J.-C., Eaton, S., and Zallen, J. A. (2009). Myosin II Dynamics Are Regulated by Tension in Intercalating Cells. *Developmental Cell*, 17(5):736–743.
- [Fernandez-Gonzalez and Zallen, 2009] Fernandez-Gonzalez, R. and Zallen, J. A. (2009). Cell Mechanics and Feedback Regulation of Actomyosin Networks. *Science Signaling*, 2(101):pe78–pe78. Publisher: American Association for the Advancement of Science.
- [Fernández et al., 2007] Fernández, B. G., Arias, A. M., and Jacinto, A. (2007). Dpp signalling orchestrates dorsal closure by regulating cell shape changes both in the amnioserosa and in the epidermis. *Mechanisms of Development*, 124(11):884–897.
- [Figard et al., 2013] Figard, L., Xu, H., Garcia, H. G., Golding, I., and Sokac, A. M. (2013). The Plasma Membrane Flattens Out to Fuel Cell-Surface Growth during *Drosophila* Cellularization. *Developmental Cell*, 27(6):648–655.

- [Foe and Alberts, 1983] Foe, V. and Alberts, B. (1983). Studies of nuclear and cytoplasmic behaviour during the five mitotic cycles that precede gastrulation in *Drosophila* embryogenesis. *Journal of Cell Science*, 61(1):31–70.
- [Foe, 1989] Foe, V. E. (1989). Mitotic domains reveal early commitment of cells in *Drosophila* embryos. *Development*, 107(1):1–22. Publisher: Company of Biologists
The Company of Biologists, Bidder Building, 140 Cowley
- [FOE, 1993] FOE, V. E. (1993). Mitosis and morphogenesis in the *Drosophila* embryo: point and counterpoint. *The development of Drosophila melanogaster*, 1:149–300. Publisher: Cold Spring Harbor Laboratory Press.
- [Forgacs et al., 1998] Forgacs, G., Foty, R. A., Shafrir, Y., and Steinberg, M. S. (1998). Viscoelastic properties of living embryonic tissues: a quantitative study. *Biophysical journal*, 74(5):2227–2234. Publisher: Elsevier.
- [Frasch, 1995] Frasch, M. (1995). Induction of visceral and cardiac mesoderm by ectodermal Dpp in the early *Drosophila* embryo. *Nature*, 374(6521):464–467.
- [Frasch, 1999] Frasch, M. (1999). Controls in patterning and diversification of somatic muscles during *Drosophila* embryogenesis. *Current opinion in genetics & development*, 9(5):522–529. Publisher: Elsevier.
- [Fremion et al., 1999] Fremion, F., Astier, M., Zaffran, S., Guillen, A., Homburger, V., and Semeriva, M. (1999). The heterotrimeric protein Go is required for the formation of heart epithelium in *Drosophila*. *The Journal of cell biology*, 145(5):1063–1076. Publisher: The Rockefeller University Press.
- [Fullilove and Jacobson, 1971] Fullilove, S. L. and Jacobson, A. G. (1971). Nuclear elongation and cytokinesis in *Drosophila montana*. *Developmental biology*, 26(4):560–577. Publisher: Elsevier.
- [Fuss et al., 2001] Fuss, B., Meissner, T., Bauer, R., Lehmann, C., Eckardt, F., and Hoch, M. (2001). Control of endoreduplication domains in the *Drosophila* gut by the knirps and knirps-related genes. *Mechanisms of Development*, 100(1):15–23.

- [Gallaud et al., 2017] Gallaud, E., Pham, T., and Cabernard, C. (2017). *Drosophila melanogaster* neuroblasts: a model for asymmetric stem cell divisions. *Asymmetric Cell Division in Development, Differentiation and Cancer*, pages 183–210. Publisher: Springer.
- [Garcia and Stathopoulos, 2011] Garcia, M. and Stathopoulos, A. (2011). Lateral gene expression in *Drosophila* early embryos is supported by Grainyhead-mediated activation and tiers of dorsally-localized repression. *PLoS one*, 6(12):e29172. Publisher: Public Library of Science San Francisco, USA.
- [Gardel et al., 2010] Gardel, M. L., Schneider, I. C., Aratyn-Schaus, Y., and Waterman, C. M. (2010). Mechanical Integration of Actin and Adhesion Dynamics in Cell Migration. *Annual Review of Cell and Developmental Biology*, 26(1):315–333.
- [Gelbart et al., 2012] Gelbart, M. A., He, B., Martin, A. C., Thiberge, S. Y., Wieschaus, E. F., and Kaschube, M. (2012). Volume conservation principle involved in cell lengthening and nucleus movement during tissue morphogenesis. *Proceedings of the National Academy of Sciences*, 109(47):19298–19303. Publisher: Proceedings of the National Academy of Sciences.
- [Ghabrial and Krasnow, 2006] Ghabrial, A. S. and Krasnow, M. A. (2006). Social interactions among epithelial cells during tracheal branching morphogenesis. *Nature*, 441(7094):746–749. Publisher: Nature Publishing Group.
- [Ghysen and Dambly-Chaudière, 2004] Ghysen, A. and Dambly-Chaudière, C. (2004). Development of the Zebrafish Lateral Line. *Current Opinion in Neurobiology*, 14(1):67–73.
- [Glise et al., 1995] Glise, B., Bourbon, H., and Noselli, S. (1995). hemipterous encodes a novel *Drosophila* MAP kinase kinase, required for epithelial cell sheet movement. *Cell*, 83(3):451–461.
- [Glise and Noselli, 1997] Glise, B. and Noselli, S. (1997). Coupling of Jun amino-terminal kinase and Decapentaplegic signaling pathways in *Drosophila* morpho-

- genesis. *Genes & Development*, 11(13):1738–1747. Company: Cold Spring Harbor Laboratory Press Distributor: Cold Spring Harbor Laboratory Press Institution: Cold Spring Harbor Laboratory Press Label: Cold Spring Harbor Laboratory Press Publisher: Cold Spring Harbor Lab.
- [Goldenberg and Harris, 2013] Goldenberg, G. and Harris, T. J. (2013). Adherens junction distribution mechanisms during cell-cell contact elongation in *Drosophila*. *PLoS One*, 8(11):e79613. Publisher: Public Library of Science San Francisco, USA.
- [Goodwin et al., 2016] Goodwin, K., Ellis, S. J., Lostchuck, E., Zulueta-Coarasa, T., Fernandez-Gonzalez, R., and Tanentzapf, G. (2016). Basal Cell-Extracellular Matrix Adhesion Regulates Force Transmission during Tissue Morphogenesis. *Developmental Cell*, 39(5):611–625.
- [Goodwin et al., 2017] Goodwin, K., Lostchuck, E. E., Cramb, K. M. L., Zulueta-Coarasa, T., Fernandez-Gonzalez, R., and Tanentzapf, G. (2017). Cell-cell and cell-extracellular matrix adhesions cooperate to organize actomyosin networks and maintain force transmission during dorsal closure. *Molecular Biology of the Cell*, 28(10):1301–1310. Publisher: American Society for Cell Biology (mboc).
- [Gorfinkiel and Arias, 2007] Gorfinkiel, N. and Arias, A. M. (2007). Requirements for adherens junction components in the interaction between epithelial tissues during dorsal closure in *Drosophila*. *Journal of Cell Science*, 120(18):3289–3298.
- [Gorfinkiel et al., 2009] Gorfinkiel, N., Blanchard, G. B., Adams, R. J., and Martinez Arias, A. (2009). Mechanical control of global cell behaviour during dorsal closure in *Drosophila*. *Development*, 136(11):1889–1898.
- [Grammont, 2007] Grammont, M. (2007). Adherens junction remodeling by the Notch pathway in *Drosophila melanogaster* oogenesis. *Journal of Cell Biology*, 177(1):139–150.

- [Gregory, 2006] Gregory, P. J. (2006). *Plant roots: growth, activity, and interaction with soils*. Blackwell Pub, Oxford ; Ames, Iowa. OCLC: ocm61461581.
- [Grieder et al., 1995] Grieder, N. C., Nellen, D., Burke, R., Basler, K., and Affolter, M. (1995). Schnurri is required for Drosophila Dpp signaling and encodes a zinc finger protein similar to the mammalian transcription factor PRDII-BF1. *Cell*, 81(5):791–800.
- [Guillot and Lecuit, 2013] Guillot, C. and Lecuit, T. (2013). Mechanics of Epithelial Tissue Homeostasis and Morphogenesis. *Science*, 340(6137):1185–1189. Publisher: American Association for the Advancement of Science.
- [Haack et al., 2014] Haack, T., Schneider, M., Schwendele, B., and Renault, A. D. (2014). Drosophila heart cell movement to the midline occurs through both cell autonomous migration and dorsal closure. *Developmental Biology*, 396(2):169–182.
- [Haas and Gilmour, 2006] Haas, P. and Gilmour, D. (2006). Chemokine Signaling Mediates Self-Organizing Tissue Migration in the Zebrafish Lateral Line. *Developmental Cell*, 10(5):673–680.
- [Hartenstein et al., 1985] Hartenstein, V., Technau, G. M., and Campos-Ortega, J. A. (1985). Fate-mapping in wild-type Drosophila melanogaster. *Wilhelm Roux's archives of developmental biology*, 194(4):213–216.
- [Hayashi and Kondo, 2018] Hayashi, S. and Kondo, T. (2018). Development and Function of the Drosophila Tracheal System. *Genetics*, 209(2):367–380.
- [Hayes and Solon, 2017] Hayes, P. and Solon, J. (2017). Drosophila dorsal closure: An orchestra of forces to zip shut the embryo. *Mechanisms of Development*, 144:2–10.
- [Hemavathy et al., 1997] Hemavathy, K., Meng, X., and Ip, Y. T. (1997). Differential regulation of gastrulation and neuroectodermal gene expression by Snail in

- the *Drosophila* embryo. *Development*, 124(19):3683–3691. Publisher: Company of Biologists The Company of Biologists, Bidder Building, 140 Cowley
- [Herranz and Morata, 2001] Herranz, H. and Morata, G. (2001). The functions of *pannier* during *Drosophila* embryogenesis. *Development*, 128(23):4837–4846.
- [Homsy et al., 2006] Homsy, J. G., Jasper, H., Peralta, X. G., Wu, H., Kiehart, D. P., and Bohmann, D. (2006). JNK signaling coordinates integrin and actin functions during *Drosophila* embryogenesis. *Developmental Dynamics*, 235(2):427–434. eprint: <https://onlinelibrary.wiley.com/doi/pdf/10.1002/dvdy.20649>.
- [Hou et al., 1997] Hou, X. S., Goldstein, E. S., and Perrimon, N. (1997). *Drosophila* Jun relays the Jun amino-terminal kinase signal transduction pathway to the Decapentaplegic signal transduction pathway in regulating epithelial cell sheet movement. *Genes & Development*, 11(13):1728–1737.
- [Hunter et al., 2018] Hunter, M. V., Willoughby, P. M., Bruce, A. E. E., and Fernandez-Gonzalez, R. (2018). Oxidative Stress Orchestrates Cell Polarity to Promote Embryonic Wound Healing. *Developmental Cell*, 47(3):377–387.e4.
- [Hutson et al., 2003] Hutson, M. S., Tokutake, Y., Chang, M.-S., Bloor, J. W., Venakides, S., Kiehart, D. P., and Edwards, G. S. (2003). Forces for morphogenesis investigated with laser microsurgery and quantitative modeling. *Science (New York, N.Y.)*, 300(5616):145–149.
- [Hwang and Rulifson, 2011] Hwang, H. J. and Rulifson, E. (2011). Serial specification of diverse neuroblast identities from a neurogenic placode by Notch and Egfr signaling. *Development*, 138(14):2883–2893. Publisher: Company of Biologists.
- [Häcker and Perrimon, 1998] Häcker, U. and Perrimon, N. (1998). DRhoGEF2 encodes a member of the Dbl family of oncogenes and controls cell shape changes during gastrulation in *Drosophila*. *Genes & Development*, 12(2):274–284. Company: Cold Spring Harbor Laboratory Press Distributor: Cold Spring Harbor

Laboratory Press Institution: Cold Spring Harbor Laboratory Press Label: Cold Spring Harbor Laboratory Press Publisher: Cold Spring Harbor Lab.

[Ikeya and Hayashi, 1999] Ikeya, T. and Hayashi, S. (1999). Interplay of Notch and FGF signaling restricts cell fate and MAPK activation in the *Drosophila* trachea. *Development*, 126(20):4455–4463.

[Inoue et al., 1998] Inoue, H., Imamura, T., Ishidou, Y., Takase, M., Udagawa, Y., Oka, Y., Tsuneizumi, K., Tabata, T., Miyazono, K., and Kawabata, M. (1998). Interplay of signal mediators of decapentaplegic (Dpp): molecular characterization of mothers against dpp, Medea, and daughters against dpp. *Molecular Biology of the Cell*, 9(8):2145–2156.

[Irish and Gelbart, 1987] Irish, V. F. and Gelbart, W. M. (1987). The decapentaplegic gene is required for dorsal-ventral patterning of the *Drosophila* embryo. *Genes & Development*, 1(8):868–879.

[Irvine and Wieschaus, 1994] Irvine, K. D. and Wieschaus, E. (1994). Cell intercalation during *Drosophila* germband extension and its regulation by pair-rule segmentation genes. *Development*, 120.

[Iwaki et al., 2001] Iwaki, D. D., Johansen, K. A., Singer, J. B., and Lengyel, J. A. (2001). drumstick, bowl, and lines are required for patterning and cell rearrangement in the *Drosophila* embryonic hindgut. *Developmental Biology*, 240(2):611–626.

[Iyer et al., 2019] Iyer, K. V., Piscitello-Gómez, R., Paijmans, J., Jülicher, F., and Eaton, S. (2019). Epithelial Viscoelasticity Is Regulated by Mechanosensitive E-cadherin Turnover. *Current Biology*, 29(4):578–591.e5.

[Jacinto et al., 2000] Jacinto, A., Wood, W., Balayo, T., Turmaine, M., Martinez-Arias, A., and Martin, P. (2000). Dynamic actin-based epithelial adhesion and cell matching during *Drosophila* dorsal closure. *Current Biology*, 10(22):1420–1426. Publisher: Elsevier.

- [Jacinto et al., 2002] Jacinto, A., Woolner, S., and Martin, P. (2002). Dynamic Analysis of Dorsal Closure in *Drosophila*: From Genetics to Cell Biology. *Developmental Cell*, 3(1):9–19.
- [Jacobs, 2000] Jacobs, J. R. (2000). The Midline Glia of *Drosophila*: a molecular genetic model for the developmental functions of Glia. *Progress in Neurobiology*, 62(5):475–508.
- [Jankovics and Brunner, 2006] Jankovics, F. and Brunner, D. (2006). Transiently Reorganized Microtubules Are Essential for Zippering during Dorsal Closure in *Drosophila melanogaster*. *Developmental Cell*, 11(3):375–385.
- [Jayasinghe et al., 2013] Jayasinghe, A., Crews, S., Mashburn, D., and Hutson, M. (2013). Apical Oscillations in Amnioserosa Cells: Basolateral Coupling and Mechanical Autonomy. *Biophysical Journal*, 105(1):255–265.
- [Jaźwińska et al., 1999] Jaźwińska, A., Kirov, N., Wieschaus, E., Roth, S., and Rushlow, C. (1999). The *Drosophila* Gene *brinker* Reveals a Novel Mechanism of Dpp Target Gene Regulation. *Cell*, 96(4):563–573.
- [Jiménez and Campos-Ortega, 1990] Jiménez, F. and Campos-Ortega, J. (1990). Defective neuroblast commitment in mutants of the *achaete-scute* complex and adjacent genes of *D. melanogaster*. *Neuron*, 5(1):81–89. Publisher: Elsevier.
- [Jin et al., 2005] Jin, S.-W., Beis, D., Mitchell, T., Chen, J.-N., and Stainier, D. Y. R. (2005). Cellular and molecular analyses of vascular tube and lumen formation in zebrafish. *Development*, 132(23):5199–5209.
- [Jurado et al., 2005] Jurado, C., Haserick, J. R., and Lee, J. (2005). Slipping or Gripping? Fluorescent Speckle Microscopy in Fish Keratocytes Reveals Two Different Mechanisms for Generating a Retrograde Flow of Actin. *Molecular Biology of the Cell*, 16(2):507–518. Publisher: American Society for Cell Biology (mboc).
- [Jürgens et al., 1984] Jürgens, G., Wieschaus, E., Nüsslein-Volhard, C., and Kluding, H. (1984). Mutations affecting the pattern of the larval cuticle in *Drosophila*

- melanogaster. *Wilhelm Roux's archives of developmental biology*, 193(5):283–295. Publisher: Springer.
- [Kaltschmidt et al., 2002] Kaltschmidt, J. A., Lawrence, N., Morel, V., Balayo, T., Fernández, B. G., Pelissier, A., Jacinto, A., and Martinez Arias, A. (2002). Planar polarity and actin dynamics in the epidermis of *Drosophila*. *Nature Cell Biology*, 4(12):937–944.
- [Karpova et al., 2006] Karpova, N., Bobinnec, Y., Fouix, S., Huitorel, P., and Debec, A. (2006). Jupiter, a new *Drosophila* protein associated with microtubules. *Cell Motility*, 63(5):301–312. _eprint: <https://onlinelibrary.wiley.com/doi/pdf/10.1002/cm.20124>.
- [Keller et al., 1992] Keller, R., Shih, J., and Sater, A. (1992). The cellular basis of the convergence and extension of the *Xenopus* neural plate. *Developmental Dynamics*, 193(3):199–217. _eprint: <https://onlinelibrary.wiley.com/doi/pdf/10.1002/aja.1001930302>.
- [Kerridge et al., 2016] Kerridge, S., Munjal, A., Philippe, J.-M., Jha, A., de las Bayonas, A. G., Saurin, A. J., and Lecuit, T. (2016). Modular activation of Rho1 by GPCR signalling imparts polarized myosin II activation during morphogenesis. *Nature Cell Biology*, 18(3):261–270. Number: 3 Publisher: Nature Publishing Group.
- [Kiehart et al., 2017] Kiehart, D. P., Crawford, J. M., Aristotelous, A., Venakides, S., and Edwards, G. S. (2017). Cell Sheet Morphogenesis: Dorsal Closure in *Drosophila melanogaster* as a Model System. *Annual Review of Cell and Developmental Biology*, 33(1):169–202. Publisher: Annual Reviews.
- [Kiehart et al., 2000] Kiehart, D. P., Galbraith, C. G., Edwards, K. A., Rickoll, W. L., and Montague, R. A. (2000). Multiple forces contribute to cell sheet morphogenesis for dorsal closure in *Drosophila*. *The Journal of Cell Biology*, 149(2):471–490.

- [Kockel et al., 1997] Kockel, L., Zeitlinger, J., Staszewski, L. M., Mlodzik, M., and Bohmann, D. (1997). Jun in Drosophila development: redundant and nonredundant functions and regulation by two MAPK signal transduction pathways. *Genes & Development*, 11(13):1748–1758. Company: Cold Spring Harbor Laboratory Press Distributor: Cold Spring Harbor Laboratory Press Institution: Cold Spring Harbor Laboratory Press Label: Cold Spring Harbor Laboratory Press Publisher: Cold Spring Harbor Lab.
- [Kolahi et al., 2009] Kolahi, K. S., White, P. F., Shreter, D. M., Classen, A. K., Bilder, D., and Mofrad, M. R. K. (2009). Quantitative analysis of epithelial morphogenesis in Drosophila oogenesis: New insights based on morphometric analysis and mechanical modeling. *Developmental Biology*, 331(2):129–139.
- [Lada et al., 2012] Lada, K., Gorfinkiel, N., and Martinez Arias, A. (2012). Interactions between the amnioserosa and the epidermis revealed by the function of the *u-shaped* gene. *Biology Open*, 1(4):353–361.
- [Lamiré et al., 2020] Lamiré, L.-A., Milani, P., Runel, G., Kiss, A., Arias, L., Vergier, B., Bossoreille, S. d., Das, P., Cluet, D., Boudaoud, A., and Grammont, M. (2020). Gradient in cytoplasmic pressure in germline cells controls overlying epithelial cell morphogenesis. *PLOS Biology*, 18(11):e3000940. Publisher: Public Library of Science.
- [Lawson et al., 2002] Lawson, N. D., Vogel, A. M., and Weinstein, B. M. (2002). sonic hedgehog and vascular endothelial growth factor Act Upstream of the Notch Pathway during Arterial Endothelial Differentiation. *Developmental Cell*, 3(1):127–136.
- [Lawson and Weinstein, 2002] Lawson, N. D. and Weinstein, B. M. (2002). Arteries and veins: making a difference with zebrafish. *Nature Reviews Genetics*, 3(9):674–682. Number: 9 Publisher: Nature Publishing Group.

- [Lecuit and Lenne, 2007] Lecuit, T. and Lenne, P.-F. (2007). Cell surface mechanics and the control of cell shape, tissue patterns and morphogenesis. *Nature Reviews Molecular Cell Biology*, 8(8):633–644. Number: 8 Publisher: Nature Publishing Group.
- [Lecuit and Wieschaus, 2000] Lecuit, T. and Wieschaus, E. (2000). Polarized Insertion of New Membrane from a Cytoplasmic Reservoir during Cleavage of the *Drosophila* Embryo. *Journal of Cell Biology*, 150(4):849–860.
- [Lee and Frasch, 2005] Lee, H.-H. and Frasch, M. (2005). Nuclear integration of positive Dpp signals, antagonistic Wg inputs and mesodermal competence factors during *Drosophila* visceral mesoderm induction. Publisher: Oxford University Press for The Company of Biologists Limited.
- [Lehmann et al., 1983] Lehmann, R., Jiménez, F., Dietrich, U., and Campos-Ortega, J. A. (1983). On the phenotype and development of mutants of early neurogenesis in *Drosophila melanogaster*. *Wilhelm Roux's archives of developmental biology*, 192(2):62–74. Publisher: Springer.
- [Leptin, 1999] Leptin, M. (1999). Gastrulation in *Drosophila*: the logic and the cellular mechanisms. *The EMBO Journal*, 18(12):3187–3192.
- [Lerit and Gavis, 2011] Lerit, D. A. and Gavis, E. R. (2011). Transport of Germ Plasm on Astral Microtubules Directs Germ Cell Development in *Drosophila*. *Current Biology*, 21(6):439–448.
- [Letsou et al., 1995] Letsou, A., Arora, K., Wrana, J. L., Simin, K., Twombly, V., Jamal, J., Staehling-Hampton, K., Hoffmann, F. M., Gelbart, W. M., and Massagué, J. (1995). *Drosophila* Dpp signaling is mediated by the punt gene product: a dual ligand-binding type II receptor of the TGF beta receptor family. *Cell*, 80(6):899–908.

- [Levayer and Lecuit, 2013] Levayer, R. and Lecuit, T. (2013). Oscillation and Polarity of E-Cadherin Asymmetries Control Actomyosin Flow Patterns during Morphogenesis. *Developmental Cell*, 26(2):162–175.
- [Levayer et al., 2011] Levayer, R., Pelissier-Monier, A., and Lecuit, T. (2011). Spatial regulation of Dia and Myosin-II by RhoGEF2 controls initiation of E-cadherin endocytosis during epithelial morphogenesis. *Nature Cell Biology*, 13(5):529–540. Number: 5 Publisher: Nature Publishing Group.
- [Li et al., 2016] Li, Z., Lee, H., and Zhu, C. (2016). Molecular mechanisms of mechanotransduction in integrin-mediated cell-matrix adhesion. *Experimental Cell Research*, 349(1):85–94.
- [Lockwood and Bodmer, 2002] Lockwood, W. K. and Bodmer, R. (2002). The patterns of wingless, decapentaplegic, and tinman position the Drosophila heart. *Mechanisms of Development*, 114(1):13–26.
- [Lu et al., 2016] Lu, H., Sokolow, A., Kiehart, D. P., and Edwards, G. S. (2016). Quantifying dorsal closure in three dimensions. *Molecular Biology of the Cell*, 27(25):3948–3955. Publisher: American Society for Cell Biology (mboc).
- [Lv et al., 2022] Lv, Z., Zhang, N., Zhang, X., Großhans, J., and Kong, D. (2022). The Lateral Epidermis Actively Counteracts Pulling by the Amnioserosa During Dorsal Closure. *Frontiers in Cell and Developmental Biology*, 10:865397.
- [Lynch et al., 2013] Lynch, H. E., Crews, S. M., Rosenthal, B., Kim, E., Gish, R., Echiverri, K., and Hutson, M. S. (2013). Cellular mechanics of germ band retraction in Drosophila. *Developmental Biology*, 384(2):205–213.
- [Magie et al.,] Magie, C. R., Pinto-Santini, D., and Parkhurst, S. M. Rho1 interacts with p120ctn and -catenin, and regulates cadherin-based adherens junction components in Drosophila. page 12.
- [Maienschein, 1991] Maienschein, J. (1991). The Origins of. *A Conceptual History of Modern Embryology*, pages 43–61. Publisher: Springer, Boston, MA.

- [Manning et al., 2019] Manning, L. A., Perez-Vale, K. Z., Schaefer, K. N., Sewell, M. T., and Peifer, M. (2019). The *Drosophila* Afadin and ZO-1 homologues Canoe and Polychaetoid act in parallel to maintain epithelial integrity when challenged by adherens junction remodeling. *Molecular Biology of the Cell*, 30(16):1938–1960. Publisher: American Society for Cell Biology (mboc).
- [Martin et al., 2010] Martin, A. C., Gelbart, M., Fernandez-Gonzalez, R., Kaschube, M., and Wieschaus, E. F. (2010). Integration of contractile forces during tissue invagination. *Journal of Cell Biology*, 188(5):735–749.
- [Martin-Bermudo et al., 1999] Martin-Bermudo, M., Alvarez-Garcia, I., and Brown, N. (1999). Migration of the *Drosophila* primordial midgut cells requires coordination of diverse PS integrin functions. *Development*, 126(22):5161–5169.
- [Marty et al., 2000] Marty, T., Müller, B., Basler, K., and Affolter, M. (2000). Schnurri mediates Dpp-dependent repression of brinker transcription. *Nature Cell Biology*, 2(10):745–749.
- [Martín-Blanco et al., 1998] Martín-Blanco, E., Gampel, A., Ring, J., Virdee, K., Kirov, N., Tolkovsky, A. M., and Martinez-Arias, A. (1998). puckered encodes a phosphatase that mediates a feedback loop regulating JNK activity during dorsal closure in *Drosophila*. *Genes & Development*, 12(4):557–570.
- [Matsuda and Chitnis, 2010] Matsuda, M. and Chitnis, A. B. (2010). *Atoh1a* expression must be restricted by Notch signaling for effective morphogenesis of the posterior lateral line primordium in zebrafish. *Development*, 137(20):3477–3487.
- [Medioni et al., 2008] Medioni, C., Astier, M., Zmojdzian, M., Jagla, K., and Sémériva, M. (2008). Genetic control of cell morphogenesis during *Drosophila melanogaster* cardiac tube formation. *Journal of Cell Biology*, 182(2):249–261.
- [Millard and Martin, 2008] Millard, T. H. and Martin, P. (2008). Dynamic analysis of filopodial interactions during the zipper phase of *Drosophila* dorsal closure. *Development*, 135(4):621–626.

- [Mogilner and Oster, 1996] Mogilner, A. and Oster, G. (1996). The physics of lamellipodial protrusion. *European Biophysics Journal*, 25(1):47–53.
- [Molnar and Labouesse, 2021] Molnar, K. and Labouesse, M. (2021). The plastic cell: mechanical deformation of cells and tissues. *Open Biology*, 11(2):rsob.210006, 210006.
- [Montero and Hurlé, 2010] Montero, J. A. and Hurlé, J. M. (2010). Sculpturing digit shape by cell death. *Apoptosis*, 15(3):365–375.
- [Morgan, 1895] Morgan, T. H. (1895). Half-Embryos and Whole-Embryos from one of the first two Blastomeres of the Frog’s Egg. *Anat. Anz.*, 10:623–628.
- [Muliyil et al., 2011] Muliyil, S., Krishnakumar, P., and Narasimha, M. (2011). Spatial, temporal and molecular hierarchies in the link between death, delamination and dorsal closure. *Development*, 138(14):3043–3054.
- [Murray and Saint, 2007] Murray, M. J. and Saint, R. (2007). Photoactivatable GFP resolves Drosophila mesoderm migration behaviour. Publisher: Oxford University Press for The Company of Biologists Limited.
- [Murrell et al., 2015] Murrell, M., Oakes, P. W., Lenz, M., and Gardel, M. L. (2015). Forcing cells into shape: the mechanics of actomyosin contractility. *Nature Reviews Molecular Cell Biology*, 16(8):486–498. Number: 8 Publisher: Nature Publishing Group.
- [Nandadasa et al., 2009] Nandadasa, S., Tao, Q., Menon, N. R., Heasman, J., and Wylie, C. (2009). N- and E-cadherins in Xenopus are specifically required in the neural and non-neural ectoderm, respectively, for F-actin assembly and morphogenetic movements. *Development*, 136(8):1327–1338.
- [Narasimha and Brown, 2004] Narasimha, M. and Brown, N. H. (2004). Novel functions for integrins in epithelial morphogenesis. *Current biology: CB*, 14(5):381–385.

- [Nassif et al., 1998] Nassif, C., Daniel, A., Lengyel, J. A., and Hartenstein, V. (1998). The Role of Morphogenetic Cell Death during *Drosophila* Embryonic Head Development. *Developmental biology*, 197(2):170–186. Publisher: Elsevier.
- [Nellen et al., 1996] Nellen, D., Burke, R., Struhl, G., and Basler, K. (1996). Direct and long-range action of a DPP morphogen gradient. *Cell*, 85(3):357–368.
- [Neuman-Silberberg and Schüpbach, 1993] Neuman-Silberberg, F. S. and Schüpbach, T. (1993). The *Drosophila* dorsoventral patterning gene *gurken* produces a dorsally localized RNA and encodes a TGF-like protein. *Cell*, 75(1):165–174. Publisher: Elsevier.
- [Nishimura et al., 2012] Nishimura, T., Honda, H., and Takeichi, M. (2012). Planar cell polarity links axes of spatial dynamics in neural-tube closure. *Cell*, 149.
- [Nishimura and Takeichi, 2008] Nishimura, T. and Takeichi, M. (2008). Shroom3-mediated recruitment of Rho kinases to the apical cell junctions regulates epithelial and neuroepithelial planar remodeling. *Development*, 135(8):1493–1502.
- [Nüsslein-Volhard et al., 1987] Nüsslein-Volhard, C., Frohnhofer, H. G., and Lehmann, R. (1987). Determination of anteroposterior polarity in *Drosophila*. *Science*, 238(4834):1675–1681. Publisher: American Association for the Advancement of Science.
- [Nüsslein-Volhard et al., 1984] Nüsslein-Volhard, C., Wieschaus, E., and Kluding, H. (1984). Mutations affecting the pattern of the larval cuticle in *Drosophila melanogaster*. *Wilhelm Roux's archives of developmental biology*, 193(5):267–282. Publisher: Springer.
- [Oda et al., 1998] Oda, H., Tsukita, S., and Takeichi, M. (1998). Dynamic behavior of the cadherin-based cell–cell adhesion system during *drosophilagastrulation*. *Developmental biology*, 203(2):435–450. Publisher: Elsevier.
- [Pare, 2014] Pare, A. C. (2014). A positional Toll receptor code directs convergent extension in *Drosophila*. *Nature*, 515.

- [Paré et al., 2019] Paré, A. C., Naik, P., Shi, J., Mirman, Z., Palmquist, K. H., and Zallen, J. A. (2019). An LRR Receptor-Teneurin System Directs Planar Polarity at Compartment Boundaries. *Developmental Cell*, 51(2):208–221.e6.
- [Pasakarnis et al., 2016] Pasakarnis, L., Frei, E., Caussinus, E., Affolter, M., and Brunner, D. (2016). Amnioserosa cell constriction but not epidermal actin cable tension autonomously drives dorsal closure. *Nature Cell Biology*, 18(11):1161–1172.
- [Penton et al., 1994] Penton, A., Chen, Y., Staehling-Hampton, K., Wrana, J. L., Attisano, L., Szidonya, J., Cassill, J. A., Massagué, J., and Hoffmann, F. M. (1994). Identification of two bone morphogenetic protein type I receptors in *Drosophila* and evidence that Brk25D is a decapentaplegic receptor. *Cell*, 78(2):239–250.
- [Peralta et al., 2007] Peralta, X. G., Toyama, Y., Hutson, M. S., Montague, R., Venakides, S., Kiehart, D. P., and Edwards, G. S. (2007). Upregulation of forces and morphogenic asymmetries in dorsal closure during *Drosophila* development. *Biophysical Journal*, 92(7):2583–2596.
- [Peri et al., 1999] Peri, F., Bökel, C., and Roth, S. (1999). Local Gurken signaling and dynamic MAPK activation during *Drosophila* oogenesis. *Mechanisms of Development*, 81(1):75–88.
- [Pitsidianaki et al., 2021] Pitsidianaki, I., Morgan, J., Adams, J., and Campbell, K. (2021). Mesenchymal-to-epithelial transitions require tissue-specific interactions with distinct laminins. *Journal of Cell Biology*, 220(8):e202010154.
- [Plotnikov et al., 2014] Plotnikov, S. V., Sabass, B., Schwarz, U. S., and Waterman, C. M. (2014). High-resolution traction force microscopy. In *Methods in cell biology*, volume 123, pages 367–394. Elsevier.
- [Polyakov et al., 2014] Polyakov, O., He, B., Swan, M., Shaevitz, J. W., Kaschube, M., and Wieschaus, E. (2014). Passive Mechanical Forces Control Cell-Shape

- Change during *Drosophila* Ventral Furrow Formation. *Biophysical Journal*, 107(4):998–1010.
- [Poole et al., 2001] Poole, T. J., Finkelstein, E. B., and Cox, C. M. (2001). The role of FGF and VEGF in angioblast induction and migration during vascular development. *Developmental Dynamics*, 220(1):1–17. eprint: <https://onlinelibrary.wiley.com/doi/pdf/10.1002/1097-0177%282000%299999%3A9999%3C%3A%3AAID-DVDY1087%3E3.0.CO%3B2-2>.
- [Pope and Harris, 2008] Pope, K. L. and Harris, T. J. (2008). Control of cell flattening and junctional remodeling during squamous epithelial morphogenesis in *Drosophila*. Publisher: Oxford University Press for The Company of Biologists Limited.
- [Poulson, 1950] Poulson, D. (1950). Histogenesis, organogenesis, and differentiation in the embryo of *Drosophila melanogaster* Meigen. *Biology of Drosophila*, pages 168–274. Publisher: John Wiley and Sons.
- [R Core Team, 2022] R Core Team (2022). *R: A Language and Environment for Statistical Computing*. R Foundation for Statistical Computing, Vienna, Austria.
- [Rabinowitz, 1941a] Rabinowitz, M. (1941a). Studies on the cytology and early embryology of the egg of *Drosophila melanogaster*. *Journal of Morphology*, 69(1):1–49. Publisher: Wiley Online Library.
- [Rabinowitz, 1941b] Rabinowitz, M. (1941b). Yolk nuclei in the egg of *Drosophila melanogaster*. *Anat Rec*, 81:80–81.
- [Raftery and Sutherland, 2003] Raftery, L. A. and Sutherland, D. J. (2003). Gradients and thresholds: BMP response gradients unveiled in *Drosophila* embryos. *Trends in Genetics*, 19(12):701–708.

- [Rafferty et al., 1995] Rafferty, L. A., Twombly, V., Wharton, K., and Gelbart, W. M. (1995). Genetic Screens to Identify Elements of the Decapentaplegic Signaling Pathway in *Drosophila*. *Genetics*, 139(1):241–254.
- [Rahimi et al., 2019] Rahimi, N., Averbukh, I., Carmon, S., Schejter, E. D., Barkai, N., and Shilo, B.-Z. (2019). Dynamics of Spaetzle morphogen shuttling in the *Drosophila* embryo shapes gastrulation patterning. *Development*, 146(21):dev181487.
- [Raspopovic et al., 2014] Raspopovic, J., Marcon, L., Russo, L., and Sharpe, J. (2014). Digit patterning is controlled by a Bmp-Sox9-Wnt Turing network modulated by morphogen gradients. *Science*, 345(6196):566–570. Publisher: American Association for the Advancement of Science.
- [Rebay and Rubin, 1995] Rebay, I. and Rubin, G. M. (1995). Yan functions as a general inhibitor of differentiation and is negatively regulated by activation of the Ras1/MAPK pathway. *Cell*, 81(6):857–866.
- [Reed et al., 2001] Reed, B. H., Wilk, R., and Lipshitz, H. D. (2001). Downregulation of Jun kinase signaling in the amnioserosa is essential for dorsal closure of the *Drosophila* embryo. *Current biology: CB*, 11(14):1098–1108.
- [Reed et al., 2004] Reed, B. H., Wilk, R., Schöck, F., and Lipshitz, H. D. (2004). Integrin-Dependent Apposition of *Drosophila* Extraembryonic Membranes Promotes Morphogenesis and Prevents Anoikis. *Current Biology*, 14(5):372–380.
- [Reuter et al., 1993] Reuter, R., Grunewald, B., and Leptin, M. (1993). A role for the mesoderm in endodermal migration and morphogenesis in *Drosophila*. *Development*, 119(4):1135–1145.
- [Riesgo-Escovar and Hafen, 1997] Riesgo-Escovar, J. R. and Hafen, E. (1997). *Drosophila* Jun kinase regulates expression of decapentaplegic via the ETS-domain protein Aop and the AP-1 transcription factor DJun during dorsal closure. *Genes & Development*, 11(13):1717–1727.

- [Riesgo-Escovar et al., 1996] Riesgo-Escovar, J. R., Jenni, M., Fritz, A., and Hafen, E. (1996). The *Drosophila* Jun-N-terminal kinase is required for cell morphogenesis but not for DJun-dependent cell fate specification in the eye. *Genes & Development*, 10(21):2759–2768. Company: Cold Spring Harbor Laboratory Press Distributor: Cold Spring Harbor Laboratory Press Institution: Cold Spring Harbor Laboratory Press Label: Cold Spring Harbor Laboratory Press Publisher: Cold Spring Harbor Lab.
- [Rodriguez-Diaz et al., 2008] Rodriguez-Diaz, A., Toyama, Y., Abravanel, D. L., Wiemann, J. M., Wells, A. R., Tulu, U. S., Edwards, G. S., and Kiehart, D. P. (2008). Actomyosin purse strings: Renewable resources that make morphogenesis robust and resilient. *HFSP Journal*, 2(4):220–237.
- [Rogulja-Ortmann et al., 2007] Rogulja-Ortmann, A., Lüer, K., Seibert, J., Rickert, C., and Technau, G. M. (2007). Programmed cell death in the embryonic central nervous system of *Drosophila melanogaster*. *Development*, 134(1):105–116.
- [Rothenberg and Fernandez-Gonzalez, 2019] Rothenberg, K. E. and Fernandez-Gonzalez, R. (2019). Forceful closure: cytoskeletal networks in embryonic wound repair. *Molecular Biology of the Cell*, 30(12):1353–1358. Publisher: American Society for Cell Biology (mboc).
- [Rousset et al., 2010] Rousset, R., Bono-Lauriol, S., Gettings, M., Suzanne, M., Spéder, P., and Noselli, S. (2010). The *Drosophila* serine protease homologue Scarface regulates JNK signalling in a negative-feedback loop during epithelial morphogenesis. *Development (Cambridge, England)*, 137(13):2177–2186.
- [Roux, 1888] Roux, W. (1888). Contributions to the developmental mechanics of the embryo. On the artificial production of half-embryos by destruction of one of the first two blastomeres, and the later development (postgeneration) of the missing half of the body. *Foundations of experimental embryology*, pages 2–37. Publisher: Hafner New York.

- [Royou et al., 2002] Royou, A., Sullivan, W., and Karess, R. (2002). Cortical recruitment of nonmuscle myosin II in early syncytial *Drosophila* embryos : its role in nuclear axial expansion and its regulation by Cdc2 activity. *Journal of Cell Biology*, 158(1):127–137.
- [RStudio Team, 2020] RStudio Team (2020). *RStudio: Integrated Development Environment for R*. RStudio, PBC., Boston, MA.
- [Ruberte et al., 1995] Ruberte, E., Marty, T., Nellen, D., Affolter, M., and Basler, K. (1995). An absolute requirement for both the type II and type I receptors, punt and thick veins, for dpp signaling in vivo. *Cell*, 80(6):889–897.
- [Rushlow et al., 2001] Rushlow, C., Colosimo, P. F., Lin, M.-c., Xu, M., and Kirov, N. (2001). Transcriptional regulation of the *Drosophila* gene *zen* by competing Smad and Brinker inputs. *Genes & development*, 15(3):340–351. Publisher: Cold Spring Harbor Lab.
- [Rushlow et al., 1989] Rushlow, C. A., Han, K., Manley, J. L., and Levine, M. (1989). The graded distribution of the dorsal morphogen is initiated by selective nuclear transport in *Drosophila*. *Cell*, 59(6):1165–1177.
- [Ríos-Barrera and Riesgo-Escovar, 2013] Ríos-Barrera, L. D. and Riesgo-Escovar, J. R. (2013). Regulating cell morphogenesis: The *drosophila* jun N-terminal kinase pathway. *genesis*, 51(3):147–162. eprint: <https://onlinelibrary.wiley.com/doi/pdf/10.1002/dvg.22354>.
- [Saias et al., 2015] Saias, L., Swoger, J., D’Angelo, A., Hayes, P., Colombelli, J., Sharpe, J., Salbreux, G., and Solon, J. (2015). Decrease in Cell Volume Generates Contractile Forces Driving Dorsal Closure. *Developmental Cell*, 33(5):611–621.
- [Sausedo et al., 1997] Sausedo, R. A., Smith, J. L., and Schoenwolf, G. C. (1997). Role of nonrandomly oriented cell division in shaping and bending of the neural plate. *Journal of Comparative Neurology*, 381(4):473–488.

_eprint: <https://onlinelibrary.wiley.com/doi/pdf/10.1002/%28SICI%291096-9861%2819970519%29381%3A4%3C473%3A%3AAID-CNE7%3E3.0.CO%3B2-%23>.

[Schindelin et al., 2012] Schindelin, J., Arganda-Carreras, I., Frise, E., Kaynig, V., Longair, M., Pietzsch, T., Preibisch, S., Rueden, C., Saalfeld, S., Schmid, B., Tinevez, J.-Y., White, D. J., Hartenstein, V., Eliceiri, K., Tomancak, P., and Cardona, A. (2012). Fiji: an open-source platform for biological-image analysis. *Nature Methods*, 9(7):676–682. Number: 7 Publisher: Nature Publishing Group.

[Schoenwolf and Smith, 1990] Schoenwolf, G. and Smith, J. (1990). Mechanisms of neurulation: traditional viewpoint and recent advances. *Development*, 109(2):243–270.

[Schoenwolf and Franks, 1984] Schoenwolf, G. C. and Franks, M. V. (1984). Quantitative analyses of changes in cell shapes during bending of the avian neural plate. *Developmental Biology*, 105(2):257–272.

[Schulman et al., 2015] Schulman, V. K., Dobi, K. C., and Baylies, M. K. (2015). Morphogenesis of the somatic musculature in *Drosophila melanogaster*. *WIREs Developmental Biology*, 4(4):313–334. _eprint: <https://onlinelibrary.wiley.com/doi/pdf/10.1002/wdev.180>.

[Schöck and Perrimon, 2002] Schöck, F. and Perrimon, N. (2002). Cellular processes associated with germ band retraction in *Drosophila*. *Developmental Biology*, 248(1):29–39.

[Schüpbach and Wieschaus, 1986] Schüpbach, T. and Wieschaus, E. (1986). Maternal-effect mutations altering the anterior-posterior pattern of the *Drosophila* embryo. *Roux's archives of developmental biology*, 195(5):302–317.

[Scuderi et al., 2006] Scuderi, A., Simin, K., Kazuko, S. G., Metherall, J. E., and Letsou, A. (2006). scylla and charybde, homologues of the human apoptotic gene

- RTP801, are required for head involution in *Drosophila*. *Developmental biology*, 291(1):110–122. Publisher: Elsevier.
- [Seher et al., 2007] Seher, T. C., Narasimha, M., Vogelsang, E., and Leptin, M. (2007). Analysis and reconstitution of the genetic cascade controlling early mesoderm morphogenesis in the *Drosophila* embryo. *Mechanisms of Development*, 124(3):167–179.
- [Sekelsky et al., 1995] Sekelsky, J. J., Newfeld, S. J., Raftery, L. A., Chartoff, E. H., and Gelbart, W. M. (1995). Genetic characterization and cloning of mothers against dpp, a gene required for decapentaplegic function in *Drosophila melanogaster*. *Genetics*, 139(3):1347–1358.
- [Selvaggi et al., 2022] Selvaggi, L., Ackermann, M., Pasakarnis, L., Brunner, D., and Aegerter, C. M. (2022). Force measurements of Myosin II waves at the yolk surface during *Drosophila* dorsal closure. *Biophysical Journal*, 121(3):410–420.
- [Sen et al., 1998] Sen, J., Goltz, J. S., Stevens, L., and Stein, D. (1998). Spatially restricted expression of pipe in the *Drosophila* egg chamber defines embryonic dorsal–ventral polarity. *Cell*, 95(4):471–481. Publisher: Elsevier.
- [Shindo et al., 2008] Shindo, M., Wada, H., Kaido, M., Tateno, M., Aigaki, T., Tsuda, L., and Hayashi, S. (2008). Dual function of Src in the maintenance of adherens junctions during tracheal epithelial morphogenesis. Publisher: Oxford University Press for The Company of Biologists Limited.
- [Shoval et al., 2007] Shoval, I., Ludwig, A., and Kalcheim, C. (2007). Antagonistic roles of full-length N-cadherin and its soluble BMP cleavage product in neural crest delamination. Publisher: Oxford University Press for The Company of Biologists Limited.
- [Singh et al., 2018] Singh, A., Saha, T., Begemann, I., Ricker, A., Nüsse, H., Thorn-Seshold, O., Klingauf, J., Galic, M., and Matis, M. (2018). Polarized microtubule

- dynamics directs cell mechanics and coordinates forces during epithelial morphogenesis. *Nature Cell Biology*, 20(10):1126–1133.
- [Skeath and Carroll, 1992] Skeath, J. and Carroll, S. (1992). Regulation of proneural gene expression and cell fate during neuroblast segregation in the *Drosophila* embryo. *Development*, 114(4):939–946.
- [Skeath et al., 1992] Skeath, J. B., Panganiban, G., Selegue, J., and Carroll, S. (1992). Gene regulation in two dimensions: the proneural achaete and scute genes are controlled by combinations of axis-patterning genes through a common intergenic control region. *Genes & Development*, 6(12b):2606–2619. Publisher: Cold Spring Harbor Lab.
- [Sluss et al., 1996] Sluss, H. K., Han, Z., Barrett, T., Goberdhan, D. C., Wilson, C., Davis, R. J., and Ip, Y. T. (1996). A JNK signal transduction pathway that mediates morphogenesis and an immune response in *Drosophila*. *Genes & Development*, 10(21):2745–2758.
- [Smith and Schoenwolf, 1991] Smith, J. L. and Schoenwolf, G. C. (1991). Further evidence of extrinsic forces in bending of the neural plate. *Journal of Comparative Neurology*, 307(2):225–236. eprint: <https://onlinelibrary.wiley.com/doi/pdf/10.1002/cne.903070206>.
- [Sokolow et al., 2012] Sokolow, A., Toyama, Y., Kiehart, D. P., and Edwards, G. S. (2012). Cell Ingression and Apical Shape Oscillations during Dorsal Closure in *Drosophila*. *Biophysical Journal*, 102(5):969–979.
- [Solon et al., 2009] Solon, J., Kaya-Copur, A., Colombelli, J., and Brunner, D. (2009). Pulsed forces timed by a ratchet-like mechanism drive directed tissue movement during dorsal closure. *Cell*, 137.
- [Sorrosal et al., 2010] Sorrosal, G., Pérez, L., Herranz, H., and Milán, M. (2010). Scarface, a secreted serine protease-like protein, regulates polarized localization of

- laminin A at the basement membrane of the *Drosophila* embryo. *EMBO reports*, 11(5):373–379.
- [Spemann, 1921] Spemann, H. (1921). Die Erzeugung tierischer Chimären durch heteroplastische embryonale Transplantation zwischen *Triton cristatus* und *taeniatus*. *Archiv für Entwicklungsmechanik der Organismen*, 48(4):533–570. Publisher: Springer-Verlag.
- [Spemann, 1988] Spemann, H. (1988). Embryonic development and induction, vol. 10. Publisher: Taylor & Francis.
- [Spemann and Mangold, 1924] Spemann, H. and Mangold, H. (1924). Induction of embryonic primordia by implantation of organizers from a different species. *Roux Arch. Entwickl. Mech.*, 100.
- [Spencer et al., 2015] Spencer, A. K., Siddiqui, B. A., and Thomas, J. H. (2015). Cell shape change and invagination of the cephalic furrow involves reorganization of F-actin. *Developmental Biology*, 402(2):192–207.
- [Staehling-Hampton and Hoffmann, 1994] Staehling-Hampton, K. and Hoffmann, F. M. (1994). Ectopic decapentaplegic in the *Drosophila* midgut alters the expression of five homeotic genes, *dpp*, and *wingless*, causing specific morphological defects. *Developmental Biology*, 164(2):502–512.
- [Stollewerk, 2000] Stollewerk, A. (2000). Changes in cell shape in the ventral neuroectoderm of *Drosophila melanogaster* depend on the activity of the achaete-scute complex genes. *Development genes and evolution*, 210(4):190–199. Publisher: Springer.
- [Stronach and Perrimon, 2002] Stronach, B. and Perrimon, N. (2002). Activation of the JNK pathway during dorsal closure in *Drosophila* requires the mixed lineage kinase, slipper. *Genes & Development*, 16(3):377–387.

- [Stronach and Perrimon, 2001] Stronach, B. E. and Perrimon, N. (2001). Investigation of leading edge formation at the interface of amnioserosa and dorsal ectoderm in the *Drosophila* embryo. *Development*, 128(15):2905–2913.
- [Sun et al., 2020] Sun, J., Macabenta, F., Akos, Z., and Stathopoulos, A. (2020). Collective Migrations of *Drosophila* Embryonic Trunk and Caudal Mesoderm-Derived Muscle Precursor Cells. *Genetics*, 215(2):297–322.
- [Sutherland et al., 1996] Sutherland, D., Samakovlis, C., and Krasnow, M. A. (1996). *branchless* encodes a *Drosophila* FGF homolog that controls tracheal cell migration and the pattern of branching. *Cell*, 87(6):1091–1101. Publisher: Elsevier.
- [Takeda et al., 2018] Takeda, M., Sami, M. M., and Wang, Y.-C. (2018). A homeostatic apical microtubule network shortens cells for epithelial folding via a basal polarity shift. *Nature Cell Biology*, 20(1):36–45. Number: 1 Publisher: Nature Publishing Group.
- [Tepass, 2014] Tepass, U. (2014). Polarize to elongate. *Nature*, 515(7528):499–501. Number: 7528 Publisher: Nature Publishing Group.
- [Tepass and Hartenstein, 1994] Tepass, U. and Hartenstein, V. (1994). Epithelium formation in the *Drosophila* midgut depends on the interaction of endoderm and mesoderm. *Development*, 120(3):579–590.
- [Torres-Vázquez et al., 2003] Torres-Vázquez, J., Kamei, M., and Weinstein, B. M. (2003). Molecular distinction between arteries and veins. *Cell and Tissue Research*, 314(1):43–59.
- [Toyama et al., 2008] Toyama, Y., Peralta, X. G., Wells, A. R., Kiehart, D. P., and Edwards, G. S. (2008). Apoptotic Force and Tissue Dynamics During *Drosophila* Embryogenesis. *Science (New York, N.Y.)*, 321(5896):1683–1686.

- [Trubuil et al., 2021] Trubuil, E., D'Angelo, A., and Solon, J. (2021). Tissue mechanics in morphogenesis: Active control of tissue material properties to shape living organisms. *Cells & Development*, 168:203777.
- [Tsuneizumi et al., 1997] Tsuneizumi, K., Nakayama, T., Kamoshida, Y., Kornberg, T. B., Christian, J. L., and Tabata, T. (1997). Daughters against dpp modulates dpp organizing activity in *Drosophila* wing development. *Nature*, 389(6651):627–631.
- [Turner and Mahowald, 1979] Turner, F. R. and Mahowald, A. P. (1979). Scanning electron microscopy of *Drosophila melanogaster* embryogenesis: III. Formation of the head and caudal segments. *Developmental Biology*, 68(1):96–109.
- [VanHook and Letsou, 2008] VanHook, A. and Letsou, A. (2008). Head involution in *Drosophila*: Genetic and morphogenetic connections to dorsal closure. *Developmental Dynamics*, 237(1):28–38. eprint: <https://onlinelibrary.wiley.com/doi/pdf/10.1002/dvdy.21405>.
- [Vincent et al., 1997a] Vincent, A., Blankenship, J., and Wieschaus, E. (1997a). Integration of the head and trunk segmentation systems controls cephalic furrow formation in *Drosophila*. *Development*, 124(19):3747–3754.
- [Vincent et al., 1997b] Vincent, S., Ruberte, E., Grieder, N., Chen, C., Haerry, T., Schuh, R., and Affolter, M. (1997b). DPP controls tracheal cell migration along the dorsoventral body axis of the *Drosophila* embryo. *Development*, 124(14):2741–2750.
- [Wada et al., 2007] Wada, A., Kato, K., Uwo, M. F., Yonemura, S., and Hayashi, S. (2007). Specialized extraembryonic cells connect embryonic and extraembryonic epidermis in response to Dpp during dorsal closure in *Drosophila*. *Developmental Biology*, 301(2):340–349.
- [Waddington and Kacser, 1957] Waddington, C. and Kacser, H. (1957). The strategy of the genes. A discussion of some aspects of theoretical biology. With an

appendix by H. Kacser. *Strateg. genes. A Discuss. some Asp. Theor. Biol. With an Append. by H. Kacser.*

[Wang et al., 2012a] Wang, Q., Feng, J. J., and Pismen, L. M. (2012a). A cell-level biomechanical model of *Drosophila* dorsal closure. *Biophysical journal*, 103(11):2265–2274. Publisher: Elsevier.

[Wang et al., 2012b] Wang, Y.-C., Khan, Z., Kaschube, M., and Wieschaus, E. F. (2012b). Differential positioning of adherens junctions is associated with initiation of epithelial folding. *Nature*, 484(7394):390–393. Number: 7394 Publisher: Nature Publishing Group.

[Wang et al., 2013] Wang, Y.-C., Khan, Z., and Wieschaus, E. F. (2013). Distinct Rap1 Activity States Control the Extent of Epithelial Invagination via -Catenin. *Developmental Cell*, 25(3):299–309.

[Weber et al., 2003] Weber, A. N. R., Tauszig-Delamasure, S., Hoffmann, J. A., Lelièvre, E., Gascan, H., Ray, K. P., Morse, M. A., Imler, J.-L., and Gay, N. J. (2003). Binding of the *Drosophila* cytokine Spätzle to Toll is direct and establishes signaling. *Nature Immunology*, 4(8):794–800. Number: 8 Publisher: Nature Publishing Group.

[Wells et al., 2014] Wells, A. R., Zou, R. S., Tulu, U. S., Sokolow, A. C., Crawford, J. M., Edwards, G. S., and Kiehart, D. P. (2014). Complete canthi removal reveals that forces from the amnioserosa alone are sufficient to drive dorsal closure in *Drosophila*. *Molecular Biology of the Cell*, 25(22):3552–3568. Publisher: American Society for Cell Biology (mboc).

[Weng and Wieschaus, 2016] Weng, M. and Wieschaus, E. (2016). Myosin-dependent remodeling of adherens junctions protects junctions from Snail-dependent disassembly. *Journal of Cell Biology*, 212(2):219–229.

- [Weng and Wieschaus, 2017] Weng, M. and Wieschaus, E. (2017). Polarity protein Par3/Bazooka follows myosin-dependent junction repositioning. *Developmental biology*, 422(2):125–134. Publisher: Elsevier.
- [Wickham, 2016] Wickham, H. (2016). *ggplot2: Elegant Graphics for Data Analysis*. Springer-Verlag New York.
- [Wieschaus et al., 1984] Wieschaus, E., Nüsslein-Volhard, C., and Jürgens, G. (1984). Mutations affecting the pattern of the larval cuticle in *Drosophila melanogaster*. *Wilhelm Roux's archives of developmental biology*, 193(5):296–307. Publisher: Springer.
- [Yoo et al., 2021] Yoo, B., Kim, H.-y., Chen, X., Shen, W., Jang, J. S., Stein, S. N., Cormier, O., Pereira, L., Shih, C. R. Y., Krieger, C., Reed, B., Harden, N., and Wang, S. J. H. (2021). 20-hydroxyecdysone (20E) signaling regulates amnioserosa morphogenesis during *Drosophila* dorsal closure: EcR modulates gene expression in a complex with the AP-1 subunit, Jun. *Biology Open*, 10(8):bio058605.
- [Young et al., 1993] Young, P. E., Richman, A. M., Ketchum, A. S., and Kiehart, D. P. (1993). Morphogenesis in *Drosophila* requires nonmuscle myosin heavy chain function. *Genes & Development*, 7(1):29–41.
- [Zaffran et al., 2001] Zaffran, S., Küchler, A., Lee, H.-H., and Frasch, M. (2001). biniou (FoxF), a central component in a regulatory network controlling visceral mesoderm development and midgut morphogenesis in *Drosophila*. *Genes & Development*, 15(21):2900–2915. Company: Cold Spring Harbor Laboratory Press Distributor: Cold Spring Harbor Laboratory Press Institution: Cold Spring Harbor Laboratory Press Label: Cold Spring Harbor Laboratory Press Publisher: Cold Spring Harbor Lab.
- [Zallen and Wieschaus, 2004] Zallen, J. A. and Wieschaus, E. (2004). Patterned Gene Expression Directs Bipolar Planar Polarity in *Drosophila*. *Developmental Cell*, 6(3):343–355.

[Zalokar, 1976] Zalokar, M. (1976). Division and migration of nuclei during early embryogenesis of *Drosophila melanogaster*.

[Zalokar and Erk, 1977] Zalokar, M. and Erk, I. (1977). Phase-Partition Fixation and Staining of *Drosophzla* Eggs. *Stain Technology*, 52(2):89–95. Publisher: Taylor & Francis _eprint: <https://doi.org/10.3109/10520297709116753>.